Photochemical Studies of Jupiter and Titan

Thesis by

Ah-San Wong

In Partial Fulfillment of the Requirements

for the Degree of

Doctor of Philosophy

California Institute of Technology

Pasadena, California

2002

(Submitted January 14, 2002)

Acknowledgements

I am forever indebted to my dissertation advisor Professor Yuk Yung for this work. It would have been impossible without his initiation, guidance, and support. In the years before I joined his group, Professor Yung had already been a good mentor for me. He and his wife often inquired about my life at Caltech. On May 12, 1999, Professor Yung invited me to lunch, and suggested that I take a look at a project in his group: modeling of benzene on Jupiter. Our conversation generated great interest and fascination for planetary science in me. In shortly two and half years, he helped me grasp the new subject, finish two major projects, and become ready to move on as a planetary scientist. Over the years, he has not only given me scientific guidance, but also shared with me his experiences and insights into many philosophical issues. He has been extremely patient with me, and his conduct shows how a successful scientist thinks and works. I am very fortunate to have known him and learned from him, and to have seen this wonderful field of science. No words are enough to describe my gratitude towards him.

My work was only possible with the help of many collaborating scientists and colleagues. I thank Anthony Lee for showing me the details of the code, proofreading my papers, and valuable technical discussions; Joe Ajello for working with me on the Galileo data, and for enjoyable conversations on outdoor activities; and Gabe Morgan for his work on the chemistry in the Titan project, and for his help with the code.

In the Jupiter project, I thank Bob West for discussion on the aerosol formation, B. Bézard for result on ISO observations, and Mark Allen, M. F. Gerstell, and G. D. McDonald for helpful comments. In the Titan project, I thank F. S. Rowland for an illuminating discussion of the $^1CH_2$ and CO reaction, and W. B. DeMore and K. Bayes for valuable advice on the kinetics of hydrocarbons and CO. I thank Nicolas Biver for carrying out the observations of Titan with the JCMT, and J. I. Moses for providing the code the Titan model is based on. M. Allen provided critical input to

a preliminary version of our paper. I thank M. A. Gurwell and M. F. Gerstell for comments and suggestions.

I thank Mike Black for helping me overcome many computer problems. Several people gave me templates for this dissertation, including Adam, Anthony, Liz, Jason, and Nari. Thanks to Frank for giving me a powerful computer to work on and for being a good friend.

My thanks to Professors Fiona Harrison, Steve Fraustchi, and Ed Stone for serving on my committee and for giving me thoughtful comments on my work; to the staff in the Physics Department and Planetary Science Department for their care and help; to the planetary science community around the world for being such a friendly and supportive community. I'd also like to thank Carol for her invaluable help, and Ernie for his burritos and teriyaki sandwiches.

My parents have shown the most passionate support of my pursuit for higher education and happiness. They have been with me through thick and thin with their timeless love and unfailing encouragement. I am so glad that they will finally share the joy of my achievement. My sister has been a dependable supporter and confidant for my causes over the years. I owe my family the deepest thankfulness.

I have made great friends during my graduate life. Many thanks to Darrell, Nina, Killian, George, Junjun, and Josh for their love and encouragement, for being who they are, for letting me be who I am, and for always reminding me what life is really about.

Thanks, world.

Abstract

This study of the atmosphere of Jupiter and Titan consists in large part of three papers, each of which employs the Caltech/JPL one-dimensional photochemical model.

Paper One: Aromatic compounds have been considered a likely candidate for enhanced aerosol formation in the polar region of Jupiter. In this paper, a new chemical model for aromatic compounds in the auroral thermosphere/ionosphere is developed, which satisfies constraints from the observations of each of Voyager, Galileo and the Infrared Space Observatory. The study demonstrates that sufficient quantities of higher ring species can condense to form aerosol.

Paper Two: A comprehensive atmospheric model is put forward and used to investigate the details of benzene chemistry on Jupiter, in both its auroral and non-auroral regions. The benzene formation schemes are discussed for neutral chemistry and ion chemistry, and the major uncertainties in the chemical kinetics are identified. The model shows that ion chemistry adds an additional source of benzene in auroral regions. The results are compared with observations made by the Infrared Space Observatory. 172

Paper Three: The recent observation of the heavy isotopomers of CO, ^{13}CO and $C^{18}O$, may be used to place constraints on the evolution of the atmosphere of Titan. 200 However, the original isotopic signature may be altered by photochemical reactions. This paper explains the absence of C isotopic enrichment in Titan's atmosphere, despite the significant enrichment of heavy H, N, and O isotopes. It is shown that there is a rapid exchange for C atoms between the CH_4 and CO reservoirs, mediated by the reaction $^1CH_2 + {}^*CO \rightarrow {}^{1*}CH_2 + CO$, where $^*C$ is ^{13}C. 261 Next, the isotopic dilution of CO is investigated using a photochemical model, the results of which suggest that the time constant for isotopic exchange through the aforementioned reaction is approximately 800 Myr. This duration is considerably shorter than the age of Titan, and thus any original isotopic enhancement of ^{13}C in CO may have

been diluted by this exchange process. This paper concludes by proposing a plausible model for the evolution history of CO on Titan's atmosphere.

Contents

List of Figures

List of Tables

Chapter 1 Introduction

1.1 Photochemistry and Photochemical Models

Photochemistry is the chemistry caused or promoted by the action of light (usually ultraviolet light) which excites or dissociates some compounds and leads to the formation of new compounds. Photochemistry plays an important role in planetary atmospheres.

The Caltech/Jet Propulsion Laboratory photochemical model is a one-dimensional diffusive model that allows us to calculate the number densities of chemical species in the atmosphere as a function of space and time. The model has been developed over the past two decades and the details of the model have been presented by Yung et al. (1984), Gladstone et al. (1996), Yung and DeMore (1999), Moses et al. (2000a), and Lee et al. (2000). It serves as the basis of the investigations of the atmospheres of Titan and Jupiter in this dissertation.

In the one-dimensional numerical model, for each species in the atmosphere, we solves the steady solution of the continuity equations

$$\frac{\partial n_i}{\partial t} + \frac{\partial \phi_i}{\partial z} = P_i - L_i$$

where n_i is the number density of specie i in cm^{-3}, ϕ_i is the number flux in cm^{-2} s$-$1, z is the altitude in m, P_i is the production rate in cm^{-3} s$-$1, and L_i is the loss rate in cm^{-3} s$-$1. The flux represents transport of air masses between different parts of the atmosphere, and is expressed as

$$\phi_i = -D_i \left(\frac{\partial n_i}{\partial z} + \frac{n_i}{H_i} + \frac{1+\alpha_i}{T}\frac{\partial T}{\partial z} n \right) - K \left(\frac{\partial n_i}{\partial z} + \frac{n_i}{H_a} + \frac{1}{T}\frac{\partial T}{\partial z} n \right)$$

where D_i is the molecular diffusion coefficient in cm^{-2} s^{-1}, T is the temperature, n

is the bulk atmospheric density, α_i is the thermal diffusivity factor, H_i is the average scale height of species i, H_a is the bulk scale height of the ambient atmosphere, K is the eddy diffusion coefficient in $\mathrm{cm}^{-2}\ \mathrm{s}^{-1}$. The values of the eddy diffusion coefficient K empirically represents all kinds of motions of the bulk atmosphere, and are usually determined from atmospheric observations.

In the upper atmosphere, $D_i > K$, and the constituents are diffusively separated according to their scale heights H_i. In the lower atmosphere, $D_i < K$, and the atmosphere is homogeneously mixed. The atmospheric level where $D_i = K$ is known as the homopause.

In the one-dimensional model, all quantities n_i, ϕ_i, P_i and L_i are evaluated at each altitude z and time t. The non-linear terms P_i and L_i are calculated using chemical kinetics. The model considers the diurnally averaged quantities for the flux and the production and loss terms. The continuity equations are solved using finite-difference techniques. Newton's method is used to solve nonlinear chemistry. The details of the model are reported in Lee (2001).

Because similar photochemical processes operate in the atmospheres of both Jupiter and Titan, we adopt the same set of photochemical cross sections and chemical reactions in our models. The physical properties of the atmospheres, such as pressure, temperature, density, eddy diffusion coefficients, and basic planetary parameters, are different. We use the most complete and recently updated set of hydrocarbon photochemical reactions taken from Moses et al. (2000a) and Lee et al. (2000) for low hydrocarbons, and include new reactions that are discussed in individual chapters.

This dissertation consists of two major parts. The first part, Chapters 2 and 3, focuses on the study of hydrocarbon chemistry on Jupiter, especially the synthesis of benzene and high hydrocarbon molecules. The second part, Chapter 4, concentrates on the evolution of carbon monoxide on Titan. The appendix includes analysis of Galileo UVS spectra of the Jovian aurorae which provides information about the energy input to the ion chemistry on Jupiter.

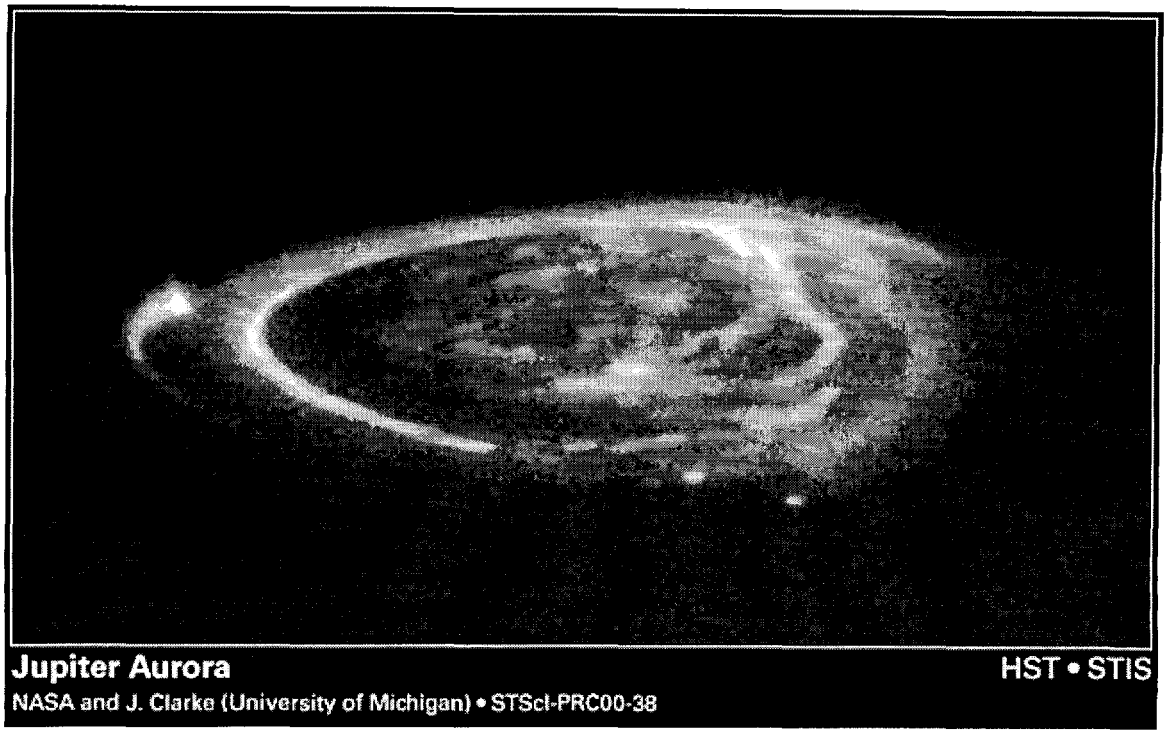

Figure 1.1 Hubble Space Telescope image of Jupiter Aurora. Credit: NASA/ESA, John Clarke.

1.2 Jupiter: Overview

Benzene has been detected since 1985. Voyager's infrared interferometer spectrometer detected benzene in the north auroral region. Lately, Galileo probe mass spectrometer has detected trace amount of benzene in the atmosphere. Most recently, the experiment of Infrared Space Observatory (ISO) has detected benzene in all regions observed. There is enhancement for benzene in the auroral regions over the disk region.

Aurora (see Figure 1.1) is caused by the precipitation of energetic particles, most likely electrons, into the atmosphere. On Jupiter, the power input of aurora is greater than that of the Sun. The precipitating electrons heat up the atmosphere and ionize the neutral species. It is likely that ion chemistry dominates the atmospheric chemistry in the auroral regions. Higher temperature and ion chemistry might lead to the formation of heavy hydrocarbon ions and compounds.

The study of hydrocarbon chemistry on Jupiter is motivated by the following open

questions:

1. What are the chemical schemes for the production of benzene on Jupiter?

2. What causes the enhancement of benzene in the polar regions?

3. What are the effects of ion chemistry on the production of benzene in auroral regions?

4. What are the chemical schemes for the production of heavy aromatic compounds?

5. Jupiter's polar haze has been observed for a long time. The haze particles are probably composed of hydrocarbons whose origins are related to ion chemistry within auroral energy deposition zone. Do polycyclic aromatic hydrocarbons (PAHs) condense to form polar haze particles?

To address these questions, we carry out three models based on the Caltech/JPL photochemical models.

Chapter 2 is a preliminary study of the formation of benzene and PAHs on Jupiter.

In Chapter 3 we investigate in details the benzene chemistry in both auroral and non-auroral regions.

1.3 Titan: Overview

We have very little knowledge of Titan. It was discovered by the Dutch astronomer Huygens in 1655. Titan is the largest satellite of Saturn, also the second largest in our solar system. Our closest encouter with Titan was the 1980 Voyager flyby which came within 4000 km of Titan's surface. In 2004, Titan will be visited by the probe Huygens carried by the Cassini spacecraft. Titan is about half water ice and half rocky material. It is the only satellite in the solar system with a massive atmosphere. At the surface, the pressure is about 1.5, 50% higher than on earth, and the temperature is about 95 K.

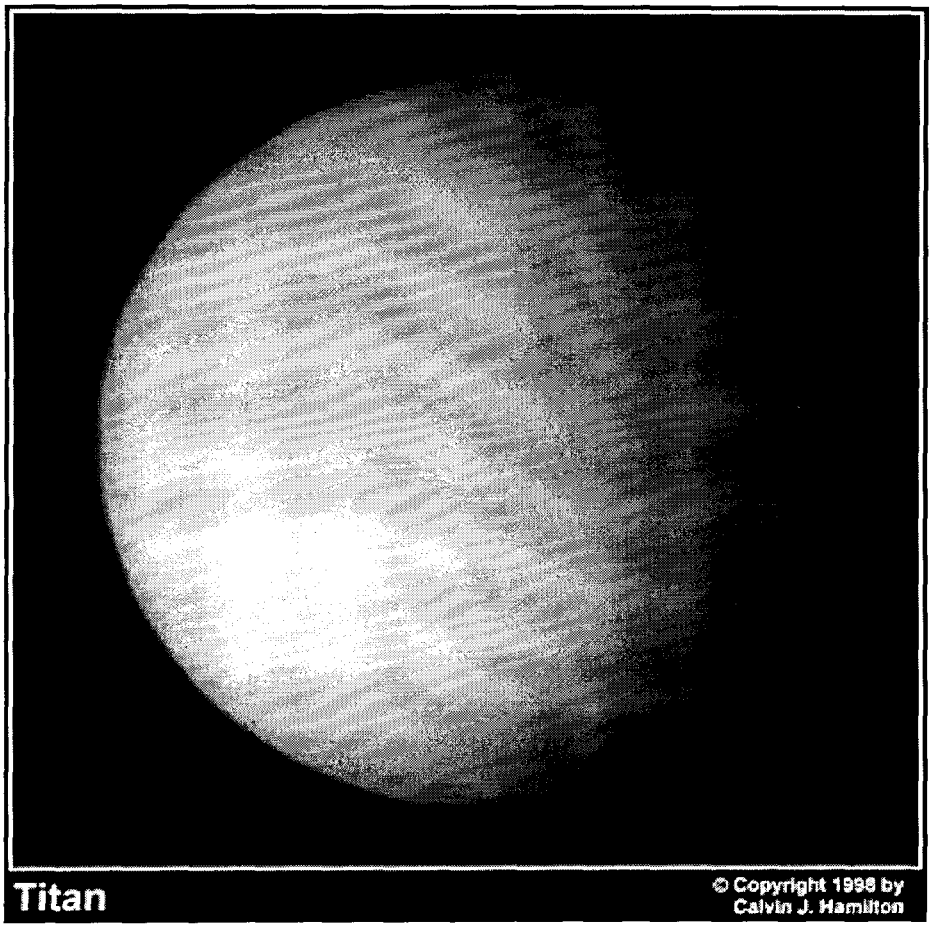

Figure 1.2 Voyager image of Titan.

The major composition of Titan's atmosphere includes molecular nitrogen, and a few percent of argon and methane. There are trace amounts of many other organic compounds such as ethane, hydrogen cyanide, carbon dioxide, carbon monoxide, and water. Since methane dominates in the upper atmosphere, the photodissociation of methane is the primary driving force of hydrocarbon chemistry in Titan's atmosphere. When methane is destroyed by sunlight, organic compounds are formed and results in very thick smog in the atmosphere.

In Chapter 4, we investigate the isotopic fractionation of carbon monoxide and its evolution history on Titan. Using the Caltech/JPL photochemical model, we re-evaluate the chemical kinetics of the important reactions with new experimental data, study a carbon atom exchange reaction that alters the isotopic signatures of carbon monoxide, and discuss the oxygen budget on Titan. Using an evolution model, we determine the evolution history of three carbon monoxide isotopomers.

Chapter 2 Jupiter: Aerosol Chemistry in the Polar Atmosphere

2.1 Abstract

Aromatic compounds have been considered a likely candidate for enhanced aerosol formation in the polar region of Jupiter. We develop a new chemical model for aromatic compounds in the Jovian auroral thermosphere/ionosphere. The model is based on a previous model for hydrocarbon chemistry in the Jovian atmosphere and is constrained by observations from Voyager, Galileo and the Infrared Space Observatory. Precipitation of energetic electrons provides the major energy source for the production of benzene and other heavier aromatic hydrocarbons. The maximum mixing ratio of benzene in the polar model is 2×10^{-9}, a value that can be compared with the observed value of $2^{+2}_{-1} \times 10^{-9}$ in the north polar auroral region. Sufficient quantities of the higher ring species are produced so that their saturated vapor pressures are exceeded. Condensation of these molecules is expected to lead to aerosol formation.

The content of this chapter is based on a paper published in *The Astrophysical Journal*, **543**, L215–L217, 2000 May 10.

2.2 Introduction

The first ring compound benzene (c-C_6H_6, also known as A_1 in this chapter) was detected on Jupiter by the Voyager Infrared Interferometer Spectrometer (IRIS) experiment around 10μm (Kim et al., 1985). Recent observations by the Infrared Space Observatory (ISO) have also identified benzene on Jupiter (Encrenaz et al., 1997). In addition, the Galileo probe mass spectrometer has detected traces of benzene (Niemann et al., 1998). The formation of benzene on Jupiter has been attributed to

successive additive reactions involving C_2H_2 (Allen and Yung, 1985), but no detailed modeling has been reported. In particular, the energy source for the synthesis of ring compounds was not identified.

In this Chapter, we present preliminary results of a chemical model of benzene and polycyclic aromatic hydrocarbons (PAHs) in the Jovian auroral region. We shall argue that charged energetic particles in addition to the enhanced auroral temperature are responsible for the production of benzene and PAHs. Our model, incorporating the most important reaction pathways for synthesizing PAHs, is a combination of a photochemical model of hydrocarbons in the outer solar system and the H atom and ion chemistry of Perry et al. (1999). We computed the concentration of various aromatic molecules, compare our results with available observational data, and show that the condensation of heavy PAHs can account for the formation of aerosols in the polar region.

2.3 Photochemical Model

We base our model on the one-dimensional hydrocarbon photochemical model developed at Caltech/Jet Propulsion Laboratory (JPL) (Gladstone et al., 1996; Lee et al., 2000). To this most comprehensive and recently updated model, we make four major modifications:

1. Adding important reactions that produce PAHs;
2. Including reactions that are the result of precipitating electrons;
3. Using a temperature profile that is appropriate for the auroral region;
4. Taking into account the condensation of higher ring molecules.

We use the same eddy diffusion coefficient as that used in the low latitude model. The latitude of the polar model is 60°, where the solar radiation is only half of that in equatorial region.

2.3.1 Reactions of PAHs

We add 98 PAH-related reactions to the Caltech/JPL model for the Jovian atmosphere. The related reactions, along with kinetic rate constants, are summarized in Table 2.1. We adopt the nomenclature used by Wang and Frenklach (1994). For example, A_i is an aromatic molecule of i fused rings, A_i- its radical, and A_iC_2H with a hydrogen atom replaced by an ethynyl group. Our calculation includes aromatic molecules up to pyrene (A_4). The reaction scheme is adopted largely from laboratory and modeling studies in flame chemistry. In the absence of laboratory data for some reactions, we estimate their rate coefficients by analogy with known reactions. Rate coefficients for reactions R266, R276, R287 and R297 (the reaction numbers refer to Table 2.1) have been set at their maximum values near 750 K. We use the same photodissociation coefficients for all A_n, since the cross section data and product information for the $n > 1$ are unavailable.

Table 2.1. Partial list of reactions and rate coefficients in Jovian aerosol chemistry model.

No.	Reaction	Rate Coefficient	Ref.
R211	$C_4H_5 + C_2H_2 \rightarrow$ l-$C_6H_6 + H$	$9.63 \times 10^{-16}\, T^{1.02}\, e^{-5489/T}$	4
R235	$C_3H_3 + C_3H_3 \xrightarrow{M} A_1$	$k_\infty = 1.66 \times 10^{-13}$	4 [a]
R241	$C_4H_3 + C_2H_2 \rightarrow$ l-$C_6H_4 + H$	$6.14 \times 10^{-8}\, T^{-1.21}\, e^{-5589/T}$	4 [a]
R242	$C_4H_3 + C_2H_2 \xrightarrow{M}$ n-C_6H_5	$k_\infty = 7.08 \times 10^{-20}\, T^{1.97}\, e^{2820/T}$	1 [a]
R243	$C_4H_3 + C_2H_2 \xrightarrow{M} A_1$-	$k_\infty = 3.82 \times 10^{44}\, T^{-17.65}\, e^{-12287/T}$	6 [ab]
R245	$C_4H_5 + C_2H_2 \rightarrow A_1 + H$	$3.49 \times 10^{-9}\, T^{-1.07}\, e^{-2417/T}$	4
R246	$C_4H_5 + C_2H_2 \xrightarrow{M} C_6H_7$	$k_\infty = 1.83 \times 10^{-10}\, T^{-1.27}\, e^{-1460/T}$	5
		$k_0 = 1.24 \times 10^{-21}\, T^{-3.28}\, e^{-5136/T}$	5
R249	$C_5H_3 + {}^3CH_2 \rightarrow$ l-$C_6H_4 + H$	8.30×10^{-11}	5
R255	l-$C_6H_4 + H \xrightarrow{M}$ n-C_6H_5	$k_\infty = 5.48 \times 10^{20}\, T^{-10.04}\, e^{-9467/T}$	4 [ab]
R256	l-$C_6H_4 + H \xrightarrow{M} A_1$-	$k_\infty = 5.98 \times 10^{53}\, T^{-20.09}\, e^{-14150/T}$	4 [ab]
R258	n-$C_6H_5 + H \rightarrow$ l-$C_6H_4 + H_2$	2.49×10^{-11}	5
R259	n-$C_6H_5 + H \xrightarrow{M}$ l-C_6H_6	$k_\infty = 1.83 \times 10^{18}\, T^{-9.65}\, e^{-3525/T}$	5 [a]
R261	l-$C_6H_6 + H \rightarrow A_1 + H$	$1.44 \times 10^{-7}\, T^{-1.34}\, e^{-1762/T}$	4
R262	l-$C_6H_6 + H \xrightarrow{M}$ n-C_6H_7	$k_\infty = 2.49 \times 10^{-8}\, T^{-1.69}\, e^{-805.7/T}$	4
		$k_0 = 8.00 \times 10^{-31}\, T^{-0.52}\, e^{-503.6/T}$	4
R264	l-$C_6H_7 \xrightarrow{M} A_1 + H$	$1.39 \times 10^{-2}\, T^{-4.22}\, e^{-5690/T}$	4
R265	A_1- $+ H \xrightarrow{M} A_1$	$k_\infty = 1.66 \times 10^{-10}$	5
		$k_0 = 1.82 \times 10^{28}\, T^{-16.3}\, e^{-3526/T}$	5
R266	A_1- $+ C_2H_2 \xrightarrow{M}$ n-$A_1C_2H_2$	$k_\infty = 1.28 \times 10^{17}\, T^{-9.19}\, e^{-6748/T}$	4 [ab]
R267	A_1- $+ C_2H_2 \rightarrow A_1C_2H + H$	$1.25 \times 10^{3}\, T^{-3.96}\, e^{-8611/T}$	5 [b]
R270	$A_1 + H \rightarrow A_1$- $+ H_2$	$4.15 \times 10^{-10}\, e^{-8057/T}$	2
R273	$A_1C_2H + H \xrightarrow{M}$ n-$A_1C_2H_2$	$k_\infty = 1.66 \times 10^{30}\, T^{-12.76}\, e^{-8661/T}$	4 [ab]
R276	n-$A_1C_2H_2 + C_2H_2 \rightarrow A_2 + H$	$3.49 \times 10^{-9}\, T^{-1.07}\, e^{-2417/T}$	5 [b]
R277	n-$A_1C_2H_2 + H \rightarrow A_1C_2H + H_2$	2.49×10^{-11}	5

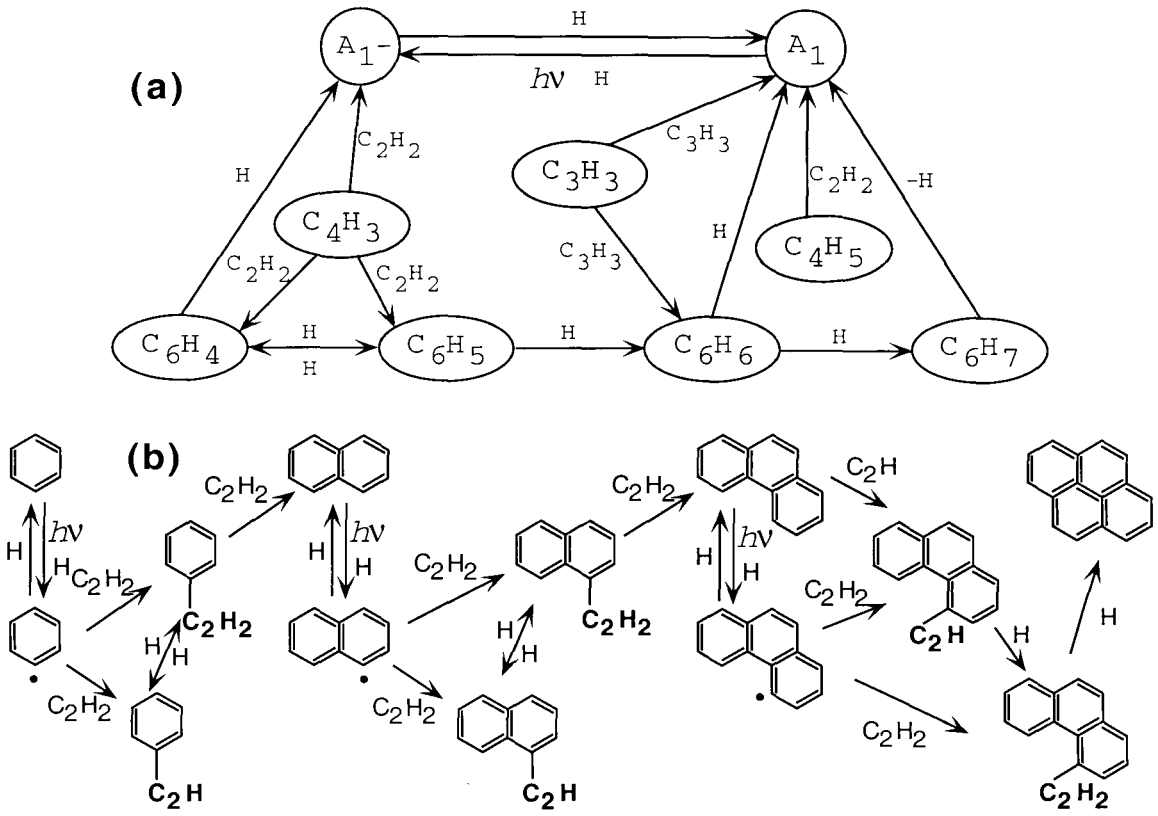

Figure 2.1 Major reaction pathways for *(a)* benzene (A_1) and *(b)* A_2, A_3, A_4 formation in the auroral atmosphere of Jupiter.

The major pathways for the formation of benzene and PAHs are shown in Figure 2.1. Benzene and phenyl (A_1-) are formed mainly through the reaction channels of R235, R243, R261 and R265. For higher ring compounds, H abstraction followed by C_2H_2 polymerization is the predominant reaction pathway.

2.3.2 Ion Chemistry

The primary driving force for aerosol chemistry in the auroral atmosphere of Jupiter is dissociative recombination of methane ions that are produced from interaction with high-energy particles. Previous studies have shown that the power of the aurorae is in the range 10^{13} – 10^{14} W and is greater than the EUV power from the sun (see, e.g., Atreya 1985, section 6.3). Perry et al. (1999) have carried out electron transport calculations for the effects of precipitating electrons with a range of energies from

Table 2.1—Continued

No.	Reaction	Rate Coefficient	Ref.
R285	$A_2\text{-}1 + H \xrightarrow{M} A_2$	$k_\infty = 1.66 \times 10^{-10}$	5
		$k_0 = 3.33 \times 10^{-12}$	5
R287	$A_2\text{-}1 + C_2H_2 \xrightarrow{M} A_2C_2H_2$	$k_\infty = 7.47 \times 10^{15}\, T^{-8.71}\, e^{-7201/T}$	4 [ab]
R288	$A_2\text{-}1 + C_2H_2 \rightarrow A_2C_2HA + H$	$2.32 \times 10^{-2}\, T^{-2.64}\, e^{-8762/T}$	4 [b]
R289	$A_2 + H \rightarrow A_2\text{-}1 + H_2$	$k_{289} = k_{270}$	
R293	$A_2C_2HA + H \xrightarrow{M} A_2C_2H_2$	$k_\infty = 3.15 \times 10^{26}\, T^{-11.63}\, e^{-8158/T}$	4 [ab]
R294	$A_2C_2H_2 + H \rightarrow A_2C_2HA + H_2$	2.49×10^{-11}	5
R297	$A_2C_2H_2 + C_2H_2 \rightarrow A_3 + H$	$k_{297} = k_{276}$	
R303	$A_3\text{-}4 + H \xrightarrow{M} A_3$	$k_\infty = 1.66 \times 10^{-10}$	5
		$k_0 = 2.21 \times 10^{-14}$	5
R304	$A_3 + C_2H \rightarrow A_3C_2H + H$	8.30×10^{-11}	5
R305	$A_3\text{-}4 + C_2H_2 \xrightarrow{M} A_3C_2H_2$	$k_\infty = 1.11 \times 10^{22}\, T^{-10.55}\, e^{-10675/T}$	5 [ab]
R306	$A_3\text{-}4 + C_2H_2 \rightarrow A_3C_2H + H$	$1.33 \times 10^{-6}\, T^{-1.21}\, e^{-11380/T}$	4 [b]
R308	$A_3C_2H + H \xrightarrow{M} A_3C_2H_2$	$k_\infty = 8.63 \times 10^{23}\, T^{-11.05}\, e^{-7402/T}$	4 [ab]
R310	$A_3C_2H_2 \xrightarrow{M} A_4 + H$	$1.12 \times 10^{25}\, T^{-11.86}\, e^{-14150/T}$	4 [b]
R312	$A_4\text{-} + H \xrightarrow{M} A_4$	$k_\infty = 1.66 \times 10^{-10}$	5 [a]
R313	$A_4\text{-} + C_2H_2 \rightarrow$ products	3.00×10^{-14}	7
R315	$H_3^+ + e \rightarrow H_2 + H$	$2.88 \times 10^{-8}\, (300/T)^{0.65}$	3
R316	$H_3^+ + e \rightarrow H + H + H$	$8.63 \times 10^{-8}\, (300/T)^{0.65}$	3
R317	$CH_5^+ + e \rightarrow {}^3CH_2 + H_2 + H$	$5.3 \times 10^{-7}\, (300/T)^{0.52}$	3
R318	$CH_5^+ + e \rightarrow CH_3 + H + H$	$1.9 \times 10^{-8}\, (300/T)^{0.52}$	3
R319	$CH_5^+ + e \rightarrow CH_3 + H_2$	$1.7 \times 10^{-8}\, (300/T)^{0.52}$	3
R320	$CH_5^+ + e \rightarrow CH_4 + H$	$9.0 \times 10^{-9}\, (300/T)^{0.52}$	3
R321	$CH_5^+ + e \rightarrow CH + H_2 + H_2$	$9.5 \times 10^{-9}\, (300/T)^{0.52}$	3

Note. — The complete set includes all the relevant reactions considered by Gladstone et al. 1996, updated by Lee et al. 2000 and some other PAH reactions studied in this work. Units for two-body and three-body rate coefficients are $cm^3\ s^{-1}$ and $cm^6\ s^{-1}$, respectively. k_0 and k_∞ refer to the low and high pressure limits of the rate coefficients.

[a] $k_0 = 10^{-27}$, estimated

[b] Set at maximum value near 750 K

References. — (1) Colket (1986); (2) Keifer et al. (1985); (3) Perry et al. (1999); (4) Wang and Frenklach (1994); (5) Wang and Frenklach (1997); (6) Westmoreland (1989); (7) Estimated.

20 to 100 keV and have presented dissociation and ionization rates of various ionic species. In our study, we adopt their calculated reaction rates (model B) for seven reactions involving the dissociative recombination reactions of H_3^+ and CH_5^+, obtained from their Figure 4 (see reactions R315–321 in Table 2.1) [1]. The total input energy is about 11 erg cm^{-2} s^{-1}. The destruction rate of methane by precipitating electrons is about 25 times higher than that by photolysis at 60°.

2.3.3 Temperature Profile

Although there is no direct measurement of the temperature profile, the temperature in the auroral region is known to be much higher than that in nonauroral regions because of the heat deposition from precipitating particles. We use a temperature profile deduced by Trafton et al. (1994), which is consistent with observed rotational temperatures of H_2 (Clarke et al., 1994; Liu and Dalgarno, 1996; Kim et al., 1997). To reconcile the higher observed thermospheric temperature with the low temperature computed in the model of Perry et al. (1999), we suggest that the former is a sporadic phenomenon, whereas the model calculation is for the time-averaged atmosphere. Since the synthesis of PAHs occurs primarily during the transient high temperature phase, the higher temperature profile should be more appropriate.

2.3.4 Condensation

Ring compounds A_1 through A_4 are condensed when their vapor pressures are exceeded. We define the loss rate of a condensing species A by a procedure described in Summers and Strobel (1989) as

$$k = \begin{cases} \dfrac{[A] - [A_s]}{[A]\,\tau}, & \text{if } [A] \geq [A_s]; \\ 0, & \text{otherwise.} \end{cases}$$

where $[A]$ is concentration in unit of molecules per cm^3, $[A_s]$ is the concentration corresponding to local saturation of the molecule, and τ is an assumed time constant

[1] This adopted ionization rates are revised in our new model in Chapter 3. See Section 3.4.3

for the condensation process. In the equation, $[A_s]$ is given by $[A_s] = n\,P_V/P$ where P_V is the local vapor pressure, P is the pressure, and n is the number density. The condensation time constant is set to be 10^6 s. The vapor pressures are taken from Yaws (1994).

2.4 Results and Discussion

The results of the model calculations are shown in Figure 2.2. Figure 2.2a presents the mixing ratios for CH_4, C_2H_6, C_2H_4 and C_2H_2. The polar model demonstrates one order of magnitude greater C_2 hydrocarbon concentration than the solar-driven model at lower latitudes (Lee et al., 2000). This is due, as discussed earlier, to the greater rate of CH_4 dissociation. Figure 2.2b shows that the maximum mixing ratio of benzene is 2×10^{-9}. This result is in fairly good agreement with the Voyager observation of $2^{+2}_{-1} \times 10^{-9}$ in the north polar auroral region (Kim et al., 1985). Above 1 mb, the column density is 9.3×10^{13} cm^{-2}, which can be compared with the preliminary result of stratospheric mid-latitude (not the auroral region) benzene column density at 2×10^{14} cm^{-2} from the ISO observation (B. Bézard 1999, private communication).

We study the response of the model to various effects including temperature, precipitating electrons, and condensation. Using a much lower temperature profile from Voyager measurements, we find that the total benzene concentration does not vary much, although the production and destruction rates are both decreased by a factor of 10. The concentration of higher ring compounds A_2, A_3 and A_4 are decreased by factors of 2, 100 and 20000 times, respectively. Without the ion-related reactions, benzene concentration is reduced by a factor of 550. This confirms that the energetic particles are essential to benzene formation. Test runs show that 62% of the higher ring molecules are condensed. The sensitivity of the benzene mixing ratio to the eddy diffusion coefficient will be tested in future works.

The total dissociation rate of CH_4 in the model is 6.7×10^{10} molecules cm^{-2} s^{-1}. About 1% of this leads to the production of A_n species, resulting in a mass flux of about 10^{-14} g cm^{-2} s^{-1}. Polar haze particles occupy the region $\sim$0.3 mb – 50 mb

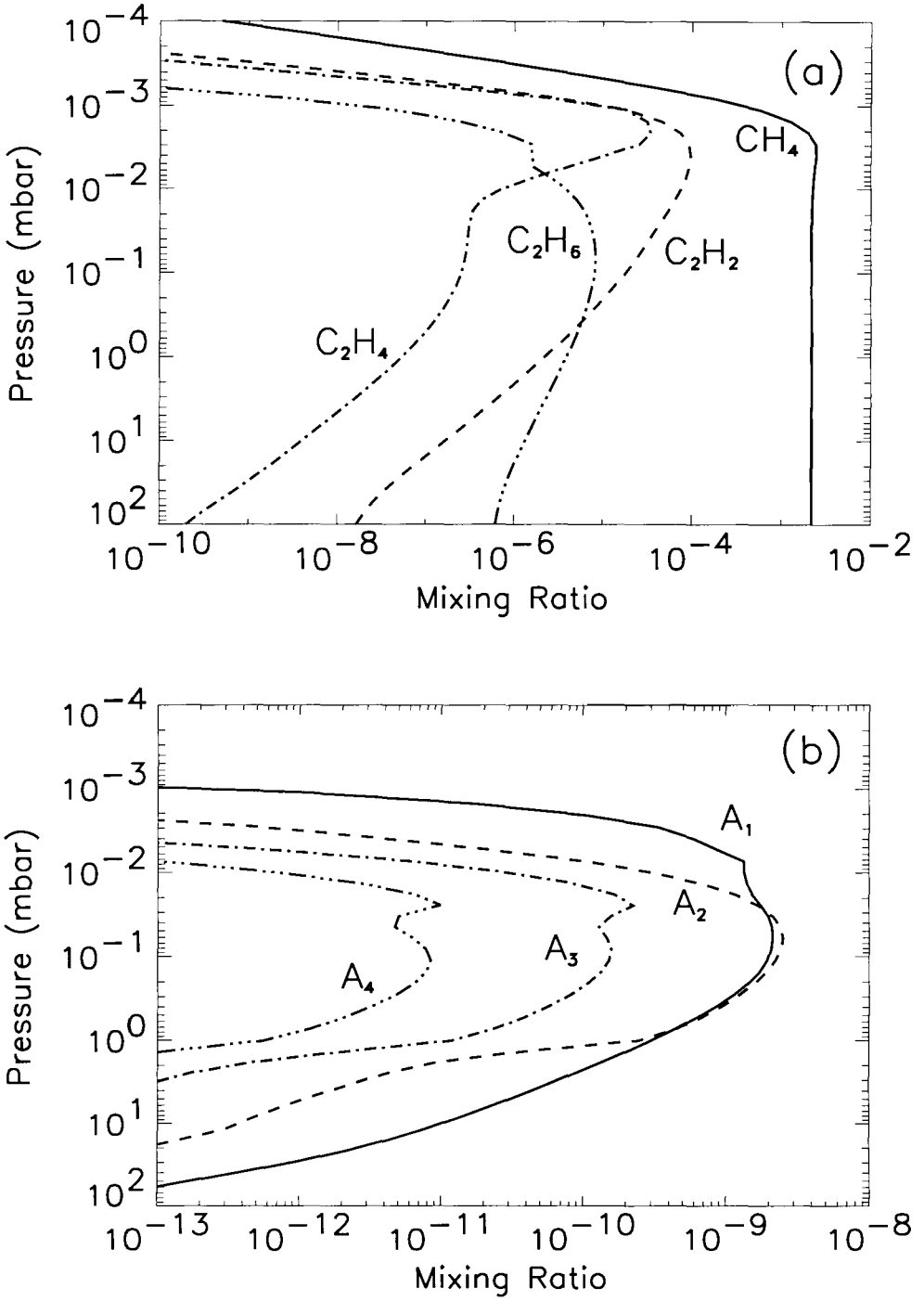

Figure 2.2 Computed hydrocarbon mixing ratio profiles as a function of pressure in the polar model for *(a)* CH_4, C_2H_2, C_2H_4 and C_2H_6; *(b)* A_1, A_2, A_3 and A_4.

(West, 1988; Pryor et al., 1991), probably concentrated near 10 mb (R. A. West 1999, private communication). Assuming the particles have a mean radius of 0.1 μm, we estimate that a haze layer with optical depth of 0.1 in the near UV could be generated by the mass flux computed in our model. Our model yields for PAHs are considerably larger than what was generated in a laboratory study for Titan's atmosphere (Sagan et al., 1993).

2.5 Conclusion

Benzene was discovered on Jupiter over a decade ago, and the origin of polar aerosols on Jupiter has remained a puzzle for a long time. This is the first quantitative chemical model that attempts to simulate the production of aromatic compounds. Our simple model can account for most of the relevent observations, and suggests that the condensation of heavy aromatic molecules is a source for the aerosols. Our model can be tested by new observations. PAH concentrations should vary as the auroral temperature changes. The difference in benzene concentrations should be observable at different latitudes, as the IRIS observations (Kim et al., 1985) suggested. More extensive observations of benzene and PAHs are needed to test our theory.

Chapter 3 Benzene on Jupiter

3.1 Abstract

Benzene was first detected on Jupiter by the Voyager Infrared Interferometer Spectrometer (IRIS) in the northern auroral region in 1985. Recently, the Short-Wavelength Spectrometer (SWS) on the Infrared Space Observatory (ISO) has made extensive observations of benzene on Jupiter. The results show enhancement of benzene abundance in the auroral regions over the Jupiter disk. To study the details of benzene chemistry on Jupiter, we have developed a one-dimensional photochemical model that couples updated neutral and ion chemistry. We discuss six neutral and six ion chemical schemes for benzene formation in auroral and non-auroral regions, identifying major uncertainties in the chemical kinetics. The benzene abundance at low latitude is computed to be 1.0×10^{15} molecules cm^{-2} above 50-mbar pressure level, which is consistent with the ISO observation. The model shows that in auroral regions, ion chemistry alters neutral chemistry and enhances the production of benzene and other heavy hydrocarbons.

3.2 Introduction

Benzene was first detected on Jupiter by the Voyager Infrared Interferometer Spectrometer (IRIS) experiment from emission from the ν_4 rovibrational band in the northern auroral region near 60° N and 180° W (Kim et al., 1985). The mixing ratio of benzene is determined to be $2^{+2}_{-1} \times 10^{-9}$. Recently, observation with the Short-Wavelength Spectrometer (SWS) of the Infrared Space Observatory (ISO) has detected benzene in all regions (Bézard et al., 2001), with some enhancement in the auroral regions over the Jupiter disk. The inferred abundance is $9^{+4.5}_{-7.5} \times 10^{14}$ molecules cm^{-2} above the 50-mbar level in mid-latitude non-auroral regions. The benzene observations are summarized in Table 3.1.

The first attempt to model the benzene on Jupiter is reported in Chapter 2 (Wong et al., 2000). In that Chapter, we present a preliminary result of a photochemical model for benzene and polycyclic aromatic hydrocarbons (PAHs) that lead to aerosol formation in the Jovian auroral region. Our model shows that charged energetic particles in combination with the enhanced auroral temperature are responsible for the production of benzene and PAHs in polar regions. The aerosol model, incorporating several important reaction pathways for synthesizing PAHs, is based on the Caltech/JPL photochemical model of hydrocarbons in the outer solar system (Gladstone et al., 1996; Moses et al., 2000a; Lee et al., 2000), with estimated temperature profile, selected ion chemistry from Perry et al. (1999), and mechanism of condensation for PAHs. The mixing ratio of benzene calculated in the model is 2×10^{-9} at altitude 60°. Above the 50-mbar level, the integrated abundance is 1.9×10^{14} molecules cm^{-2}, which is much smaller than the ISO observation. Without the ion-related reactions, in non-auroral regions at the same latitude, benzene concentration is reduced further by a factor of 550. The aerosol model does not predict the observed abundance of benzene due to several possible reasons:

1. The kinetics of some key reactions is subject to great uncertainties due to lack of available or consistent experimental data.

2. The ion chemistry in auroral regions is incomplete.

Table 3.1. Summary of benzene observation on Jupiter.

Technique	Region	Benzene Observation	Ref.
IUE[a]	mid-latitudes	mixing ratio $< 1 \times 10^{-10}$	1
IRIS[b]	60° N, 180° W auroral	mixing ratio $2^{+2}_{-1} \times 10^{-9}$	2
GPMS[c]	0.51–21.1 bars	traces level	3
ISO-SWS[d]	mid-latitudes non-auroral	$9^{+4.5}_{-7.5} \times 10^{14}$ cm^{-2} above 50 mbar	4
ISO-SWS	auroral	enhancement over the disk region	4

[a]International Ultraviolet Explorer

[b]Voyager Infrared Interferometer Spectrometer

[c]Galileo Probe Mass Spectrometer

[d]Infrared Space Observatory, Short-Wavelength Spectrometer

References. — (1) Waganer et al. (1985); (2) Kim et al. (1985); (3) Niemann et al. (1998); (4) Bézard et al. (2001)

3. The accuracy of the energy source used in the model that drives the ion chemistry in the auroral regions is questionable.

The goal of this work is to investigate the possibility of improving the model using available experimental and observational data. We update neutral reaction kinetics for benzene formation, and develop two models. Using the non-auroral model, we evaluate the complete neutral reaction scheme for benzene chemistry and compare the result with observation. For the non-auroral regions, we establish an extensive ion reaction scheme from available ion chemistry data, and investigate the effects of ion chemistry on neutral chemistry. We then propose necessary future experimental and modeling work.

3.3 Non-Auroral Model

3.3.1 The Model

Both auroral and non-auroral models are based on the Caltech/JPL photochemical model of hydrocarbons in the outer solar system (Gladstone et al., 1996; Moses et al., 2000a; Lee et al., 2000; Wong et al., 2000). We include only the neutral reactions in the non-auroral model, because at low latitudes, solar energy is the major energy input that drives the atmospheric chemistry, and ion chemistry is relatively unimportant. We use a fixed H_2 density profile, and compute the density profiles of all other hydrocarbon neutral species studied in Chapter 2 (Wong et al., 2000). The temperature profile for the non-auroral model is taken from Voyager (Gladstone et al., 1996), shown in Figure 3.1.

3.3.2 Neutral Chemistry

Agreement has not yet been reached concerning the dominant reactions responsible for the first aromatic ring formation. Lindstedt (1998) summarizes the current knowledge of the ring formation processes. The two most important pathways proposed and evaluated are (1) the C_2H_2 addition to the n-C_4H_3 (HCCCHCH) or n-C_4H_5 ($CH_2CHCHCH$), and (2) the combination of propargyl radicals C_3H_3. Each of the two processes has been the subject of debate. For the purpose of consistency, we adopt the values for the rate coefficients for these reactions from the assessment of D'Anna et al. (2001), the most recent published work on the subject. The related rate coefficients are listed in Table 3.2, along with the values used in our previous model (Wong et al., 2000). The nomenclature used here is the same as in Chapter 2 (see Section 2.3.1). Note that for the C_3H_3 reactions, we replace the single-step reaction R230 with two reactions R231 and R232 which form phenyl (A_1-).

The primary emphasis of this study is benzene chemistry, and as such we will not re-evaluate other PAHs chemistry reported in the previous work.

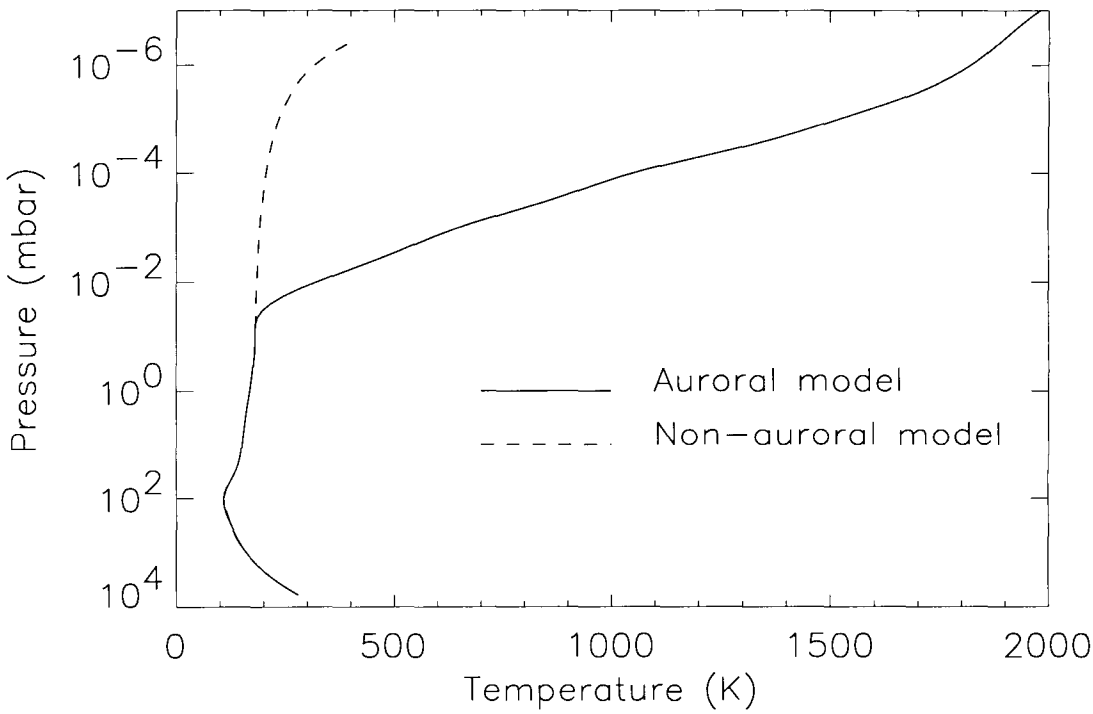

Figure 3.1 Temperature profiles adopted for non-auroral and auroral models. For non-auroral model, the temperature profile is taken from Voyager observation (Gladstone et al., 1996); for auroral model, the temperature profile is deduced from the spectroscopic observation of Hubble Space Telescope Trafton et al. (1994).

Table 3.2. Updated neutral reactions in auroral model.

Number	Reaction	Rate Coefficient	
		Wong et al. (2000)	D'Anna et al. (2001)
R230	$2C_3H_3 \xrightarrow{M} A_1$	1.66×10^{-13}	...
R231	$2C_3H_3 \rightarrow A_1\text{-} + H$	...	4.98×10^{-12}
R232	$C_3H_3 + C_3H_2 \xrightarrow{M} A_1\text{-}$	...	4.98×10^{-12}
R240	$C_4H_3 + C_2H_2 \xrightarrow{M} A_1\text{-}$	$3.82 \times 10^{44}\, T^{-17.65} \exp(-12287/T)$	$4.65 \times 10^{-21}\, T^{-2.9} \exp(-703.59/T)$
R242	$C_4H_5 + C_2H_2 \rightarrow A_1 + H$ $1.66 \times 10^{-8}\, T^{-1.33} \exp(-2714.54/T)$	$3.49 \times 10^{-9}\, T^{-1.07} \exp(-2417/T)$	

Note. — Two-body rate coefficients and high-pressure limiting rate coefficients for three-body reactions (k_∞) are in units of $cm^3\ s^{-1}$. Low-pressure limiting rate coefficients for three-body reactions (k_0) are in units of $cm^6\ s^{-1}$, and are estimated to be 10^{-27}. M represents any third body such as H_2. The reaction numbers refer to the complete list of reactions in the auroral model. Our model adopts the values of D'Anna et al. (2001).

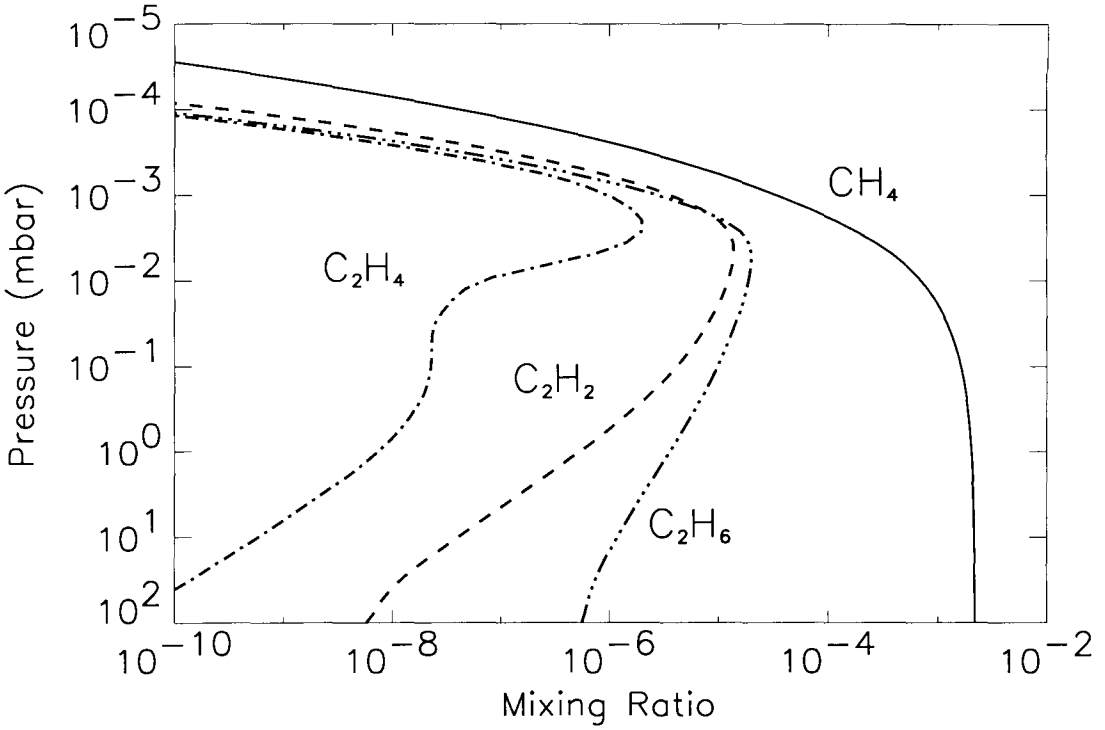

Figure 3.2 Computed mixing ratios for CH_4, C_2H_6, C_2H_4, and C_2H_2 for non-auroral model.

3.3.3 Results for Non-Auroral Model

In this section we discuss the result of Jovian photochemical model in non-auroral regions with our updated reaction scheme.

The mixing ratios for CH_4, C_2H_6, C_2H_4, and C_2H_2 are shown in Figure 3.2. It is consistent with the result from Gladstone et al. (1996) and Lee et al. (2000). The mixing ratios for benzene (A_1), naphthalene (A_2), and phenanthrene (A_3) are shown in Figure 3.3. The maximum mixing ratio for pryrene (A_4) is smaller than 10^{-13} and beyond the range of the plot. In this model, we do not consider the condensation of aromatic molecules therefore, at lower altitudes the concentrations of these molecules do not decrease as shown in Figure 2.2 of the aerosol model in Chapter 2 (Wong et al., 2000).

We calculated the benzene production at two difference latitutes (model A and

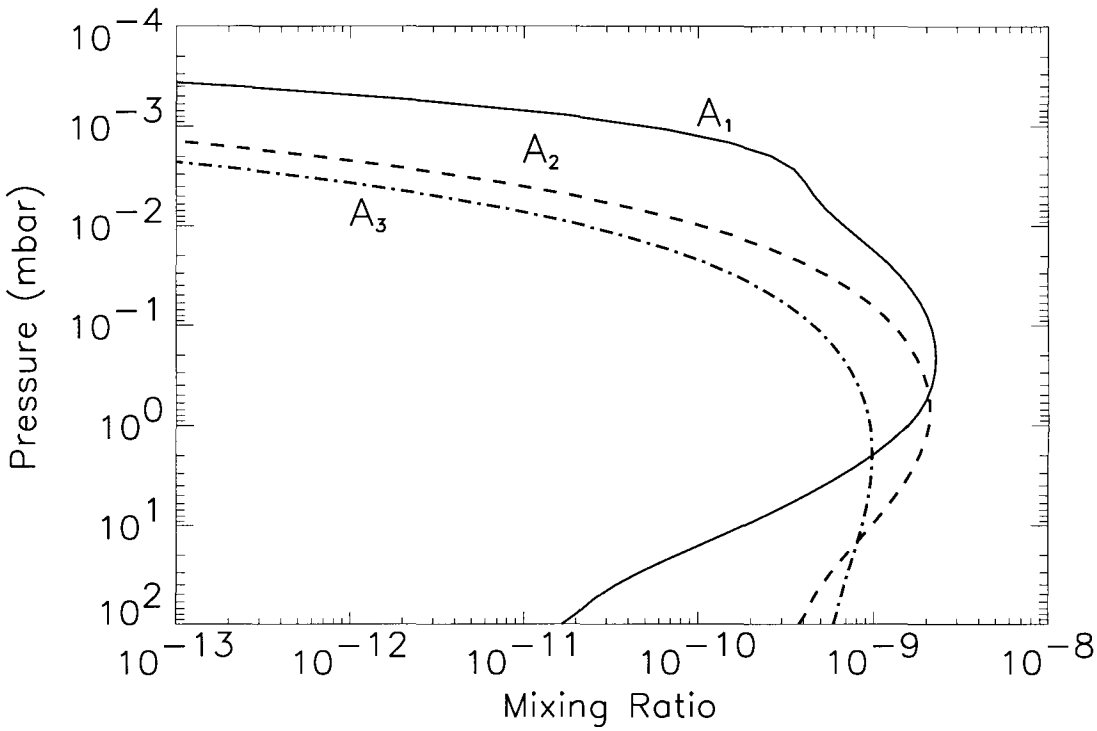

Figure 3.3 Computed mixing ratios for benzene (A_1), naphthalene (A_2), and phenanthrene (A_3) for non-auroral model at 0° latitute.

B). The abundance of benzene (A_1) above 50 mbar pressure level at 0° latitude is calculated to be 1.02×10^{15} molecules cm^{-2}, which is comparable to the ISO observation of $9^{+4.5}_{-7.5} \times 10^{14}$ molecules cm^{-2} (Bézard et al., 2001). At 60° latitude, the same reaction scheme yields a benzene abundance of 4.63×10^{14} molecules cm^{-2} above 50 mbar, or a mixing ratio of 6×10^{-10}, which is significantly lower than the IRIS observed value of $2^{+2}_{-1} \times 10^{-9}$ in that region (Kim et al., 1985). The results of these two cases (A and B) are summarized in Table 3.3.

3.3.4 Neutral Reaction Schemes for Benzene Production

Six major pathways leading to the first ring formation are discussed in this section. Related reactions are listed in Table 3.4. Schematic diagram illustrating the reaction pathways is shown in Figure 3.4. In the discussion of reaction schemes, the limiting steps are marked with a '†', and the ring closing steps are marked with a '$*$'. The altitude profiles of the reaction rates for the limiting steps of each of the six most important reaction pathways involving production and loss of benzene in our non-auroral model are shown in Figure 3.5.

Table 3.3. Summary and comparison of model results.

Case	Model Chemistry	Region	Energy Flux (ergs cm^{-2} s^{-1})	Mixing Ratio Benzene	Column Abundance (cm^{-2}) Benzene	PAHs
A	neutral	0°	···	2.3×10^{-9}	1.0×10^{15}	9.8×10^{15}
B	neutral	60°	···	6.3×10^{-10}	4.6×10^{14}	2.5×10^{15}
C	neutral + ion	60°	11.2	3.2×10^{-8}	2.4×10^{14}	4.8×10^{15}
D	neutral + ion	60°	15.7	2.6×10^{-8}	2.6×10^{14}	5.1×10^{15}

Table 3.4. Partial list of neutral reactions and rate coefficients in benzene model.

No.	Reaction			Rate Coefficient	Ref.
R8	CH_4	$\xrightarrow{h\nu}$	$^3CH_2 + 2H$	5.158×10^{-8} [a]	(1)
R10	C_2H_2	$\xrightarrow{h\nu}$	$C_2H + H$	5.773×10^{-8} [a]	(1)
R90	$H + {}^3CH_2$	$\rightarrow$	$CH + H_2$	2.66×10^{-10}	(1)
R96	$H + C_2H_2$	$\xrightarrow{M}$	C_2H_3	$k_0 = 8.20 \times 10^{-31} \exp(-352/T)$	(1)
				$k_\infty = 1.40 \times 10^{-11} \exp(-1300/T)$	(1)
R104	$H + C_3H_2$	$\xrightarrow{M}$	C_3H_3	$k_0 = 2.52 \times 10^{-28}$	(1)
				$k_\infty = 5.00 \times 10^{-11}$	(1)
R123	$H + C_4H_2$	$\xrightarrow{M}$	C_4H_3	$k_0 = 1.00 \times 10^{-28}$	(1)
				$k_\infty = 1.39 \times 10^{-10} \exp(-1184/T)$	(1)
R125	$H + C_4H_3$	$\xrightarrow{M}$	C_4H_4	$k_0 = 6.00 \times 10^{-30} \exp(1680/T)$	(1)
				$k_\infty = 8.56 \times 10^{-10} \exp(-405/T)$	(1)
R126	$H + C_4H_4$	$\xrightarrow{M}$	C_4H_5	$k_0 = 6.00 \times 10^{-31} \exp(1680/T)$	(1)
				$k_\infty = 3.30 \times 10^{-12}$	(1)
R138	$CH + C_2H_2$	$\rightarrow$	$C_3H_2 + H$	$3.49 \times 10^{-10} \exp(61/T)$	(1)
R175	$C_2H + C_2H_2$	$\rightarrow$	$C_4H_2 + H$	$1.10 \times 10^{-10} \exp(28/T)$	(1)
R184	$C_2H_3 + C_2H_2$	$\xrightarrow{M}$	C_4H_5	$k_0 = 8.20 \times 10^{-30} \exp(-352/T)$	(1)
				$k_\infty = 4.17 \times 10^{-19} \exp(-1058/T)$	(1)
R229	A_1	$\xrightarrow{h\nu}$	$A_1\text{-} + H$	2.999×10^{-7} [a]	(1)
R230	$2C_3H_3$	$\xrightarrow{M}$	A_1	$k_0 = 0$	(2)
				$k_\infty = 0$	(2)
R231		$\rightarrow$	$A_1\text{-} + H$	4.98×10^{-12}	(3)
R232	$C_3H_3 + C_3H_2$	$\xrightarrow{M}$	$A_1\text{-}$	$k_0 = 1.00 \times 10^{-27}$	(4)
				$k_\infty = 4.98 \times 10^{-12}$	(3)
R233	$C_4H_2 + CH$	$\rightarrow$	$C_5H_2 + H$	8.30×10^{-11}	(5)
R234	$C_4H_2 + {}^3CH_2$	$\rightarrow$	$C_5H_3 + H$	$2.16 \times 10^{-11} \exp(-3334/T)$	(5)
R235	$C_4H_2 + {}^1CH_2$	$\rightarrow$	$C_5H_3 + H$	3.32×10^{-11}	(5)
R236	$C_4H_2 + C_2H$	$\rightarrow$	$C_6H_2 + H$	1.59×10^{-10}	(5)
R237		$\xrightarrow{M}$	C_6H_3	$k_0 = 1.00 \times 10^{-27}$	(5)
				$k_\infty = 1.83 \times 10^{6} \exp(-1405/T)$	(5)

Table 3.4—Continued

No.	Reaction			Rate Coefficient	Ref.
R238	$C_4H_3 + C_2H_2$	$\rightarrow$	$C_6H_4 + H$	$6.14 \times 10^{-08}\, T^{-1.2} \exp(-5589/T)$	(5)
R239		$\xrightarrow{M}$	n-C_6H_5	$k_0 = 1.00 \times 10^{-27}$	(5)
				$k_\infty = 7.08 \times 10^{-20}$	(5)
R240	$C_4H_3 + C_2H_2$	$\xrightarrow{M}$	A_1-	$k_0 = 1.00 \times 10^{-27}$	(4)
				$k_\infty = 4.65 \times 10^{-21} \exp(-704/T)$	(3)
R241	$C_4H_4 + C_2H_3$	$\rightarrow$	$C_6H_6 + H$	$1.23 \times 10^{-09}\, T^{-0.7} \exp(-4240/T)$	(5)
R242	$C_4H_5 + C_2H_2$	$\rightarrow$	$A_1 + H$	$1.66 \times 10^{-08}\, T^{-1.3} \exp(-2715/T)$	(3)
R243		$\xrightarrow{M}$	C_6H_7	$k_0 = 1.24 \times 10^{-21}\, T^{-3.3} \exp(-5136/T)$	(5)
				$k_\infty = 1.83 \times 10^{-10}\, T^{-1.3} \exp(-1460/T)$	(5)
R244	$C_5H_2 + CH$	$\rightarrow$	$C_6H_2 + H$	8.30×10^{-11}	(5)
R245	$C_5H_3 + CH$	$\rightarrow$	$C_6H_2 + 2H$	8.30×10^{-11}	(5)
R246	$C_5H_3 + {}^3CH_2$	$\rightarrow$	$C_6H_4 + H$	8.30×10^{-11}	(5)
R247	$C_6H + H$	$\xrightarrow{M}$	C_6H_2	$k_0 = 1.03 \times 10^{-14}\, T^{-4.8} \exp(-957/T)$	(5)
				$k_\infty = 1.66 \times 10^{-07}\, T^{-1.0}$	(5)
R248	$C_6H_2 + H$	$\xrightarrow{M}$	C_6H_3	$k_0 = 1.00 \times 10^{-27}$	(5)
				$k_\infty = 6.43 \times 10^{-12}$	(5)
R249	$C_6H_3 + H$	$\rightarrow$	$C_4H_2 + C_2H_2$	$3.99 \times 10^{-05}\, T^{-1.6} \exp(-1410/T)$	(5)
R250		$\xrightarrow{M}$	C_6H_4	$k_0 = 1.00 \times 10^{-27}$	(5)
				$k_\infty = 6.97 \times 10^{20} \exp(-3973/T)$	(5)
R251	$C_6H_4 + H$	$\rightarrow$	$C_6H_3 + H_2$	$1.10 \times 10^{-17}\, T^{2.5} \exp(-4653/T)$	(5)
R252		$\xrightarrow{M}$	n-C_6H_5	$k_0 = 1.00 \times 10^{-27}$	(5)
				$k_\infty = 2.46 \times 10^{-14}$	(5)
R253		$\xrightarrow{M}$	A_1-	$k_0 = 1.00 \times 10^{-27}$	(5)
				$k_\infty = 6.65 \times 10^{-13}$	(5)
R254	n-$C_6H_5 + H$	$\rightarrow$	$C_4H_4 + C_2H_2$	$2.66 \times 10^{-05}\, T^{-1.6} \exp(-1118/T)$	(5)
R255		$\rightarrow$	$C_6H_4 + H_2$	2.49×10^{-11}	(5)
R256		$\xrightarrow{M}$	C_6H_6	$k_0 = 1.00 \times 10^{-27}$	(5)
				$k_\infty = 1.83 \times 10^{18} \exp(-3525/T)$	(5)
R257	$C_6H_6 + H$	$\rightarrow$	n-$C_6H_5 + H_2$	$1.10 \times 10^{-18}\, T^{2.5} \exp(-6163/T)$	(5)

Table 3.4—Continued

No.	Reaction			Rate Coefficient	Ref.
R258		$\rightarrow$	$A_1 + H$	$1.44 \times 10^{-07} T^{-1.3} \exp(-1762/T)$	(5)
R259		$\xrightarrow{M}$	C_6H_7	$k_0 = 8.00 \times 10^{-31} T^{-0.5} \exp(-504/T)$	(5)
				$k_\infty = 2.49 \times 10^{-08} T^{-1.7} \exp(-806/T)$	(5)
R260	$C_6H_7 + H$	$\rightarrow$	$C_6H_6 + H_2$	2.49×10^{-11}	(5)
R261	C_6H_7	$\xrightarrow{M}$	$A_1 + H$	$1.39 \times 10^{-02} T^{-4.2} \exp(-5690/T)$	(5)
R262	$A_1\text{-} + H$	$\xrightarrow{M}$	A_1	$k_0 = 1.82 \times 10^{28} T^{-16.3} \exp(-3526/T)$	(5)
				$k_\infty = 1.66 \times 10^{-10}$	(5)
R263	$A_1\text{-} + C_2H_2$	$\rightarrow$	PAHs	1.60×10^{-13}	(6)
R264	$A_1 + H$	$\rightarrow$	$A_1\text{-} + H_2$	$5.00 \times 10^{-12} \exp(-4076/T)$	(5)
R265	$A_1 + C_2H$	$\rightarrow$	PAHs	8.30×10^{-11}	(6)

Note. — The complete set includes all the relevant reactions considered by Gladstone et al. (1996), updated by Moses et al. (2000a), Lee et al. (2000), and Wong et al. (2000). Units for two-body and three-body rate coefficients are cm^3s^{-1} and cm^6s^{-1}, respectively. k_0 and k_∞ refer to the low and high pressure limits of the rate coefficients.

[a]photolysis rate J (s^{-1}) at the top of the atmosphere

References. — (1) Moses et al. (2000a); (2) this work; (3) D'Anna et al. (2001) (4) three-body rate estimated to be 10^{-27}; (5) Wong et al. (2000); (6) rate estimated using the result from Wong et al. (2000)

3.3.4.1 Combination of propargyl radicals C_3H_3

Scheme N1:

$$CH_4 + h\nu \rightarrow {}^3CH_2 + 2H \qquad \text{(R8)}$$

$$^3CH_2 + H \rightarrow CH + H_2 \qquad \text{(R90)}$$

$$CH + C_2H_2 \rightarrow C_3H_2 + H \qquad \text{(R138)}$$

$$C_3H_2 + H \xrightarrow{M} C_3H_3 \qquad \text{(R104)}$$

$$C_3H_3 + C_3H_3 \rightarrow A_1\text{-} + H \qquad \text{(R325)} * \dagger$$

$$\text{Net:} \quad 2CH_4 + 2C_2H_2 \rightarrow A_1\text{-} + 3H + 2H_2 \qquad \text{(Scheme N1)}$$

An alternative pathway to form phenyl (A_1-) from C_3H_3 is

$$C_3H_3 + C_3H_2 \xrightarrow{M} A_1\text{-} \qquad \text{(R326)} * \dagger$$

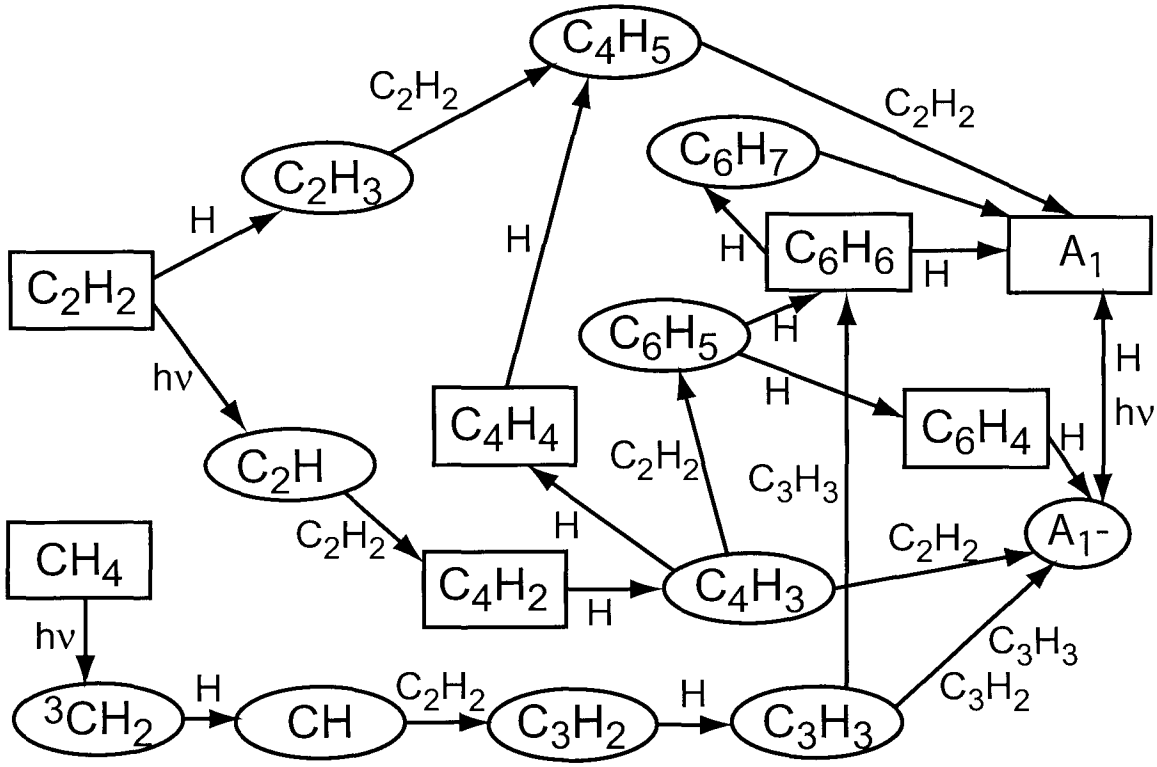

Figure 3.4 Major reaction pathways for benzene production in non-auroral model. The symbol hν corresponds to a solar ultraviolet photon. Radical species are outlined as ovals and stable molecules as rectangles.

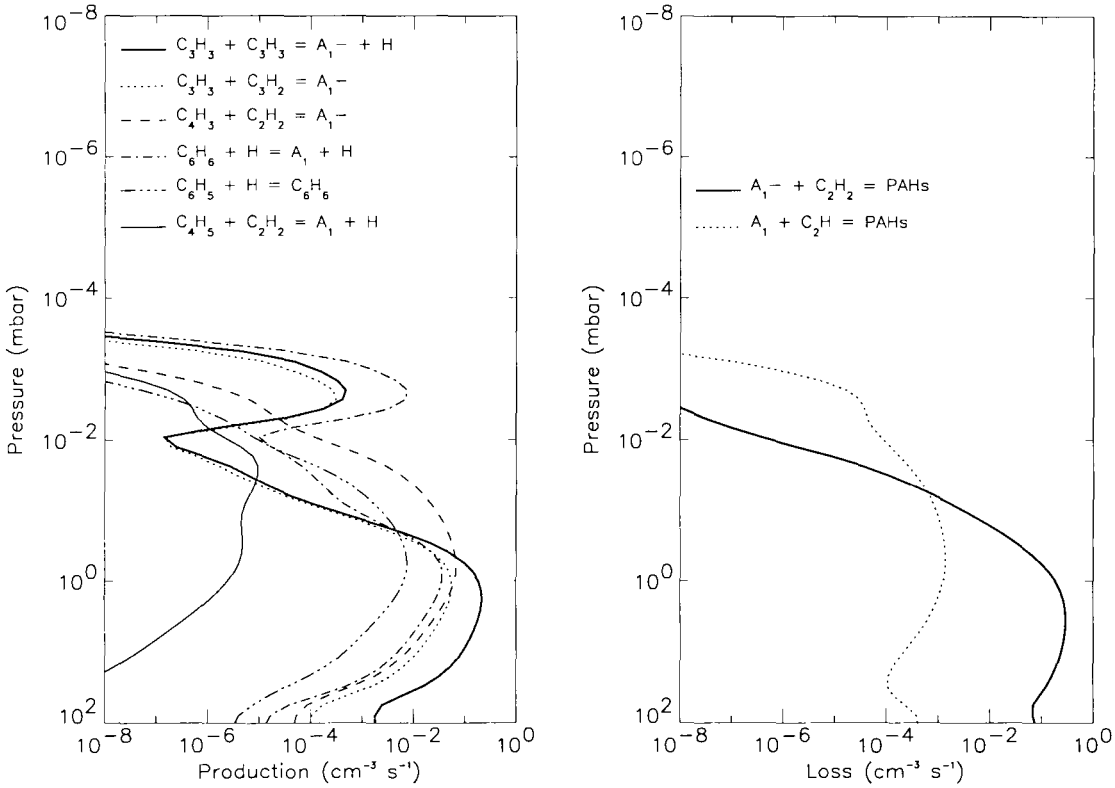

Figure 3.5 Computed altitude profiles of the reaction rates for the limiting steps of each of the six most important reaction pathways involving production (left panel) and loss (right panel) of benzene for non-auroral model. The reactions are listed in order of decreasing column reaction rate.

Scheme N2:

	$CH_4 + h\nu \rightarrow {}^3CH_2 + 2H$	(R8)
	${}^3CH_2 + H \rightarrow CH + H_2$	(R90)
	$CH + C_2H_2 \rightarrow C_3H_2 + H$	(R138)
	$C_3H_2 + H \xrightarrow{M} C_3H_3$	(R104)
	$C_3H_3 + C_3H_3 \xrightarrow{M} C_6H_6$	(R200)
	$C_6H_6 + H \rightarrow A_1 + H$	(R261) $*$ †
Net:	$2CH_4 + 2C_2H_2 \rightarrow A_1 + 2H + 2H_2$	(Scheme N2)

Instead of reaction R261, a slower alternative pathway from C_6H_6 to A_1 is via the intermediate step to form C_6H_7 with the following two reactions:

$C_6H_6 + H \xrightarrow{M} C_6H_7$	(R262)
$C_6H_7 \xrightarrow{M} A_1 + H$	(R264)

3.3.4.2 C_2H_2 addition to n-C_4H_3 or n-C_4H_5

Scheme N3:

	$C_2H_2 + h\nu \rightarrow C_2H + H$	(R10)
	$C_2H + C_2H_2 \rightarrow C_4H_2 + H$	(R175)
	$C_4H_2 + H \xrightarrow{M} C_4H_3$	(R123)
	$C_4H_3 + C_2H_2 \xrightarrow{M} A_1\text{-}$	(R243) $*$ †
Net:	$3C_2H_2 \rightarrow A_1\text{-} + H$	(Scheme N3)

Scheme N4:

	$C_2H_2 + h\nu \rightarrow C_2H + H$	(R10)
	$C_2H + C_2H_2 \rightarrow C_4H_2 + H$	(R175)
	$C_4H_2 + H \xrightarrow{M} C_4H_3$	(R123)
	$C_4H_3 + C_2H_2 \xrightarrow{M}$ n-C_6H_5	(R242)
	n-$C_6H_5 + H \xrightarrow{M} C_6H_6$	(R259) †
	$C_6H_6 + H \rightarrow A_1 + H$	(R261) $*$

Net: $3C_2H_2 \rightarrow A_1$ (Scheme N4)

Scheme N5:

$C_2H_2 + h\nu \rightarrow C_2H + H$ (R10)

$C_2H + C_2H_2 \rightarrow C_4H_2 + H$ (R175)

$C_4H_2 + H \xrightarrow{M} C_4H_3$ (R123)

$C_4H_3 + H \xrightarrow{M} C_4H_4$ (R125)

$C_4H_4 + H \xrightarrow{M} n\text{-}C_4H_5$ (R126)

$C_4H_5 + C_2H_2 \rightarrow A_1 + H$ (R245) $*$ †

Net: $3C_2H_2 \rightarrow A_1$ (Scheme N5)

An alternative route to form n-C_4H_5 from C_2H_2 is via the following reactions:

$C_2H_2 + H \xrightarrow{M} C_2H_3$ (R96)

$C_2H_3 + C_2H_2 \xrightarrow{M} n\text{-}C_4H_5$ (R184)

Scheme N6:

$C_2H_2 + h\nu \rightarrow C_2H + H$ (R10)

$C_2H + C_2H_2 \rightarrow C_4H_2 + H$ (R175)

$C_4H_2 + H \xrightarrow{M} C_4H_3$ (R123)

$C_4H_3 + C_2H_2 \xrightarrow{M} n\text{-}C_6H_5$ (R242)

$n\text{-}C_6H_5 + H \rightarrow C_6H_4 + H_2$ (R258)

$C_6H_4 + H \xrightarrow{M} A_1\text{-}$ (R256) $*$ †

Net: $3C_2H_2 + H \rightarrow A_1\text{-} + H_2$ (Scheme N6)

3.4 Auroral Model

3.4.1 The Model

For the auroral model, we use the same H_2 density profile as in the non-auroral model and compute the densities of all other hydrocarbon neutral and ion species

simultaneously. The density of all PAHs is computed as a single species. The electron density is calculated by summing up the densities of all other positive charged species.

In the auroral regions, the precipitating electrons heat up the atmosphere and increase its temperature. We use the same temperature profile as in Wong et al. (2000), deduced by Trafton et al. (1994), for the auroral model. At the peak of the energy deposition of the precipitating electrons where the pressure is 5×10^{-3} mbar, the temperature is about 400 K, which is consistent with the derived temperatures by Clarke et al. (1994) (400–700 K), Kim et al. (1995) (200–800 K), Liu and Dalgarno (1996) (400–500 K), and Kim et al. (1997) (400 K). The temperature profile is shown in Figure 3.1.

3.4.2 Energy Source

In the auroral atmosphere of Jupiter, the primary driving force for the chemistry of high hydrocarbons is dissociative recombination of methane ions that are produced from interaction with high-energy particles. A crucial piece of information in the calculation of ion chemistry in the auroral atmosphere is a statistical compilation of energy flux input and distribution of particles with altitude that will affect the neutral composition.

In order to estimate the effects of ion chemistry on the neutral chemistry, our aerosol model in Chapter 2 adopted the calculated reaction rates for the dissociative recombination reactions of H_3^+ and CH_5^+, two of the most abundant ions in the atmosphere, from Figure 4 of Perry et al. (1999). The calculation reflects the influence of precipitating electrons of 30 keV and 11 ergs cm^{-2} s^{-1} energy flux. However, in their paper, Perry et al. (1999) discuss that the H_2 density profile used in their model is derived from Galielo data, which is different from the Voyager data that we use. According to the rates of the recombination reactions, the altitude of the peak of ionization is around 350 km, which corresponds to a H_2 density of 2×10^{13} cm^{-2} in their model. The H_2 density in our model at that altitude is 2.6×10^{13} cm^{-2}, 30% more than in their model. This means that it is important to take the difference in

H_2 densities of the two models into account when using computed reaction rates from their models.

To evaluate the effects of energetic particles on atmospheric chemistry in the polar regions, it is necessary to validate and/or update the energy source of the precipitating electrons used in the model of Perry et al. (1999). The energy of the primary electrons determines the altitude of the peak ionization, and therefore determines which part of the atmosphere is ionized. If it is well above the methane homopause, then the ions will have little effect on the chemistry of hydrocarbons. The energy flux of the precipitating particles determines the amount of the ionization in the atmosphere.

Analysis of Galielo UVS spectra will enable us to determine the total input energy flux and the energy of the electrons of the aurora. We have cataloged over 100 UVS spectra from the Galielo experiment, and it is our future research goal to model these spectra and obtain necessary information about the aurora. The preliminary studies and the catalog of the spectra is included in the Appendix.

In the present work, we adopt the electron energy of 50 keV, used in Perry et al. (1999) for their model A. We evaluate the energy flux using the calculation result from Grodent et al. (2001). They develop a one-dimensional model that investigates the links between auroral heat input and the vertical temperature of Jupiter's upper atmosphere, and calculate a self-consistent model atmosphere. In their model, the total energy fluxes for the discrete and the diffuse auroral distributions are 110.5 ergs cm^{-2} s^{-1} and 30.5 ergs cm^{-2} s^{-1}, respectively. The exospheric temperatures reached by these two distributions are 1309 K and 1271 K, respectively, which is higher than the temperature 900 K used in Perry et al. (1999). Since the energy flux is proportional to the heating of the atmosphere (Chamberlain and Hunten, 1987), the energy fluxes should be 71 ergs cm^{-2} s^{-1} and 20 ergs cm^{-2} s^{-1} for the discrete and the diffuse auroral distributions, respectively. These values are factors of 6.5 and 1.8 greater than the flux 11 ergs cm^{-2} s^{-1} used in Perry et al. (1999). In this study we use two different values, 11 and 16 ergs cm^{-2} s^{-1}, as the input energy flux, in order to evaluate the effect of ion chemistry on benzene formation.

3.4.3 Ion Chemistry

The previous aerosol model has included recombination reactions for H_3^+ and CH_5^+ (R315–R321 in Table 2.1), the most abundant ions in the atmosphere. The production rates of these reactions are taken directly from Perry et al. (1999), producing large amounts of CH_3 at the altitude of energy deposition without removing an appropriate amount of methane from the atmosphere. This method incorrectly predicts excessive production of large amounts of CH_4 in that region.

In this work, instead of inserting the products of the recombination reactions into the atmosphere directly, we compute the densities of each ion in the model. After examing over 4000 reactions from the literature, we expand the list of ion reactions to include 8 photo-ionization reactions, 4 electron-ionization reactions, 312 ion-neutral exchange reactions, and 88 electron-ion recombination reactions. We add 7 heavy hydrocarbon classes (C_iH_n, $i = 3, 4, 5, 6, 7, 8, 9$), 54 ions (up to $C_6H_7^+$), electron, $H_2(\nu \geq 2)$ and $H_2(\nu \geq 4)$ to our list of species.

3.4.3.1 Photo-ionization reactions

Although solar EUV radiation is not the dominant source of ionization at high latitudes, we include eight most important photo-ionization reactions; the reactions (R266–R273) and their column production rates calculated in our model are listed in Table 3.5. Among these, the major ionizable constituents are H_2, H, and CH_3 due to their greater abundance or lower ionization potential. The ionization rates for the these three reactions are plotted in Figure 3.6.

3.4.3.2 Electron-ionization reactions

Precipitating electrons ionize the atmosphere and have significant effects on the chemical structure of the auroral regions. In the auroral model, we include four electron-ionization reactions (R274–R277), listed in Table 3.6. The production rates of these reactions are digitized from Figure 7 of Perry et al. (1999), "selected altitude profiles of the direct ionization rates for model A with 50 keV precipitating electrons." Since

Table 3.5. Photo-ionization reactions in auroral model.

Number	Reaction	Column Production Rate (cm^{-2} s^{-1})
R266	$H \xrightarrow{h\nu} H^+ + e$	2.86×10^8
R267	$He \xrightarrow{h\nu} He^+ + e$	3.32×10^3
R268	$H_2 \xrightarrow{h\nu} H_2^+ + e$	6.07×10^7
R269	$H_2 \xrightarrow{h\nu} H^+ + H + e$	1.07×10^6
R270	$C \xrightarrow{h\nu} C^+ + e$	2.21×10^5
R271	$CH_3 \xrightarrow{h\nu} CH_3^+ + e$	2.29×10^7
R272	$CH_4 \xrightarrow{h\nu} CH_4^+ + e$	1.63×10^5
R273	$C_2H_2 \xrightarrow{h\nu} C_2H_2^+ + e$	1.15×10^5

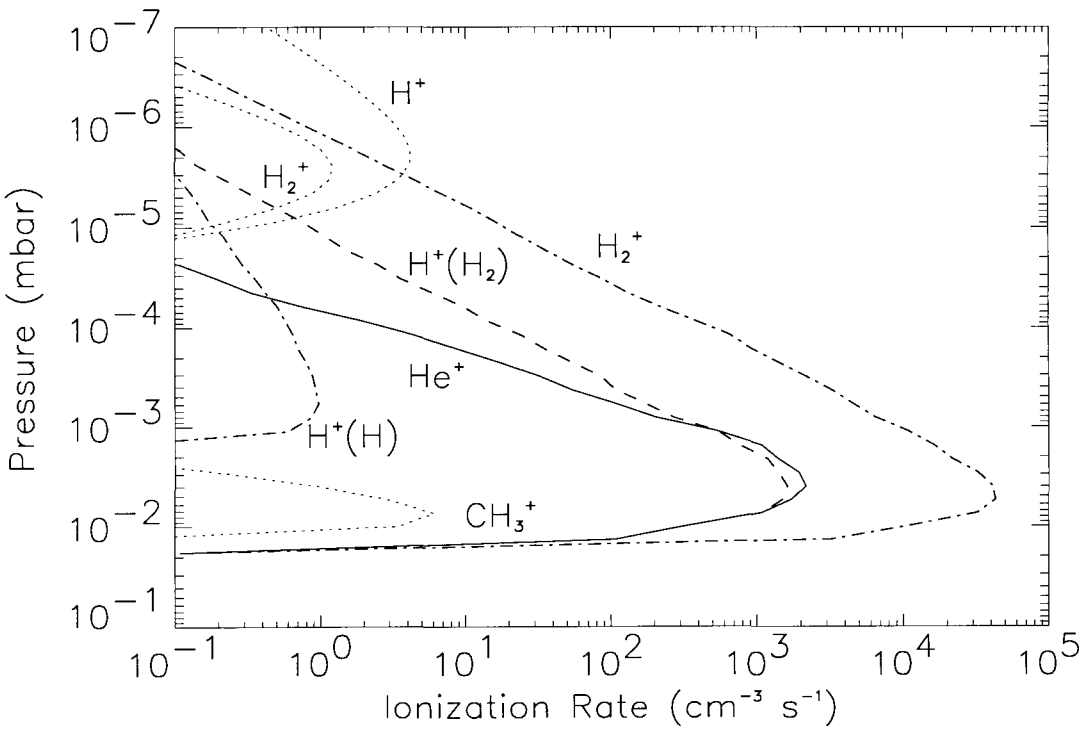

Figure 3.6 Altitude profiles of the ionization reaction rates. The thick curves are rates for electron impact ionization reactions used in auroral model. The electron impact ionization reactions are for 50 keV precipitating electrons with energy fluxes of 11 ergs cm^{-2} s^{-1}. The dotted curves are rates for photoionization and photodissociative ionization, calculated by the auroral model.

Table 3.6. Electron-ionization reactions in auroral model.

Number	Reaction	Column Production Rate (cm^{-2} s^{-1})
R274	$H_2 + e \rightarrow H_2^+ + 2e$	5.17×10^{11}
R275	$H_2 + e \rightarrow H^+ + H + 2e$	2.13×10^{10}
R276	$H + e \rightarrow H^+ + 2e$	5.04×10^{7}
R277	$He + e \rightarrow He^+ + 2e$	2.41×10^{10}

Note. — The reaction rates are based on Perry et al. (1999) model A with 50 keV precipitating electrons, energy fluxes of 11 ergs cm^{-2} s^{-1}, and H_2 density profile from Wong et al. (2000).

they use H_2 densities derived from Galielo data which is different from our model, the production rates of these electron impact ionization reactions are evaluated with respect to H_2 density. The peak of ionization in our model is at about 5×10^{-3} mbar pressure. The electron ionization rates are shown in Figure 3.6.

3.4.3.3 Ion-neutral exchange reactions

Since the peak of ionization in our model is at pressure 5×10^{-3} mbar, below the methane homopause, ion-neutral chemistry can be a dominant factor in determining the hydrocarbon abundances in the auroral regions. Kim and Fox (1994) include 156 ion-neutral reactions producing hydrocarbons of up to two carbon atoms in their model, and have concluded that it is likely that successive ion-neutral reactions will lead to production of heavier hydrocarbon ions and neutral molecules.

We have examined a great number of ion-neutral exchange reactions from the literature, including the 156 ion-molecule reactions listed in Kim and Fox (1994) with updated reaction rates and 5 additional reactions from Perry et al. (1999), about 1000 ion-molecule reactions listed in the Titan model of Anicich et al. (2000), reactions with estimated branching ratios and rates from Keller et al. (1998)'s Titan model, the reactions that contribute to benzene synthesis in dense interstellar clouds studied

by McEwan et al. (1999), the reactions in the UMIST database for astrochemistry (Millar et al., 1997; Le Teuff and Markwick, 2000), the $C_mH_n^+$ reactions with H or H_2 by Scott et al. (1997), and reaction schemes that may lead to benzene formation proposed by Anicich (private communication) and Bayes (Vinckier et al. (1962), and private communication).

From this extensive list of ion-neutral exchange reactions, we first eliminate those reactions that have little or no effect on benzene chemistry in the region of our concern. To simply the calculation, some hydrocarbon ions ($C_3H_6^+$, $C_3H_7^+$, $C_4H_7^+$, $C_4H_8^+$, $C_4H_9^+$, $C_5H_7^+$, $C_5H_9^+$, $C_7H_n^+$, $C_8H_n^+$, $C_9H_n^+$, $C_{10}H_n^+$, $C_{11}H_n^+$) are not calculated individually in the model. They are represented by $C_3H_n^+$, $C_4H_n^+$, $C_5H_n^+$, $C_7H_n^+$, $C_8H_n^+$, $C_9H_n^+$, $C_{10}H_n^+$, and $C_{11}H_n^+$.

In adopting the rate coefficients or branching ratios of the reactions, whenever there is any large discrepancy for a given reaction from different sources of literature, we follow the selection rules outlined below. We first select the value that is in the UMIST database (Millar et al., 1997; Le Teuff and Markwick, 2000) for the purpose of maximum consistency, then the value that is reported latest, then the value that is obtained from experimental data, then the value that promote benzene production, and finally the value that seems the most reasonable to the authors.

Several uncertainties exist for our selection rules. First, in the literature most reactions that form $C_6H_5^+$ or $C_6H_7^+$ are not indicated whether these species are in cyclic form or not, because most of the experimental data are based on mass spectrometric studies. We follow the argument of McEwan et al. (1999) that it is reasonable to assume ring closure "will occur under where radiative stabilization dominates," and assume the cyclic forms for the species in doubt. Similarly, we do not have some of the isomeric information about several other species such as C_3H_4, C_4H_6, $C_3H_2^+$, and $C_3H_3^+$ in the reaction lists. In the case of $C_3H_3^+$ vs. c-$C_3H_3^+$, we exercise our best judgement. For C_3H_4 and C_4H_6, it turns out that these species are not crucial for the analysis of benzene synthesis, and therefore we assume each is in the isomeric form of the greatest abundance whenever in doubt. In addition, the rate coefficients or branching ratios of some reactions are unavailable. For these

Table 3.7. Ion-neutral exchange reactions in auroral model.

Number	Reaction			Rate coefficients	Ref.
R278	$H^+ + H$	$\rightarrow$	$H_2^+ + h\nu$	$6.67 \times 10^{-20} T^{1.0}$	U97
R279	$H^+ + H_2$	$\rightarrow$	$H_2^+ + H$	$1.00 \times 10^{-10} \exp(-21200/T)$	U97
R280	$H^+ + 2H_2$	$\rightarrow$	$H_3^+ + H_2$	$k_0 = 3.20 \times 10^{-29}$	K94
				$k_\infty = 0$	K94
R281	$H^+ + H_2(\nu \geq 4)$	$\rightarrow$	$H_2^+ + H$	2.00×10^{-9}	P99
R282	$H^+ + CH$	$\rightarrow$	$CH^+ + H$	1.90×10^{-9}	U97 [a]
R283	$H^+ + {}^3CH_2$	$\rightarrow$	$CH^+ + H_2$	1.40×10^{-9}	U97 [a]
R284		$\rightarrow$	$CH_2^+ + H$	1.40×10^{-9}	U97 [a]
R285	$H^+ + CH_3$	$\rightarrow$	$CH_3^+ + H$	3.40×10^{-9}	U97 [a]
R286	$H^+ + CH_4$	$\rightarrow$	$CH_3^+ + H_2$	3.40×10^{-9}	A97
R287		$\rightarrow$	$CH_4^+ + H$	7.47×10^{-10}	A97
R288	$H^+ + C_2H_2$	$\rightarrow$	$C_2H^+ + H_2$	4.30×10^{-9}	U97
R289		$\rightarrow$	$C_2H_2^+ + H$	2.00×10^{-9}	U97
R290	$H^+ + C_2H_4$	$\rightarrow$	$C_2H_2^+ + H_2 + H$	1.00×10^{-9}	U00
R291		$\rightarrow$	$C_2H_3^+ + H_2$	3.00×10^{-9}	U00
R292		$\rightarrow$	$C_2H_4^+ + H$	1.00×10^{-9}	U00
R293	$H^+ + C_2H_6$	$\rightarrow$	$C_2H_3^+ + 2H_2$	1.30×10^{-9}	K94
R294		$\rightarrow$	$C_2H_4^+ + H_2 + H$	1.30×10^{-9}	K94
R295		$\rightarrow$	$C_2H_5^+ + H_2$	1.30×10^{-9}	K94
R296	$H^+ + C_3H_2$	$\rightarrow$	$C_3H^+ + H_2$	2.00×10^{-9}	U97
R297		$\rightarrow$	$C_3H_2^+ + H$	2.00×10^{-9}	U97
R298	$H^+ + C_3H_3$	$\rightarrow$	$C_3H_2^+ + H_2$	2.00×10^{-9}	U97
R299		$\rightarrow$	$C_3H_3^+ + H$	2.00×10^{-9}	U97
R300	$H^+ + CH_3C_2H$	$\rightarrow$	$C_3H_3^+ + H_2$	2.00×10^{-9}	U97
R301		$\rightarrow$	$C_3H_4^+ + H$	2.00×10^{-9}	U97
R302	$He^+ + H$	$\rightarrow$	$H^+ + He$	1.90×10^{-15}	U97
R303	$He^+ + H_2$	$\rightarrow$	$H_2^+ + He$	9.35×10^{-15}	K94
R304		$\rightarrow$	$H^+ + H + He$	8.80×10^{-14}	
R305	$He^+ + H_2(\nu \geq 2)$	$\rightarrow$	$H^+ + H + He$	1.00×10^{-9}	K94

reactions, we estimate the total rate coefficient to be 10^{-9} cm^3 s^{-1} following the recommendation of Anicich (private communication), and assume equal branching ratio for all branches when applicable. Lastly, three-body reaction rate coefficients are not available for most ion-neutral exchange reactions, and we use an estimated rate coefficient of 1.0×10^{-27} cm^{-6} s^{-1}.

Table 3.7 lists the ion-neutral exchange reactions investigated in our model.

Table 3.7—Continued

Number	Reaction			Rate coefficients	Ref.
R306	$He^+ + H_2$	$\rightarrow$	$HeH^+ + H$	4.21×10^{-13}	P99
R307	$He^+ + C$	$\rightarrow$	$C^+ + He$	$8.74 \times 10^{-17} T^{0.8}$	U97
R308	$He^+ + {}^3CH_2$	$\rightarrow$	$CH^+ + H + He$	7.50×10^{-10}	U97
R309		$\rightarrow$	$C^+ + H_2 + He$	1.10×10^{-9}	
R310	$He^+ + CH_4$	$\rightarrow$	$H^+ + CH_3 + He$	4.76×10^{-10}	K94
R311		$\rightarrow$	$CH^+ + H + H_2 + He$	2.38×10^{-10}	K94
R312		$\rightarrow$	$CH_2^+ + H_2 + He$	8.50×10^{-10}	K94
R313		$\rightarrow$	$CH_3^+ + H + He$	8.50×10^{-11}	K94
R314		$\rightarrow$	$CH_4^+ + He$	5.10×10^{-11}	K94
R315	$He^+ + C_2H_2$	$\rightarrow$	$CH^+ + CH + He$	7.70×10^{-10}	K94
R316		$\rightarrow$	$C_2^+ + H_2 + He$	1.61×10^{-9}	K94
R317		$\rightarrow$	$C_2H^+ + H + He$	8.75×10^{-10}	K94
R318		$\rightarrow$	$C_2H_2^+ + He$	2.45×10^{-10}	K94
R319	$He^+ + C_2H_4$	$\rightarrow$	$CH_2^+ + {}^3CH_2 + He$	4.08×10^{-10}	K94
R320		$\rightarrow$	$C_2H^+ + H + H_2 + He$	4.42×10^{-10}	K94
R321		$\rightarrow$	$C_2H_2^+ + H_2 + He$	2.18×10^{-9}	K94
R322		$\rightarrow$	$C_2H_3^+ + H + He$	1.70×10^{-10}	K94
R323		$\rightarrow$	$C_2H_4^+ + He$	2.38×10^{-10}	K94
R324	$He^+ + C_2H_6$	$\rightarrow$	$C_2H_2^+ + 2H_2 + He$	8.40×10^{-10}	K94
R325		$\rightarrow$	$C_2H_3^+ + H + H_2 + He$	1.74×10^{-9}	K94
R326		$\rightarrow$	$C_2H_4^+ + H_2 + He$	4.20×10^{-10}	K94
R327	$He^+ + C_3H_2$	$\rightarrow$	$C_3^+ + H_2 + He$	1.00×10^{-9}	U97 [a]
R328		$\rightarrow$	$C_3H^+ + H + He$	1.00×10^{-9}	U97 [a]
R329	$He^+ + C_3H_3$	$\rightarrow$	$c\text{-}C_3H_2^+ + H + He$	6.70×10^{-10}	U97 [a]
R330		$\rightarrow$	$C_3H^+ + H_2 + He$	6.70×10^{-10}	U97 [a]
R331		$\rightarrow$	$C_3^+ + H + H_2 + He$	6.70×10^{-10}	U97 [a]
R332	$He^+ + A_1$	$\rightarrow$	$C_5H_5^+ + CH + He$	7.00×10^{-10}	M99
R333		$\rightarrow$	$c\text{-}C_6H_5^+ + H + He$	7.00×10^{-10}	M99
R334	$H_2^+ + H$	$\rightarrow$	$H^+ + H_2$	6.40×10^{-10}	K94

Table 3.7—Continued

Number	Reaction	Rate coefficients	Ref.
R335	$H_2^+ + H_2 \rightarrow H_3^+ + H$	2.00×10^{-9}	K94
R336	$H_2^+ + C \rightarrow CH^+ + H$	2.40×10^{-9}	U97
R337	$H_2^+ + {}^3CH_2 \rightarrow CH_3^+ + H$	1.00×10^{-9}	U97
R338	$\rightarrow CH_2^+ + H_2$	1.00×10^{-9}	U97
R339	$H_2^+ + CH_4 \rightarrow CH_3^+ + H + H_2$	2.28×10^{-9}	K94
R340	$\rightarrow CH_4^+ + H_2$	1.41×10^{-9}	K94
R341	$\rightarrow CH_5^+ + H$	1.10×10^{-10}	K94
R342	$H_2^+ + C_2H_2 \rightarrow C_2H_2^+ + H_2$	4.82×10^{-9}	K94
R343	$\rightarrow C_2H_3^+ + H$	4.77×10^{-10}	K94
R344	$H_2^+ + C_2H_4 \rightarrow C_2H_2^+ + 2H_2$	8.82×10^{-10}	U97
R345	$\rightarrow C_2H_3^+ + H + H_2$	1.81×10^{-9}	U97
R346	$\rightarrow C_2H_4^+ + H_2$	2.21×10^{-9}	U97
R347	$H_2^+ + C_2H_6 \rightarrow C_2H_6^+ + H_2$	2.94×10^{-10}	K94
R348	$\rightarrow C_2H_5^+ + H + H_2$	1.37×10^{-9}	K94
R349	$\rightarrow C_2H_4^+ + 2H_2$	2.35×10^{-9}	K94
R350	$\rightarrow C_2H_3^+ + H + 2H_2$	6.86×10^{-10}	K94
R351	$\rightarrow C_2H_2^+ + 3H_2$	1.96×10^{-10}	K94
R352	$HeH^+ + H \rightarrow H_2^+ + He$	9.10×10^{-10}	K94
R353	$HeH^+ + H_2 \rightarrow H_3^+ + He$	1.50×10^{-9}	K94
R354	$HeH^+ + C_2H_4 \rightarrow C_2H_3^+ + H_2 + He$	2.10×10^{-9}	K94
R355	$\rightarrow C_2H_4^+ + H + He$	7.00×10^{-10}	K94
R356	$HeH^+ + C_2H_6 \rightarrow C_2H_3^+ + He + 2H_2$	1.05×10^{-9}	K94
R357	$\rightarrow C_2H_5^+ + He + H_2$	1.05×10^{-9}	K94
R358	$H_3^+ + C \rightarrow CH^+ + H_2$	2.00×10^{-9}	U97
R359	$H_3^+ + CH \rightarrow CH_2^+ + H_2$	1.20×10^{-9}	U97
R360	$H_3^+ + {}^3CH_2 \rightarrow CH_3^+ + H_2$	1.70×10^{-9}	U97
R361	$H_3^+ + CH_3 \rightarrow CH_4^+ + H_2$	2.10×10^{-9}	U97
R362	$H_3^+ + CH_4 \rightarrow CH_5^+ + H_2$	2.40×10^{-9}	K94
R363	$H_3^+ + C_2H_2 \rightarrow C_2H_3^+ + H_2$	3.20×10^{-9}	A97

Table 3.7—Continued

Number	Reaction			Rate coefficients	Ref.
R364	$H_3^+ + C_2H_3$	$\rightarrow$	$C_2H_4^+ + H_2$	2.00×10^{-9}	U97
R365	$H_3^+ + C_2H_4$	$\rightarrow$	$C_2H_3^+ + 2H_2$	2.03×10^{-9}	A97
R366		$\rightarrow$	$C_2H_5^+ + H_2$	8.70×10^{-10}	A97
R367	$H_3^+ + C_2H_5$	$\rightarrow$	$C_2H_6^+ + H_2$	1.40×10^{-9}	U97 [a]
R368	$H_3^+ + C_2H_6$	$\rightarrow$	$C_2H_5^+ + 2H_2$	2.90×10^{-10}	
R369		$\rightarrow$	$C_2H_7^+ + H_2$	2.90×10^{-11}	P99
R370	$H_3^+ + C_3H_2$	$\rightarrow$	$C_3H_3^+ + H_2$	2.00×10^{-9}	U97
R371	$H_3^+ + CH_3C_2H$	$\rightarrow$	$C_3H_5^+ + H_2$	6.75×10^{-10}	M99
R372		$\rightarrow$	$C_3H_3^+ + 2H_2$	2.25×10^{-9}	U97
R373	$H_3^+ + C_4H_2$	$\rightarrow$	$C_4H_3 + H_2$	2.60×10^{-9}	A97
R374	$H_3^+ + A_1$	$\rightarrow$	$c\text{-}C_6H_7^+ + H_2$	3.90×10^{-9}	M99
R375	$C^+ + H_2$	$\rightarrow$	$CH_2^+ + h\nu$	$1.25 \times 10^{-15} T^{-0.2}$	U97
R376	$C^+ + CH_4$	$\rightarrow$	$C_2H_2^+ + H_2$	3.64×10^{-10}	P99
R377		$\rightarrow$	$C_2H_3^+ + H$	9.36×10^{-10}	P99
R378	$C^+ + C_2H_2$	$\rightarrow$	$C_3H^+ + H$	2.63×10^{-9}	A97
R379	$C^+ + C_2H_4$	$\rightarrow$	$C_2H_3^+ + CH$	1.20×10^{-10}	A97
R380		$\rightarrow$	$C_2H_4^+ + C$	2.25×10^{-10}	A97
R381		$\rightarrow$	$C_3H^+ + H + H_2$	7.50×10^{-11}	A97
R382		$\rightarrow$	$C_3H_2^+ + H_2$	4.35×10^{-10}	A97
R383		$\rightarrow$	$C_3H_3^+ + H$	6.30×10^{-10}	A97
R384	$C^+ + C_2H_6$	$\rightarrow$	$C_2H_2^+ + CH_4$	1.70×10^{-10}	K94
R385		$\rightarrow$	$C_2H_3^+ + CH_3$	5.10×10^{-10}	K94
R386		$\rightarrow$	$C_2H_5^+ + CH$	1.70×10^{-10}	K94
R387		$\rightarrow$	$C_3H_3^+ + H + H_2$	8.50×10^{-10}	K94
R388	$CH^+ + H$	$\rightarrow$	$C^+ + H_2$	7.50×10^{-10}	K94
R389	$CH^+ + H_2$	$\rightarrow$	$CH_2^+ + H$	1.20×10^{-9}	K94
R390	$CH^+ + CH_4$	$\rightarrow$	$C_2H_2^+ + H + H_2$	1.40×10^{-10}	K94
R391		$\rightarrow$	$C_2H_3^+ + H_2$	1.10×10^{-9}	K94
R392		$\rightarrow$	$C_2H_4^+ +$ products	6.50×10^{-11}	K94

Table 3.7—Continued

Number	Reaction			Rate coefficients	Ref.
R393	$CH^+ + C_2H_2$	$\rightarrow$	$C_3H_2^+ + H$	2.40×10^{-9}	K94
R394	$CH_2^+ + H_2$	$\rightarrow$	$CH_3^+ + H$	1.16×10^{-9}	K94
R395	$CH_2^+ + CH_4$	$\rightarrow$	$C_2H_4^+ + H_2$	9.10×10^{-10}	A97
R396		$\rightarrow$	$C_2H_5^+ + H$	3.90×10^{-10}	A97
R397	$CH_2^+ + C_2H_2$	$\rightarrow$	$c\text{-}C_3H_3^+ + H$	2.50×10^{-9}	K94
R398	$CH_3^+ + H$	$\rightarrow$	$CH_2^+ + H_2$	$7.00 \times 10^{-10} \exp(-10560/T)$	U97 [a]
R399	$CH_3^+ + H_2$	$\rightarrow$	$CH_5^+ + h\nu$	$3.90 \times 10^{-12} T^{-1.0}$	U97
R400	$CH_3^+ + H_2 + He$	$\rightarrow$	$CH_5^+ + He$	$k_0 = 1.10 \times 10^{-28}$	K94
				$k_\infty = 0$	K94
R401	$CH_3^+ + C$	$\rightarrow$	$C_2H^+ + H_2$	1.20×10^{-9}	U00
R402	$CH_3^+ + CH$	$\rightarrow$	$C_2H_2^+ + H_2$	7.10×10^{-10}	U97
R403	$CH_3^+ + {}^3CH_2$	$\rightarrow$	$C_2H_3^+ + H_2$	9.90×10^{-10}	U97
R404	$CH_3^+ + CH_4$	$\rightarrow$	$C_2H_5^+ + H_2$	1.10×10^{-9}	
R405	$CH_3^+ + 2H_2$	$\rightarrow$	$CH_5^+ + H_2$	$k_0 = 3.30 \times 10^{-29}$	
				$k_\infty = 0$	
R406	$CH_3^+ + C_2H_2$	$\rightarrow$	$C_3H_3^+ + H_2$	1.15×10^{-9}	K98
R407	$CH_3^+ + C_2H_4$	$\rightarrow$	$C_2H_3^+ + CH_4$	4.88×10^{-10}	P99
R408		$\rightarrow$	$C_3H_3^+ + 2H_2$	4.24×10^{-11}	P99
R409		$\rightarrow$	$C_3H_5^+ + H_2$	5.40×10^{-10}	P99
R410	$CH_3^+ + C_2H_6$	$\rightarrow$	$C_2H_5^+ + CH_4$	1.50×10^{-9}	K94
R411		$\rightarrow$	$C_3H_5^+ + 2H_2$	1.60×10^{-10}	K94
R412		$\rightarrow$	$C_3H_n^+ + H_2$	1.00×10^{-10}	K94
R413	$CH_3^+ + C_3H_2$	$\rightarrow$	$C_4H_3^+ + H_2$	2.70×10^{-9}	U97
R414	$CH_3^+ + C_3H_3$	$\rightarrow$	$C_4H_5^+ + H$	4.00×10^{-9}	U97
R415	$CH_4^+ + H$	$\rightarrow$	$CH_3^+ + H_2$	1.00×10^{-11}	U97
R416	$CH_4^+ + H_2$	$\rightarrow$	$CH_5^+ + H$	3.50×10^{-11}	P99
R417	$CH_4^+ + CH_4$	$\rightarrow$	$CH_5^+ + CH_3$	1.14×10^{-9}	A97
R418	$CH_4^+ + C_2H_2$	$\rightarrow$	$C_2H_2^+ + CH_4$	1.44×10^{-9}	A97
R419		$\rightarrow$	$C_2H_3^+ + CH_3$	1.12×10^{-9}	A97

Table 3.7—Continued

Number	Reaction	Rate coefficients	Ref.
R420	$\rightarrow$ $C_3H_3^+ + H + H_2$	1.63×10^{-10}	A97
R421	$CH_4^+ + C_2H_4$ $\rightarrow$ $C_2H_4^+ + CH_4$	1.70×10^{-9}	P99
R422	$\rightarrow$ $C_2H_5^+ + CH_3$	2.60×10^{-10}	P99
R423	$\rightarrow$ $C_3H_5^+ + H + H_2$	6.00×10^{-11}	P99
R424	$CH_4^+ + C_2H_6$ $\rightarrow$ $C_2H_4^+ + CH_4 + H_2$	1.91×10^{-9}	K94
R425	$CH_5^+ + H$ $\rightarrow$ $CH_4^+ + H_2$	1.50×10^{-10}	K94
R426	$CH_5^+ + C$ $\rightarrow$ $CH^+ + CH_4$	1.20×10^{-9}	U97
R427	$CH_5^+ + CH$ $\rightarrow$ $CH_2^+ + CH_4$	6.90×10^{-10}	U97
R428	$CH_5^+ + {}^3CH_2$ $\rightarrow$ $CH_3^+ + CH_4$	9.60×10^{-10}	U97
R429	$CH_5^+ + C_2H_2$ $\rightarrow$ $C_2H_3^+ + CH_4$	1.48×10^{-9}	A97
R430	$CH_5^+ + C_2H_4$ $\rightarrow$ $C_2H_5^+ + CH_4$	1.50×10^{-9}	K94
R431	$CH_5^+ + C_2H_6$ $\rightarrow$ $C_2H_5^+ + CH_4 + H_2$	2.03×10^{-10}	P99
R432	$\rightarrow$ $C_2H_7^+ + CH_4$	1.15×10^{-9}	P99
R433	$CH_5^+ + A_1$ $\rightarrow$ $c\text{-}C_6H_7^+ + CH_4$	2.00×10^{-9}	M99
R434	$C_2^+ + H_2$ $\rightarrow$ $C_2H^+ + H$	1.20×10^{-9}	K94
R435	$C_2^+ + CH_4$ $\rightarrow$ $C_2H^+ + CH_3$	2.38×10^{-10}	K94
R436	$\rightarrow$ $C_2H_2^+ + {}^3CH_2$	1.82×10^{-10}	K94
R437	$\rightarrow$ $C_3H^+ + H_2 + H$	1.96×10^{-10}	K94
R438	$\rightarrow$ $C_3H_2^+ + H_2$	5.74×10^{-10}	K94
R439	$\rightarrow$ $C_3H_3^+ + H$	2.10×10^{-10}	K94
R440	$C_2^+ + C_2H_2$ $\rightarrow$ $C_4H^+ + H$	1.20×10^{-9}	K94
R441	$C_2^+ + C_2H_4$ $\rightarrow$ $C_4H_n^+$	1.90×10^{-9}	K94
R442	$C_2H^+ + H_2$ $\rightarrow$ $C_2H_2^+ + H$	1.24×10^{-9}	A97
R443	$C_2H^+ + CH_4$ $\rightarrow$ $C_2H_2^+ + CH_3$	3.74×10^{-10}	K94
R444	$\rightarrow$ $C_3H_3^+ + H_2$	3.74×10^{-10}	K94
R445	$\rightarrow$ $C_3H_4^+ + H$	1.32×10^{-10}	K94
R446	$\rightarrow$ $C_3H_5^+$	2.20×10^{-10}	K94
R447	$C_2H^+ + C_2H_2$ $\rightarrow$ $C_4H_2^+ + H$	1.85×10^{-9}	A97
R448	$C_2H^+ + C_2H_4$ $\rightarrow$ $C_4H_n^+$	1.71×10^{-9}	K94

Table 3.7—Continued

Number	Reaction			Rate coefficients	Ref.
R449	$C_2H_2^+ + H_2$	$\rightarrow$	$C_2H_3^+ + H$	1.00×10^{-11}	A97
R450		$\rightarrow$	$C_2H_4^+ + h\nu$	$1.22 \times 10^{-10} T^{-1.5}$	U97
R451	$C_2H_2^+ + H_2 + He$	$\rightarrow$	$C_2H_4^+ + He$	$k_0 = 1.20 \times 10^{-27}$	K94
				$k_\infty = 0$	K94
R452	$C_2H_2^+ + C$	$\rightarrow$	$C_3H^+ + H$	1.10×10^{-9}	U97
R453	$C_2H_2^+ + {}^3CH_2$	$\rightarrow$	$C_3H_3^+ + H$	8.80×10^{-10}	U97
R454	$C_2H_2^+ + CH_4$	$\rightarrow$	$C_3H_4^+ + H_2$	1.87×10^{-10}	P99
R455		$\rightarrow$	$C_3H_5^+ + H$	7.00×10^{-10}	P99
R456	$C_2H_2^+ + C_2H_2$	$\rightarrow$	$C_4H_2^+ + H_2$	4.48×10^{-10}	A97
R457		$\rightarrow$	$C_4H_3^+ + H$	9.52×10^{-10}	A97
R458	$C_2H_2^+ + C_2H_4$	$\rightarrow$	$C_2H_4^+ + C_2H_2$	4.14×10^{-10}	P99
R459		$\rightarrow$	$C_3H_3^+ + CH_3$	6.62×10^{-10}	P99
R460		$\rightarrow$	$C_4H_5^+ + H$	3.17×10^{-10}	P99
R461	$C_2H_2^+ + C_2H_6$	$\rightarrow$	$C_2H_4^+ + C_2H_4$	2.63×10^{-10}	K94
R462		$\rightarrow$	$C_2H_5^+ + C_2H_3$	1.31×10^{-10}	K94
R463		$\rightarrow$	$C_3H_3^+ + CH_3 + H_2$	8.76×10^{-11}	K94
R464		$\rightarrow$	$C_3H_4^+ + CH_4$	1.46×10^{-11}	K94
R465		$\rightarrow$	$C_3H_5^+ + CH_3$	7.88×10^{-10}	K94
R466		$\rightarrow$	$C_4H_5^+ + H + H_2$	7.30×10^{-11}	K94
R467		$\rightarrow$	$C_4H_n^+ + H$	1.31×10^{-10}	K94
R468	$C_2H_2^+ + C_3H_2$	$\rightarrow$	$C_5H_3^+ + H$	1.30×10^{-9}	U97
R469	$C_2H_2^+ + C_3H_3$	$\rightarrow$	$C_5H_4^+ + H$	1.00×10^{-9}	U97
R470		$\rightarrow$	$C_5H_3^+ + H_2$	1.00×10^{-9}	U97
R471	$C_2H_3^+ + H$	$\rightarrow$	$C_2H_2^+ + H_2$	6.80×10^{-11}	A97
R472	$C_2H_3^+ + C$	$\rightarrow$	$c\text{-}C_3H_2^+ + H$	1.00×10^{-9}	U97
R473	$C_2H_3^+ + CH_4$	$\rightarrow$	$C_3H_5^+ + H_2$	1.90×10^{-10}	A97
R474	$C_2H_3^+ + C_2H_2$	$\rightarrow$	$C_4H_3^+ + H_2$	2.16×10^{-10}	K94
R475		$\xrightarrow{M}$	$C_4H_5^+$	$k_0 = 1.00 \times 10^{-27}$	c
				$k_\infty = 1.00 \times 10^{-9}$	V62 [h]

Table 3.7—Continued

Number	Reaction			Rate coefficients	Ref.
R476	$C_2H_3^+ + C_2H_4$	$\rightarrow$	$C_2H_5^+ + C_2H_2$	8.20×10^{-10}	A97
R477	$C_2H_3^+ + C_2H_6$	$\rightarrow$	$C_2H_5^+ + C_2H_4$	2.91×10^{-10}	K94
R478		$\rightarrow$	$C_3H_5^+ + CH_4$	2.48×10^{-10}	K94
R479		$\rightarrow$	$C_4H_n^+ + H_2$	8.06×10^{-11}	K94
R480	$C_2H_3^+ + C_3H_2$	$\rightarrow$	$C_3H_3^+ + C_2H_2$	8.00×10^{-10}	U97
R481		$\rightarrow$	$C_5H_3^+ + H_2$	8.00×10^{-10}	U97
R482		$\rightarrow$	$C_5H_4^+ + H$	8.00×10^{-10}	U97
R483	$C_2H_3^+ + C_3H_3$	$\rightarrow$	$C_3H_4^+ + C_2H_2$	1.00×10^{-9}	U97
R484		$\rightarrow$	$C_5H_5^+ + H$	1.00×10^{-9}	U97
R485		$\rightarrow$	$C_5H_4^+ + H_2$	1.00×10^{-9}	U97
R486	$C_2H_3^+ + CH_3C_2H$	$\rightarrow$	$C_3H_5^+ + C_2H_2$	5.00×10^{-10}	U97 [b]
R487		$\rightarrow$	$C_5H_5^+ + H_2$	5.00×10^{-10}	U97
R488	$C_2H_3^+ + A_1$	$\rightarrow$	c-$C_6H_7^+ + C_2H_2$	1.60×10^{-9}	M99
R489	$C_2H_4^+ + H$	$\rightarrow$	$C_2H_3^+ + H_2$	3.00×10^{-10}	K94
R490	$C_2H_4^+ + C$	$\rightarrow$	$C_3H_3^+ + H$	1.00×10^{-9}	U97
R491		$\rightarrow$	c-$C_3H_2^+ + H_2$	1.00×10^{-9}	U97
R492	$C_2H_4^+ + C_2H_2$	$\rightarrow$	$C_3H_3^+ + CH_3$	6.47×10^{-10}	A97
R493		$\rightarrow$	$C_4H_5^+ + H$	1.93×10^{-10}	A97
R494	$C_2H_4^+ + C_2H_4$	$\rightarrow$	$C_3H_5^+ + CH_3$	7.55×10^{-10}	A97
R495		$\rightarrow$	$C_4H_n^+ + H$	7.47×10^{-11}	A97
R496	$C_2H_4^+ + C_2H_6$	$\rightarrow$	$C_3H_n^+ + CH_4$	3.71×10^{-13}	K94
R497		$\rightarrow$	$C_3H_n^+ + CH_3$	4.93×10^{-12}	K94
R498	$C_2H_4^+ + C_3H_2$	$\rightarrow$	$C_4H_3^+ + CH_3$	1.50×10^{-9}	U97
R499		$\rightarrow$	$C_5H_5^+ + H$	5.00×10^{-10}	U97
R500	$C_2H_4^+ + C_3H_3$	$\rightarrow$	$C_4H_3^+ + CH_4$	8.00×10^{-10}	U97
R501		$\rightarrow$	$C_5H_5^+ + H_2$	8.00×10^{-10}	U97
R502	$C_2H_5^+ + H$	$\rightarrow$	$C_2H_4^+ + H_2$	1.00×10^{-11}	K94
R503	$C_2H_5^+ + CH_4$	$\rightarrow$	$C_3H_n^+ + H_2$	9.00×10^{-14}	P99
R504	$C_2H_5^+ + C_2H_2$	$\rightarrow$	c-$C_3H_3^+ + CH_4$	7.20×10^{-12}	A97

Table 3.7—Continued

Number	Reaction			Rate coefficients	Ref.
R505		$\rightarrow$	$C_4H_5^+ + H_2$	1.17×10^{-10}	A97
R506	$C_2H_5^+ + C_2H_4$	$\rightarrow$	$C_3H_5^+ + CH_4$	3.55×10^{-10}	P99
R507	$C_2H_5^+ + C_2H_6$	$\rightarrow$	$C_3H_n^+ + CH_4$	5.50×10^{-12}	P99
R508		$\rightarrow$	$C_4H_n^+ + H_2$	3.35×10^{-11}	P99
R509	$C_2H_5^+ + C_3H_8$	$\rightarrow$	$C_3H_n^+ + C_2H_6$	6.30×10^{-10}	A97
R510	$C_2H_6^+ + H$	$\rightarrow$	$C_2H_5^+ + H_2$	1.00×10^{-10}	K94
R511	$C_2H_6^+ + C_2H_2$	$\rightarrow$	$C_2H_5^+ + C_2H_3$	2.22×10^{-10}	K94
R512		$\rightarrow$	$C_3H_5^+ + CH_3$	8.19×10^{-10}	K94
R513		$\rightarrow$	$C_4H_n^+ + H$	1.29×10^{-10}	K94
R514	$C_2H_6^+ + C_2H_4$	$\rightarrow$	$C_2H_4^+ + C_2H_6$	1.15×10^{-9}	K94
R515	$C_2H_6^+ + C_2H_6$	$\rightarrow$	$C_3H_n^+ + CH_4$	7.98×10^{-12}	K94
R516		$\rightarrow$	$C_3H_n^+ + CH_3$	1.10×10^{-11}	K94
R517	$C_2H_7^+ + C_2H_2$	$\rightarrow$	$C_2H_3^+ + C_2H_6$	1.00×10^{-9}	K94
R518	$C_2H_7^+ + C_2H_4$	$\rightarrow$	$C_2H_5^+ + C_2H_6$	1.00×10^{-9}	K94
R519	$C_3^+ + H_2$	$\rightarrow$	$C_3H^+ + H$	3.00×10^{-10}	U97
R520	$C_3H^+ + H_2$	$\rightarrow$	c-$C_3H_2^+ + H$	1.04×10^{-12}	A97
R521		$\rightarrow$	$C_3H_2^+ + H$	4.16×10^{-12}	A97
R522		$\xrightarrow{M}$	c-$C_3H_3^+$	$k_0 = 1.00 \times 10^{-27}$	c
				$k_\infty = 1.35 \times 10^{-11}$	A97
R523		$\xrightarrow{M}$	$C_3H_3^+$	$k_0 = 1.00 \times 10^{-27}$	c
				$k_\infty = 7.28 \times 10^{-12}$	A97
R524	$C_3H_2^+ + H$	$\rightarrow$	$C_3H^+ + H_2$	6.00×10^{-11}	A97
R525	$C_3H_2^+ + C_2H_2$	$\rightarrow$	$C_5H_3^+ + H$	1.10×10^{-9}	A97
R526	c-$C_3H_2^+ + C$	$\rightarrow$	$C_4^+ + H_2$	1.00×10^{-9}	U97 [d]
R527		$\rightarrow$	$C_4H^+ + H$	1.00×10^{-9}	U97 [d]
R528	c-$C_3H_2^+ + C_2H_2$	$\rightarrow$	$C_5H_3^+ + H$	9.00×10^{-10}	A97
R529	c-$C_3H_2^+ + C_2H_4$	$\rightarrow$	$C_4H_3^+ + CH_3$	3.00×10^{-10}	U97 [d]
R530		$\rightarrow$	$C_5H_5^+ + H$	3.00×10^{-10}	U97, [d]
R531	c-$C_3H_2^+ + C_3H_2$	$\rightarrow$	$C_6H_2^+ + H_2$	1.00×10^{-9}	U97 [d]

Table 3.7—Continued

Number	Reaction			Rate coefficients	Ref.
R532		$\rightarrow$	$C_6H_3^+ + H$	1.00×10^{-9}	U97 [d]
R533	c-$C_3H_2^+ + C_3H_3$	$\rightarrow$	$C_6H_4^+ + H$	2.00×10^{-9}	U97 [d]
R534	c-$C_3H_3^+ + CH_3C_2H$	$\rightarrow$	$C_6H_5^+ + H_2$	1.00×10^{-9}	U97 [b]
R535	$C_3H_3^+ + C$	$\rightarrow$	$C_4H_2^+ + H$	1.00×10^{-9}	U97
R536		$\rightarrow$	$C_4H^+ + H_2$	1.00×10^{-9}	U97
R537	$C_3H_3^+ + C_2H_2$	$\rightarrow$	c-$C_3H_3^+ + C_2H_2$	2.10×10^{-10}	A97
R538	$C_3H_3^+ + CH_3C_2H$	$\rightarrow$	$C_6H_5^+ + H_2$	1.00×10^{-9}	U97 [e]
R539	c-$C_3H_3^+ + C$	$\rightarrow$	$C_4H_2^+ + H$	1.00×10^{-9}	U97
R540		$\rightarrow$	$C_4H^+ + H_2$	1.00×10^{-9}	U97
R541	$C_3H_4^+ + H$	$\rightarrow$	$C_3H_3^+ + H_2$	3.00×10^{-11}	
R542	$C_3H_4^+ + C$	$\rightarrow$	$C_4H_2^+ + H_2$	1.00×10^{-9}	U97
R543	$C_3H_4^+ + C$	$\rightarrow$	$C_4H_3^+ + H$	1.00×10^{-9}	U97
R544	$C_3H_4^+ + C_2H_2$	$\rightarrow$	$C_5H_5^+ + H$	4.90×10^{-10}	A97
R545	$C_3H_5^+ + H$	$\rightarrow$	$C_2H_2^+ + CH_4$	5.00×10^{-13}	A97
R546		$\rightarrow$	$C_2H_3^+ + CH_3$	9.60×10^{-12}	A97
R547	$C_3H_5^+ + C$	$\rightarrow$	$C_4H_3^+ + H_2$	1.00×10^{-9}	U97
R548	$C_3H_5^+ + C_2H_2$	$\rightarrow$	$C_5H_5^+ + H_2$	3.80×10^{-10}	A97
R549	$C_3H_5^+ + C_2H_4$	$\rightarrow$	$C_5H_n^+ + H_2$	1.19×10^{-10}	A97
R550		$\xrightarrow{M}$	$C_5H_n^+$	$k_0 = 1.00 \times 10^{-27}$	[c]
				$k_\infty = 5.10 \times 10^{-11}$	A97
R551	$C_3H_5^+ + CH_3C_2H$	$\rightarrow$	c-$C_6H_7^+ + H_2$	1.00×10^{-9}	A01
R552	$C_3H_5^+ + A_1$	$\rightarrow$	c-$C_6H_7^+ + CH_3C_2H$	1.15×10^{-10}	M99
R553	$C_4^+ + H_2$	$\rightarrow$	$C_4H^+ + H$	3.00×10^{-10}	U97
R554	$C_4H^+ + H_2$	$\rightarrow$	$C_4H_2^+ + H$	7.00×10^{-10}	U97
R555	$C_4H^+ + CH_4$	$\rightarrow$	$C_5H_3^+ + H_2$	1.10×10^{-9}	U97
R556	$C_4H^+ + C_3H_3$	$\rightarrow$	$C_7H_n^+ + H$	2.50×10^{-9}	U97
R557	$C_4H_2^+ + H$	$\rightarrow$	$C_4H_3^+ + h\nu$	$1.24 \times 10^{-11}\, T^{-0.1}$	M99
R558	$C_4H_2^+ + C$	$\rightarrow$	$C_5^+ + H_2$	5.00×10^{-10}	U97
R559		$\rightarrow$	$C_5H^+ + H$	5.00×10^{-10}	U97

Table 3.7—Continued

Number	Reaction			Rate coefficients	Ref.
R560	$C_4H_2^+ + CH_4$	$\rightarrow$	$C_5H_4^+ + H_2$	2.00×10^{-10}	U97
R561		$\rightarrow$	$C_5H_5^+ + H$	5.00×10^{-10}	U97
R562	$C_4H_2^+ + C_2H_2$	$\rightarrow$	$C_6H_3^+ + H$	1.40×10^{-11}	A97
R563		$\rightarrow$	$C_6H_4^+ + h\nu$	2.66×10^{-10}	A97
R564	$C_4H_2^+ + C_2H_4$	$\rightarrow$	$C_6H_4^+ + H_2$	2.00×10^{-10}	U97
R565		$\rightarrow$	$C_6H_5^+ + H$	8.00×10^{-10}	U97
R566	$C_4H_2^+ + C_3H_2$	$\rightarrow$	$C_7H_n^+ + H$	2.20×10^{-9}	U97
R567	$C_4H_2^+ + C_3H_3$	$\rightarrow$	$C_7H_n^+$	2.50×10^{-9}	U97
R568	$C_4H_3^+ + H$	$\rightarrow$	$C_4H_4^+ + h\nu$	$3.25 \times 10^{-12}\,T^{-0.7}$	M99
R569	$C_4H_3^+ + C$	$\rightarrow$	$C_5H^+ + H_2$	5.00×10^{-10}	U97
R570	$C_4H_3^+ + CH_4$	$\rightarrow$	$C_5H_5^+ + H_2$	5.00×10^{-10}	U97
R571	$C_4H_3^+ + C_2H_2$	$\rightarrow$	c-$C_6H_5^+$	2.20×10^{-10}	A97 [f]
R572	$C_4H_3^+ + A_1$	$\rightarrow$	c-$C_6H_7^+ + C_4H_2$	1.00×10^{-9}	A97 [c]
R573	$C_4H_3^+ + C$	$\rightarrow$	$C_5H_2^+ + H$	5.00×10^{-10}	U97
R574	$C_4H_3^+ + C_3H_2$	$\rightarrow$	$C_7H_4^+ + H$	1.50×10^{-9}	U97
R575	$C_4H_3^+ + C_3H_3$	$\rightarrow$	$C_7H_n^+$	2.00×10^{-9}	U97
R576	$C_4H_4^+ + C_2H_2$	$\rightarrow$	$C_6H_4^+ + H_2$	1.20×10^{-11}	M99
R577		$\rightarrow$	c-$C_6H_5^+ + H$	9.00×10^{-11}	M99
R578	$C_4H_5^+ + C_2H_2$	$\xrightarrow{M}$	c-$C_6H_7^+$	$k_0 = 1.00 \times 10^{-27}$	[c]
				$k_\infty = 1.00 \times 10^{-9}$	V62 [h]
R579	$C_4H_5^+ + CH_3C_2H$	$\rightarrow$	$C_6H_5^+ + CH_4$	4.00×10^{-10}	A97 [g]
R580		$\rightarrow$	$C_7H_n^+ + H_2$	6.00×10^{-10}	A97 [g]
R581	$C_4H_5^+ + C_4H_2$	$\rightarrow$	$C_6H_5^+ + C_2H_2$	1.00×10^{-9}	A97 [h]
R582	$C_4H_5^+ + C_4H_4$	$\rightarrow$	$C_6H_7^+ + C_2H_2$	1.00×10^{-9}	A97 [h]
R583	$C_5^+ + H_2$	$\rightarrow$	$C_5H^+ + H$	7.30×10^{-10}	U97
R584	$C_5H^+ + H_2$	$\rightarrow$	$C_5H_2^+ + H$	1.00×10^{-17}	U97
R585	$C_5H^+ + C$	$\rightarrow$	$C_6^+ + H$	1.00×10^{-9}	U97
R586	$C_5H_2^+ + C$	$\rightarrow$	$C_6^+ + H_2$	5.00×10^{-10}	U97
R587		$\rightarrow$	$C_6H^+ + H$	5.00×10^{-10}	U97

3.4.3.4 Electron-ion recombination reactions

The ions produced by direct ionization or by ion-neutral exchange reactions are destroyed by further ion-neutral reactions or recombination with electrons. We include 88 electron-ion recombination reactions in the present work, listed in Table 3.8. Most of these recombination reactions and rate coefficients are adopted from the work of Kim and Fox (1994), Perry et al. (1999), McEwan et al. (1999), and the UMIST database (Millar et al., 1997; Le Teuff and Markwick, 2000).

There are considerable uncertainties with the recombination reactions. Although the rate coefficients are easily calculated, the products are very difficult to measure, and experimental results performed on these ions have been very limited. For those recombination reactions (R694, R697–R702) with unavailable product and rate information, we follow the example of Perry et al. (1999) and Rebrion-Rowe et al. (1998), and estimate a removal rate coefficient of 7.5×10^{-7}. In the recombination reactions with unknown products, or reactions with known neutral products that are not studied in our neutral model, we use C_iH_n to represent a product molecule with a total of i carbon atoms.

Unfortunately, the set of recombination reactions included is far from being complete and accurate because of lack of available information about the rate coefficients and product yields. Such an incomplete recombination reaction set poses potential problems to our benzene studies. For example, a great number of heavy hydrocarbon molecules (C_iH_n) are accumulated in our model. There is no mechanism in the model to break them down so the products may contribute to benzene production. Also, some products of the recombination reactions may be important for benzene formation, but we are unable to obtain the rates at which these products form. Kim and Fox (1994) also speculate the formidable problem associated with accurate modeling of the chemistry of hydrocarbon ions. This issue receives more attention in Section 3.4.4 of this study.

Table 3.7—Continued

Number	Reaction			Rate coefficients	Ref.
R588	$C_5H_2^+ + CH_4$	$\rightarrow$	$C_6H_4^+ + H_2$	2.00×10^{-10}	U97
R589		$\rightarrow$	$C_6H_5^+ + H$	8.00×10^{-10}	U97
R590	$C_5H_2^+ + C_2H_2$	$\rightarrow$	$C_7H_n^+ + H_2$	3.00×10^{-10}	U97
R591	$C_5H_2^+ + C_2H_4$	$\rightarrow$	$C_7H_n^+ + H_2$	5.00×10^{-10}	U97
R592	$C_5H_2^+ + C_3H_2$	$\rightarrow$	$C_8H_n^+ + H_2$	6.00×10^{-10}	U97
R593	$C_5H_2^+ + C_3H_3$	$\rightarrow$	$C_8H_n^+ + H$	1.20×10^{-9}	U97
R594	$C_5H_3^+ + C$	$\rightarrow$	$C_6H^+ + H_2$	5.00×10^{-10}	U97
R595		$\rightarrow$	$C_6H_2^+ + H$	5.00×10^{-10}	U97
R596	$C_5H_5^+ + C_2H_2$	$\rightarrow$	$C_7H_n^+ + h\nu$	3.10×10^{-11}	A97
R597	$C_5H_5^+ + CH_3C_2H$	$\rightarrow$	c-$C_6H_7^+ + C_2H_2$	5.60×10^{-10}	A97 [g]
R598		$\rightarrow$	$C_8H_n^+ + H_2$	4.40×10^{-10}	A97 [g]
R599	$C_5H_5^+ + C_4H_2$	$\rightarrow$	$C_7H_n^+ + C_2H_2$	1.76×10^{-10}	A97 [g]
R600		$\rightarrow$	$C_7H_n^+ + C_2$	3.30×10^{-11}	A97 [g]
R601	$C_6^+ + H_2$	$\rightarrow$	$C_6H^+ + H$	7.00×10^{-11}	U97
R602		$\rightarrow$	$C_6H_2^+ + h\nu$	$9.01 \times 10^{-13} T^{-0.5}$	U97
R603	$C_6H^+ + H_2$	$\rightarrow$	$C_6H_2^+ + H$	9.50×10^{-13}	U97
R604	$C_6H_2^+ + CH_4$	$\rightarrow$	$C_7H_n^+ + H_2$	2.00×10^{-10}	U97
R605	$C_6H_2^+ + C_2H_2$	$\rightarrow$	$C_8H_n^+ + h\nu$	1.00×10^{-9}	U97
R606	$C_6H_2^+ + C_2H_4$	$\rightarrow$	$C_8H_4^+ + H_2$	1.00×10^{-9}	U97
R607	$C_6H_2^+ + C_3H_2$	$\rightarrow$	$C_9H_n^+$	1.80×10^{-9}	U97
R608	$C_6H_2^+ + C_3H_3$	$\rightarrow$	$C_9H_n^+$	1.42×10^{-9}	U97
R609	$C_6H_3^+ + C$	$\rightarrow$	$C_7H_n^+ + H_2$	5.00×10^{-10}	U97
R610	$C_6H_4^+ + H$	$\xrightarrow{M}$	$C_6H_5^+$	$k_0 = 1.00 \times 10^{-27}$	[c]
				$k_\infty = 3.30 \times 10^{-11}$	A97
R611	$C_6H_5^+ + H_2$	$\rightarrow$	$C_6H_7^+ + h\nu$	5.00×10^{-11}	A97
R612	c-$C_6H_5^+ + H_2$	$\rightarrow$	c-$C_6H_7^+ + h\nu$	6.00×10^{-11}	M99
R613	$C_6H_7^+ + CH_3C_2H$	$\rightarrow$	$C_7H_n^+ + C_2H_4$	1.00×10^{-9}	A97 [b]

Note. — Units for two-body and three-body rate coefficients are cm^3s^{-1} and cm^6s^{-1}, respectively. k_0 and k_∞ refer to the low and high pressure limits of the rate coefficients. $C_3H_n^+$ represents $C_3H_6^+$ or $C_3H_7^+$; $C_4H_n^+$ represents $C_4H_7^+$, $C_4H_8^+$, or $C_4H_9^+$; $C_5H_n^+$ represents $C_5H_7^+$ or $C_5H_9^+$.

[a]Reaction removed from the list in final model.

[b]The form of C_3H_4 is not specified in the reference.

[c]Estimated.

[d]The form of $C_3H_2^+$ is not specified in the reference.

[e]The form of $C_6H_5^+$ is not specified in the reference.

[f]Assume cyclic form, McEwan et al. (1999).

[g]Total rate coefficient estimated to be 1.0×10^{-09}.

[h]Rate coefficient estimated to be 1.0×10^{-09}.

References. — (A01) Anicich, private communication; (A97) Anicich and McEwan (1997); (K98) Keller et al. (1998); (K94) Kim and Fox (1994); (M99) McEwan et al. (1999); (P99) Perry et al. (1999); (U97) Millar et al. (1997); (U00) Le Teuff and Markwick (2000); (V62) Vinckier et al. (1962)

Table 3.8. Electron-ion recombination reactions in auroral model.

No.	Reaction	Rate coefficient[a]	Ref.
R614	$H^+ + e \rightarrow H + h\nu$	$1.91 \times 10^{-10} T^{-0.7}$	1
R615	$He^+ + e \rightarrow He + h\nu$	$1.91 \times 10^{-10} T^{-0.7}$	1
R616	$H_2^+ + e \rightarrow 2H$	$2.25 \times 10^{-6} T^{-0.4}$	1
R617	$HeH^+ + e \rightarrow He + H$	$3.06 \times 10^{-7} T^{-0.6}$	1
R618	$H_3^+ + e \rightarrow 3H$	$3.52 \times 10^{-6} T^{-0.6}$	2
R619	$\rightarrow H_2 + H$	$1.17 \times 10^{-6} T^{-0.6}$	2
R620	$C^+ + e \rightarrow C + h\nu$	$1.91 \times 10^{-10} T^{-0.7}$	1
R621	$CH^+ + e \rightarrow C + H$	$1.65 \times 10^{-6} T^{-0.4}$	3
R622	$CH_2^+ + e \rightarrow C + H_2$	$2.17 \times 10^{-6} T^{-0.5}$	3
R623	$\rightarrow CH + H$	$2.17 \times 10^{-6} T^{-0.5}$	3
R624	$CH_3^+ + e \rightarrow CH + 2H$	$1.34 \times 10^{-6} T^{-0.5}$	3
R625	$\rightarrow CH + H_2$	$3.38 \times 10^{-6} T^{-0.5}$	3
R626	$\rightarrow {}^3CH_2 + H$	$1.34 \times 10^{-6} T^{-0.5}$	3
R627	$\rightarrow CH_3$	$1.91 \times 10^{-09} T^{-0.5}$	3
R628	$CH_4^+ + e \rightarrow CH_3 + H$	$6.06 \times 10^{-6} T^{-0.5}$	3
R629	$CH_5^+ + e \rightarrow CH + 2H_2$	$1.84 \times 10^{-7} T^{-0.5}$	2
R630	$\rightarrow {}^3CH_2 + H + H_2$	$1.03 \times 10^{-6} T^{-0.5}$	2
R631	$\rightarrow CH_3 + 2H$	$3.69 \times 10^{-6} T^{-0.5}$	2
R632	$\rightarrow CH_3 + H_2$	$3.30 \times 10^{-7} T^{-0.5}$	2
R633	$\rightarrow CH_4 + H$	$1.75 \times 10^{-7} T^{-0.5}$	2
R634	$C_2^+ + e \rightarrow 2C$	$5.20 \times 10^{-6} T^{-0.5}$	1
R635	$C_2H^+ + e \rightarrow CH + C$	$2.34 \times 10^{-6} T^{-0.5}$	1
R636	$\rightarrow C_2 + H$	$2.34 \times 10^{-6} T^{-0.5}$	1
R637	$C_2H_2^+ + e \rightarrow C_2 + 2H$	$1.56 \times 10^{-6} T^{-0.5}$	3
R638	$\rightarrow 2CH$	$1.56 \times 10^{-6} T^{-0.5}$	3

Table 3.8—Continued

No.	Reaction			Rate coefficient[a]	Ref.
R639		$\rightarrow$	$C_2H + H$	$1.56 \times 10^{-6} T^{-0.5}$	3
R640	$C_2H_3^+ + e$	$\rightarrow$	$^3CH_2 + CH$	$3.98 \times 10^{-6} T^{-0.5}$	1
R641		$\rightarrow$	$C_2H_2 + H$	$3.98 \times 10^{-6} T^{-0.5}$	1
R642	$C_2H_4^+ + e$	$\rightarrow$	$C_2H_2 + 2H$	$5.20 \times 10^{-6} T^{-0.5}$	3
R643	$C_2H_5^+ + e$	$\rightarrow$	$C_2H + 2H_2$	$2.60 \times 10^{-6} T^{-0.5}$	3
R644		$\rightarrow$	$C_2H_2 + H_2 + H$	$5.20 \times 10^{-6} T^{-0.5}$	3
R645		$\rightarrow$	$C_2H_3 + H_2$	$2.60 \times 10^{-6} T^{-0.5}$	3
R646		$\rightarrow$	$C_2H_4 + H$	$2.60 \times 10^{-05} T^{-0.5}$	3
R647	$C_2H_6^+ + e$	$\rightarrow$	$C_2H_4 + H_2$	$2.60 \times 10^{-6} T^{-0.5}$	1
R648		$\rightarrow$	$C_2H_5 + H$	$2.60 \times 10^{-6} T^{-0.5}$	1
R649	$C_2H_7^+ + e$	$\rightarrow$	$C_2H_5 + H_2$	$2.60 \times 10^{-6} T^{-0.5}$	3
R650		$\rightarrow$	$C_2H_6 + H$	$2.60 \times 10^{-6} T^{-0.5}$	3
R651	$C_3^+ + e$	$\rightarrow$	$C_2 + C$	$5.20 \times 10^{-6} T^{-0.5}$	3
R652	$C_3H^+ + e$	$\rightarrow$	$C_3 + H$	$2.60 \times 10^{-6} T^{-0.5}$	3
R653		$\rightarrow$	$C_2H + C$	$2.60 \times 10^{-6} T^{-0.5}$	3
R654	$c\text{-}C_3H_2^+ + e$	$\rightarrow$	$C_2H_2 + C$	$5.20 \times 10^{-7} T^{-0.5}$	3
R655		$\rightarrow$	$C_3 + H_2$	$1.04 \times 10^{-6} T^{-0.5}$	3
R656		$\rightarrow$	$C_3 + 2H$	$1.04 \times 10^{-6} T^{-0.5}$	3
R657		$\rightarrow$	$C_2 + {}^3CH_2$	$5.20 \times 10^{-7} T^{-0.5}$	3
R658		$\rightarrow$	$C_3H + H$	$5.20 \times 10^{-6} T^{-0.5}$	3
R659	$C_3H_3^+ + e$	$\rightarrow$	$C_3H_2 + H$	$8.66 \times 10^{-7} T^{-0.5}$	3
R660		$\rightarrow$	$C_2H_2 + CH$	$8.66 \times 10^{-7} T^{-0.5}$	3
R661	$c\text{-}C_3H_3^+ + e$	$\rightarrow$	C_3H_n	$8.66 \times 10^{-7} T^{-0.5}$	3
R662	$C_3H_4^+ + e$	$\rightarrow$	$C_3H_2 + H_2$	$3.46 \times 10^{-6} T^{-0.5}$	3
R663		$\rightarrow$	$C_3H_3 + H$	$3.46 \times 10^{-6} T^{-0.5}$	3

Table 3.8--Continued

No.	Reaction			Rate coefficient[a]	Ref.
R664	$C_3H_5^+ + e$	$\rightarrow$	$C_3H_3 + H_2$	$2.60 \times 10^{-6} T^{-0.5}$	3
R665		$\rightarrow$	$CH_3C_2H + H$	$2.60 \times 10^{-6} T^{-0.5}$	3
R666	$C_4^+ + e$	$\rightarrow$	$2C_2$	$5.20 \times 10^{-6} T^{-0.5}$	3
R667	$C_4H^+ + e$	$\rightarrow$	C_4H_n	$5.20 \times 10^{-6} T^{-0.5}$	3
R668	$C_4H_2^+ + e$	$\rightarrow$	$C_4H + H$	$5.20 \times 10^{-6} T^{-0.5}$	3
R669	$C_4H_3^+ + e$	$\rightarrow$	$C_4H + H_2$	$5.37 \times 10^{-6} T^{-0.5}$	3
R670		$\rightarrow$	$C_4H_2 + H$	$5.37 \times 10^{-6} T^{-0.5}$	3
R671	$C_4H_4^+ + e$	$\rightarrow$	$C_4H_3 + H$	$5.72 \times 10^{-6} T^{-0.5}$	4
R672	$C_4H_5^+ + e$	$\rightarrow$	$CH_3C_2H + CH$	$2.60 \times 10^{-6} T^{-0.5}$	3 [b]
R673		$\rightarrow$	$C_4H_2 + H + H_2$	$2.60 \times 10^{-6} T^{-0.5}$	3
R674	$C_5^+ + e$	$\rightarrow$	$C_3 + C_2$	$5.20 \times 10^{-6} T^{-0.5}$	3
R675	$C_5H^+ + e$	$\rightarrow$	$C_4H + C$	$5.54 \times 10^{-6} T^{-0.3}$	3
R676		$\rightarrow$	C_5H_n	$5.20 \times 10^{-6} T^{-0.5}$	3
R677	$C_5H_2^+ + e$	$\rightarrow$	C_5H_n	$5.20 \times 10^{-6} T^{-0.5}$	3
R678	$C_5H_3^+ + e$	$\rightarrow$	$C_5H_n + H_2$	$2.60 \times 10^{-6} T^{-0.5}$	3
R679		$\rightarrow$	$C_5H_2 + H$	$2.60 \times 10^{-6} T^{-0.5}$	3
R680	$C_5H_4^+ + e$	$\rightarrow$	$C_5H_n + H + H_2$	$5.54 \times 10^{-6} T^{-0.3}$	3
R681		$\rightarrow$	$C_5H_2 + H_2$	$5.54 \times 10^{-6} T^{-0.3}$	3
R682	$C_5H_5^+ + e$	$\rightarrow$	$C_5H_2 + H + H_2$	$5.54 \times 10^{-6} T^{-0.3}$	3
R683		$\rightarrow$	$C_5H_n + H$	$5.20 \times 10^{-6} T^{-0.5}$	3
R684	$C_6^+ + e$	$\rightarrow$	C_6H_n	$1.11 \times 10^{-05} T^{-0.3}$	3
R685	$C_6H^+ + e$	$\rightarrow$	C_6H_n	$1.11 \times 10^{-05} T^{-0.3}$	3
R686	$C_6H_2^+ + e$	$\rightarrow$	$C_6H_n + H_2$	$5.54 \times 10^{-6} T^{-0.3}$	3
R687		$\rightarrow$	$C_6H + H$	$5.54 \times 10^{-6} T^{-0.3}$	3
R688	$C_6H_3^+ + e$	$\rightarrow$	$C_6H + H_2$	$5.54 \times 10^{-6} T^{-0.3}$	3

Table 3.8—Continued

No.	Reaction	Rate coefficient[a]	Ref.
R689	$\rightarrow C_6H_2 + H$	$5.54 \times 10^{-6} T^{-0.3}$	3
R690	$C_6H_4^+ + e \rightarrow C_6H + H + H_2$	$5.54 \times 10^{-6} T^{-0.3}$	3
R691	$\rightarrow C_6H_2 + H_2$	$5.54 \times 10^{-6} T^{-0.3}$	3
R692	$C_6H_5^+ + e \rightarrow C_6H + 2H_2$	$5.54 \times 10^{-6} T^{-0.3}$	3
R693	$\rightarrow C_6H_2 + H + H_2$	$5.54 \times 10^{-6} T^{-0.3}$	3
R694	$C_6H_7^+ + e \rightarrow C_6H_n$	7.50×10^{-7}	5
R695	$c\text{-}C_6H_7^+ + e \rightarrow A_1 + H$	$8.66 \times 10^{-6} T^{-0.5}$	6
R696	$\rightarrow C_6H_2 + H + 2H_2$	$8.66 \times 10^{-6} T^{-0.5}$	6
R697	$C_3H_n^+ + e \rightarrow C_3H_n$	7.50×10^{-7}	5
R698	$C_4H_n^+ + e \rightarrow C_4H_n$	7.50×10^{-7}	5
R699	$C_5H_n^+ + e \rightarrow C_5H_n$	7.50×10^{-7}	5
R700	$C_7H_n^+ + e \rightarrow C_7H_n$	7.50×10^{-7}	5
R701	$C_8H_n^+ + e \rightarrow C_8H_n$	7.50×10^{-7}	5
R702	$C_9H_n^+ + e \rightarrow C_9H_n$	7.50×10^{-7}	5

[a]Unit is cm^3s^{-1}.

[b]The form of C_3H_4 is not specified in the reference.

References. — (1) Kim and Fox (1994); (2) Perry et al. (1999); (3) Millar et al. (1997); (4) Le Teuff and Markwick (2000); (5) estimated using Rebrion-Rowe et al. (1998); (6) McEwan et al. (1999)

3.4.4 Results for Auroral Model

It is believed that ion chemistry in auroral regions increases the production of heavy hydrocarbon molecules including benzene, and thereby explains the observation of benzene enhancement in those regions. In our auroral model, we include a large set of ion chemical reactions described above to help investigate the effect of ion reactions on benzene production. For electron-ionization, the energy of the precipitating electrons is 50 keV, and the energy flux is 11 ergs cm^{-2} s^{-1}. The peak of ionization is at about 5×10^{-3} mbar. The latitude is 60°.

Table 3.3 summarizes the model results for four cases: two of non-auroral model for low latitude regions and for polar regions, and two of auroral model for polar regions with energy flux of 16 ergs cm^{-2} s^{-1} and 11 ergs cm^{-2} s^{-1}.

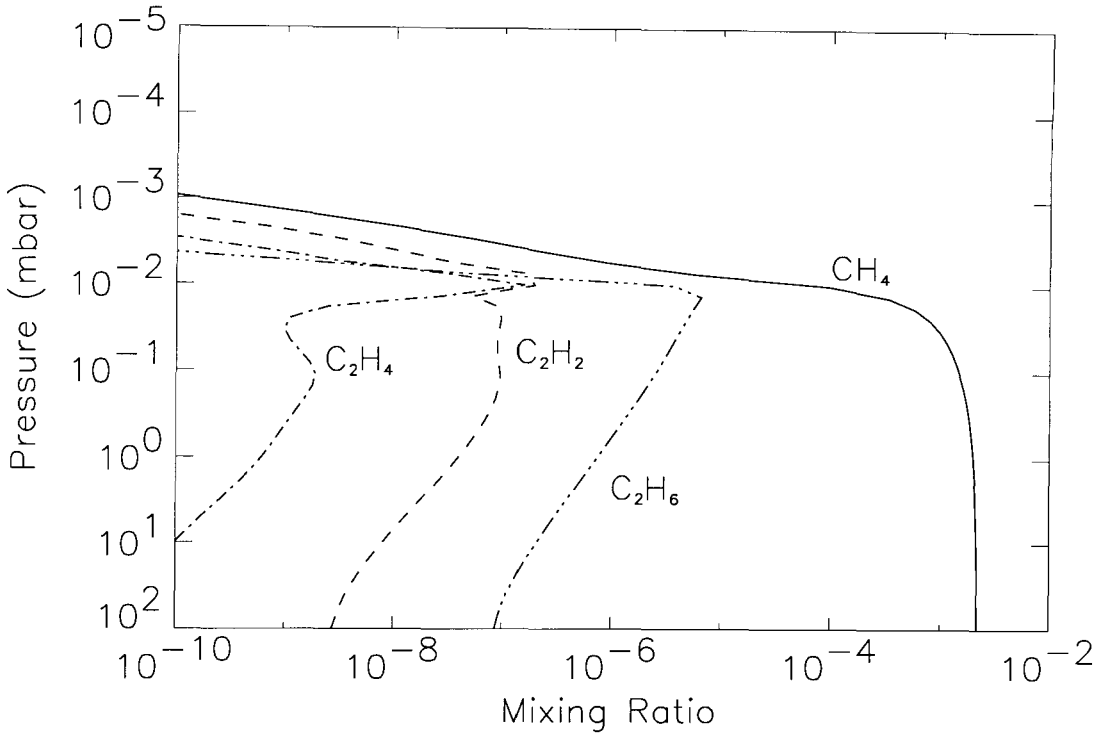

Figure 3.7 Computed mixing ratios for CH_4, C_2H_6, C_2H_4, and C_2H_2 for auroral model.

The calculated mixing ratios for CH_4, C_2H_6, C_2H_4, and C_2H_2 are shown in Figure 3.7. The mixing ratios for benzene (A_1), polycyclic aromatic hydrocarbons (PAHs), and heavy hydrocarbons ($C_{5-9}H_n$) are shown in Figure 3.8.

The result indicates that above 1×10^{-2} mbar, the abundances of the neutral species CH_4, C_2H_6, C_2H_4, C_2H_2 and benzene are significantly reduced. This is caused by the rapid loss due to ionization in that region. For example, methane is ionized by H_3^+ to form CH_5^+, as

$$H_3^+ + CH_4 \rightarrow CH_5^+ + H_2 \qquad \text{(R362)}$$

and some of the CH_5^+ recombine with electrons to form CH_3 via

$$CH_5^+ + e \rightarrow CH_3 + 2H \qquad \text{(R631)}$$

and then most of the CH_3 react with H_2 to form CH_4 again. However, some of the CH_5^+ react with other species to form higher hydrocarbons, which might not recycle back to form methane in our model.

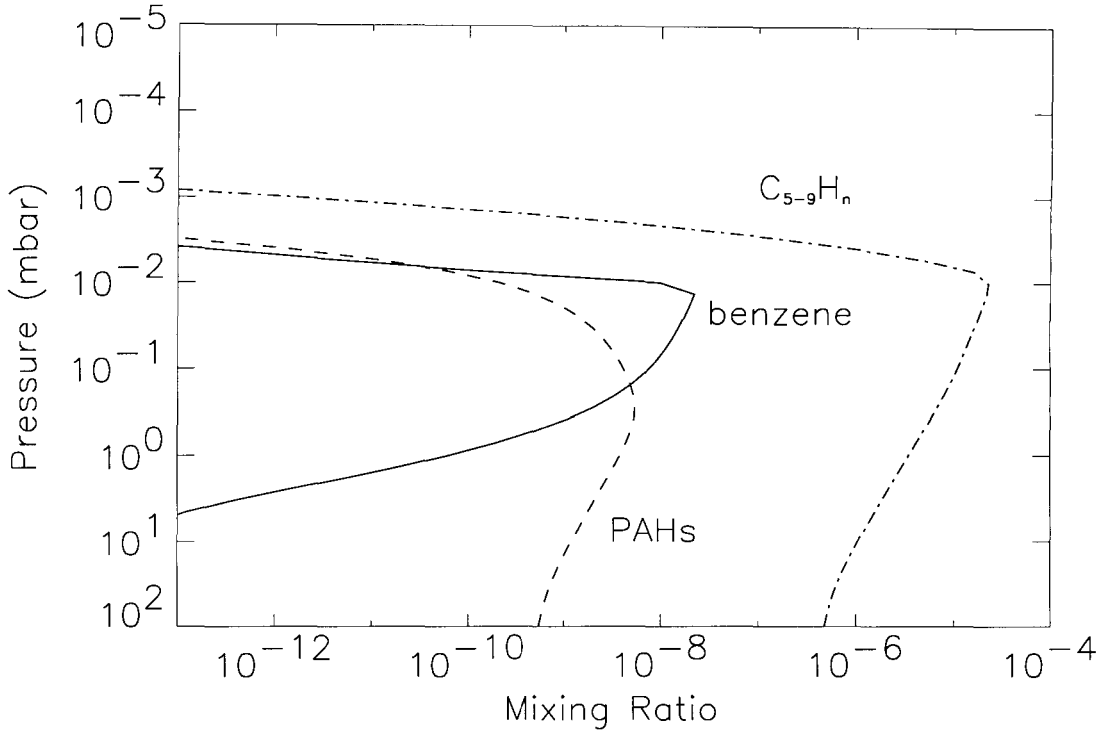

Figure 3.8 Computed mixing ratios for benzene (A_1), polycyclic aromatic hydrocarbons (PAHs), and heavy hydrocarbons ($C_{5-9}H_n$) for auroral model.

Similarly, in the model benzene is rapidly lost due to ionization in the same region by H_3^+, CH_5^+, $C_2H_3^+$, $C_3H_5^+$ and other ions to produce c-$C_6H_7^+$, half of which recombine with electrons to form benzene again (R695), while the other half produce C_6H_2 (R696). Some of C_6H_2 eventually recycle back to form benzene, but some will form the unrecoverable heavy hydrocarbons C_iH_n. On the other hand, since the PAHs and heavy hydrocarbons do not have a removal scheme, in our model, either by chemical reactions or condensation, their abundances do not suffer the irreversible loss due to the incompleteness of the reaction scheme available.

The calculated column abundance of benzene (A_1) above 50 mbar pressure level in the auroral model is 2.37×10^{14} molecules cm^{-2}. Because of the difference in the completeness of the reaction schemes of the two models due to the aforementioned problem, we should not compare this value with the calculated abundance in the non-auroral model. However, the auroral model shows that the mixing ratio of benzene can be as high as 2.2×10^{-8}, 35 times more enhanced than that from the non-auroral model of the same region (see Table 3.3, Case B).

Although the model results do not reflect accurate atmosphere composition, it is clear that ion chemistry promotes the production of heavy hydrocarbons. Compare two model results with different input energy fluxes (see models C and D in Table 3.3), we find that when the energy flux increases 40% from 11 to 16 ergs cm^{-2} s^{-1}, the concentrations of benzene and PAHs increase 8% and 7%, respectively.

3.4.5 Ion Chemistry Schemes for Benzene Production

There are two types of effects of ion chemistry on the benzene formation scheme. The first one is the formation of cyclic ions from reactions of non-cyclic molecules and ions. The major pathway for this type of reaction is the formation of c-$C_6H_7^+$ or c-$C_6H_5^+$ ions, which will recombine with electrons to form benzene. The second effect is the production of neutral species that are important for benzene production in the neutral scheme. In this section we discuss the ion chemistry schemes that lead to benzene formation in auroral model. First we will describe the chemistry of major

ions in the atmosphere, and then we will propose ion chemistry schemes for benzene production, and at last we will discuss the effects of ion chemistry on neutral species which will lead to benzene formation.

3.4.5.1 Chemistry of major ions

The schematic diagram illustrating the most important reaction pathways discussed in this section is shown in Figure 3.9.

Initial ionization Initial electron impact ionizes H_2, H, and He to produce large amounts of H_2^+, H^+, and He^+ due to reactions R274–277 (see Table 3.6). The ions quickly react with H_2 to form H_3^+:

$$H_2^+ + H_2 \rightarrow H_3^+ + H \quad \text{(R335)}$$

$$H^+ + 2H_2 \rightarrow H_3^+ + H_2 \quad \text{(R280)}$$

and the following two steps:

$$He^+ + H_2 \rightarrow HeH^+ + H \quad \text{(R306)}$$

$$HeH^+ + H_2 \rightarrow H_3^+ + He \quad \text{(R353)}$$

H_3^+ then transfers charges to carbon species to produce carbon ions via exchange reactions, such as the following important reactions:

$$H_3^+ + C \rightarrow CH^+ + H_2 \quad \text{(R358)}$$

$$H_3^+ + CH_3 \rightarrow CH_4^+ + H_2 \quad \text{(R361)}$$

$$H_3^+ + CH_4 \rightarrow CH_5^+ + H_2 \quad \text{(R362)}$$

$$H_3^+ + C_2H_2 \rightarrow C_2H_3^+ + H_2 \quad \text{(R363)}$$

$$H_3^+ + C_2H_4 \rightarrow C_2H_3^+ + 2H_2 \quad \text{(R365)}$$

Ions with two carbon atoms Ions with one carbon atom react with other carbon species to form ions with two carbon atoms. The most important reactions are

$$CH_3^+ + CH_4 \rightarrow C_2H_5^+ + H_2 \quad \text{(R404)}$$

$$CH_5^+ + C_2H_2 \rightarrow C_2H_3^+ + CH_4 \quad \text{(R429)}$$

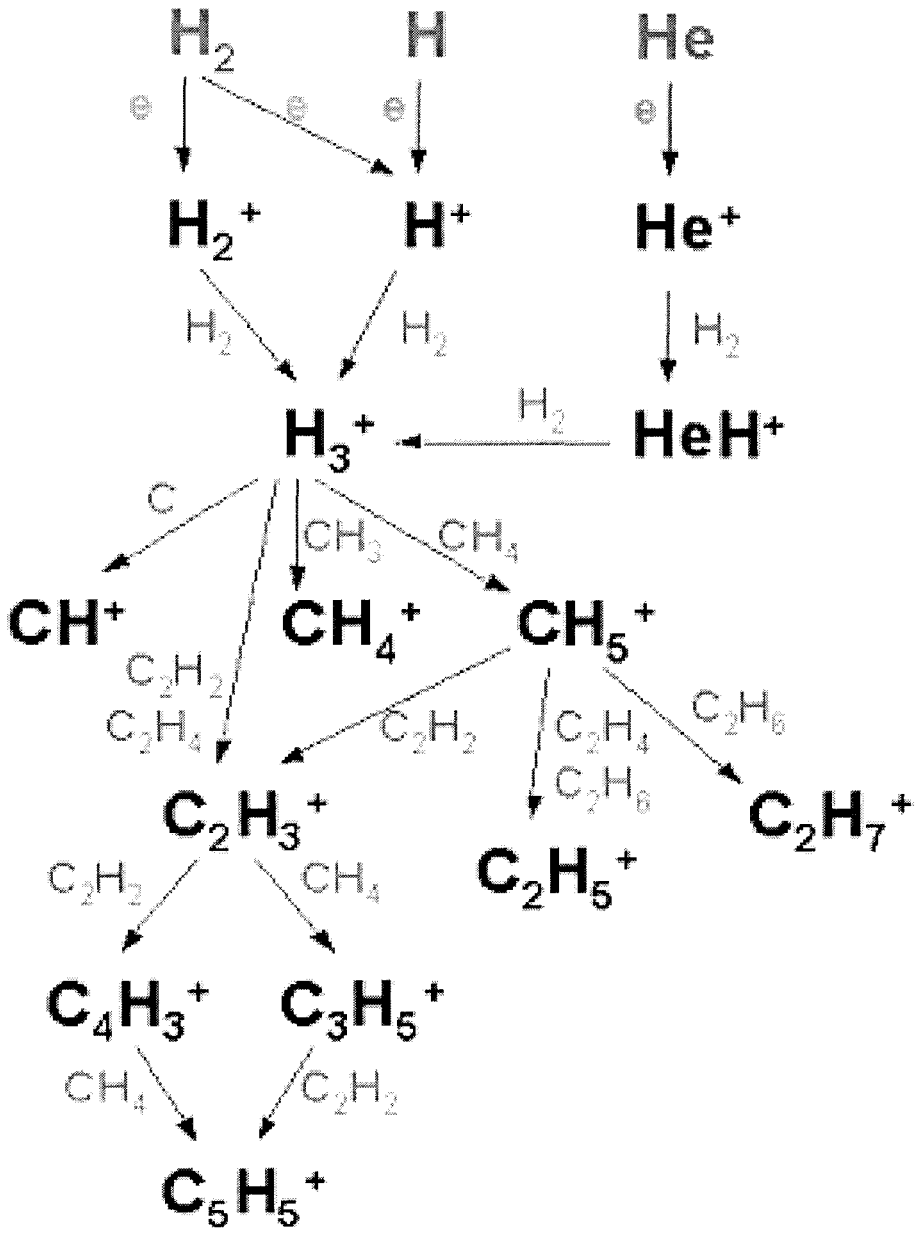

Figure 3.9 Important reaction pathways for the production of major ions.

$$CH_5^+ + C_2H_4 \rightarrow C_2H_5^+ + CH_4 \quad \text{(R430)}$$

$$CH_5^+ + C_2H_6 \rightarrow C_2H_5^+ + CH_4 + H_2 \quad \text{(R431)}$$

$$CH_5^+ + C_2H_6 \rightarrow C_2H_7^+ + CH_4 \quad \text{(R432)}$$

$C_2H_3^+$ is a very abundant ion species in the atmosphere. It reacts with neutral carbon species to form ions with higher carbon numbers, such as c-$C_3H_2^+$, $C_3H_5^+$, and $C_4H_3^+$, which will lead to benzene formation.

$C_3H_5^+$ The major production pathway for $C_3H_5^+$ is through reaction R473:

$$C_2H_3^+ + CH_4 \rightarrow C_3H_5^+ + H_2 \quad \text{(R473)}$$

$C_4H_3^+$ The major production pathways for $C_4H_3^+$ include the following four schemes:
Scheme A:

$$C_2H_3^+ + C_2H_2 \rightarrow C_4H_3^+ + H_2 \quad \text{(R474)}$$

Scheme B:

$$C_2H_3^+ + C \rightarrow \text{c-}C_3H_2^+ + H \quad \text{(R472)}$$

$$\text{c-}C_3H_2^+ + C \rightarrow C_4H^+ + H \quad \text{(R527)}$$

$$C_4H^+ + H_2 \rightarrow C_4H_2^+ + H \quad \text{(R554)}$$

$$C_4H_2^+ + H \rightarrow C_4H_3^+ + h\nu \quad \text{(R557)}$$

Net: $C_2H_3^+ + 2C + H_2 \rightarrow C_4H_3^+ + 2H$

This scheme describes a pathway to increase ion mass by addition of carbon atoms, which is similar to that proposed in McEwan et al. (1999). Instead of reaction R527, an alternative pathway to form C_4H^+ from c-$C_3H_2^+$ is the following two steps of reactions:

$$\text{c-}C_3H_2^+ + C \rightarrow C_4^+ + H_2 \quad \text{(R526)}$$

$$C_4^+ + H_2 \rightarrow C_4H^+ + H \quad \text{(R553)}$$

Scheme C:

$$C_3H_5^+ + C \rightarrow C_4H_3^+ + H_2 \quad \text{(R547)}$$

Scheme D:

$$H_3^+ + C_4H_2 \rightarrow C_4H_3^+ + H_2 \quad \text{(R373)}$$

$C_5H_5^+$ $C_5H_5^+$ is an important ion in benzene formation, the major production pathways for which include

$$C_3H_5^+ + C_2H_2 \rightarrow C_5H_5^+ + H_2 \quad \text{(R548)}$$

and

$$C_4H_3^+ + CH_4 \rightarrow C_5H_5^+ + H_2 \quad \text{(R570)}$$

The density profiles of the most important ions discussed above are shown in Figure 3.10 and Figure 3.11.

3.4.5.2 Benzene formation via c-$C_6H_7^+$

The schematic diagram illustrating the most important reaction pathways discussed in this section is shown in Figure 3.12.

A major pathway to produce benzene (A_1) is by the dissociative recombination of c-$C_6H_7^+$ with electrons:

$$c\text{-}C_6H_7^+ + e \rightarrow A_1 + H \quad \text{(R695)}$$

There are three major sets of pathways that lead to c-$C_6H_7^+$ formation: (1) reactions with C_2H_2 or C_3H_4; (2) cyclization of c-$C_6H_5^+$; (3) polymerization of ion by C_2H_2. In Figure 3.13, the reaction rates of the c-$C_6H_7^+$ production in each of the pathways is plotted, along with the rate for the recombination reaction R695 which forms benzene.

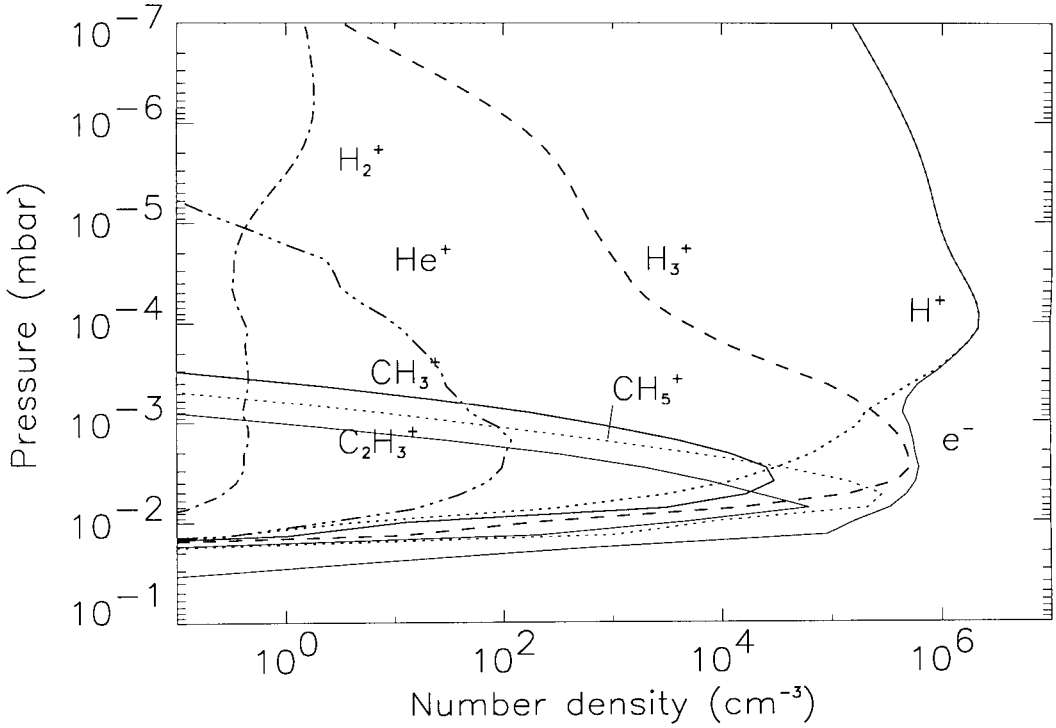

Figure 3.10 Computed density profiles of electron, H^+, He^+, H_2^+, H_3^+, CH_3^+, CH_5^+, and $C_2H_3^+$, for auroral model.

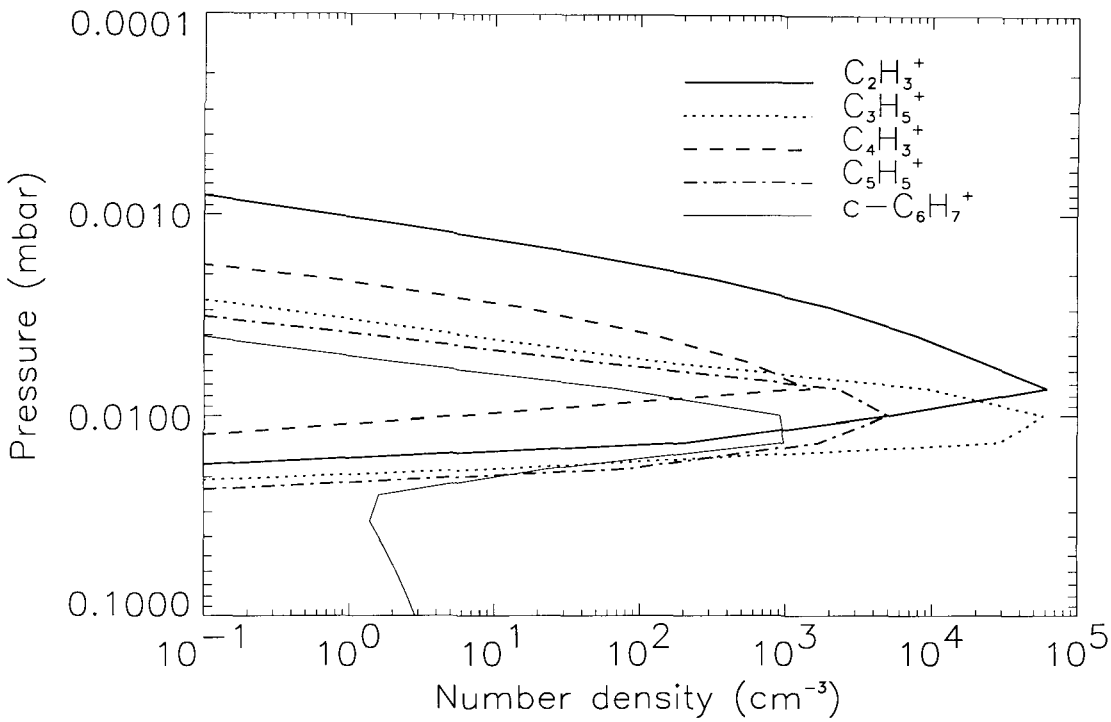

Figure 3.11 Computed density profiles of $C_2H_3^+$ (thick solid), $C_3H_5^+$ (thick dotted), $C_4H_3^+$ (thick dashed), $C_4H_5^+$ (thick dash-dot-dash), and c-$C_6H_7^+$ (thin solid) for auroral model.

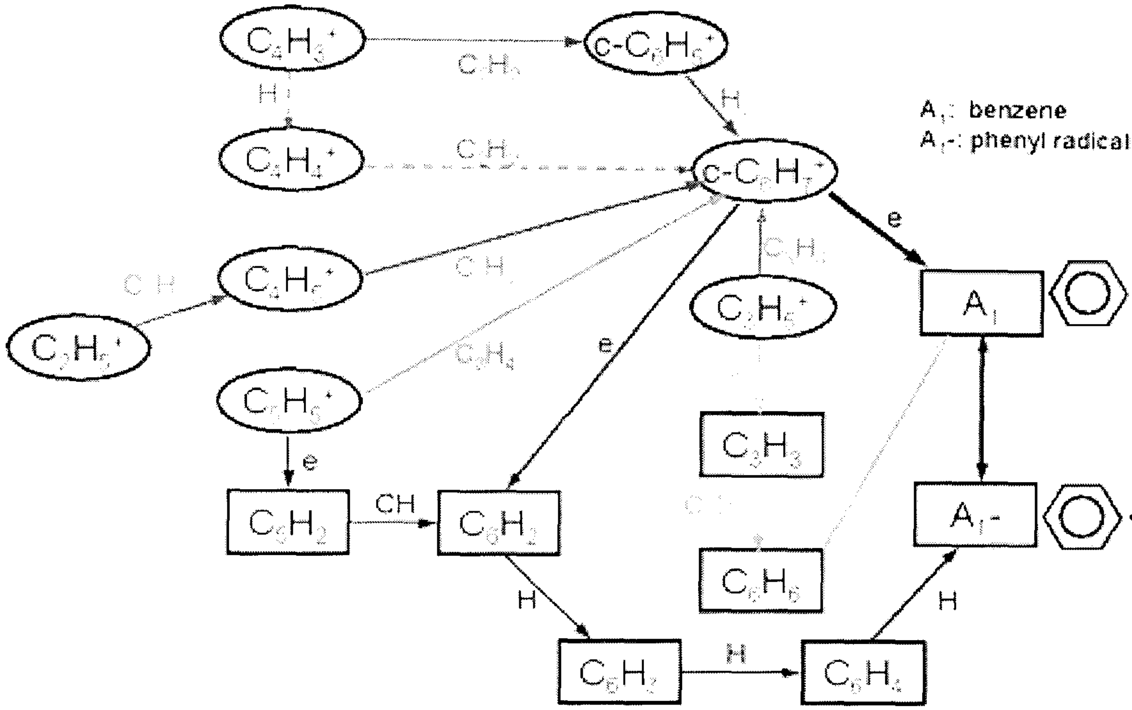

Figure 3.12 Major reaction pathways for benzene production in auroral model.

Reactions with C_2H_2 or C_3H_4 Anicich proposes a pathway to form $C_6H_7^+$ via reactions with C_2H_2 and C_3H_4 (private communication). Like most other similar reactions, it is unclear whether the product $C_6H_7^+$ is in cyclic form or not. We assume the cyclic form so the upper limit of the reaction rate for this pathway is established.

Scheme A1:

$$C_3H_5^+ + C_3H_4 \rightarrow \text{c-}C_6H_7^+ + H_2 \qquad \text{(R551)}$$

Scheme A2:

$$C_5H_5^+ + C_3H_4 \rightarrow \text{c-}C_6H_7^+ + H_2 \qquad \text{(R597)} \dagger$$

In our model, Scheme A1 is more than ten times faster than Scheme A2 due to the greater abundance of $C_3H_5^+$ than $C_5H_5^+$ and the faster exchange rate of R551 than R597. Scheme A1 is the most significant ion reaction scheme leading to the formation of benzene.

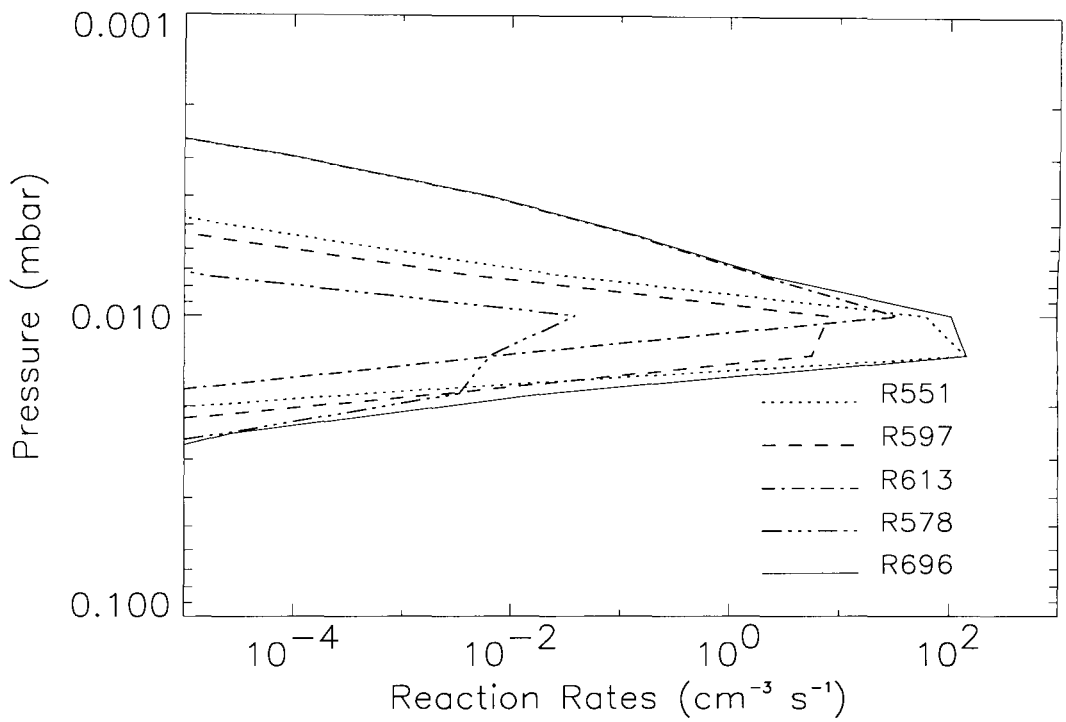

Figure 3.13 Computed altitude profiles of the reaction rates involving production and loss of c-$C_6H_7^+$ for auroral model. Production: R551 ($C_3H_5^+ + CH_3C_2H \rightarrow$ c-$C_6H_7^+ + H_2$), R612 (c-$C_6H_5^+ + H_2 \rightarrow$ c-$C_6H_7^+ + h\nu$), R597 ($C_5H_5^+ + CH_3C_2H \rightarrow$ c-$C_6H_7^+ + C_2H_2$), and R578 ($C_4H_5^+ + C_2H_2 \xrightarrow{M}$ c-$C_6H_7^+$). Loss: R695 (c-$C_6H_7^+ + e \rightarrow A_1 + H$).

Cyclization of c-$C_6H_5^+$ This set of pathways is similar to that outlined by McEwan et al. (1999) in their study of the benzene synthesis in dense interstellar clouds. The cyclic ion c-$C_6H_7^+$ is formed from c-$C_6H_5^+$, which is mainly formed from $C_4H_3^+$ or $C_4H_4^+$.

Scheme A3a:

	$C_4H_3^+ + C_2H_2 \rightarrow$ c-$C_6H_5^+ + h\nu$	(R571) $*$ †
	c-$C_6H_5^+ + H_2 \rightarrow$ c-$C_6H_7^+ + h\nu$	(R612)
Net:	$C_4H_3^+ + C_2H_2 + H_2 \rightarrow$ c-$C_6H_7^+$	(Scheme A3a)

Scheme A3b:

	$C_4H_3^+ + H \rightarrow C_4H_4^+ + h\nu$	(R568)
	$C_4H_4^+ + C_2H_2 \rightarrow$ c-$C_6H_5^+ + H$	(R577) $*$ †
	c-$C_6H_5^+ + H_2 \rightarrow$ c-$C_6H_7^+ + h\nu$	(R612)
Net:	$C_4H_3^+ + C_2H_2 + H_2 \rightarrow$ c-$C_6H_7^+$	(Scheme A3b)

Reaction R568 is a rather slow step therefore, Scheme A3a is a significantly faster pathway than Scheme A2b.

Polymerization of ion by C_2H_2 Bayes proposes the polymerization of ions by C_2H_2 to form benzene (Vinckier et al. (1962), and private communication). There are major uncertainties in this set of pathways. First of all, the rate coefficients for the polymerization reactions R475 and R578 (see below) are unknown, and we estimate the two-body rates to be 1.0×10^{-9} cm^3 s^{-1}, and three-body rates to be 1.0×10^{-27} cm^{-6} s^{-1}. In addition, it is unknown what form the product $C_6H_7^+$ is in, and we assume the branching ratio for producing the cyclic form of $C_6H_7^+$ to be the upper limit of one. With these uncertainties, this set of pathways only gives an estimated production rate for benzene formation via C_2H_2 polymerization.

Scheme A4:

	$C_2H_3^+ + C_2H_2 \xrightarrow{M} C_4H_5^+$	(R475)
	$C_4H_5^+ + C_2H_2 \xrightarrow{M}$ c-$C_6H_7^+$	(R578) $*$ †

Net: $C_2H_3^+ + 2C_2H_2 \rightarrow c\text{-}C_6H_7^+$ (Scheme A4)

Note that instead of reaction R475, a much faster pathway to form $C_4H_5^+$ is from $C_2H_5^+$:

$$C_2H_5^+ + C_2H_2 \rightarrow C_4H_5^+ + H_2 \quad \text{(R505)}$$

In our auroral model, the total production of benzene through ion reactions is greater than that through neutral reactions, and it can be concluded that ion chemistry adds a considerable amount of benzene in the polar atmosphere.

3.4.5.3 Effects on neutral species

Reactions of hydrocarbon ions have great effects on the chemical composition of neutral species in the region of particle deposition. Heavy hydrocarbons are likely formed through successive ion-neutral reactions. In this section we discuss the relevant ion reactions that promote the production of neutral species which are important in benzene formation. The schematic diagram illustrating the most important reaction pathways discussed in this section is shown in Figure 3.12. The altitude profiles of the reaction rates for the limiting steps of each of the six most important benzene production pathways, including both neutral chemistry and ion chemistry, are shown in Figure 3.14.

C_3H_3 production Because of the great abundance of $C_3H_5^+$ ions, the electron recombination reaction of $C_3H_5^+$ produces large amounts of C_3H_3, which is an important neutral species in Schemes N1 and N2. The production rate of C_3H_3 through recombination is comparable to that through neutral reactions. The following is an example of of this scheme.

Scheme A5:

$$C_3H_5^+ + e \rightarrow C_3H_3 + H_2 \quad \text{(R664)}$$

$$C_3H_3 + C_3H_3 \xrightarrow{M} C_6H_6 \quad \text{(R200)}$$

$$C_6H_6 + H \rightarrow A_1 + H \quad \text{(R261)} * \dagger$$

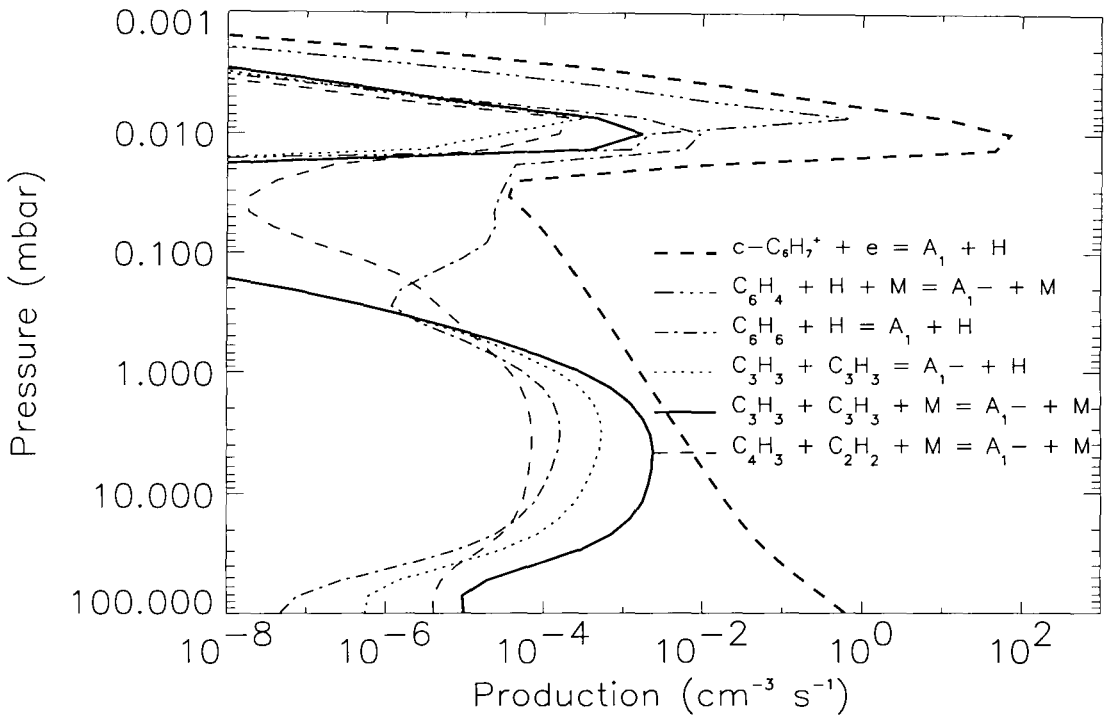

Figure 3.14 Computed altitude profiles of the reaction rates for the limiting steps of each of the six most important benzene production pathways, including both neutral chemistry and ion chemistry, for auroral model. The reactions are listed in order of decreasing column reaction rate.

C_6H_2 and C_6H_4 In our model, ion chemistry produces a large amount of C_6H_2 through recombination reactions (R689, R691, R693 and R696). C_6H_2 subsequently reacts with H to produce C_6H_4, which may form phenyl (A_1-). This is a variation to Scheme N6.

Scheme N6v:

$$C_6H_2 + H \xrightarrow{M} C_6H_3 \qquad \text{(R248)}$$
$$C_6H_3 + H \xrightarrow{M} C_6H_4 \qquad \text{(R250)}$$
$$C_6H_4 + H \xrightarrow{M} A_1\text{-} \qquad \text{(R253)} * \dagger$$

Net: $C_6H_2 + 3H \rightarrow A_1$- (Scheme N6v)

The reaction of C_6H_4 to phenyl (A_1-) is very slow without the additional source of C_6H_4 produced from the ion chemistry. Schemes A7a and A7b illustrate the major pathways to produce C_6H_4 from ion reactions.

Scheme A6a:

$$C_5H_5^+ + e \rightarrow C_5H_2 + H + H_2 \qquad \text{(R682)}$$
$$C_5H_2 + CH \rightarrow C_6H_2 + H \qquad \text{(R244)} *$$

Scheme A6b:

$$c\text{-}C_6H_7^+ + e \rightarrow C_6H_2 + H + 2H_2 \qquad \text{(R696)}$$

Other neutral species The production of other neutral species such as C_3H_2, C_4H_3 and C_4H_5 through known recombination reactions are small compared to their neutral reaction counterparts, thus ion chemistry has little effect on the benzene formation pathways through these molecules.

3.5 Conclusion

It is our intent to study the complete chemical scheme for the formation of benzene on Jupiter and to explain the recent observations. In this work we have proposed two models. The first model investigates the reaction pathways of neutral chemistry

to form benzene in non-auroral regions. The second model investigates the effect of ion chemistry on the neutral composition and the benzene formation in the auroral regions.

In the neutral model, we have updated the neutral reaction kinetics, and are successful in predicting the observed benzene concentration. Six major chemical schemes for benzene formation are discussed in detail. However, there are still uncertanties in the reaction kinetics of the ring production process. Resolution of these uncertainties will improve the accuracy of our model.

In the auroral model, we couple ion chemistry with neutral chemistry and propose six major ion-related chemical schemes for benzene production. Our model is able to show that ion chemistry increases the production of heavy hydrocarbons, and explain the observed enhancement of benzene concentration in the polar regions. However, because our current knowledge of ion chemistry is incomplete, it is impossible at this stage to produce an accurate model to describe the chemistry of hydrocarbon ions and its effect on benzene formation.

In order to fully understand and model the benzene on Jupiter, it is necessary to

1. carefully evaluate the key reactions in benzene formation process;

2. measure important ion-related reaction rates and products;

3. improve our understanding of Jupiter's aurora.

Chapter 4 Evolution of CO on Titan

4.1 Abstract

The early evolution of Titan's atmosphere is expected to have produced enrichment in the heavy isotopomers of CO, ^{13}CO and $C^{18}O$, relative to $^{12}C^{16}O$. However, the original isotopic signatures may be altered by photochemical reactions. This chapter explains why there is no isotopic enrichment in C in Titan's atmosphere, despite significant enrichment of heavy H, N, and O isotopes. We show that there is a rapid exchange for C atoms between the CH_4 and CO reservoirs, mediated by the reaction $^1CH_2 + {}^*CO \rightarrow {}^{1*}CH_2 + CO$, where $^*C$ is ^{13}C. Based on recent laboratory measurements, we estimate the rate coefficient for this reaction to be 3.2×10^{-12} cm^3 s^{-1} at the temperatures consistent with those of Titan's upper atmosphere. We investigate the isotopic dilution of CO using the Caltech/JPL one-dimensional photochemical model of Titan. Our model suggests that the time constant for isotopic exchange through the above reaction is about 800 Myr, which is significantly shorter than the age of Titan, and therefore any original isotopic enhancement of ^{13}C in CO may have been diluted by the exchange process. In addition, a plausible model for the evolution history of CO on Titan after the initial escape is proposed.

The content of this chapter is based on a paper accepted in *Icarus*, July 2001.

4.2 Introduction

In the first paper on the photochemistry of hydrocarbons on Titan, Strobel (1974) pointed out the fundamental difference between the stability of methane on Jupiter and Titan. On Jupiter, CH_4 is destroyed in the upper atmosphere by photolysis and converted to higher hydrocarbons and hydrogen. The products are eventually transported to the lower atmosphere, where thermodynamic equilibrium at high temperature and pressure recycles the hydrocarbons and hydrogen back to CH_4. However, on Titan the destruction of CH_4 is irreversible. The higher hydrocarbons condense on the surface, and hydrogen escapes to space. To maintain the atmosphere in a steady state, Strobel (1974) suggested that CH_4 must be replenished by outgassing from the crust, which is thought to be composed of CH_4 and NH_3 hydrates (Lewis, 1971). Subsequent observations by Voyager and modeling largely confirmed the idea of the transient nature of Titan's atmosphere (see, for example, Yung et al. (1984)). From the photochemical model of Yung et al. (1984), the column abundance and rate of destruction for CH_4 are 4.6×10^{24} cm^{-2} and 1.5×10^{10} cm^{-2} s^{-1}, respectively. Therefore the lifetime of CH_4 in the atmosphere is about 10 Myr, which is very short compared with the age of the solar system, 4.6 Gyr. Yung et al. (1984) also extended Strobel's idea to N_2 and CO on Titan, and the relevant quantities are summarized in Table 4.1. Their work concludes that over the age of the solar system, N_2 is fairly stable, and CO is much less stable. In this work, we will revise the quantitative rate of change of CO in Table 4.1. It should be emphasized that the destruction rates are based on extrapolation of present photochemical rates in the model. It does not include alternative models of evolution (see, for example, Lorenz et al. (1997)) or what might have happened during the period close to the origin of the atmosphere (Atreya et al., 1978; Lunine et al., 1999; Lammer et al., 2000).

Pinto et al. (1986) pointed out that the relative abundances of the isotopomers of CH_4 could be used to constrain the evolutionary history of Titan's atmosphere. This idea is based on the fact that chemical destruction or escape to space differentiates between isotopomers, resulting in measurable isotopic fractionations. This idea can

Table 4.1. Summary of column abundances, destruction rates and lifetimes of CH_4, N_2 and CO on Titan.

	Column abundance (cm^{-2})	Destruction rate (cm^{-2} s^{-1})	Lifetime (year)
CH_4	4.59×10^{24}	1.5×10^{10}	9.7×10^{6}
N_2	2.30×10^{26}	2.8×10^{8}	2.6×10^{10}
CO	1.38×10^{22}	6.1×10^{5}	2.1×10^{9}

References. — All values are taken from Yung et al. (1984).

be applied to all other species, such as CO, N_2, or HCN. Figure 4.1 summarizes the isotopic measurements on Titan for hydrogen, carbon, nitrogen and oxygen, plotted relative to the protosolar (for deuterium) or terrestrial values (for carbon, nitrogen and oxygen). All D/H enhancements are inferred from measurements of CH_3D/CH_4 ratios, which are: D/H = $16.1^{+16.5}_{-8} \times 10^{-5}$ from ground-based data (De Bergh et al., 1988), $15.0^{+14.0}_{-5.0} \times 10^{-5}$ from Voyager spectra (Coustenis et al., 1989), $7.75(\pm 2.25) \times 10^{-5}$ from Infrared Telescope Facility (IRTF) measurements at 8.7-micron wavelength (Orton, 1992), and $9.5(\pm 2.5) \times 10^{-5}$ from the Short Wavelength Spectrometer (SWS) on-board ESA's Infrared Space Observatory (ISO) spectrum (Coustenis and Taylor, 1999). The protosolar value of D/H is $2.6(\pm 0.7) \times 10^{-5}$ (Geiss and Gloeckler, 1998; Mahaffy et al., 1998), 25% of the CH_3D/CH_4 ratio. The $^{13}C/^{12}C$ measurements are: $H^{13}CN/H^{12}CN$ through Earth-based millimeter measurements at 88.63 GHz by Hidayat et al. (1997), and $^{12}C^{13}CH_6/^{12}C^{12}CH_6$ from 12-micron wavelength spectra measurements by Orton (1992). The terrestrial value for $^{13}C/^{12}C$ adopted here is 0.011 (Van Dishoeck et al., 1993). The $^{15}N/^{14}N$ enrichment is determined from Earth-based millimetric wavelength spectroscopic observations of $HC^{15}N/HC^{14}N$ and the ratio is determined to be 4.5 times that of the Earth value (Hidayat and Marten, 1998). For $^{18}O/^{16}O$ enhancement, Owen et al. (1999) report a preliminary value of $^{18}O/^{16}O$ about two times the terrestrial value of 2×10^{-3} in the detection of the (3-2)

line of $C^{18}O$ at 329.33 GHz in the radio spectrum. Figure 4.1 clearly shows that on Titan there is enrichment in the heavy isotopes of H, N and O, but not in C.

According to Yung et al. (1984), about 17% of the original N_2 on Titan has been destroyed by escape to space and loss to the ground. However, on the basis of the isotopic data, Lunine et al. (1999) proposed that there was an early period of massive escape of atmospheric species. The driving force could have been the more active phase of the sun in the early history of Titan (Pepin, 1991; Kass and Yung, 1995; Lammer et al., 2000). Similar to N_2, a large amount of CO could have been lost by escape from Titan in the past. We expect by analogy with N_2 that the heavy isotopomers of CO, ^{13}CO and $C^{18}O$, would be enriched relative to $^{12}C^{16}O$. However, because of the source of new CH_4 from the interior of the satellite, carbon enrichment in CO could be diluted, if a chemical pathway exists for exchange between the carbon atoms in CH_4 and CO. This latter possibility is investigated in this chapter using an updated version of the Caltech/JPL one-dimensional photochemical model of Titan.

The present work is primarily motivated by the curious isotopic fractionation of CO, as summarized in Figure 4.1. According to Hidayat et al. (1997); Hidayat and Marten (1998), the $^{13}CO/^{12}CO$ ratio is the same as $H^{13}CN/H^{12}CN$, which is close to the terrestrial value. On the other hand, the $C^{18}O/C^{16}O$ ratio is two times the terrestrial value (Owen et al., 1999). Why is there an enrichment in $C^{18}O$ but not in ^{13}CO? To address this question, we will carry out a critical examination of the chemical kinetics relevant to CO on Titan, followed by modeling of the evolution of CO and its isotopomers. The methodology adopted in the evolution model is based on that of McElroy and Yung (1976).

4.3 Kinetics

The photochemical model adopted in this work is based on Yung et al. (1984) and Moses et al. (2000a). There are several important modifications of the kinetics, which will be discussed in detail in this section. All reaction numbers refer to the reaction list of the complete Titan model. The reactions discussed in this chapter are listed

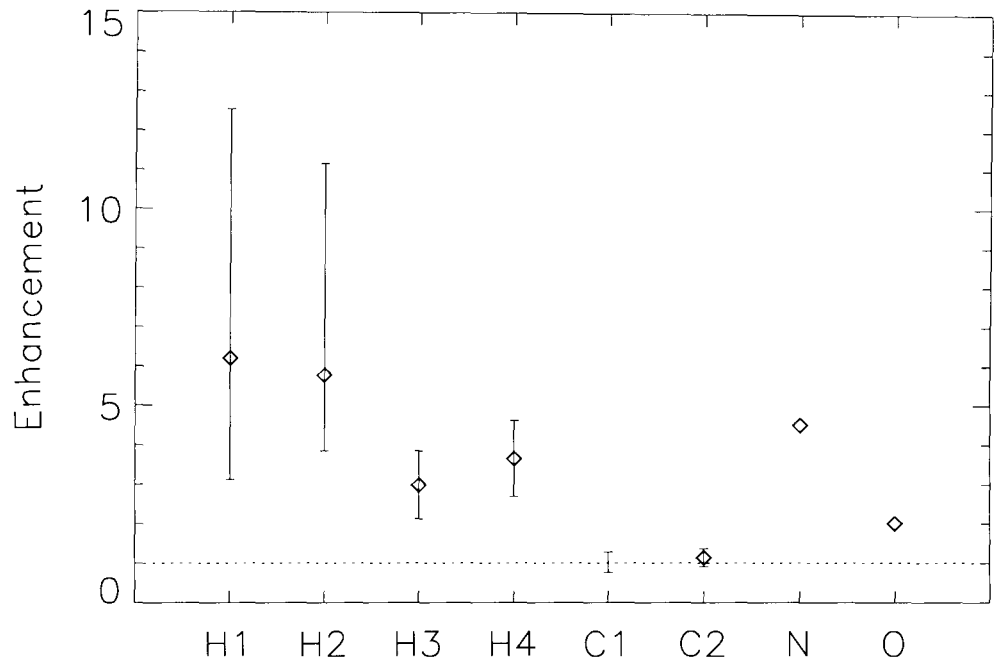

Figure 4.1 Summary of the hydrogen, carbon, nitrogen and oxygen isotopic measurements on Titan, plotted relative to the protosolar (for deuterium) or terrestrial value (for carbon, nitrogen and oxygen). For D/H, H1 is from De Bergh et al. (1988); H2 is from Coustenis et al. (1989); H3 is from Orton (1992); H4 is from Coustenis and Taylor (1999). For $^{13}C/^{12}C$, C1 is from HCN by Hidayat et al. (1997); C2 is from C_2H_6 by Orton (1992). N is $^{15}N/^{14}N$ from Hidayat and Marten (1998). O is $^{18}O/^{16}O$ from CO by Owen et al. (1999). The protosolar value of D/H is $2.6(\pm 0.7) \times 10^{-5}$ (Geiss and Gloeckler, 1998; Mahaffy et al., 1998). The terrestrial value for $^{13}C/^{12}C$ is 0.011 (Van Dishoeck et al., 1993), for $^{15}N/^{14}N$ is 3.68×10^{-3}, for $^{18}O/^{16}O$ is 2×10^{-3}.

in Table 4.2. The species $^1CH_2$ and $^3CH_2$ refer to the singlet (excited) and triplet (ground) state of the methylene radical, respectively. A schematic diagram showing the major reaction pathways and ultimate fate of the oxygen atom derived from meteoritic H_2O is shown in Figure 4.2.

4.3.1 OH + CH_3

We will examine three reaction channels for the reaction between OH and CH_3:

$$OH + CH_3 \rightarrow CO + 2H_2 \quad (1)$$

$$OH + CH_3 \rightarrow H_2O + {}^1CH_2 \quad (2)$$

$$OH + CH_3 \rightarrow HCOH + H_2 \quad (3)$$

Channel (1) is the major pathway to produce CO in Yung et al. (1984), where k_1 (Yung) = 6.7×10^{-12} cm^3 s^{-1}. This is actually the overall reaction rate coefficient measured by Fenimore (1968). Although possible products may lead to the formation of CO, the products formed in his experiment and the branching ratios are unknown. Therefore channel (1) should no longer be included in our reaction list.

Channel (2) is the major channel for this reaction used by Moses et al. (2000a), where k_2 (Moses) = 1.0×10^{-12} cm^3 s^{-1}, taken from the experiment of Oser et al. (1992). We examined the work of the Oser group (Oser et al., 1992; Humpfer et al., 1995). They describe difficult and complicated experiments, and the analysis of the data is subject to many uncertainties. In particular, their reliance on the H versus D experiments is unreliable as there are many potential traps that they may not have encountered. For example, exchange of H_2O and HDO on the walls is common and depends on the history of past experiments. Even though they were generating sufficient quantities of D atoms from OD + OD, their model does not appear to include the exchange reaction, $CH_3 + D \rightarrow CH_2D + H$, which is very fast at all pressures. Therefore, we no longer use their result for channel (2).

The reaction OH + CH_3 is investigated by Deters et al. (1998). They observed singlet methylene directly in this reaction by laser magnetic resonance (LMR). They studied the rate coefficient and the product distribution of the reaction at room

Table 4.2. Partial list of reactions in standard Titan model.

No.	Reaction	Rate Coefficient	Ref.
R136	$C + H_2 \xrightarrow{M} {}^3CH_2$	$k_0 = 7.00 \times 10^{-32}$ $k_\infty = 2.06 \times 10^{-11} \exp(-57/T)$	1
R137	$C + C_2H_2 \xrightarrow{M} C_3H_2$	$k_0 = 1.00 \times 10^{-31}$ $k_\infty = 2.10 \times 10^{-10}$	1
R247	$H_2O + h\nu \rightarrow H + OH$	4.947×10^{-8}	1
R248	$H_2O + h\nu \rightarrow 2H + O$	3.197×10^{-9}	1
R250	$CO + h\nu \rightarrow C + O$	3.450×10^{-9}	1
R251	$CO_2 + h\nu \rightarrow CO + O$	6.801×10^{-11}	1
R253	$HCO + h\nu \rightarrow H + CO$	5.390×10^{-6}	1
R254	$H_2CO + h\nu \rightarrow HCO + H$	4.307×10^{-7}	1
R255	$H_2CO + h\nu \rightarrow H_2 + CO$	5.619×10^{-7}	1
R269	$O + CH_3 \rightarrow H_2CO + H$	1.40×10^{-10}	1
R280	$O + C_2H_4 \rightarrow H_2CCO + H_2$	$1.50 \times 10^{-19} T^{2.08}$	1
R315	$OH + CH_3 \rightarrow H_2O + {}^1CH_2$	$1.0 \times 10^{-10}(T/300)^{-0.91} \exp(-275/T)$	2
R320	$OH + C_2H_2 \xrightarrow{M} CH_3CO$	$k_0 = 2.6 \times 10^{-26} T^{-1.5}$ $k_\infty = 1.0 \times 10^{-17} T^{-2}$	1
R329	$OH + CO \rightarrow CO_2 + H$	1.5×10^{-13}	1
R344	$CO_2 + {}^3CH_2 \rightarrow CO + H_2CO$	2.8×10^{-15}	3
R407	$CH_3CO + H \rightarrow HCO + CH_3$	3.57×10^{-11}	1
R410	$CH_3CO + CH_3 \rightarrow CO + C_2H_6$	4.9×10^{-11}	1
R446	${}^1CH_2 + {}^*CO \rightarrow {}^{1*}CH_2 + CO$	3.2×10^{-12}	4
R447	${}^1CH_2 + N_2 \rightarrow {}^3CH_2 + N_2$	$5.1 \times 10^{-13} T^{0.5}$	5
R448	$OH + CH_3 \rightarrow H_2CO + H_2$	$1.9 \times 10^{-14}(T/300)^{-0.12} \exp(209/T)$	2

Note. — Two-body rate coefficients and high-pressure limiting rate coefficients for three-body reactions (k_∞) are in units of $cm^3\ s^{-1}$. Low-pressure limiting rate coefficients for three-body reactions (k_0) are in units of $cm^6\ s^{-1}$. M represents any third body such as H_2. For photolysis reactions, the rate coefficients are the rate at 5×10^{-10} mbar.

References. — (1) Moses et al. (2000a); (2) Pereira et al. (1997); (3) Darwin and Moore (1995); (4) this work; (5) Ashfold et al. (1981)

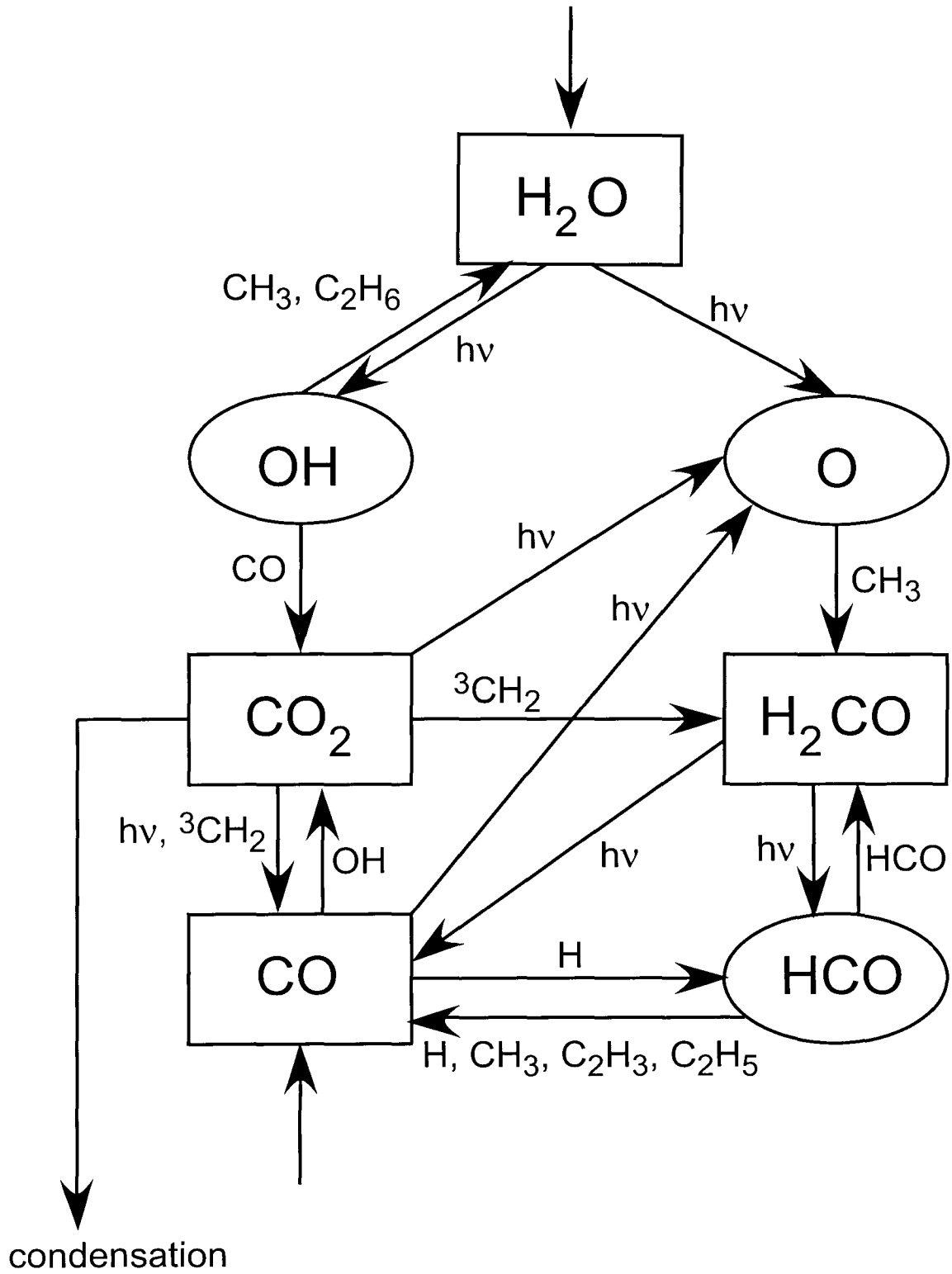

Figure 4.2 Major reaction pathways for oxygen species in Titan model. The symbol $h\nu$ corresponds to a solar ultraviolet photon. Radical species are outlined as ovals and stable molecules as rectangles.

temperature in low pressures down to 0.7 mbar. The branching ratio for reaction channel (2) is 0.89 ± 0.09 at 1.33 mbar and 298 K. From their Figure 7, extrapolating the fall-off curve of the overall rate coefficient down to the low-pressure limit, we get $k_{overall}$ (Deters) $= 3.3 \times 10^{-11}$ cm^3 s^{-1}. Using branching ratio 0.89, we determined that k_2 (Deters) $= 3.0 \times 10^{-11}$ cm^3 s^{-1} for channel (2).

The experimental measurements by Pereira et al. (1997) confirm the high-pressure limiting value for the overall reaction that several other groups have measured. They make a good case that channel (2) is approximately thermo-neutral and not endothermic as suggested by Oser et al. (1992). Consequently, they also favor channel (2) as the dominant reaction at the low pressures that are of interest to our modeling.

We use Pereira et al. (1997)'s calculations as a consistent set of rate coefficients for the different channels. Of the six possible product channels they studied, only channels (2) and (3) are significant at the low temperatures we are interested in. From their Appendix B, using statistical mechanics, their results can be applied for temperatures 200 K $\leq T \leq$ 1200 K. Extrapolation to 150 K should not add very much uncertainty to our model.

In our work, the reactions and the rate coefficients we adopted are

$$OH + CH_3 \rightarrow H_2O + {}^1CH_2 \qquad \text{(R315)}$$

$$k_{315} = 1.0 \times 10^{-10}(T/300)^{-0.91} \exp(-275/T) \text{cm}^3 \text{ s}^{-1}$$

$$OH + CH_3 \rightarrow H_2CO + H_2 \qquad \text{(R448)}$$

$$k_{448} = 1.9 \times 10^{-14}(T/300)^{-0.12} \exp(209/T) \text{ cm}^3 \text{ s}^{-1}$$

We note that the rate coefficient for R315 at 150 K is 3.0×10^{-11} cm^3 s^{-1}, which is consistent with the value obtained from Deters et al. (1998). For reaction R448, the rate coefficient at 150 K is 8.3×10^{-14} cm^3 s^{-1}. We assume that HCOH isomerizes to H_2CO rapidly.

4.3.2 $CO_2 + {}^3CH_2$

An important major pathway for the production of CO is the reaction

$$CO_2 + {}^3CH_2 \rightarrow CO + H_2CO \qquad \text{(R344)}$$

In Moses et al. (2000a), the rate coefficient for this reaction is taken from Laufer and Bass (1977) as 3.9×10^{-14} cm^3 s^{-1}. However, in a more recent work, Darwin and Moore (1995) measured the reactive removal rate of $^3CH_2$ with CO_2 directly and could not detect any reaction. Their upper limit of the rate coefficient of R344 is at least a factor of 3-5 lower than 1.4×10^{-14} cm^3 s^{-1}, much smaller than the value from Laufer and Bass (1977). In our Titan model, we set the rate coefficient to be $k_{344} = 2.8 \times 10^{-15}$ cm^3 s^{-1}.

4.3.3 $^1CH_2 + N_2 \rightarrow {}^3CH_2 + N_2$

We add the quenching reaction (R447) of $^1CH_2$ by N_2,

$$^1CH_2 + N_2 \rightarrow {}^3CH_2 + N_2 \qquad \text{(R447)}$$

Ashfold et al. (1981) measured the cross section for quenching of $^3CH_2$ by collisions with N_2 to be 1.1×10^{-16} cm^2. The temperature-dependent rate coefficient for quenching of $^1CH_2$ and N_2 is $k_{447} = 5.1 \times 10^{-13} T^{0.5}$ cm^3 s^{-1}. Note that Langford et al. (1983) reported a larger collisional cross section for $^1CH_2$ and N_2 than the one reported in Ashfold et al. (1981), but their experimental method measured the collisional cross section for removal of a specific rotational and vibrational state of $^1CH_2$ rather than the cross-section for removal from the singlet electronic state.

4.3.4 Carbon Exchange Reaction

Carbon atom exchange has been observed between $^1CH_2$ and CO (Montague and Rowland, 1971). The reaction rate for the exchange reaction (R446)

$$^1CH_2 + {}^*CO \rightarrow {}^{1*}CH_2 + CO \qquad \text{(R446)}$$

has a corresponding rate coefficient k_{446}. A reaction scheme for the exchange mechanism, which involves a ketene intermediary, is shown below,

$$^1CH_2 + {}^*CO \xrightarrow{k_a} CH_2{}^*CO$$

$$CH_2{}^*CO \xrightarrow{k_d} {}^1CH_2 + {}^*CO$$

$$CH_2{}^*CO \xleftrightarrow{k_i} {}^*CH_2CO$$

$${}^*CH_2CO \xrightarrow{k_d} {}^{1*}CH_2 + CO,$$

where $^*C$ represents ^{13}C, k_a is the rate coefficient for association of $^1CH_2$ and $^*CO$, k_d is the rate coefficient of ketene dissociation, and k_i is the rate coefficient for isomerization. The rate coefficients of dissociation and isomerization have been shown, within experimental error, to be the same for both ketene isotopomers (Lovejoy et al., 1991).

If steady-state concentrations are assumed for both ketene species, then the rate of carbon atom exchange between $^1CH_2$ and $^*CO$ is

$$\text{Rate} = k_{446}\left[^1CH_2\right]\left[^*CH_2\right] = \frac{k_a k_i}{k_d + 2k_i}\left[^1CH_2\right]\left[^*CH_2\right]$$

The quantity $\frac{k_i}{k_d+2k_i}$ is equal to the yield for carbon atom exchange (Y) for a given association of $^1CH_2$ and $^*CO$. The yield for carbon atom exchange between $^1CH_2$ and CO can be quantitatively estimated from the experimental work of the Moore group (Lovejoy et al., 1991; Lovejoy and Moore, 1993). In their work, $CH_2{}^{13}CO$ was photodissociated and the appearance of CO and ^{13}CO was monitored as a function of photolysis wavelength. During the ketene photolysis, the molecule is promoted to an excited singlet state. It then undergoes a radiationless transition to the ground-state singlet manifold. At that point, ketene can either transfer through intersystem crossing to the triplet manifold or undergo either isomerization or dissociation in the ground-state singlet manifold (Cui and Morokuma, 1997). In the carbon exchange reaction (R446), the $^1CH_2$ and CO also form a ketene intermediary in the ground-state singlet manifold. Since both the ketene intermediary during carbon atom exchange

and the ketene in the photolysis experiments undergo isomerization from the ground singlet state, the pathways for carbon exchange for the $^1CH_2$ + CO reaction and the photodissociation reaction are the same. Therefore, the photodissociation studies of ketene are a suitable proxy for us to deduce the rate coefficients of the reaction scheme listed above.

The threshold for singlet CH_2*CO dissociation is 30137 cm^{-1} (Chen et al., 1988; Lovejoy et al., 1991). The data of Lovejoy et al. (1991), taken between 30137 and 32000 cm^{-1}, are fit to a quadratic function (see Figure 4.3). Since we are only interested in the order of magnitude of the exchange rate, we have greatly simplified the calculation by assuming that in the reaction of $^1CH_2$ and CO, only translational energy will provide the excess energy of the complex formation. More detailed calculations of the exchange rate, including the role rotational and vibrational energy, are left for later study. If the quadratic function in Figure 4.3 is convolved over the Boltzmann translational energy distribution, a temperature-dependent yield for carbon atom exchange ($Y(T)$) can be calculated, as shown below

$$\frac{k_i}{k_d + 2k_i} = Y(T) = 0.100 - 1.11 \times 10^{-4}T + 8.0 \times 10^{-8}T^2$$

At a temperature typical of the upper atmosphere of Titan, 200 K, the yield is $Y = 0.081$.

The association rate coefficient of $^1CH_2$ and *CO, k_a, can be estimated using the reactive hard sphere model, which states that the association rate coefficient is equal to the products of the total cross section for association (σ_a) between $^1CH_2$ and *CO and the average relative velocity (Steinfeld et al., 1989), or

$$k_a = \sigma_a \sqrt{\frac{8RT}{\pi M}}$$

where R is the ideal gas constant, and M is the reduced mass of the system. Using σ_a rather than a simple collisional cross section takes into account the fact that only inelastic collisions between $^1CH_2$ and CO lead to the formation of the ketene

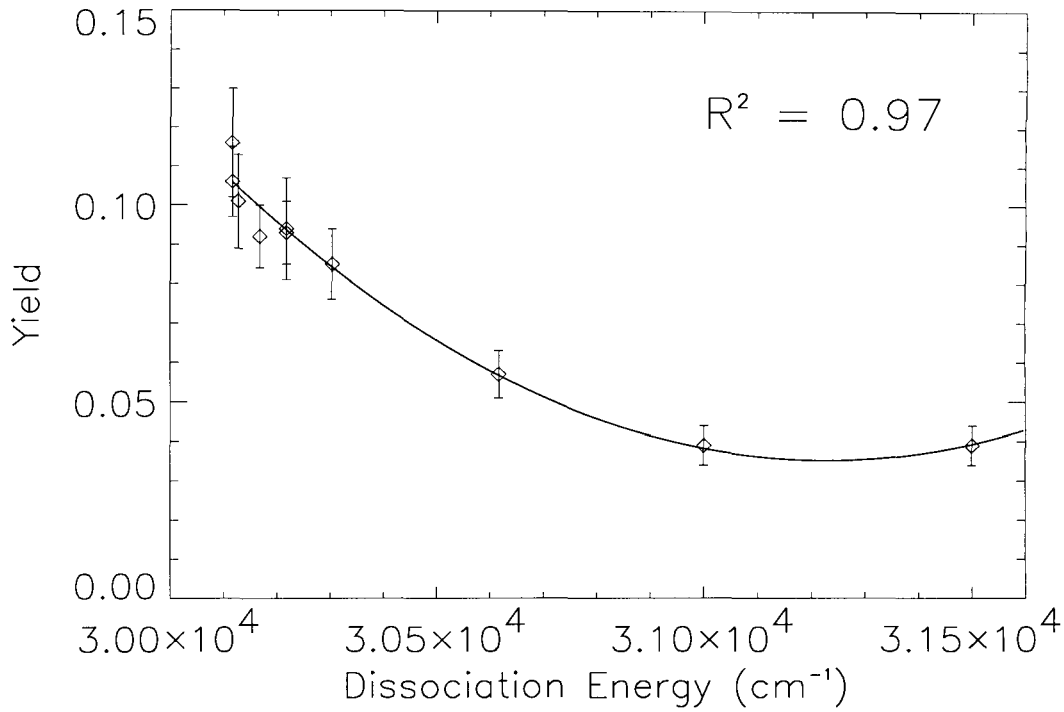

Figure 4.3 Carbon atom exchange yields as a function of photodissociation energy. The diamonds (with error bars) are the carbon atom exchange yields between $^1CH_2$ and CO, measured by Lovejoy et al. (1991) as a function of photodissociation energy. The solid line is the quadratic fit to the data (with $R^2 = 0.97$).

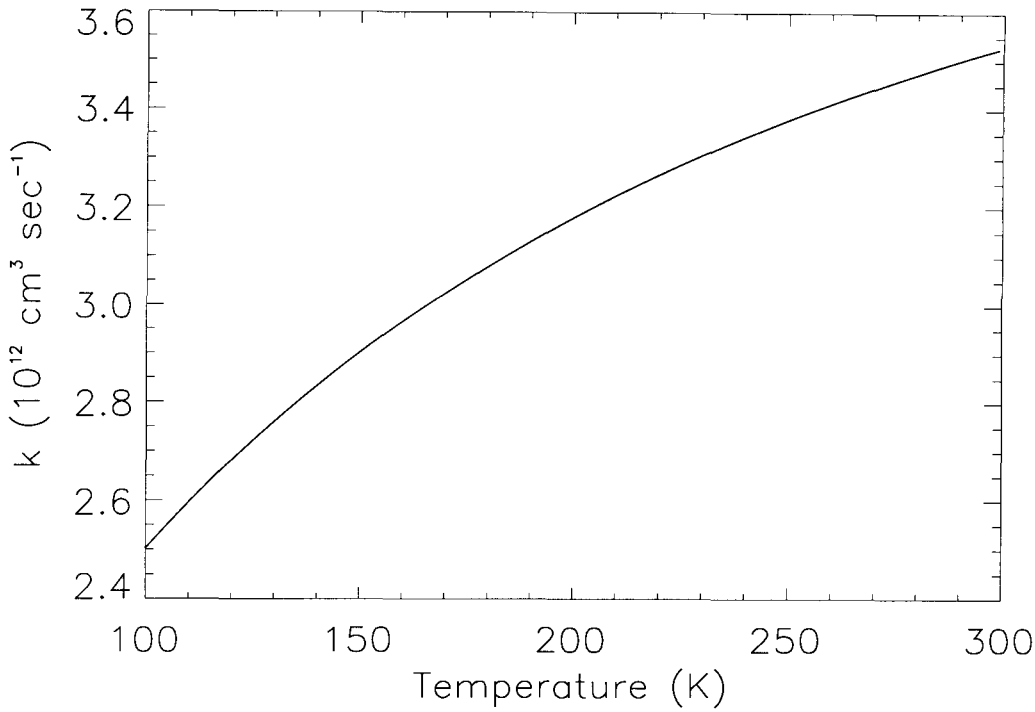

Figure 4.4 Carbon exchange rate coefficient k_{446} between $^1CH_2$ and CO as a function of temperature.

intermediary. Langford et al. (1983) have measured the cross section for these inelastic collisions to be 6.0×10^{-16} cm^2. Therefore, the temperature-dependent rate coefficient for carbon atom exchange between $^1CH_2$ and CO is

$$k_{446} = k_a Y(T) = 2.8 \times 10^{-13} T^{1/2} - 3.2 \times 10^{-16} T^{3/2} + 2.2 \times 10^{-19} T^{5/2} \text{cm}^3 \text{ s}^{-1}$$

A plot of the rate coefficient versus temperature is shown in Figure 4.4. At 200 K, the above expression gives a rate coefficient of $k_{446} = 3.2 \times 10^{-12}$ cm^{-3} s^{-1}.

If this reaction is fast enough, the carbon atoms in CO will be exchanged with the carbon atoms in the CH_4 in the atmosphere, and *any original isotopic fractionation of carbon in CO can be diluted by this process over time*, assuming the presence of a major source/reservoir of CH_4, already required by the short lifetime of this species in the atmosphere (see above).

4.3.5 Dissociation of CO

We will investigate other possible processes involved in isotopic exchange in CO. An important process is the dissociation of CO into C and O via the following reactions R250:

$$CO + h\nu \rightarrow C + O \quad \text{(R250a)}$$

$$CO + e^- \rightarrow C + O + e^- \quad \text{(R250b)}$$

$$CO + h\nu \rightarrow CO^+ + e^- \quad \text{(R250c)}$$

$$CO^+ + e^- \rightarrow C + O \quad \text{(R250d)}$$

While some of the C and O atoms produced in the breakup processes can escape to space, for those C and O that remain in the atmosphere, their fates are quite different with respect to exchange with other reservoirs.

The most important reactions for O are insertions into CH_3 and C_2H_4 (Yung et al., 1984), such as

$$O + CH_3 \rightarrow H_2CO + H \quad \text{(R269)}$$

followed by

$$H_2CO + h\nu \rightarrow H_2 + CO \quad \text{(R255)}$$

$$H_2CO + h\nu \rightarrow HCO + H \quad \text{(R254)}$$

$$HCO + h\nu \rightarrow H + CO \quad \text{(R253)}$$

Four different product channels result from the reaction between O and C_2H_4

$$O + C_2H_4 \rightarrow \text{products}, \quad \text{(R277-280)}$$

but they all eventually produce a CO molecule via reactions similar to R253-255. In the reformation of the CO molecule, the O atom is derived originally from CO, because CO is the principal atmospheric reservoir of oxygen. *Thus the isotopic signature of O in CO will be preserved.*

We make a similar inquiry into the fate of the C atom produced in the CO breakup (R250). The C atom in the reformed CO comes from CH_3 and C_2H_4, which in turn are derived from CH_4 photolysis. The primary reactions removing C atoms are the following (Moses et al., 2000a):

$$C + H_2 \xrightarrow{M} {}^3CH_2 \qquad \text{(R136)}$$

$$C + C_2H_2 \xrightarrow{M} C_3H_2 \qquad \text{(R137)}$$

The ultimate fate of the CH_2 and C_3H_2 radicals on Titan is to form heavier hydrocarbons that condense on the surface and are *permanently sequestered* in the ground reservoir (Yung et al., 1984). This process does *not* preserve the isotopic signature of C in CO.

If the rate for the CO dissociation reaction R250 is slow compared with the age of the solar system, then this process is not important to alter the isotopic fractionation of CO. The reaction rate is calculated and shown in the next section.

4.4 Model and Results

We updated the H_2O influx at the upper boundary from 6.1×10^5 cm^{-2} s^{-1} Yung et al. (1984) to 1.5×10^6 cm^{-2} s^{-1} in order to agree with observations (Coustenis et al., 1998). This updated flux is within the predicted range of $(0.8 - 2.8) \times 10^6$ cm^{-2} s^{-1} from Moses et al. (2000b).

In our standard model, the CO mixing ratio is set to 5.2×10^{-5}, which is consistent with the measurements of Lutz et al. (1983), Muhleman et al. (1984), Gurwell and Muhleman (1995), and Gurwell and Muhleman (2000). However, Marten et al. (1988), Noll et al. (1996), and Hidayat and Marten (1998) found significantly lower

values. Since the chemical lifetime of CO on Titan is very long (on the order of 10^9 years) compared with atmospheric transport, we expect CO to be well mixed in the atmosphere and there should be little change from year to year. In the unlikely event that CO is not well mixed in the atmosphere, we will have to conclude that there is an unknown reaction that destroys CO on Titan. Thus the discrepancies between the observations are puzzling and must be resolved by future measurements.

From the model we can calculate the time constants for carbon exchange reaction R446 and CO dissociation reaction R250. The reaction rates for these two reactions are plotted in Figure 4.5. The column integrated rates for R446 and R250 are 5.68×10^5 cm^{-2} s^{-1}, 8.15×10^4 cm^{-2} s^{-1}, respectively. Since the column abundance of CO in the model is 1.42×10^{22} cm^{-2}, we get an exchange time constant of 792 Myr, and a time constant for CO dissociation of 5.52 Gyr. The exchange reaction time constant is short compared with the age of the solar system, which implies that the carbon atoms in CO will be exchanged with the carbon atoms in the atmospheric methane many times, and the original isotopic fractionation of carbon in CO can be diluted over time. On the other hand, the CO dissociation reaction time constant is long, which suggests that the process of CO dissociation is less important in the carbon exchange scheme and will not alter the isotopic signature of CO.

With the update of the kinetics, the dominant CO production pathways are (in decreasing order of importance):

Scheme 1:

	$H_2O + h\nu \rightarrow H + OH$	(R247)
	$OH + CO \rightarrow CO_2 + H$	(R329)
	$CO_2 + {}^3CH_2 \rightarrow CO + H_2CO$	(R344)*
	$H_2CO + h\nu \rightarrow H_2 + CO$	(R255)
Net:	$H_2O + {}^3CH_2 \rightarrow CO + H_2 + 2H$	(scheme 1)

Scheme 2:

	$H_2O + h\nu \rightarrow 2H + O$	(R248)*

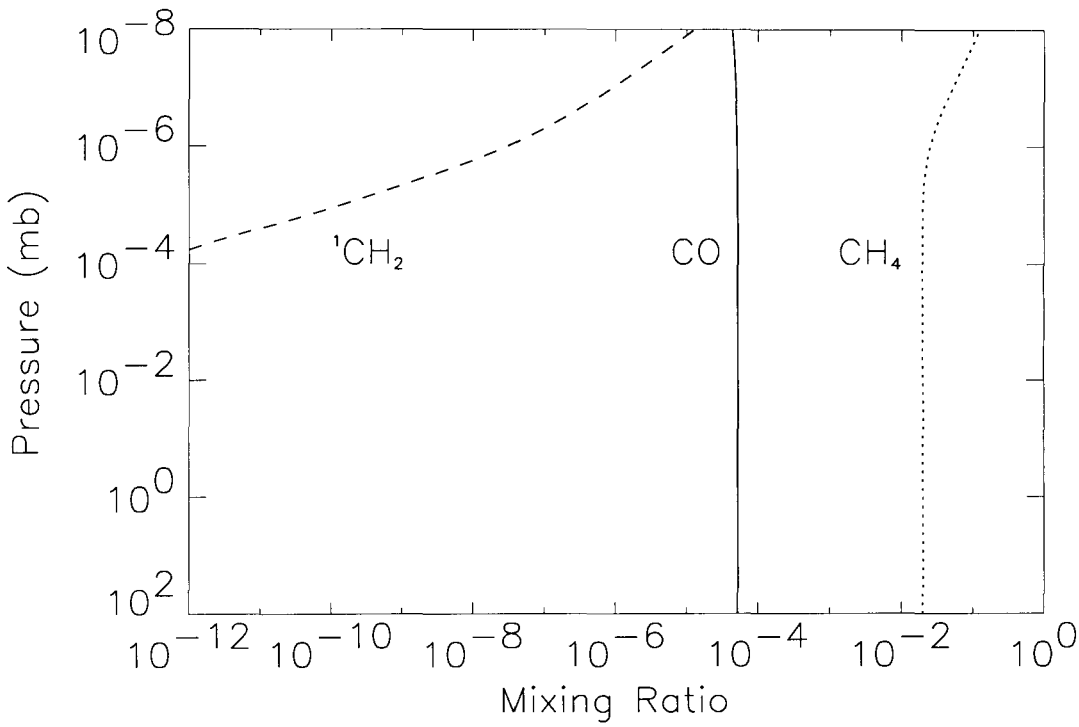

Figure 4.5 Reaction rates for carbon exchange (R446) $^1CH_2 + {}^*CO \rightarrow {}^*CH_2 + CO$, and CO dissociation (R250) $CO \rightarrow C + O$.

	$O + CH_3 \rightarrow H_2CO + H$	(R269)
	$H_2CO + h\nu \rightarrow H_2 + CO$	(R255)
Net:	$H_2O + CH_3 \rightarrow CO + H_2 + 3H$	(scheme 2)

Scheme 3:

	$H_2O + h\nu \rightarrow H + OH$	(R247)
	$OH + C_2H_2 \rightarrow CH_3CO$	(R320)
	$CH_3CO + CH_3 \rightarrow CO + C_2H_6$	(R410)*
Net:	$H_2O + C_2H_2 + CH_3 \rightarrow CO + C_2H_6 + H$	(scheme 3)

Scheme 4:

	$H_2O + h\nu \rightarrow H + OH$	(R247)
	$OH + C_2H_2 \rightarrow CH_3CO$	(R320)
	$CH_3CO + H \rightarrow HCO + CH_3$	(R407)*
	HCO + hydrocarbons $\rightarrow$ CO + hydrocarbons	(R345-352)
Net:	$H_2O + C_2H_2$ + hydrocarbons $\rightarrow$ CO + hydrocarbons	(scheme 4)

The limiting step for each scheme is labeled with an asterisk (*). Figure 4.2 shows the most important reaction pathways for oxygen species on Titan.

The mixing ratios for $^1CH_2$, CH_4 and CO in our model are shown in Figure 4.6. The values for $^1CH_2$ and CH_4 are not significantly different from those reported in the models of Yung et al. (1984) and Lara et al. (1996). Table 4.3 summarizes the results from different models.

The production rate of CO is much smaller than the loss rate. The CO mixing ratio of 5.2×10^{-5} is achieved through an upward flux of CO of about 1.1×10^6 cm^{-2} s^{-1} from the surface. This can be compared to the model of Lara et al. (1996, 1998), where an upward flux of 8.3×10^5 cm^{-2} s^{-1} CO is needed to maintain the conservation of O atoms and account for the mixing ratio of 5×10^{-5}. The influx of water in Lara et al. (1996, 1998) is about two times greater than in our standard

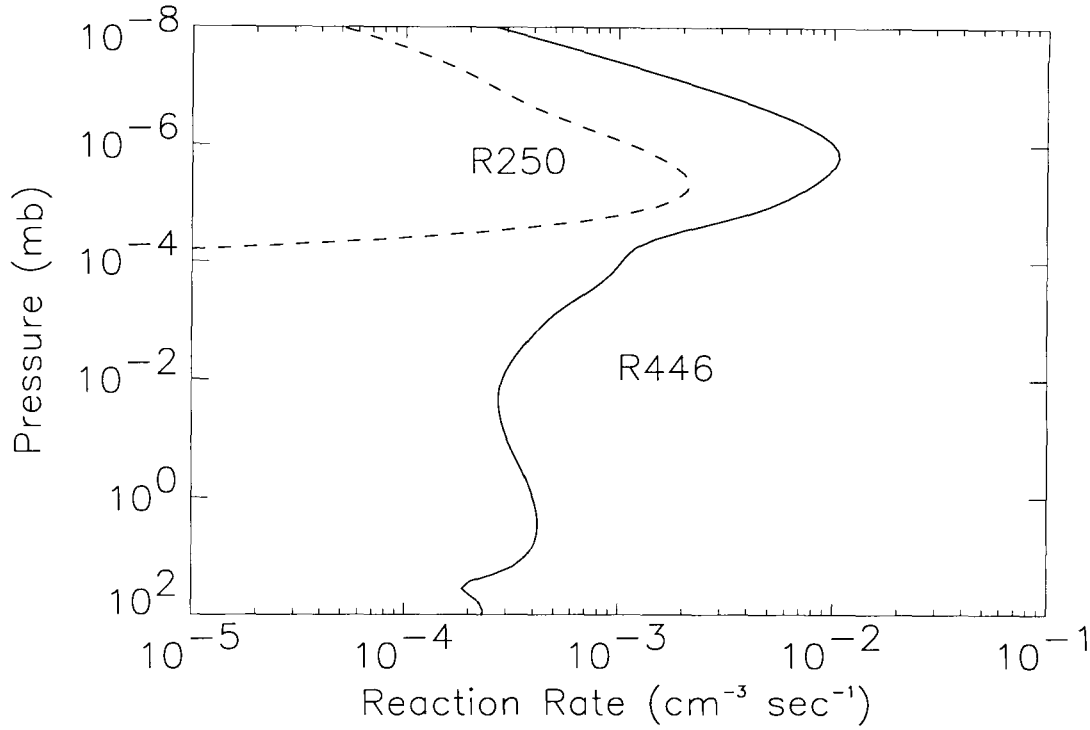

Figure 4.6 Computed mixing ratios for CO, $^1CH_2$, and CH_4 in the standard Titan model.

Table 4.3. Comparison of model results.

	CO mixing ratio	CO upward flux	CO influx	H_2O influx
Yung et al. (1984)	1.8×10^{-4}	0	8.8×10^{4}	6.1×10^{5}
Lara et al. (1996, 1998)	5.0×10^{-5}	8.3×10^{5}	0	3.0×10^{6}
Lara et al. (1996, 1998) (equilibrium)	1.0×10^{-5}	0	0	3.0×10^{6}
Lara et al. (1996, 1998) (alternative)	5.0×10^{-5}	0	1.6×10^{6}	3.0×10^{6}
this work (standard)	5.2×10^{-5}	1.1×10^{6}	0	1.5×10^{6}
this work (equilibrium)	1.8×10^{-6}	0	0	1.5×10^{6}

Note. — All flux is in unit of (cm^{-2} s^{-1}).

model. They also proposed an alternative model in which, instead of an upward flux of CO from the surface, an influx of CO of 1.6×10^6 cm^{-2} s^{-1} from meteoroids is required to reproduce the desired CO mixing ratio.

For CO to be in equilibrium and allow no external and/or internal source of CO to be supplied to the atmosphere, our model shows the CO mixing ratio must be 1.8×10^{-6}, only 3% of the observed value. In a similar fashion, the steady state CO mixing ratio found in Yung et al. (1984) is 100 times greater than our value, because of the inclusion of a fast CO production channel in their model (see above). The steady state CO mixing ratio found in Lara et al. (1996) is 5.6 times greater than ours, and we note the greater amount of water influx in their model (see above).

4.5 Evolution Model of CO Isotopes

Since the water in meteorites is the major incoming source of oxygen on Titan, our model shows that the water influx is not large enough to sustain the observed amount of CO in the atmosphere. The possible explanations are as follows:

1. There is a continuous supply of CO from the interior of Titan (Dubouloz et al., 1989);

2. CO is directly injected into the atmosphere from incoming meteorites;

3. The amount of CO in the atmosphere is gradually decreasing;

4. A combination of the above cases.

We have discussed cases (1) and (2) in the previous section.

For case (3), we can calculate the evolution history of CO in the atmosphere over time. In order to reach the CO mixing ratio of the present day with no external and internal supply thereof, the mixing ratio after the initial escape state at 4.6 Gyr ago would have to be 7.2×10^{-4}, fourteen times more than the value observed today. This is labeled model A. We have also calculated the evolution of CO with five times more and five times less initial CO concentrations. For models B and C, the initial

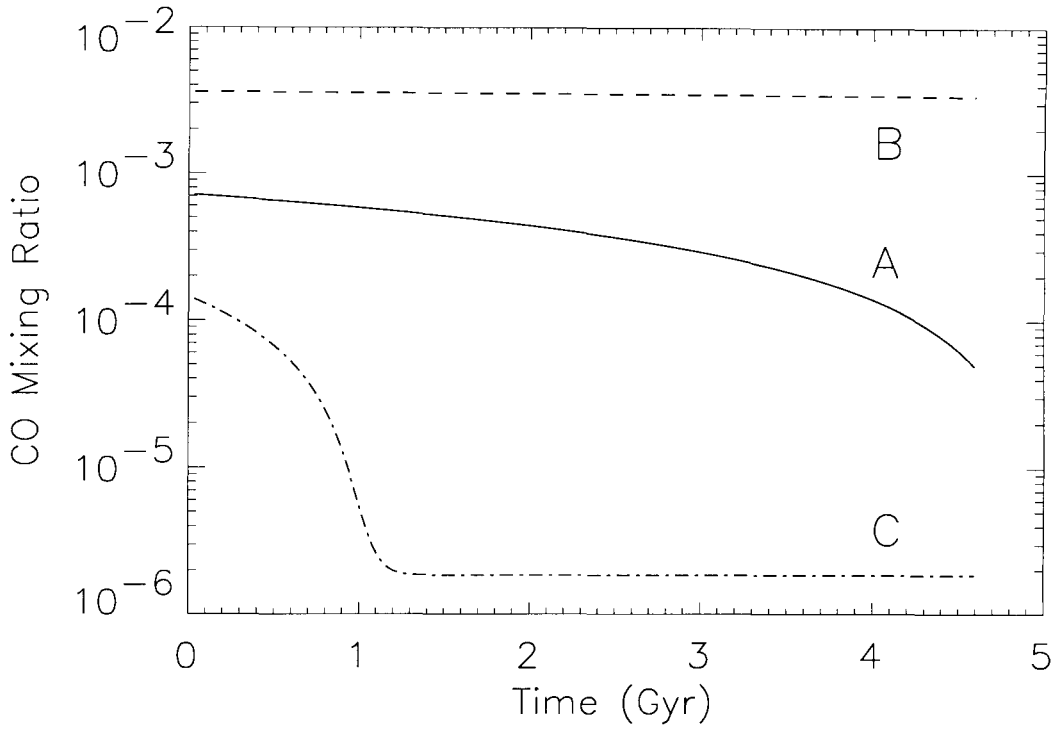

Figure 4.7 Computed mixing ratio for CO as a function of time. Model A produces a value of mixing ratio of 5.2×10^{-5}, which is consistent with observation (Gurwell and Muhleman, 2000), at present time 4.6 Gyr. Models B and C show the evolution with initial CO concentration 5 and 0.2 times of the initial value in solid line, respectively.

CO concentrations are 3.6×10^{-3}, 1.44×10^{-4}, respectively. Figure 4.7 shows the calculated mixing ratios as a function of time for the three models. The amount of CO lost over 4.6×10^{9} year for models A, B, and C are 93.1%, 5.3%, and 98.7%, respectively. In model C, the CO abundance reaches a state of equilibrium and the final mixing ratio is 1.8×10^{-6}.

The evolution paths of the isotopomers of CO, ^{13}CO and C^{18}O, are different from ^{12}C^{16}O, and therefore the initial isotopic ratios in CO will be altered over time. In order to calculate the change of the isotopomers of CO, we need to determine the production rate $P(t)$, loss rate $L(t)$, and carbon atom exchange rate $E(t)$ for each isotopomer.

The production rate of each CO isotopomer is directly proportional to the ratio of the corresponding isotopes in the atmosphere. The destruction of CO occurs mainly through the reaction with OH:

$$OH + CO \rightarrow CO_2 + H \qquad \text{(R329)}$$

Since R329 is the major destruction route of CO, the loss rate of CO can be estimated as the column rate, or the vertically integrated chemical reaction rate, of R329. The reaction rate for R329 is slightly different for different isotopomers of CO due to mass-independent fractionation of the reaction. Let ${}^{12}k = k_{329}$, and ${}^{13}k$, ${}^{18}k$ be the overall rate coefficients for the system CO + OH for the isotopomers ${}^{13}CO$, $C^{18}O$, respectively. From the work of Röckmann et al. (1998), by taking the low-pressure limit, we obtain the ratios ${}^{13}k/{}^{12}k = 1.005$, and ${}^{18}k/{}^{12}k = 1.011$.

To calculate the carbon atom exchange rate for ${}^{13}CO$, consider the exchange reactions R446 and its backward reaction R446a.

$$^1CH_2 + {}^*CO \rightarrow {}^{1*}CH_2 + CO \qquad \text{(R446)}$$

$$^{1*}CH_2 + CO \rightarrow {}^1CH_2 + {}^*CO \qquad \text{(R446a)}$$

where *C represents ${}^{13}C$. If k_{446} and k_{446a} are the rate coefficients of the above two reactions, then the rate of change in the concentration of *CO from the contribution of these two reactions is

$$\frac{d\left[{}^*CO\right]}{dt} = -k_{446}\left[{}^1CH_2\right]\left[{}^*CO\right] + k_{446a}\left[{}^{1*}CH_2\right]\left[CO\right]$$

Since $k_{446} = k_{446a}$, the above expression can be reduced to

$$\frac{d\left[{}^*CO\right]}{dt} = k_{446}[{}^1CH_2]\left(\frac{[{}^{1*}CH_2]}{[{}^1CH_2]}[CO] - [{}^*CO]\right)$$

Letting the time constant of reaction R446 be $\tau_e x = (k_{446}\left[{}^1CH_2\right])^{-1}$, we have

$$E(t) = \frac{d\left[{}^*CO\right]}{dt} = \left(\frac{[{}^{1*}CH_2]}{[{}^1CH_2]}[CO] - [{}^*CO]\right)\tau_e x^{-1}$$

The theory of isotopic enrichment in a planetary atmosphere due to photochemical processes has been worked out by McElroy and Yung (1976), whose methodology and notation we follow. Let $N_{12}(t)$, $N_{13}(t)$, and $N_{18}(t)$ be the total column abundance of $^{12}C^{16}O$, ^{13}CO, and $C^{18}O$, respectively, on Titan at time t. The evolution of $N_{12}(t)$ is given by

$$\frac{dN_{12}(t)}{dt} = P_{12}(t) - L_{12}(t)$$

where time t is defined so that $t = 0$ refers to the time of formation of Titan and $t = 4.6 \times 10^9$ yr corresponds to the present, and $P_{12}(t)$ and $L_{12}(t)$ are the production rate and loss rate of $^{12}C^{16}O$ respectively, from the evolution model.

Similarly, the evolution of ^{13}CO, in terms of$N_{13}(t)$, is given by

$$\frac{dN_{13}(t)}{dt} = P_{13}(t) - L_{13}(t) + E_{13}(t)$$

where $P_{13}(t)$, $L_{13}(t)$ and $E_{13}(t)$ are the production rate, loss rate, and exchange rate of ^{13}CO respectively. Here

$$P_{13}(t) = P_{12}(t) \left(\frac{^{13}C}{^{12}C} \right)_{CH_4}$$

$$L_{13}(t) = L_{12}(t) \frac{^{13}k}{^{12}k} \frac{N_{13}(t)}{N_{12}(t)}$$

$$E_{13}(t) = \left(\frac{\left[^{13(1)}CH_2\right]}{\left[^{12(1)}CH_2\right]} N_{12}(t) - N_{13}(t) \right) \tau_{ex}^{-1}$$

and $\left[^{13(1)}CH_2\right] / \left[^{12(1)}CH_2\right] = 0.011$ (Van Dishoeck et al., 1993), $\tau_{ex} = 7.92 \times 10^8$ yr is the time constant for the exchange reaction calculated in the previous section.

For $C^{18}O$, the evolution of $N_{18}(t)$ is given by

$$\frac{dN_{18}(t)}{dt} = P_{18}(t) - L_{18}(t)$$

where the production and loss rates are

$$P_{18}(t) = P_{12}(t) \left(\frac{^{18}\mathrm{O}}{^{16}\mathrm{O}} \right)_{\mathrm{H_2O}}$$

$$L_{18}(t) = L_{12}(t) \frac{^{18}k}{^{12}k} \frac{N_{18}(t)}{N_{12}(t)}$$

We solve this set of equations by using the observed present value of $N_{12}(4.6 \times 10^9\mathrm{yr}) = 5.2 \times 10^{-5}$ and integrating the equations backwards to $t = 0$ to obtain $N_{12}(t)$, and consequently $N_{13}(t)$, and $N_{18}(t)$. This gives us the enrichment factors of ^{13}CO to $^{12}\mathrm{C}^{16}\mathrm{O}$, $\mathrm{C}^{18}\mathrm{O}$ to $^{12}\mathrm{C}^{16}\mathrm{O}$ as a function of time.

The result for model A is plotted in Figure 4.8. We assume an initial enhancement of 3.23 for $\mathrm{C}^{18}\mathrm{O}/^{12}\mathrm{C}^{16}\mathrm{O}$ in order for the enhancement to reach the observed value (two times the terrestrial value) at present day. We set the initial enhancement for $^{13}\mathrm{CO}/^{12}\mathrm{C}^{16}\mathrm{O}$ to be the same for the purpose of comparison. It is clear that if initially both heavy isotopomers of CO are enriched, through atmospheric evolution, ^{13}CO enrichment will dilute to close to unity (1.097), but $\mathrm{C}^{18}\mathrm{O}$ enrichment will dilute at a much slower rate. The results for models B and C are shown in Figure 4.9 together. In both models, ^{13}CO is diluted rapidly to unity (1.105 and 1.095) because of the exchange of carbon atoms with the $\mathrm{CH_4}$ reservoir in the atmosphere. The dilution of $\mathrm{C}^{18}\mathrm{O}$ is more gradual, especially in model B. Note that in model C, when the equilibrium is reached, the $\mathrm{C}^{18}\mathrm{O}$ enrichment is close to the terrestrial value (0.989).

4.6 Conclusion

Our study of the evolution history of CO on Titan has four implications:

1. There is evidence for massive loss of CO during Titan's early history, resulting in the enrichment of the isotopomers of CO except for ^{13}CO.

2. There has been a gradual decline in the concentration of CO in the atmosphere by a factor of approximately 14.

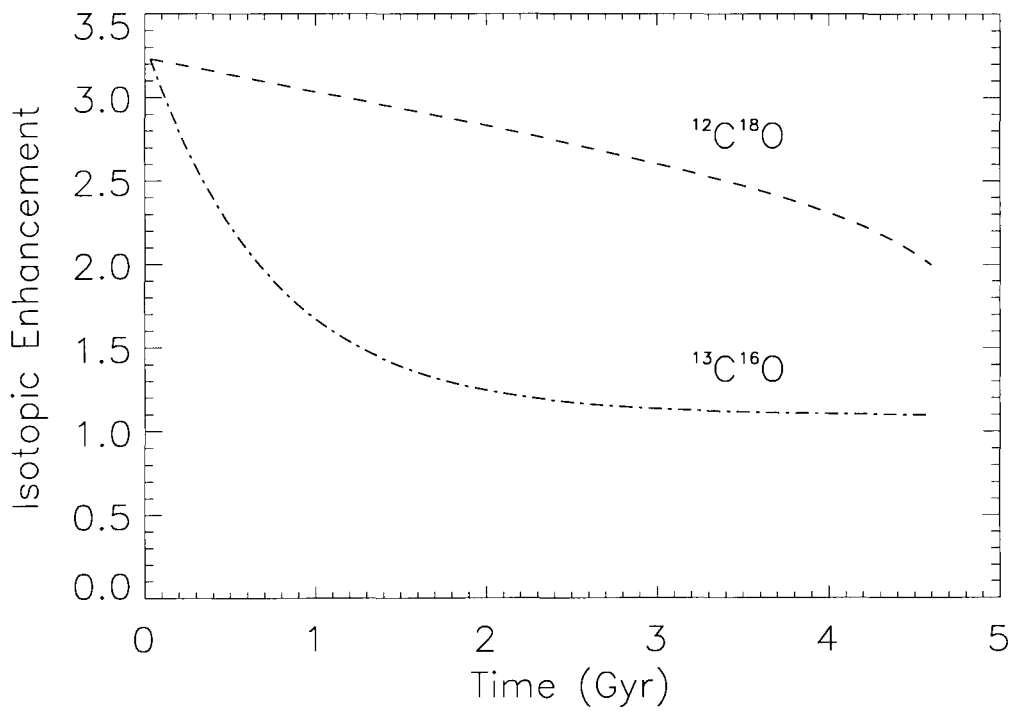

Figure 4.8 Evolution of enrichment factors of $^{13}CO/^{12}C^{16}O$ and $C^{18}O/^{12}C^{16}O$ for model A, assuming an enrichment of 3.23 to the terrestrial value at time 0. The dashed line represents the enrichment of $C^{18}O$, and the dash-dot-dash line represents the enrichment of $C^{18}O$.

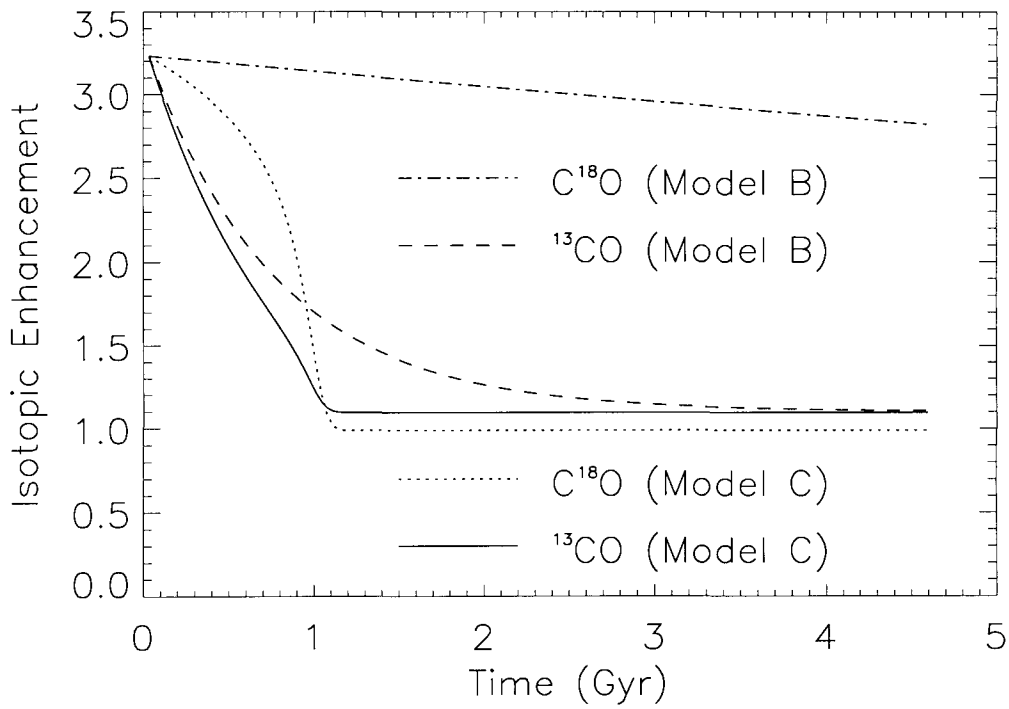

Figure 4.9 Evolution of enrichment factors of ^{13}CO and $C^{18}O$ with respect to $^{12}C^{16}O$ for models B and C, assuming an enrichment of 3.23 to the terrestrial value at time 0.

3. As a result of an exchange reaction for carbon atoms, it is not possible to preserve the isotopic signature of ^{13}CO for longer than 800 Myr.

4. The isotopic signatures of ^{17}O and ^{18}O isotopomers of CO are not diluted over the age of the solar system.

Our model presents a plausible but not unique interpretation of the known observations of Titan. To further our understanding of the evolution history of CO on Titan, it is most important to

1. Resolve the differences in the measurements of CO abundance.

2. Measure the isotopic fractionation of all three isotopomers, ^{13}CO, $C^{17}O$ and $C^{18}O$.

3. Measure the isotopic fractionation of all three isotopomers of CO on Saturn, where the source is exogenic, for comparison with Titan.

New laboratory measurements are needed to remove the uncertainties in the photochemistry and chemical kinetics of key reactions identified in our model. These include

1. the branching ratio producing $^1CH_2$ in the UV photolysis of CH_4;

2. the products and branching ratio of reaction OH + CH_3.

Appendix A Galileo UVS Spectra of the Jovian Aurorae

A.1 Abstract

Analysis of over 100 UV spectra obtained by the spacecraft Galileo of the Jovian auroral emission indicates that the Jovian auroral brightness is modulated in longitude. It is brighter near 180° in the north and 54° in the south. There is also a color ratio asymmetry associated with the brightening. We catalog the Galileo ultraviolet spectrometer (UVS) spectra and compare the statistical measurement with that of the International Ultraviolet Explorer (IUE). This will enable us to determine the total input energy and the energy of the primary electrons of the aurora and study the effect of precipitation of energetic charged particles on the polar atmosphere in the future.

A.2 Introduction

Jupiter's extensive magnetic fields give rise to complex interactions with the solar wind. Auroral phenomena result from precipitation of energetic charged particles in the polar regions. Jupiter's aurora is the brightest source of UV radiation in the solar system, save for that of the sun. Its enormous power input into the auroral region dominates the atmospheric chemistry. Heavy molecules such as polycyclic aromatic hydrocarbons (PAHs) can be formed in auroral regions and lead to the production of polar haze.

Early efforts had been made to detect ultraviolet aurora utilizing rocket experiments. Voyager 1 and 2 spacecrafts carried ultraviolet spectrometers (UVS) and observed Jupiter's aurora in the region 500-1700 Å and identified H_2 Lyman- and Werner-bands and H Ly-α emissions. An Earth-orbiting observatory, the International Ultraviolet Explorer (IUE), studied Jovian ultraviolet aurora in the wavelength range 1200-1700 Å. Recently, intensive study of the ultraviolet aurora was made with the Hopkins Ultraviolet Telescope (HUT) and with the Hubble Space Telescope (HST).

The Galileo Orbiter has been obtaining ultraviolet spectra of Jupiter's intense polar aurora since December 1995. The UV instrument on the Galileo Orbiter consists of two separate spectrometers, one of which is the ultraviolet spectrometer (UVS), operating over the range 1130-4320 Å. Over 100 spectra were taken by the UVS for both north and south polar regions of Jupiter. Some UVS data sets were analyzed by Ajello et al. (1998, 2001) and Pryor et al. (1998, 2000), and gave important information about the energetics and structure of the aurora, such as the absolute surface brightness of the aurora from the H_2 Rydberg Systems, column abundance of H_2 and CH_4, and total power input.

However, there has been no study of the spectral data set as a whole. In this work we catalog the UVS spectra and compare the statistical measurement with that of the IUE.

A.3 Catalog the UVS Spectra and HST Images

Observations of FUV auroral emission from Jupiter using the Earth-orbiting the ultraviolet observatory IUE have induced studies of the longitudinal variation of the aurorae (Livengood et al., 1990; Harris et al., 1996). Livengood et al. (1990) analyzed 229 IUE spectra (1150-1950 Å) of the Jovian north polar emissions over the period of 1978-1989 and studied the variability of the aurora. This study established that the locus of UV auroral brightness is fixed in magnetic longitude rather than local time as for the terrestrial aurora.

We carry out similar analysis with the Galileo UVS spectra. From 109 UVS spectra (67 north spectra and 42 south spectra), we select 63 spectra that cover the polar regions for our analysis. These include 37 North spectra and 26 South spectra. There are 4 spectra that cover both north and south region during the observation (Nos. 16, 27, 30 in the north, and No. 21 in the south; see Table A.1). All the latitude and longitude values designate locations within the middle of each observation period. We calculate the time-averaged fill factor – the fraction of the slit that overlaps with the Jupiter disk – for each spectrum from the map. The method to determine the fill factor is different from Ajello et al. (1998, 2001) and Pryor et al. (1998, 2000), where they define the fill factor as the fraction of the slit that is filled with aurora. Since it is difficult to determine the exact size of the aurora, using the new fill factors enables us to calculate the averaged emisson.

Table A.1 and Table A.2 summarize the north and the south spectra with UT time stamp, latitude, longitude, background, total background, total H_2 band emission, and Lyman-α intensity. All longitude is in System III central meridian longitude (λ_{CML}).

Table A.1. Catalog of Galileo UVS spectra, north.

No.	Time	Latitude	Longitude	Background	– Total	H_2	Ly-α
0	3493218-3493247	61.862	149.418	8.123	12.630	3.18	1.695
1	3493248-3493277	57.748	156.309	8.637	13.471	3.63	2.090
2	3493278-3493307	57.107	175.817	11.811	18.350	10.28	3.171
3	3493308-3493337	52.895	186.979	9.535	14.916	19.96	4.845
4	3594518-3594547	66.066	139.648	7.341	11.496	4.04	2.590
5	3594548-3594577	62.142	145.988	7.516	11.739	4.72	3.311
6	3594578-3594607	57.080	157.188	9.057	14.048	9.38	3.419
7	3594608-3594637	56.877	174.850	9.290	14.490	10.46	3.855
8	3594638-3594667	62.103	200.867	11.088	17.303	19.66	7.237
9	3594668-3594697	68.153	234.927	10.983	17.003	9.99	5.165
10	3595058-3595087	70.945	99.990	7.446	11.619	1.85	1.497
11	3675880-3675939	58.950	186.922	31.010	142.725	13.06	3.359
12	3675940-3675999	63.981	207.106	29.265	134.770	11.75	2.986
13	3676000-3676059	68.182	219.640	31.517	145.129	11.31	3.368
14	3676060-3676119	70.352	221.721	44.774	206.020	7.17	3.957
15	3676120-3676179	67.308	229.135	68.263	314.342	3.57	4.618
16	3737639-3737698	56.252	165.969	8.190	17.395	16.64	3.327
17	3737699-3737728	56.896	174.297	11.462	11.966	17.05	3.712
18	3737729-3737758	58.364	183.225	9.852	10.286	18.46	3.991
19	3737759-3737788	60.450	192.704	8.870	9.261	17.57	3.768
20	3737789-3737818	62.515	202.319	10.577	11.042	13.26	3.619
21	3737819-3737878	66.608	214.776	8.277	17.580	12.88	3.438
22	3737879-3737938	68.663	219.799	8.506	18.067	9.61	3.997
23	3834148-3834207	80.035	11.010	13.375	19.261	3.99	4.260
24	3895559-3895599	51.196	173.644	87.463	91.311	58.19	11.636
25	3895600-3895629	59.773	189.104	66.792	69.731	31.30	6.708
26	3895660-3895680	56.821	159.238	32.820	23.630	27.47	8.918
27	3947734-3947823	56.800	171.700	290.995	657.994	30.93	6.379
28	4018986-4019015	59.689	189.356	309.617	222.924	33.17	10.510

Table A.1—Continued

No.	Time	Latitude	Longitude	Background	– Total	H_2	Ly-α
29	4019016-4019045	56.389	169.927	120.145	86.504	31.58	6.954
30	4134696-4134725	56.867	158.410	310.131	223.294	14.95	3.204
31	4204194-4204253	58.853	185.113	54.120	77.933	42.03	9.040
32	4204254-4204295	67.393	218.207	20.252	21.143	39.05	8.861
33	4204296-4204325	64.560	208.319	20.091	20.975	22.98	5.279
34	4204326-4204355	63.303	205.551	24.872	25.966	30.67	5.316
35	4204356-4204385	63.108	202.965	34.515	36.034	33.03	6.437
36	4204386-4204445	59.946	193.392	129.654	182.034	20.30	8.435

We also investigate the distribution of color ratio as a function of magnetic longitude, where color ratio is proposed by Yung et al. (1982) as a measure of atmospheric absorption, and thus the penetration depth and energy, or auroral primary particles. Color ratio is defined as

$$C = \frac{< I_{1557-1619} >}{< I_{1230-1310} >}$$

where the numerator and denomitor are the intensities averaged over the indicated range of wavelengths. This ratio is the reciprocal of the ratio R2 proposed by Yung et al. (1982) times the factor 70/62, corresponding to the weighting by the wavelength intervals introduced by the averaging. The ratio C varies such that increased C corresponds to increased attenuation of the short-wavelength emission and increased hydrocarbon column abundance.

The north brightness peak is at $\lambda_{III} \sim 180°$ and the south peak at $\lambda_{III} \sim 54°$. These can be compared with IUE data of 200° and 20° respectively.

Figure A.1 shows the spectral observables, the 1150-1619 Å brightness and the color ratio, as a function of longitude.

The average emission is summarized in Table A.3.

Table A.2. Catalog of Galileo UVS spectra, south.

No.	Time	Latitude	Longitude	Background	– Total	H_2	Ly-α
0	3488687-3488716	-83.828	189.499	53.688	56.050	7.04	3.958
1	3488747-3488806	-73.218	200.625	54.843	252.356	7.58	4.925
2	3493156-3493185	-70.313	22.479	8.999	14.006	37.83	9.064
3	3493186-3493203	-69.478	43.408	8.376	11.129	30.57	7.793
4	3595484-3595513	-63.427	14.685	14.127	27.468	11.35	4.424
5	3595514-3595536	-76.335	315.414	9.125	15.678	26.98	10.237
6	3595544-3595573	-64.840	320.204	8.861	17.381	19.40	11.293
7	3675620-3675699	-68.763	46.411	8.740	24.857	13.89	3.296
8	3675700-3675729	-69.006	56.055	9.868	10.303	13.26	3.228
9	3675730-3675759	-68.903	59.114	7.293	7.613	14.40	4.036
10	3675760-3675789	-68.846	65.970	7.325	7.647	9.48	3.607
11	3675790-3675819	-69.283	70.775	8.258	8.622	7.35	3.331
12	3675820-3675879	-69.537	79.595	10.568	48.543	8.33	4.192
13	3681110-3681127	-69.688	78.906	12.866	17.020	23.84	5.669
14	3681140-3681160	-69.557	73.092	21.394	33.378	35.97	7.615
15	3738121-3738180	-57.719	79.862	6.797	14.437	3.08	2.099
16	3738181-3738240	-73.947	110.018	7.050	14.975	16.05	4.122
17	3738241-3738300	-73.490	113.837	9.915	21.059	9.80	3.394
18	3738303-3738362	-57.886	91.863	11.379	24.168	5.50	6.232
19	3742781-3742811	-65.002	316.725	27.591	64.373	23.50	11.539
20	3742812-3742868	-63.821	333.614	10.392	21.927	31.84	10.750
21	3834026-3834086	-63.226	30.666	60.177	86.655	10.85	3.402
22	3834872-3834891	-68.981	69.670	32.667	48.289	13.12	8.951
23	3895478-3895507	-70.237	80.386	14.150	14.773	21.19	6.909
24	3895630-3895659	-78.264	130.546	47.474	49.563	11.77	6.076
25	4134645-4134665	-69.109	68.362	285.352	444.899	11.56	6.535

Table A.3. Average emission of Galileo spectra.

Feature	Mean values North	South	Total
H_2 intensity (1150-1625 Å) (kR)	18.1 ± 12.9	16.4 ± 9.7	17.4 ± 11.6
Ly-α intensity (1208-1223 Å) (kR)	5.00 ± 2.48	6.03 ± 2.82	5.42 ± 2.66
red intensity (kR)	4.28 ± 3.11	4.46 ± 3.63	3.97 ± 3.03
red/blue (1557-1619 Å) / (1230-1310 Å)	1.30 ± 0.28	1.75 ± 1.13	1.49 ± 0.78
red/green (1557-1619 Å) / (1310-1410 Å)	2.88 ± 0.65	3.69 ± 2.15	3.22 ± 1.51

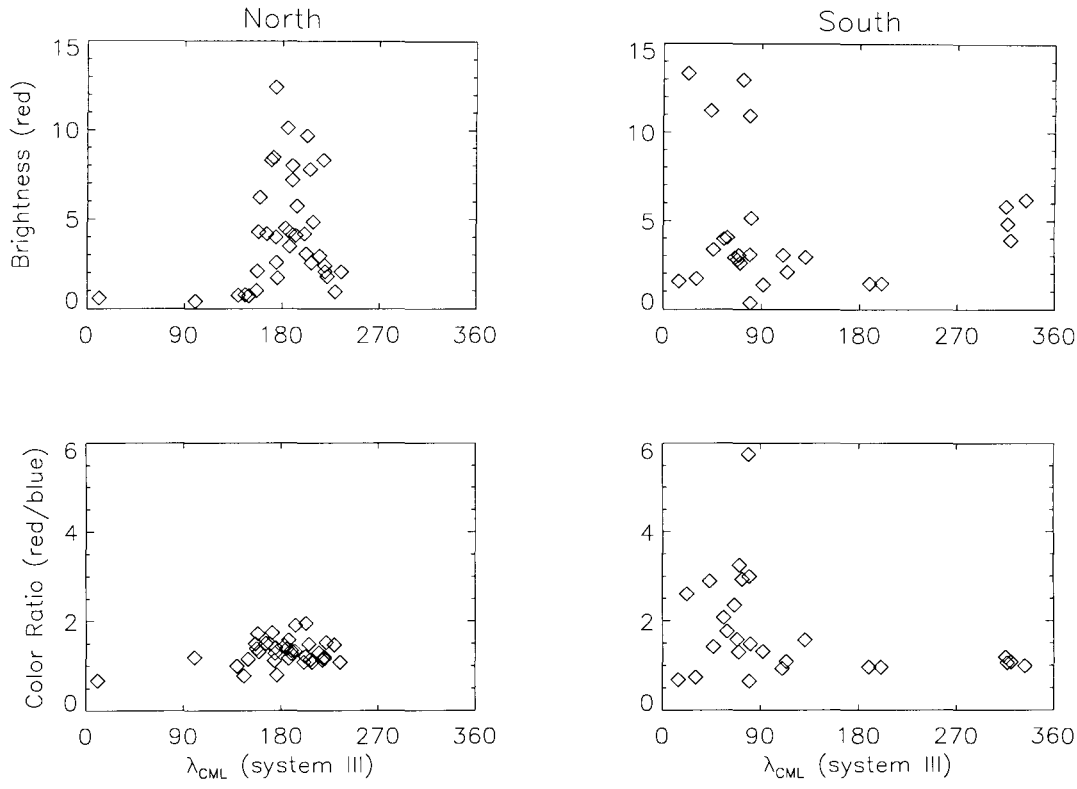

Figure A.1 Galileo spectral observables of Jovian as a function of CML.

A.4 Conclusion

The north brightness peak is at $\lambda_{III} \sim 180°$ and the south peak at $\lambda_{III} \sim 54°$. These can be compared with IUE data of 200° and 20° respectively.

Appendix B Inputs and Outputs for Jupiter Auroral Model

B.1 Model Inputs

Input parameters and reaction list for auroral model.

B.1.1 Input Parameters

```
 OPERATING SYSTEM:
VMS
 DIMENSIONS:
 NATOM NMOL NREACT NPART NFIX NVARYS NVARYF NOVARF NVARFM NVARYFT NOTZERO
     3  120    702   200    7      0    112      1    112     112        1
 NALT1 NALT2 NALTTP NLAT NLON NMONTH NMONJ  NIMP NTIMES NLEV NTEMP
     1    80     80    1    1      1     1     5     0    0     0
 NPHOTC NPHOTCT NPHOTO NPHOTS NPHOTR NPHOTD NWAVE1 NWAVE2 NWAVEM NZEN NWAVES NTAU NGA MPHI IDZEN
    104       0      9      0      0      0     20    157    176    0     43  550   8    3     0
 IFIX,IVARYS,IVARYF:
    3   50   51  116  117  118  119    1    2    4    5    6    7    8    9   10   11   12   13   14
   15   16   17   18   19   20   21   22   23   24   25   26   27   28   29   30   31   32   33   34
   35   36   37   38   39   40   41   42   43   44   45   46   47   48   49   52   53   54   55   56
   57   58   59   60   61   62   63   64   65   66   67   68   69   70   71   72   73   74   75   76
   77   78   79   80   81   82   83   84   85   86   87   88   89   90   91   92   93   94   95   96
   97   98   99  100  101  102  103  104  105  106  107  108  109  110  111  112  113  114  115
 NUMBER OF SPECIES IN EACH DIFFUS GROUP:
  112
 IPHOTO:  220  221  222  223  224  225  226  227  228
 IPHOTS:
 IPHOTR:
 IPHOTD:
 PLANET PARAMETERS:
    AU    PE PAXINC  PYEAR   PDAY PERIH DAYSPR       PRAD  PDEN   GRAV   ADIFH2 SDIFH2
   5.2 0.000   3.08  4332.7   9.8   0.0    0.0    71284.0   1.3 2325.0 3.64E-05   1.75
 MONDAY:
  10576
 DLAT:
  60.00
 BASIC RADIATION PARAMETERS:
 MODE ISPHER ISUN JUPDAT
    0      0    1      1
 BASIC RUN PARAMETERS:
 MOTION IVEC IATM ICOEF ITRCHM ITER IDBUG LOG IPRES ITAPE IPUN MUPDAT ICONT  LAGLEV
      0    0    0     1      8    8    -1   0     1     0    1     0      0     20
 DIRECTORY PATH FOR PUNCH OUTPUT FILES:
 SCR:
 RUN CONVERGENCE:
```

```
 CONVT       CONVF    IDAMP     ICNV
 -1.0E-10  5.0E-03        1        0
 RUN TIMING:
 ICYEAR   DAY     HOUR    DELTIM    DELTTRM
      1 180.00    0.00  -1.0E+15    0.000E+00
 SPECIFIC RUN PARAMETERS:
 NTIME  IEND YEND        DEND  ITRY IPRNT IPRNTD IPRNTF IPRNTN    TPRNT ISTART
      1    0 -1.000E+00   0.00    2     1      0     -1      0  0.0E+00      2
0
 NPHOTO =   9
 OPTICAL OPACITY DUE TO REACTIONS   220  221  222  223  224  225  226  227  228
0
 NPHOTS =   0
0
 NPHOTR =   0
0
 NPHOTD =   0
1KINETIC MODEL INVOLVES   3 DIFFERENT ATOMS, 120 CHEMICAL SPECIES, AND 702 REACTIONS


 ATOMS:         H  HE C
```

B.1.2 Other Input Information

```
CONCENTRATIONS OF   7 SPECIES ARE HELD CONSTANT:
H2        H2V2      H2V4      EL        PROD      Y         V


CONCENTRATIONS OF   0 SPECIES TO BE CALCULATED ASSUMING LOCAL INSTANTANEOUS PHOTOCHEMICAL STEADY-STATE:


CONCENTRATIONS OF 112 SPECIES TO BE CALCULATED WITH VERTICAL TRANSPORT:

     GROUP  1 : H         HE        C         CH        (1)CH2    (3)CH2    CH3       CH4       C2        C2H
                C2H2      C2H3      C2H4      C2H5      C2H6      C3        C3H       C3H2      C3H3      CH3C2H
                CH2CCH2   C3H5      C3H6      C3H7      C3H8      C4H       C4H2      C4H3      C4H4      C4H5
                1-C4H6    1,2-C4H6  1,3-C4H6  C4H8      C4H9      C4H10     C6H       C6H2      C6H3      C6H6
                C8H2      C5H2      C5H3      C6H4      NC6H5     C6H7      A1-       A1        HP        HEP
                H2P       H3P       HEHP      CP        CHP       CH2P      CH3P      CH4P      CH5P      C2P
                C2HP      C2H2P     C2H3P     C2H4P     C2H5P     C2H6P     C2H7P     C3P       C3HP      C3H2P
                C-C3H2P   C3H3P     C-C3H3P   CH3C2HP   C3H5P     C4P       C4HP      C4H2P     C4H3P     C4H4P
                C4H5P     C5P       C5HP      C5H2P     C5H3P     C5H4P     C5H5P     C6P       C6HP      C6H2P
                C6H3P     C6H4P     C6H5P     C-C6H5P   C6H7P     C-C6H7P   PAH       CC        C3HN      C4HN
                C5HN      C6HN      C7HN      C8HN      C9HN      CCP       C3HNP     C4HNP     C5HNP     C7HNP
                C8HNP     C9HNP
```

B.1.3 Species List

```
SPECIES:
  1) H          1  0  0
  2) HE         0  1  0
  3) H2         2  0  0
  4) C          0  0  1
```

5)	CH	1	0	1
6)	(1)CH2	2	0	1
7)	(3)CH2	2	0	1
8)	CH3	3	0	1
9)	CH4	4	0	1
10)	C2	0	0	2
11)	C2H	1	0	2
12)	C2H2	2	0	2
13)	C2H3	3	0	2
14)	C2H4	4	0	2
15)	C2H5	5	0	2
16)	C2H6	6	0	2
17)	C3	0	0	3
18)	C3H	1	0	3
19)	C3H2	2	0	3
20)	C3H3	3	0	3
21)	CH3C2H	4	0	3
22)	CH2CCH2	4	0	3
23)	C3H5	5	0	3
24)	C3H6	6	0	3
25)	C3H7	7	0	3
26)	C3H8	8	0	3
27)	C4H	1	0	4
28)	C4H2	2	0	4
29)	C4H3	3	0	4
30)	C4H4	4	0	4
31)	C4H5	5	0	4
32)	1-C4H6	6	0	4
33)	1,2-C4H6	6	0	4
34)	1,3-C4H6	6	0	4
35)	C4H8	8	0	4
36)	C4H9	9	0	4
37)	C4H10	10	0	4
38)	C6H	1	0	6
39)	C6H2	2	0	6
40)	C6H3	3	0	6
41)	C6H6	6	0	6
42)	C8H2	2	0	8
43)	C5H2	2	0	5
44)	C5H3	3	0	5
45)	C6H4	4	0	6
46)	NC6H5	5	0	6
47)	C6H7	7	0	6
48)	A1-	5	0	6
49)	A1	6	0	6

50) H2V2	2	0	0
51) H2V4	2	0	0
52) HP	1	0	0
53) HEP	0	1	0
54) H2P	2	0	0
55) H3P	3	0	0
56) HEHP	1	1	0
57) CP	0	0	1
58) CHP	1	0	1
59) CH2P	2	0	1
60) CH3P	3	0	1
61) CH4P	4	0	1
62) CH5P	5	0	1
63) C2P	0	0	2
64) C2HP	1	0	2
65) C2H2P	2	0	2
66) C2H3P	3	0	2
67) C2H4P	4	0	2
68) C2H5P	5	0	2
69) C2H6P	6	0	2
70) C2H7P	7	0	2
71) C3P	0	0	3
72) C3HP	1	0	3
73) C3H2P	2	0	3
74) C-C3H2P	2	0	3
75) C3H3P	3	0	3
76) C-C3H3P	3	0	3
77) CH3C2HP	4	0	3
78) C3H5P	5	0	3
79) C4P	0	0	4
80) C4HP	1	0	4
81) C4H2P	2	0	4
82) C4H3P	3	0	4
83) C4H4P	4	0	4
84) C4H5P	5	0	4
85) C5P	0	0	5
86) C5HP	1	0	5
87) C5H2P	2	0	5
88) C5H3P	3	0	5
89) C5H4P	4	0	5
90) C5H5P	5	0	5
91) C6P	0	0	6
92) C6HP	1	0	6
93) C6H2P	2	0	6
94) C6H3P	3	0	6

95)	C6H4P	4	0	6
96)	C6H5P	5	0	6
97)	C-C6H5P	5	0	6
98)	C6H7P	7	0	6
99)	C-C6H7P	7	0	6
100)	PAH	6	0	8
101)	CC	0	0	1
102)	C3HN	0	0	3
103)	C4HN	0	0	4
104)	C5HN	0	0	5
105)	C6HN	0	0	6
106)	C7HN	0	0	7
107)	C8HN	0	0	8
108)	C9HN	0	0	9
109)	CCP	0	0	1
110)	C3HNP	0	0	3
111)	C4HNP	0	0	4
112)	C5HNP	0	0	5
113)	C7HNP	0	0	7
114)	C8HNP	0	0	8
115)	C9HNP	0	0	9
116)	EL	0	0	0
117)	PROD	0	0	0
118)	Y	0	0	0
119)	V	0	0	0
120)	M	0	0	0

B.1.4 Reaction List

REACTIONS:

1)	H2	=	2H					k	=	0.00E+00	EXP(0./T)
2)	(3)CH2	=	CH	+	H			k	=	0.00E+00	EXP(0./T)
3)	CH3	=	CH	+	H2			k	=	0.00E+00	EXP(0./T)
4)	CH3	=	(1)CH2	+	H			k	=	0.00E+00	EXP(0./T)
5)	CH4	=	CH3	+	H			k	=	0.00E+00	EXP(0./T)
6)	CH4	=	(1)CH2	+	H2			k	=	0.00E+00	EXP(0./T)
7)	CH4	=	(1)CH2	+	2H			k	=	0.00E+00	EXP(0./T)
8)	CH4	=	(3)CH2	+	2H			k	=	0.00E+00	EXP(0./T)
9)	CH4	=	CH	+	H	+	H2	k	=	0.00E+00	EXP(0./T)
10)	C2H2	=	C2H	+	H			k	=	0.00E+00	EXP(0./T)
11)	C2H2	=	C2	+	H2			k	=	0.00E+00	EXP(0./T)
12)	C2H3	=	C2H2	+	H			k	=	0.00E+00	EXP(0./T)
13)	C2H4	=	C2H2	+	H2			k	=	0.00E+00	EXP(0./T)
14)	C2H4	=	C2H2	+	2H			k	=	0.00E+00	EXP(0./T)
15)	C2H4	=	C2H3	+	H			k	=	0.00E+00	EXP(0./T)
16)	C2H5	=	CH3	+	(1)CH2			k	=	0.00E+00	EXP(0./T)
17)	C2H6	=	C2H4	+	H2			k	=	0.00E+00	EXP(0./T)
18)	C2H6	=	C2H4	+	2H			k	=	0.00E+00	EXP(0./T)
19)	C2H6	=	C2H2	+	2H2			k	=	0.00E+00	EXP(0./T)

20)	C2H6 = CH4 + (1)CH2	k = 0.00E+00 EXP(0./T)
21)	C2H6 = 2CH3	k = 0.00E+00 EXP(0./T)
22)	C3H2 = C3 + H2	k = 0.00E+00 EXP(0./T)
23)	C3H3 = C3H2 + H	k = 0.00E+00 EXP(0./T)
24)	C3H3 = C3 + H2 + H	k = 0.00E+00 EXP(0./T)
25)	CH3C2H = C3H3 + H	k = 0.00E+00 EXP(0./T)
26)	CH3C2H = C3H2 + H2	k = 0.00E+00 EXP(0./T)
27)	CH3C2H = (1)CH2 + C2H2	k = 0.00E+00 EXP(0./T)
28)	CH2CCH2 = C3H3 + H	k = 0.00E+00 EXP(0./T)
29)	CH2CCH2 = C3H2 + H2	k = 0.00E+00 EXP(0./T)
30)	C3H5 = CH3C2H + H	k = 0.00E+00 EXP(0./T)
31)	C3H5 = CH2CCH2 + H	k = 0.00E+00 EXP(0./T)
32)	C3H5 = C2H2 + CH3	k = 0.00E+00 EXP(0./T)
33)	C3H6 = C3H5 + H	k = 0.00E+00 EXP(0./T)
34)	C3H6 = CH3C2H + H2	k = 0.00E+00 EXP(0./T)
35)	C3H6 = CH2CCH2 + H2	k = 0.00E+00 EXP(0./T)
36)	C3H6 = C2H4 + (1)CH2	k = 0.00E+00 EXP(0./T)
37)	C3H6 = C2H3 + CH3	k = 0.00E+00 EXP(0./T)
38)	C3H6 = C2H2 + CH4	k = 0.00E+00 EXP(0./T)
39)	C3H8 = C3H6 + H2	k = 0.00E+00 EXP(0./T)
40)	C3H8 = C2H6 + (1)CH2	k = 0.00E+00 EXP(0./T)
41)	C3H8 = C2H5 + CH3	k = 0.00E+00 EXP(0./T)
42)	C3H8 = C2H4 + CH4	k = 0.00E+00 EXP(0./T)
43)	C4H2 = C4H + H	k = 0.00E+00 EXP(0./T)
44)	C4H2 = C2H2 + C2	k = 0.00E+00 EXP(0./T)
45)	C4H2 = 2C2H	k = 0.00E+00 EXP(0./T)
46)	C4H4 = C4H2 + H2	k = 0.00E+00 EXP(0./T)
47)	C4H4 = 2C2H2	k = 0.00E+00 EXP(0./T)
48)	1-C4H6 = C4H4 + 2H	k = 0.00E+00 EXP(0./T)
49)	1-C4H6 = C3H3 + CH3	k = 0.00E+00 EXP(0./T)
50)	1-C4H6 = C2H5 + C2H	k = 0.00E+00 EXP(0./T)
51)	1-C4H6 = C2H4 + C2H + H	k = 0.00E+00 EXP(0./T)
52)	1-C4H6 = C2H3 + C2H + H2	k = 0.00E+00 EXP(0./T)
53)	1-C4H6 = 2C2H2 + H2	k = 0.00E+00 EXP(0./T)
54)	1,2-C4H6= C4H5 + H	k = 0.00E+00 EXP(0./T)
55)	1,2-C4H6= C4H4 + 2H	k = 0.00E+00 EXP(0./T)
56)	1,2-C4H6= C3H3 + CH3	k = 0.00E+00 EXP(0./T)
57)	1,2-C4H6= C2H4 + C2H2	k = 0.00E+00 EXP(0./T)
58)	1,2-C4H6= C2H3 + C2H2 + H	k = 0.00E+00 EXP(0./T)
59)	1,2-C4H6= C2H3 + C2H + H2	k = 0.00E+00 EXP(0./T)
60)	1,2-C4H6= 2C2H2 + H2	k = 0.00E+00 EXP(0./T)
61)	1,3-C4H6= C4H5 + H	k = 0.00E+00 EXP(0./T)
62)	1,3-C4H6= C4H4 + H2	k = 0.00E+00 EXP(0./T)
63)	1,3-C4H6= C3H3 + CH3	k = 0.00E+00 EXP(0./T)
64)	1,3-C4H6= C2H4 + C2H2	k = 0.00E+00 EXP(0./T)
65)	1,3-C4H6= 2C2H3	k = 0.00E+00 EXP(0./T)
66)	C4H8 = 1,3-C4H6+ 2H	k = 0.00E+00 EXP(0./T)
67)	C4H8 = C3H5 + CH3	k = 0.00E+00 EXP(0./T)
68)	C4H8 = CH3C2H + CH4	k = 0.00E+00 EXP(0./T)
69)	C4H8 = CH2CCH2 + CH4	k = 0.00E+00 EXP(0./T)
70)	C4H8 = C2H5 + C2H3	k = 0.00E+00 EXP(0./T)
71)	C4H8 = 2C2H4	k = 0.00E+00 EXP(0./T)
72)	C4H8 = C2H2 + 2CH3	k = 0.00E+00 EXP(0./T)
73)	C4H10 = C4H8 + H2	k = 0.00E+00 EXP(0./T)
74)	C4H10 = C3H8 + (1)CH2	k = 0.00E+00 EXP(0./T)
75)	C4H10 = C3H6 + CH4	k = 0.00E+00 EXP(0./T)
76)	C4H10 = C3H6 + CH3 + H	k = 0.00E+00 EXP(0./T)
77)	C4H10 = C2H6 + C2H4	k = 0.00E+00 EXP(0./T)
78)	C4H10 = 2C2H5	k = 0.00E+00 EXP(0./T)
79)	C4H10 = C2H4 + 2CH3	k = 0.00E+00 EXP(0./T)
80)	C6H2 = C6H + H	k = 0.00E+00 EXP(0./T)

81)	C6H2 = C4H + C2H	k = 0.00E+00 EXP(0./T)	
82)	C6H6 = C4H2 + C2H4	k = 0.00E+00 EXP(0./T)	
83)	C6H6 = 2C3H3	k = 0.00E+00 EXP(0./T)	
84)	C6H6 = 3C2H2	k = 0.00E+00 EXP(0./T)	
85)	C8H2 = C6H + C2H	k = 0.00E+00 EXP(0./T)	
86)	C8H2 = 2C4H	k = 0.00E+00 EXP(0./T)	
87)	2H + M = H2 + M	k0 = 2.70E-31 (T/ 1.)** -0.6 EXP(0./T)	
		koo = 0.00E+00 (T/ 1.)** 0.0 EXP(0./T)	
88)	H + CH = C + H2	k = 1.30E-10 EXP(-80./T)	
89)	H + (1)CH2 = CH + H2	k = 2.00E-10 EXP(0./T)	
90)	H + (3)CH2 = CH + H2	k = 2.66E-10 EXP(0./T)	
91)	H + (3)CH2 + M = CH3 + M	k0 = 3.40E-32 EXP(736./T)	
		koo = 7.30E-12 EXP(0./T)	
92)	H + CH3 + M = CH4 + M	k0 = 2.52E-29 EXP(0./T)	
		koo = 3.23E-10 EXP(0./T)	
93)	H + CH4 = CH3 + H2	k = 6.40E-18 T** 2.1 EXP(-3900./T)	
94)	H + C2H + M = C2H2 + M	k0 = 1.26E-18 (T/ 1.)** -3.1 EXP(-721./T)	
		koo = 3.00E-10 (T/ 1.)** 0.0 EXP(0./T)	
95)	H + C2H2 = C2H + H2	k = 1.00E-38 EXP(0./T)	
96)	H + C2H2 + M = C2H3 + M	k0 = 8.20E-31 EXP(-352./T)	
		koo = 1.40E-11 EXP(-1300./T)	
97)	H + C2H3 = C2H2 + H2	k = 2.00E-11 EXP(0./T)	
98)	H + C2H3 + M = C2H4 + M	k0 = 5.50E-27 EXP(0./T)	
		koo = 1.82E-10 EXP(0./T)	
99)	H + C2H4 + M = C2H5 + M	k0 = 1.30E-29 (T/ 1.)** 0.0 EXP(-380./T)	
		koo = 6.60E-15 (T/ 1.)** 1.3 EXP(-650./T)	
100)	H + C2H5 = 2CH3	k = 1.25E-10 EXP(0./T)	
101)	H + C2H5 = C2H4 + H2	k = 3.00E-12 EXP(0./T)	
102)	H + C2H5 + M = C2H6 + M	k0 = 5.50E-22 (T/ 1.)** -2.0 EXP(-1040./T)	
		koo = 2.60E-10 (T/ 1.)** 0.0 EXP(0./T)	
103)	H + C2H6 = C2H5 + H2	k = 2.35E-15 T** 1.5 EXP(-3725./T)	
104)	H + C3H2 + M = C3H3 + M	k0 = 2.52E-28 EXP(0./T)	
		koo = 5.00E-11 EXP(0./T)	
105)	H + C3H3 + M = CH3C2H + M	k0 = 5.50E-27 EXP(0./T)	
		koo = 1.15E-10 EXP(-276./T)	
106)	H + C3H3 + M = CH2CCH2 + M	k0 = 5.50E-27 EXP(0./T)	
		koo = 1.15E-10 EXP(-276./T)	
107)	H + CH3C2H = CH3 + C2H2	k = 9.63E-12 EXP(-1560./T)	
108)	H + CH3C2H + M = C3H5 + M	k0 = 2.00E-29 EXP(0./T)	
		koo = 3.98E-11 EXP(-1152./T)	
109)	H + CH2CCH2 = CH3C2H + H	k = 4.00E-12 EXP(-1006./T)	
110)	H + CH2CCH2 + M = C3H5 + M	k0 = 2.00E-29 EXP(0./T)	
		koo = 1.00E-11 EXP(-1006./T)	
111)	H + C3H5 = CH3C2H + H2	k = 1.40E-11 EXP(0./T)	
112)	H + C3H5 = CH2CCH2 + H2	k = 1.40E-11 EXP(0./T)	
113)	H + C3H5 = CH3 + C2H3	k = 1.40E-11 EXP(0./T)	
114)	H + C3H5 + M = C3H6 + M	k0 = 2.00E-28 EXP(0./T)	
		koo = 2.80E-10 EXP(0./T)	
115)	H + C3H6 = C3H5 + H2	k = 2.87E-19 T** 2.5 EXP(-1254./T)	
116)	H + C3H6 = CH3 + C2H4	k = 2.20E-11 EXP(-1641./T)	
117)	H + C3H6 + M = C3H7 + M	k0 = 1.30E-28 EXP(-380./T)	
		koo = 2.20E-11 EXP(-785./T)	
118)	H + C3H7 = C3H6 + H2	k = 3.00E-12 EXP(0./T)	
119)	H + C3H7 = C2H5 + CH3	k = 6.00E-11 EXP(0./T)	
120)	H + C3H7 + M = C3H8 + M	k0 = 5.50E-22 (T/ 1.)** -2.0 EXP(-1040./T)	
		koo = 2.49E-10 (T/ 1.)** 0.0 EXP(0./T)	
121)	H + C3H8 = C3H7 + H2	k = 2.20E-18 T** 2.5 EXP(-3400./T)	
122)	H + C4H + M = C4H2 + M	k0 = 1.26E-18 (T/ 1.)** -3.1 EXP(-721./T)	
		koo = 3.00E-10 (T/ 1.)** 0.0 EXP(0./T)	
123)	H + C4H2 + M = C4H3 + M	k0 = 1.00E-28 EXP(0./T)	
		koo = 1.39E-10 EXP(-1184./T)	

124)	H + C4H3 = C4H2 + H2	k = 5.00E-12 EXP(0./T)	
125)	H + C4H3 + M = C4H4 + M	k0 = 6.00E-30 EXP(1680./T)	
		koo = 8.56E-10 EXP(-405./T)	
126)	H + C4H4 + M = C4H5 + M	k0 = 6.00E-31 EXP(1680./T)	
		koo = 3.30E-12 EXP(0./T)	
127)	H + C4H5 = C4H4 + H2	k = 2.00E-11 EXP(0./T)	
128)	H + C4H5 + M = 1-C4H6 + M	k0 = 6.00E-30 EXP(1680./T)	
		koo = 1.00E-10 EXP(0./T)	
129)	H + C4H9 = C4H8 + H2	k = 1.50E-12 EXP(0./T)	
130)	H + C4H9 + M = C4H10 + M	k0 = 6.00E-30 EXP(1680./T)	
		koo = 6.00E-11 EXP(0./T)	
131)	H + C6H2 + M = C6H3 + M	k0 = 1.00E-28 EXP(0./T)	
		koo = 1.39E-10 EXP(-1184./T)	
132)	H + C6H3 = C6H2 + H2	k = 2.00E-11 EXP(0./T)	
133)	C + H2 + M = (3)CH2 + M	k0 = 7.00E-32 EXP(0./T)	
		koo = 2.06E-11 EXP(-57./T)	
134)	C + C2H2 + M = C3H2 + M	k0 = 1.00E-31 EXP(0./T)	
		koo = 2.10E-10 EXP(0./T)	
135)	CH + H2 = (3)CH2 + H	k = 3.75E-10 EXP(-1662./T)	
136)	CH + H2 + M = CH3 + M	k0 = 3.40E-31 EXP(736./T)	
		koo = 7.30E-11 EXP(0./T)	
137)	CH + CH4 = C2H4 + H	k = 5.00E-11 EXP(200./T)	
138)	CH + C2H2 = C3H2 + H	k = 3.49E-10 EXP(61./T)	
139)	CH + C2H4 = C2H2 + CH3	k = 2.23E-10 EXP(173./T)	
140)	CH + C2H6 = C3H6 + H	k = 1.80E-10 EXP(132./T)	
141)	(1)CH2 + H2 = (3)CH2 + H2	k = 1.26E-11 EXP(0./T)	
142)	(1)CH2 + H2 = CH3 + H	k = 9.24E-11 EXP(0./T)	
143)	(1)CH2 + CH4 = (3)CH2 + CH4	k = 1.20E-11 EXP(0./T)	
144)	(1)CH2 + CH4 = 2CH3	k = 5.90E-11 EXP(0./T)	
145)	2(3)CH2 = C2H2 + 2H	k = 1.80E-10 EXP(-400./T)	
146)	(3)CH2 + CH3 = C2H4 + H	k = 7.00E-11 EXP(0./T)	
147)	(3)CH2 + CH4 = 2CH3	k = 7.10E-12 EXP(-5051./T)	
148)	(3)CH2 + C2H2 = C3H2 + H2	k = 5.00E-12 EXP(-3332./T)	
149)	(3)CH2 + C2H2 = C3H3 + H	k = 1.50E-11 EXP(-3332./T)	
150)	(3)CH2 + C2H2 + M = CH3C2H + M	k0 = 6.00E-29 EXP(1680./T)	
		koo = 2.00E-12 EXP(-3330./T)	
151)	(3)CH2 + C2H3 = C2H2 + CH3	k = 8.00E-11 EXP(0./T)	
152)	(3)CH2 + C2H5 = C2H4 + CH3	k = 8.00E-11 EXP(0./T)	
153)	CH3 + H2 = CH4 + H	k = 6.60E-20 T** 2.2 EXP(-3220./T)	
154)	2CH3 + M = C2H6 + M	k0 = 6.00E-29 EXP(1680./T)	
		koo = 6.00E-11 EXP(0./T)	
155)	CH3 + C2H3 = CH4 + C2H2	k = 3.40E-11 EXP(0./T)	
156)	CH3 + C2H3 + M = C3H6 + M	k0 = 6.00E-28 EXP(1680./T)	
		koo = 1.20E-10 EXP(0./T)	
157)	CH3 + C2H5 = CH4 + C2H4	k = 2.00E-12 EXP(0./T)	
158)	CH3 + C2H5 + M = C3H8 + M	k0 = 1.01E-22 EXP(341./T)	
		koo = 6.64E-11 EXP(0./T)	
159)	CH3 + C3H3 + M = 1,2-C4H6+ M	k0 = 6.00E-28 EXP(1680./T)	
		koo = 4.20E-12 EXP(0./T)	
160)	CH3 + C3H3 + M = 1-C4H6 + M	k0 = 6.00E-28 EXP(1680./T)	
		koo = 4.20E-12 EXP(0./T)	
161)	CH3 + C3H5 = CH4 + CH3C2H	k = 2.50E-12 T** -0.3 EXP(66./T)	
162)	CH3 + C3H5 = CH4 + CH2CCH2	k = 2.50E-12 T** -0.3 EXP(66./T)	
163)	CH3 + C3H5 + M = C4H8 + M	k0 = 7.12E-22 EXP(715./T)	
		koo = 6.50E-11 EXP(0./T)	
164)	CH3 + C3H6 = CH4 + C3H5	k = 2.32E-13 EXP(-4390./T)	
165)	CH3 + C3H6 + M = C4H9 + M	k0 = 1.30E-28 EXP(-380./T)	
		koo = 1.34E-13 EXP(-3330./T)	
166)	CH3 + C3H7 = CH4 + C3H6	k = 1.90E-11 T** -0.3 EXP(0./T)	
167)	CH3 + C3H7 + M = C4H10 + M	k0 = 7.12E-22 (T/ 1.)** 0.0 EXP(715./T)	
		koo = 3.20E-10 (T/ 1.)** -0.3 EXP(0./T)	

168)	CH3 + C3H8 = CH4 + C3H7	k = 1.50E-24 T** 3.7 EXP(-3600./T)
169)	CH3 + C4H5 = CH4 + C4H4	k = 3.40E-11 EXP(0./T)
170)	CH3 + C4H5 + M = 5CC + M	k0 = 7.12E-22 (T/ 1.)** 0.0 EXP(715./T)
		koo = 3.20E-10 (T/ 1.)** -0.3 EXP(0./T)
171)	C2 + H2 = C2H + H	k = 1.77E-10 EXP(-1469./T)
172)	C2 + CH4 = C2H + CH3	k = 5.05E-11 EXP(-297./T)
173)	C2H + H2 = C2H2 + H	k = 1.20E-11 EXP(-998./T)
174)	C2H + CH4 = C2H2 + CH3	k = 1.20E-11 EXP(-491./T)
175)	C2H + C2H2 = C4H2 + H	k = 1.10E-10 EXP(28./T)
176)	C2H + C2H4 = C4H4 + H	k = 7.80E-11 EXP(134./T)
177)	C2H + C2H6 = C2H2 + C2H5	k = 3.50E-11 EXP(3./T)
178)	C2H + C4H2 = C6H2 + H	k = 1.10E-10 EXP(28./T)
179)	C2H + C4H10 = C4H9 + C2H2	k = 1.00E-11 EXP(0./T)
180)	C2H + C6H2 = C8H2 + H	k = 1.10E-10 EXP(28./T)
181)	C2H + C8H2 =10CC	k = 1.10E-10 EXP(28./T)
182)	C2H3 + H2 = C2H4 + H	k = 5.00E-20 T** 2.6 EXP(-4298./T)
183)	C2H3 + C2H2 = C4H4 + H	k = 3.31E-12 EXP(-2516./T)
184)	C2H3 + C2H2 + M = C4H5 + M	k0 = 8.20E-30 (T/ 1.)** 0.0 EXP(-352./T)
		koo = 4.17E-19 (T/ 1.)** 1.9 EXP(-1058./T)
185)	2C2H3 = C2H4 + C2H2	k = 2.40E-11 EXP(0./T)
186)	2C2H3 + M = 1,3-C4H6+ M	k0 = 6.00E-28 EXP(1680./T)
		koo = 1.20E-10 EXP(0./T)
187)	C2H3 + C2H4 = 1-C4H6 + H	k = 1.05E-12 EXP(-1559./T)
188)	C2H3 + C2H5 = 2C2H4	k = 8.00E-13 EXP(0./T)
189)	C2H3 + C2H5 = C2H6 + C2H2	k = 8.00E-13 EXP(0./T)
190)	C2H3 + C2H5 = CH3 + C3H5	k = 0.00E+00 EXP(0./T)
191)	C2H3 + C2H5 + M = C4H8 + M	k0 = 6.00E-28 EXP(1680./T)
		koo = 0.00E+00 EXP(0./T)
192)	C2H5 + H2 = C2H6 + H	k = 5.10E-24 T** 3.6 EXP(-4253./T)
193)	2C2H5 = C2H6 + C2H4	k = 2.40E-12 EXP(0./T)
194)	2C2H5 + M = C4H10 + M	k0 = 1.55E-22 EXP(586./T)
		koo = 1.40E-11 EXP(35./T)
195)	C3 + H2 = C3H + H	k = 1.00E-14 EXP(0./T)
196)	C3H + H2 = C3H2 + H	k = 1.00E-14 EXP(0./T)
197)	C3H2 + C2H2 + M = 5CC + M	k0 = 6.00E-31 EXP(1680./T)
		koo = 2.00E-11 EXP(-3330./T)
198)	C3H2 + C2H3 = C3H3 + C2H2	k = 8.00E-11 EXP(0./T)
199)	C3H2 + C2H5 = C3H3 + C2H4	k = 8.00E-11 EXP(0./T)
200)	2C3H3 + M = C6H6 + M	k0 = 6.00E-28 EXP(1680./T)
		koo = 1.20E-10 EXP(0./T)
201)	C3H5 + H2 = C3H6 + H	k = 5.25E-11 EXP(-9913./T)
202)	C3H7 + H2 = C3H8 + H	k = 3.00E-21 T** 2.8 EXP(-4600./T)
203)	C4H + H2 = C4H2 + H	k = 1.20E-11 EXP(-998./T)
204)	C4H + CH4 = C4H2 + CH3	k = 1.20E-11 EXP(-491./T)
205)	C4H + C2H2 = C6H2 + H	k = 2.50E-11 EXP(0./T)
206)	C4H + C2H6 = C4H2 + C2H5	k = 3.50E-11 EXP(3./T)
207)	C4H + C4H2 = C8H2 + H	k = 1.10E-10 EXP(28./T)
208)	C4H + C6H2 =10CC	k = 1.10E-10 EXP(28./T)
209)	C4H + C8H2 =12CC	k = 1.10E-10 EXP(28./T)
210)	C4H5 + H2 = 1-C4H6 + H	k = 6.61E-15 T** 0.5 EXP(-1864./T)
211)	C4H5 + C2H2 = C6H6 + H	k = 9.63E-16 T** 1.0 EXP(-5489./T)
212)	C6H + H2 = C6H2 + H	k = 1.20E-11 EXP(-998./T)
213)	C6H + CH4 = C6H2 + CH3	k = 1.20E-11 EXP(-491./T)
214)	C6H + C2H2 = C8H2 + H	k = 1.10E-10 EXP(28./T)
215)	C6H + C2H6 = C6H2 + C2H5	k = 3.50E-11 EXP(3./T)
216)	C6H + C4H2 =10CC	k = 1.10E-10 EXP(28./T)
217)	C6H + C6H2 =12CC	k = 1.10E-10 EXP(28./T)
218)	C6H + C8H2 =14CC	k = 1.10E-10 EXP(28./T)
219)	H + C4H3 = 2C2H2	k = 1.50E-11 EXP(0./T)
220)	H2 = H2	k = 0.00E+00 EXP(0./T)
221)	CH4 = CH4	k = 0.00E+00 EXP(0./T)

222)	C2H2	=	C2H2							
223)	C2H4	=	C2H4							
224)	C2H6	=	C2H6							
225)	C3H8	=	C3H8							
226)	C4H2	=	C4H2							
227)	C4H10	=	C4H10							
228)	C6H2	=	C6H2							
229)	A1	=	A1-	+	H					
230)	2C3H3	+	M	=	A1	+	M			
231)	2C3H3	=	A1-	+	H					
232)	C3H3	+	C3H2	+	M	=	A1-	+	M	
233)	C4H2	+	CH	=	C5H2	+	H			
234)	C4H2	+	(3)CH2	=	C5H3	+	H			
235)	C4H2	+	(1)CH2	=	C5H3	+	H			
236)	C4H2	+	C2H	=	C6H2	+	H			
237)	C4H2	+	C2H	+	M	=	C6H3	+	M	
238)	C4H3	+	C2H2	=	C6H4	+	H			
239)	C4H3	+	C2H2	+	M	=	NC6H5	+	M	
240)	C4H3	+	C2H2	+	M	=	A1-	+	M	
241)	C4H4	+	C2H3	=	C6H6	+	H			
242)	C4H5	+	C2H2	=	A1	+	H			
243)	C4H5	+	C2H2	+	M	=	C6H7	+	M	
244)	C5H2	+	CH	=	C6H2	+	H			
245)	C5H3	+	CH	=	C6H2	+	2H			
246)	C5H3	+	(3)CH2	=	C6H4	+	H			
247)	C6H	+	H	+	M	=	C6H2	+	M	
248)	C6H2	+	H	+	M	=	C6H3	+	M	
249)	C6H3	+	H	=	C4H2	+	C2H2			
250)	C6H3	+	H	+	M	=	C6H4	+	M	
251)	C6H4	+	H	=	C6H3	+	H2			
252)	C6H4	+	H	+	M	=	NC6H5	+	M	
253)	C6H4	+	H	+	M	=	A1-	+	M	
254)	NC6H5	+	H	=	C4H4	+	C2H2			
255)	NC6H5	+	H	=	C6H4	+	H2			
256)	NC6H5	+	H	+	M	=	C6H6	+	M	
257)	C6H6	+	H	=	NC6H5	+	H2			
258)	C6H6	+	H	=	A1	+	H			
259)	C6H6	+	H	+	M	=	C6H7	+	M	
260)	C6H7	+	H	=	C6H6	+	H2			
261)	C6H7	+	M	=	A1	+	H	+	M	
262)	A1-	+	H	+	M	=	A1	+	M	
263)	A1-	+	C2H2	=	PAH	+	H			
264)	A1	+	H	=	A1-	+	H2			
265)	A1	+	C2H	=	PAH	+	H			
266)	H	=	HP	+	EL					
267)	HE	=	HEP	+	EL					
268)	H2	=	H2P	+	EL					

k	=	0.00E+00	EXP(0./T)
k	=	0.00E+00	EXP(0./T)
k	=	0.00E+00	EXP(0./T)
k	=	0.00E+00	EXP(0./T)
k	=	0.00E+00	EXP(0./T)
k	=	0.00E+00	EXP(0./T)
k	=	0.00E+00	EXP(0./T)
k	=	0.00E+00	EXP(0./T)
k0	=	0.00E+00	EXP(0./T)
koo	=	0.00E+00	EXP(0./T)
k	=	4.98E-12	EXP(0./T)
k0	=	1.00E-27	EXP(0./T)
koo	=	4.98E-12	EXP(0./T)
k	=	8.30E-11	EXP(0./T)
k	=	2.16E-11	EXP(-3334./T)
k	=	3.32E-11	EXP(0./T)
k	=	1.59E-10	EXP(0./T)
k0	=	1.00E-27	(T/ 1.)** 0.0 EXP(0./T)
koo	=	1.83E+06	(T/ 1.)** -6.3 EXP(-1405./T)
k	=	6.14E-08	T** -1.2 EXP(-5589./T)
k0	=	1.00E-27	(T/ 1.)** 0.0 EXP(0./T)
koo	=	7.08E-20	(T/ 1.)** 2.0 EXP(0./T)
k0	=	1.00E-27	(T/ 1.)** 0.0 EXP(0./T)
koo	=	4.65E-21	(T/ 1.)** 2.9 EXP(-704./T)
k	=	1.23E-09	T** -0.7 EXP(-4240./T)
k	=	1.66E-08	T** -1.3 EXP(-2715./T)
k0	=	1.24E-21	(T/ 1.)** -3.3 EXP(-5136./T)
koo	=	1.83E-10	(T/ 1.)** -1.3 EXP(-1460./T)
k	=	8.30E-11	EXP(0./T)
k	=	8.30E-11	EXP(0./T)
k	=	8.30E-11	EXP(0./T)
k0	=	1.03E-14	(T/ 1.)** -4.8 EXP(-957./T)
koo	=	1.66E-07	(T/ 1.)** -1.0 EXP(0./T)
k0	=	1.00E-27	EXP(0./T)
koo	=	6.43E-12	EXP(0./T)
k	=	3.99E-05	T** -1.6 EXP(-1410./T)
k0	=	1.00E-27	(T/ 1.)** 0.0 EXP(0./T)
koo	=	6.97E+20	(T/ 1.)**-10.3 EXP(-3973./T)
k	=	1.10E-17	T** 2.5 EXP(-4653./T)
k0	=	1.00E-27	EXP(0./T)
koo	=	2.46E-14	EXP(0./T)
k0	=	1.00E-27	EXP(0./T)
koo	=	6.65E-13	EXP(0./T)
k	=	2.66E-05	T** -1.6 EXP(-1118./T)
k	=	2.49E-11	EXP(0./T)
k0	=	1.00E-27	(T/ 1.)** 0.0 EXP(0./T)
koo	=	1.83E+18	(T/ 1.)** -9.6 EXP(-3525./T)
k	=	1.10E-18	T** 2.5 EXP(-6163./T)
k	=	1.44E-07	T** -1.3 EXP(-1762./T)
k0	=	8.00E-31	(T/ 1.)** -0.5 EXP(-504./T)
koo	=	2.49E-08	(T/ 1.)** -1.7 EXP(-806./T)
k	=	2.49E-11	EXP(0./T)
k	=	1.39E-02	T** -4.2 EXP(-5690./T)
k0	=	1.82E+28	(T/ 1.)**-16.3 EXP(-3526./T)
koo	=	1.66E-10	(T/ 1.)** 0.0 EXP(0./T)
k	=	1.60E-13	EXP(0./T)
k	=	5.00E-12	EXP(-4076./T)
k	=	8.30E-11	EXP(0./T)
k	=	0.00E+00	EXP(0./T)
k	=	0.00E+00	EXP(0./T)
k	=	0.00E+00	EXP(0./T)

269)	H2	=	HP	+	H	+	EL			k	=	0.00E+00	EXP(0./T)
270)	C	=	CP	+	EL					k	=	0.00E+00	EXP(0./T)
271)	CH3	=	CH3P	+	EL					k	=	0.00E+00	EXP(0./T)
272)	CH4	=	CH4P	+	EL					k	=	0.00E+00	EXP(0./T)
273)	C2H2	=	C2H2P	+	EL					k	=	0.00E+00	EXP(0./T)
274)	2Y	=	H2P	+	EL					k	=	0.00E+00	EXP(0./T)
275)	2Y	=	HP	+	H	+	EL			k	=	0.00E+00	EXP(0./T)
276)	2Y	=	HP	+	EL					k	=	0.00E+00	EXP(0./T)
277)	2Y	=	HEP	+	EL					k	=	0.00E+00	EXP(0./T)
278)	HP	+	H	=	H2P					k	=	6.67E-20	T** 1.0 EXP(0./T)
279)	HP	+	H2	=	H2P	+	H			k	=	1.00E-10	EXP(-21200./T)
280)	HP	+	2H2	=	H3P	+	H2			k0	=	3.20E-29	EXP(0./T)
										koo	=	0.00E+00	EXP(0./T)
281)	HP	+	H2V4	=	H2P	+	H			k	=	2.00E-09	EXP(0./T)
282)	HP	+	CH	=	CHP	+	H			k	=	0.00E+00	EXP(0./T)
283)	HP	+	(3)CH2	=	CHP	+	H2			k	=	0.00E+00	EXP(0./T)
284)	HP	+	(3)CH2	=	CH2P	+	H			k	=	0.00E+00	EXP(0./T)
285)	HP	+	CH3	=	CH3P	+	H			k	=	0.00E+00	EXP(0./T)
286)	HP	+	CH4	=	CH3P	+	H2			k	=	3.40E-09	EXP(0./T)
287)	HP	+	CH4	=	CH4P	+	H			k	=	7.47E-10	EXP(0./T)
288)	HP	+	C2H2	=	C2HP	+	H2			k	=	4.30E-09	EXP(0./T)
289)	HP	+	C2H2	=	C2H2P	+	H			k	=	2.00E-09	EXP(0./T)
290)	HP	+	C2H4	=	C2H2P	+	H2	+	H	k	=	1.00E-09	EXP(0./T)
291)	HP	+	C2H4	=	C2H3P	+	H2			k	=	3.00E-09	EXP(0./T)
292)	HP	+	C2H4	=	C2H4P	+	H			k	=	1.00E-09	EXP(0./T)
293)	HP	+	C2H6	=	C2H3P	+	2H2			k	=	1.30E-09	EXP(0./T)
294)	HP	+	C2H6	=	C2H4P	+	H2	+	H	k	=	1.30E-09	EXP(0./T)
295)	HP	+	C2H6	=	C2H5P	+	H2			k	=	1.30E-09	EXP(0./T)
296)	HP	+	C3H2	=	C3HP	+	H2			k	=	2.00E-09	EXP(0./T)
297)	HP	+	C3H2	=	C3H2P	+	H			k	=	2.00E-09	EXP(0./T)
298)	HP	+	C3H3	=	C3H2P	+	H2			k	=	2.00E-09	EXP(0./T)
299)	HP	+	C3H3	=	C3H3P	+	PROD			k	=	2.00E-09	EXP(0./T)
300)	HP	+	CH3C2H	=	C3H3P	+	H2			k	=	2.00E-09	EXP(0./T)
301)	HP	+	CH3C2H	=	CH3C2HP	+	H			k	=	2.00E-09	EXP(0./T)
302)	HEP	+	H	=	HP	+	HE			k	=	1.90E-15	EXP(0./T)
303)	HEP	+	H2	=	H2P	+	HE			k	=	9.35E-15	EXP(0./T)
304)	HEP	+	H2	=	HP	+	H	+	HE	k	=	8.80E-14	EXP(0./T)
305)	HEP	+	H2V2	=	HP	+	H	+	HE	k	=	1.00E-09	EXP(0./T)
306)	HEP	+	H2	=	HEHP	+	H			k	=	4.21E-13	EXP(0./T)
307)	HEP	+	C	=	CP	+	HE			k	=	8.74E-17	T** 0.8 EXP(0./T)
308)	HEP	+	(3)CH2	=	CHP	+	PROD			k	=	7.50E-10	EXP(0./T)
309)	HEP	+	(3)CH2	=	CP	+	PROD			k	=	1.10E-09	EXP(0./T)
310)	HEP	+	CH4	=	HP	+	CH3	+	HE	k	=	4.76E-10	EXP(0./T)
311)	HEP	+	CH4	=	CHP	+	H	+	PROD	k	=	2.38E-10	EXP(0./T)
312)	HEP	+	CH4	=	CH2P	+	H2	+	HE	k	=	8.50E-10	EXP(0./T)
313)	HEP	+	CH4	=	CH3P	+	H	+	HE	k	=	8.50E-11	EXP(0./T)
314)	HEP	+	CH4	=	CH4P	+	HE			k	=	5.10E-11	EXP(0./T)
315)	HEP	+	C2H2	=	CHP	+	CH	+	HE	k	=	7.70E-10	EXP(0./T)
316)	HEP	+	C2H2	=	C2P	+	H2	+	HE	k	=	1.61E-09	EXP(0./T)
317)	HEP	+	C2H2	=	C2HP	+	H	+	HE	k	=	8.75E-10	EXP(0./T)
318)	HEP	+	C2H2	=	C2H2P	+	HE			k	=	2.45E-10	EXP(0./T)
319)	HEP	+	C2H4	=	CH2P	+	(3)CH2	+	HE	k	=	4.08E-10	EXP(0./T)
320)	HEP	+	C2H4	=	C2HP	+	H	+	PROD	k	=	4.42E-10	EXP(0./T)
321)	HEP	+	C2H4	=	C2H2P	+	H2	+	HE	k	=	2.18E-09	EXP(0./T)
322)	HEP	+	C2H4	=	C2H3P	+	H	+	HE	k	=	1.70E-10	EXP(0./T)
323)	HEP	+	C2H4	=	C2H4P	+	HE			k	=	2.38E-10	EXP(0./T)
324)	HEP	+	C2H6	=	C2H2P	+	2H2	+	HE	k	=	8.40E-10	EXP(0./T)
325)	HEP	+	C2H6	=	C2H3P	+	H	+	PROD	k	=	1.74E-09	EXP(0./T)
326)	HEP	+	C2H6	=	C2H4P	+	H2	+	HE	k	=	4.20E-10	EXP(0./T)
327)	HEP	+	C3H2	=	C3P	+	PROD			k	=	0.00E+00	EXP(0./T)
328)	HEP	+	C3H2	=	C3HP	+	PROD			k	=	0.00E+00	EXP(0./T)

329)	HEP	+	C3H3	=	C-C3H2P	+	PROD			k	=	0.00E+00	EXP(	0./T)
330)	HEP	+	C3H3	=	C3HP	+	PROD			k	=	0.00E+00	EXP(	0./T)
331)	HEP	+	C3H3	=	C3P	+	PROD			k	=	0.00E+00	EXP(	0./T)
332)	HEP	+	A1	=	C5H5P	+	CH	+	HE	k	=	7.00E-10	EXP(	0./T)
333)	HEP	+	A1	=	C-C6H5P	+	PROD			k	=	7.00E-10	EXP(	0./T)
334)	H2P	+	H	=	HP	+	H2			k	=	6.40E-10	EXP(	0./T)
335)	H2P	+	H2	=	H3P	+	H			k	=	2.00E-09	EXP(	0./T)
336)	H2P	+	C	=	CHP	+	PROD			k	=	2.40E-09	EXP(	0./T)
337)	H2P	+	(3)CH2	=	CH3P	+	PROD			k	=	1.00E-09	EXP(	0./T)
338)	H2P	+	(3)CH2	=	CH2P	+	H2			k	=	1.00E-09	EXP(	0./T)
339)	H2P	+	CH4	=	CH3P	+	H	+	H2	k	=	2.28E-09	EXP(	0./T)
340)	H2P	+	CH4	=	CH4P	+	H2			k	=	1.41E-09	EXP(	0./T)
341)	H2P	+	CH4	=	CH5P	+	H			k	=	1.10E-10	EXP(	0./T)
342)	H2P	+	C2H2	=	C2H2P	+	H2			k	=	4.82E-09	EXP(	0./T)
343)	H2P	+	C2H2	=	C2H3P	+	PROD			k	=	4.77E-10	EXP(	0./T)
344)	H2P	+	C2H4	=	C2H2P	+	2H2			k	=	8.82E-10	EXP(	0./T)
345)	H2P	+	C2H4	=	C2H3P	+	PROD			k	=	1.81E-09	EXP(	0./T)
346)	H2P	+	C2H4	=	C2H4P	+	H2			k	=	2.21E-09	EXP(	0./T)
347)	H2P	+	C2H6	=	C2H6P	+	H2			k	=	2.94E-10	EXP(	0./T)
348)	H2P	+	C2H6	=	C2H5P	+	H	+	H2	k	=	1.37E-09	EXP(	0./T)
349)	H2P	+	C2H6	=	C2H4P	+	2H2			k	=	2.35E-09	EXP(	0./T)
350)	H2P	+	C2H6	=	C2H3P	+	H	+	2H2	k	=	6.86E-10	EXP(	0./T)
351)	H2P	+	C2H6	=	C2H2P	+	3H2			k	=	1.96E-10	EXP(	0./T)
352)	HEHP	+	H	=	H2P	+	HE			k	=	9.10E-10	EXP(	0./T)
353)	HEHP	+	H2	=	H3P	+	HE			k	=	1.50E-09	EXP(	0./T)
354)	HEHP	+	C2H4	=	C2H3P	+	H2	+	HE	k	=	2.10E-09	EXP(	0./T)
355)	HEHP	+	C2H4	=	C2H4P	+	PROD			k	=	7.00E-10	EXP(	0./T)
356)	HEHP	+	C2H6	=	C2H3P	+	HE	+	2H2	k	=	1.05E-09	EXP(	0./T)
357)	HEHP	+	C2H6	=	C2H5P	+	HE	+	H2	k	=	1.05E-09	EXP(	0./T)
358)	H3P	+	C	=	CHP	+	H2			k	=	2.00E-09	EXP(	0./T)
359)	H3P	+	CH	=	CH2P	+	H2			k	=	1.20E-09	EXP(	0./T)
360)	H3P	+	(3)CH2	=	CH3P	+	H2			k	=	1.70E-09	EXP(	0./T)
361)	H3P	+	CH3	=	CH4P	+	H2			k	=	2.10E-09	EXP(	0./T)
362)	H3P	+	CH4	=	CH5P	+	H2			k	=	2.40E-09	EXP(	0./T)
363)	H3P	+	C2H2	=	C2H3P	+	H2			k	=	3.20E-09	EXP(	0./T)
364)	H3P	+	C2H3	=	C2H4P	+	H2			k	=	2.00E-09	EXP(	0./T)
365)	H3P	+	C2H4	=	C2H3P	+	2H2			k	=	2.03E-09	EXP(	0./T)
366)	H3P	+	C2H4	=	C2H5P	+	H2			k	=	8.70E-10	EXP(	0./T)
367)	H3P	+	C2H5	=	C2H6P	+	H2			k	=	0.00E+00	EXP(	0./T)
368)	H3P	+	C2H6	=	C2H5P	+	2H2			k	=	2.90E-10	EXP(	0./T)
369)	H3P	+	C2H6	=	C2H7P	+	H2			k	=	2.90E-11	EXP(	0./T)
370)	H3P	+	C3H2	=	C3H3P	+	H2			k	=	2.00E-09	EXP(	0./T)
371)	H3P	+	CH3C2H	=	C3H5P	+	H2			k	=	6.75E-10	EXP(	0./T)
372)	H3P	+	CH3C2H	=	C3H3P	+	2H2			k	=	2.25E-09	EXP(	0./T)
373)	H3P	+	C4H2	=	C4H3P	+	H2			k	=	2.60E-09	EXP(	0./T)
374)	H3P	+	A1	=	C-C6H7P	+	H2			k	=	3.90E-09	EXP(	0./T)
375)	CP	+	H2	=	CH2P					k	=	1.25E-15	T** -0.2 EXP(	0./T)
376)	CP	+	CH4	=	C2H2P	+	H2			k	=	3.64E-10	EXP(	0./T)
377)	CP	+	CH4	=	C2H3P	+	H			k	=	9.36E-10	EXP(	0./T)
378)	CP	+	C2H2	=	C3HP	+	H			k	=	2.63E-09	EXP(	0./T)
379)	CP	+	C2H4	=	C2H3P	+	CH			k	=	1.20E-10	EXP(	0./T)
380)	CP	+	C2H4	=	C2H4P	+	C			k	=	2.25E-10	EXP(	0./T)
381)	CP	+	C2H4	=	C3HP	+	PROD			k	=	7.50E-11	EXP(	0./T)
382)	CP	+	C2H4	=	C3H2P	+	H2			k	=	4.35E-10	EXP(	0./T)
383)	CP	+	C2H4	=	C3H3P	+	H			k	=	6.30E-10	EXP(	0./T)
384)	CP	+	C2H6	=	C2H2P	+	CH4			k	=	1.70E-10	EXP(	0./T)
385)	CP	+	C2H6	=	C2H3P	+	CH3			k	=	5.10E-10	EXP(	0./T)
386)	CP	+	C2H6	=	C2H5P	+	CH			k	=	1.70E-10	EXP(	0./T)
387)	CP	+	C2H6	=	C3H3P	+	H	+	H2	k	=	8.50E-10	EXP(	0./T)
388)	CHP	+	H	=	CP	+	H2			k	=	7.50E-10	EXP(	0./T)
389)	CHP	+	H2	=	CH2P	+	H			k	=	1.20E-09	EXP(	0./T)

```
390)  CHP     + CH4     =  C2H2P   +  PROD                    k   =  1.40E-10 EXP(     0./T)
391)  CHP     + CH4     =  C2H3P   +  H2                      k   =  1.10E-09 EXP(     0./T)
392)  CHP     + CH4     =  C2H4P   +  PROD                    k   =  6.50E-11 EXP(     0./T)
393)  CHP     + C2H2    =  C3H2P   +  PROD                    k   =  2.40E-09 EXP(     0./T)
394)  CH2P    + H2      =  CH3P    +  H                       k   =  1.16E-09 EXP(     0./T)
395)  CH2P    + CH4     =  C2H4P   +  H2                      k   =  9.10E-10 EXP(     0./T)
396)  CH2P    + CH4     =  C2H5P   +  H                       k   =  3.90E-10 EXP(     0./T)
397)  CH2P    + C2H2    =  C-C3H3P +  PROD                    k   =  2.50E-09 EXP(     0./T)
398)  CH3P    + H       =  CH2P    +  H2                      k   =  0.00E+00 EXP(     0./T)
399)  CH3P    + H2      =  CH5P                               k   =  3.90E-12 T** -1.0 EXP(     0./T)
400)  CH3P    + H2      +  HE      =  CH5P    +  HE           k0  =  1.10E-28 EXP(     0./T)
                                                             koo =  0.00E+00 EXP(     0./T)
401)  CH3P    + C       =  C2HP    +  H2                      k   =  1.20E-09 EXP(     0./T)
402)  CH3P    + CH      =  C2H2P   +  H2                      k   =  7.10E-10 EXP(     0./T)
403)  CH3P    + (3)CH2  =  C2H3P   +  H2                      k   =  9.90E-10 EXP(     0./T)
404)  CH3P    + CH4     =  C2H5P   +  H2                      k   =  1.10E-09 EXP(     0./T)
405)  CH3P    + 2H2     =  CH5P    +  H2                      k0  =  3.30E-29 EXP(     0./T)
                                                             koo =  0.00E+00 EXP(     0./T)
406)  CH3P    + C2H2    =  C3H3P   +  H2                      k   =  1.15E-09 EXP(     0./T)
407)  CH3P    + C2H4    =  C2H3P   +  CH4                     k   =  4.88E-10 EXP(     0./T)
408)  CH3P    + C2H4    =  C3H3P   +  2H2                     k   =  4.24E-11 EXP(     0./T)
409)  CH3P    + C2H4    =  C3H5P   +  H2                      k   =  5.40E-10 EXP(     0./T)
410)  CH3P    + C2H6    =  C2H5P   +  CH4                     k   =  1.50E-09 EXP(     0./T)
411)  CH3P    + C2H6    =  C3H5P   +  2H2                     k   =  1.60E-10 EXP(     0./T)
412)  CH3P    + C2H6    =  C3HNP   +  H2                      k   =  1.00E-10 EXP(     0./T)
413)  CH3P    + C3H2    =  C4H3P   +  H2                      k   =  2.70E-09 EXP(     0./T)
414)  CH3P    + C3H3    =  C4H5P   +  H                       k   =  4.00E-09 EXP(     0./T)
415)  CH4P    + H       =  CH3P    +  H2                      k   =  1.00E-11 EXP(     0./T)
416)  CH4P    + H2      =  CH5P    +  H                       k   =  3.50E-11 EXP(     0./T)
417)  CH4P    + CH4     =  CH5P    +  CH3                     k   =  1.14E-09 EXP(     0./T)
418)  CH4P    + C2H2    =  C2H2P   +  CH4                     k   =  1.44E-09 EXP(     0./T)
419)  CH4P    + C2H2    =  C2H3P   +  CH3                     k   =  1.12E-09 EXP(     0./T)
420)  CH4P    + C2H2    =  C3H3P   +  H       +  H2          k   =  1.63E-10 EXP(     0./T)
421)  CH4P    + C2H4    =  C2H4P   +  CH4                     k   =  1.70E-09 EXP(     0./T)
422)  CH4P    + C2H4    =  C2H5P   +  CH3                     k   =  2.60E-10 EXP(     0./T)
423)  CH4P    + C2H4    =  C3H5P   +  H       +  H2          k   =  6.00E-11 EXP(     0./T)
424)  CH4P    + C2H6    =  C2H4P   +  CH4     +  H2          k   =  1.91E-09 EXP(     0./T)
425)  CH5P    + H       =  CH4P    +  H2                      k   =  1.50E-10 EXP(     0./T)
426)  CH5P    + C       =  CHP     +  CH4                     k   =  1.20E-09 EXP(     0./T)
427)  CH5P    + CH      =  CH2P    +  CH4                     k   =  6.90E-10 EXP(     0./T)
428)  CH5P    + (3)CH2  =  CH3P    +  CH4                     k   =  9.60E-10 EXP(     0./T)
429)  CH5P    + C2H2    =  C2H3P   +  CH4                     k   =  1.48E-09 EXP(     0./T)
430)  CH5P    + C2H4    =  C2H5P   +  CH4                     k   =  1.50E-09 EXP(     0./T)
431)  CH5P    + C2H6    =  C2H5P   +  CH4     +  H2          k   =  2.03E-10 EXP(     0./T)
432)  CH5P    + C2H6    =  C2H7P   +  CH4                     k   =  1.15E-09 EXP(     0./T)
433)  CH5P    + A1      =  C-C6H7P +  CH4                     k   =  2.00E-09 EXP(     0./T)
434)  C2P     + H2      =  C2HP    +  H                       k   =  1.20E-09 EXP(     0./T)
435)  C2P     + CH4     =  C2HP    +  CH3                     k   =  2.38E-10 EXP(     0./T)
436)  C2P     + CH4     =  C2H2P   +  (3)CH2                  k   =  1.82E-10 EXP(     0./T)
437)  C2P     + CH4     =  C3HP    +  H2      +  PROD         k   =  1.96E-10 EXP(     0./T)
438)  C2P     + CH4     =  C3H2P   +  H2                      k   =  5.74E-10 EXP(     0./T)
439)  C2P     + CH4     =  C3H3P   +  PROD                    k   =  2.10E-10 EXP(     0./T)
440)  C2P     + C2H2    =  C4HP    +  PROD                    k   =  1.20E-09 EXP(     0./T)
441)  C2P     + C2H4    =  C4HNP                              k   =  1.90E-09 EXP(     0./T)
442)  C2HP    + H2      =  C2H2P   +  H                       k   =  1.24E-09 EXP(     0./T)
443)  C2HP    + CH4     =  C2H2P   +  CH3                     k   =  3.74E-10 EXP(     0./T)
444)  C2HP    + CH4     =  C3H3P   +  H2                      k   =  3.74E-10 EXP(     0./T)
445)  C2HP    + CH4     =  CH3C2HP +  PROD                    k   =  1.32E-10 EXP(     0./T)
446)  C2HP    + CH4     =  C3H5P                              k   =  2.20E-10 EXP(     0./T)
447)  C2HP    + C2H2    =  C4H2P   +  PROD                    k   =  1.85E-09 EXP(     0./T)
448)  C2HP    + C2H4    =  C4HNP                              k   =  1.71E-09 EXP(     0./T)
```

449)	C2H2P + H2 = C2H3P + H	k = 1.00E-11 EXP(0./T)
450)	C2H2P + H2 = C2H4P	k = 1.22E-10 T** -1.5 EXP(0./T)
451)	C2H2P + H2 + HE = C2H4P + HE	k0 = 1.20E-27 EXP(0./T)
		koo = 0.00E+00 EXP(0./T)
452)	C2H2P + C = C3HP + H	k = 1.10E-09 EXP(0./T)
453)	C2H2P + (3)CH2 = C3H3P + H	k = 8.80E-10 EXP(0./T)
454)	C2H2P + CH4 = CH3C2HP + H2	k = 1.87E-10 EXP(0./T)
455)	C2H2P + CH4 = C3H5P + H	k = 7.00E-10 EXP(0./T)
456)	C2H2P + C2H2 = C4H2P + H2	k = 4.48E-10 EXP(0./T)
457)	C2H2P + C2H2 = C4H3P + H	k = 9.52E-10 EXP(0./T)
458)	C2H2P + C2H4 = C2H4P + C2H2	k = 4.14E-10 EXP(0./T)
459)	C2H2P + C2H4 = C3H3P + CH3	k = 6.62E-10 EXP(0./T)
460)	C2H2P + C2H4 = C4H5P + H	k = 3.17E-10 EXP(0./T)
461)	C2H2P + C2H6 = C2H4P + C2H4	k = 2.63E-10 EXP(0./T)
462)	C2H2P + C2H6 = C2H5P + C2H3	k = 1.31E-10 EXP(0./T)
463)	C2H2P + C2H6 = C3H3P + CH3 + H2	k = 8.76E-11 EXP(0./T)
464)	C2H2P + C2H6 = CH3C2HP + CH4	k = 1.46E-11 EXP(0./T)
465)	C2H2P + C2H6 = C3H5P + CH3	k = 7.88E-10 EXP(0./T)
466)	C2H2P + C2H6 = C4H5P + H + H2	k = 7.30E-11 EXP(0./T)
467)	C2H2P + C2H6 = C4HNP + H	k = 1.31E-10 EXP(0./T)
468)	C2H2P + C3H2 = C5H3P + H	k = 1.30E-09 EXP(0./T)
469)	C2H2P + C3H3 = C5H4P + PROD	k = 1.00E-09 EXP(0./T)
470)	C2H2P + C3H3 = C5H3P + H2	k = 1.00E-09 EXP(0./T)
471)	C2H3P + H = C2H2P + H2	k = 6.80E-11 EXP(0./T)
472)	C2H3P + C = C-C3H2P + H	k = 1.00E-09 EXP(0./T)
473)	C2H3P + CH4 = C3H5P + H2	k = 1.90E-10 EXP(0./T)
474)	C2H3P + C2H2 = C4H3P + H2	k = 2.16E-10 EXP(0./T)
475)	C2H3P + C2H2 + M = C4H5P + M	k0 = 1.00E-27 EXP(0./T)
		koo = 1.00E-09 EXP(0./T)
476)	C2H3P + C2H4 = C2H5P + C2H2	k = 8.20E-10 EXP(0./T)
477)	C2H3P + C2H6 = C2H5P + C2H4	k = 2.91E-10 EXP(0./T)
478)	C2H3P + C2H6 = C3H5P + CH4	k = 2.48E-10 EXP(0./T)
479)	C2H3P + C2H6 = C4HNP + H2	k = 8.06E-11 EXP(0./T)
480)	C2H3P + C3H2 = C3H3P + C2H2	k = 8.00E-10 EXP(0./T)
481)	C2H3P + C3H2 = C5H3P + H2	k = 8.00E-10 EXP(0./T)
482)	C2H3P + C3H2 = C5H4P + H	k = 8.00E-10 EXP(0./T)
483)	C2H3P + C3H3 = CH3C2HP + C2H2	k = 1.00E-09 EXP(0./T)
484)	C2H3P + C3H3 = C5H5P + H	k = 1.00E-09 EXP(0./T)
485)	C2H3P + C3H3 = C5H4P + H2	k = 1.00E-09 EXP(0./T)
486)	C2H3P + CH3C2H = C3H5P + C2H2	k = 5.00E-10 EXP(0./T)
487)	C2H3P + CH3C2H = C5H5P + H2	k = 5.00E-10 EXP(0./T)
488)	C2H3P + A1 = C-C6H7P + C2H2	k = 1.60E-09 EXP(0./T)
489)	C2H4P + H = C2H3P + H2	k = 3.00E-10 EXP(0./T)
490)	C2H4P + C = C3H3P + H	k = 1.00E-09 EXP(0./T)
491)	C2H4P + C = C-C3H2P + H2	k = 1.00E-09 EXP(0./T)
492)	C2H4P + C2H2 = C3H3P + CH3	k = 6.47E-10 EXP(0./T)
493)	C2H4P + C2H2 = C4H5P + H	k = 1.93E-10 EXP(0./T)
494)	C2H4P + C2H4 = C3H5P + CH3	k = 7.55E-10 EXP(0./T)
495)	C2H4P + C2H4 = C4HNP	k = 7.47E-11 EXP(0./T)
496)	C2H4P + C2H6 = C3HNP + CH4	k = 3.71E-13 EXP(0./T)
497)	C2H4P + C2H6 = C3HNP + CH3	k = 4.93E-12 EXP(0./T)
498)	C2H4P + C3H2 = C4H3P + CH3	k = 1.50E-09 EXP(0./T)
499)	C2H4P + C3H2 = C5H5P + H	k = 5.00E-10 EXP(0./T)
500)	C2H4P + C3H3 = C4H3P + CH4	k = 8.00E-10 EXP(0./T)
501)	C2H4P + C3H3 = C5H5P + H2	k = 8.00E-10 EXP(0./T)
502)	C2H5P + H = C2H4P + H2	k = 1.00E-11 EXP(0./T)
503)	C2H5P + CH4 = C3HNP + H2	k = 9.00E-14 EXP(0./T)
504)	C2H5P + C2H2 = C-C3H3P + CH4	k = 7.20E-12 EXP(0./T)
505)	C2H5P + C2H2 = C4H5P + H2	k = 1.17E-10 EXP(0./T)
506)	C2H5P + C2H4 = C3H5P + CH4	k = 3.55E-10 EXP(0./T)
507)	C2H5P + C2H6 = C3HNP + CH4	k = 5.50E-12 EXP(0./T)

508)	C2H5P + C2H6 = C4HNP + H2	k = 3.35E-11 EXP(0./T)
509)	C2H5P + C3H8 = C3HNP + C2H6	k = 6.30E-10 EXP(0./T)
510)	C2H6P + H = C2H5P + H2	k = 1.00E-10 EXP(0./T)
511)	C2H6P + C2H2 = C2H5P + C2H3	k = 2.22E-10 EXP(0./T)
512)	C2H6P + C2H2 = C3H5P + CH3	k = 8.19E-10 EXP(0./T)
513)	C2H6P + C2H2 = C4HNP + PROD	k = 1.29E-10 EXP(0./T)
514)	C2H6P + C2H4 = C2H4P + C2H6	k = 1.15E-09 EXP(0./T)
515)	C2H6P + C2H6 = C3HNP + CH4	k = 7.98E-12 EXP(0./T)
516)	C2H6P + C2H6 = C3HNP + CH3	k = 1.10E-11 EXP(0./T)
517)	C2H7P + C2H2 = C2H3P + C2H6	k = 1.00E-09 EXP(0./T)
518)	C2H7P + C2H4 = C2H5P + C2H6	k = 1.00E-09 EXP(0./T)
519)	C3P + H2 = C3HP + H	k = 3.00E-10 EXP(0./T)
520)	C3HP + H2 = C-C3H2P + H	k = 1.04E-12 EXP(0./T)
521)	C3HP + H2 = C3H2P + H	k = 4.16E-12 EXP(0./T)
522)	C3HP + H2 + M = C-C3H3P + M	k0 = 1.00E-27 EXP(0./T)
		koo = 1.35E-11 EXP(0./T)
523)	C3HP + H2 + M = C3H3P + M	k0 = 1.00E-27 EXP(0./T)
		koo = 7.28E-12 EXP(0./T)
524)	C3H2P + H = C3HP + H2	k = 6.00E-11 EXP(0./T)
525)	C3H2P + C2H2 = C5H3P + H	k = 1.10E-09 EXP(0./T)
526)	C-C3H2P + C = C4P + H2	k = 1.00E-09 EXP(0./T)
527)	C-C3H2P + C = C4HP + H	k = 1.00E-09 EXP(0./T)
528)	C-C3H2P + C2H2 = C5H3P + H	k = 9.00E-10 EXP(0./T)
529)	C-C3H2P + C2H4 = C4H3P + CH3	k = 3.00E-10 EXP(0./T)
530)	C-C3H2P + C2H4 = C5H5P + H	k = 3.00E-10 EXP(0./T)
531)	C-C3H2P + C3H2 = C6H2P + H2	k = 1.00E-09 EXP(0./T)
532)	C-C3H2P + C3H2 = C6H3P + H	k = 1.00E-09 EXP(0./T)
533)	C-C3H2P + C3H3 = C6H4P + H	k = 2.00E-09 EXP(0./T)
534)	C-C3H3P + CH3C2H = C6H5P + H2	k = 1.00E-09 EXP(0./T)
535)	C3H3P + C = C4H2P + H	k = 1.00E-09 EXP(0./T)
536)	C3H3P + C = C4HP + H2	k = 1.00E-09 EXP(0./T)
537)	C3H3P + C2H2 = C-C3H3P + C2H2	k = 2.10E-10 EXP(0./T)
538)	C3H3P + CH3C2H = C6H5P + H2	k = 1.00E-09 EXP(0./T)
539)	C-C3H3P + C = C4H2P + H	k = 1.00E-09 EXP(0./T)
540)	C-C3H3P + C = C4HP + H2	k = 1.00E-09 EXP(0./T)
541)	CH3C2HP + H = C3H3P + H2	k = 3.00E-11 EXP(0./T)
542)	CH3C2HP + C = C4H2P + H2	k = 1.00E-09 EXP(0./T)
543)	CH3C2HP + C = C4H3P + H	k = 1.00E-09 EXP(0./T)
544)	CH3C2HP + C2H2 = C5H5P + H	k = 4.90E-10 EXP(0./T)
545)	C3H5P + H = C2H2P + CH4	k = 5.00E-13 EXP(0./T)
546)	C3H5P + H = C2H3P + CH3	k = 9.60E-12 EXP(0./T)
547)	C3H5P + C = C4H3P + H2	k = 1.00E-09 EXP(0./T)
548)	C3H5P + C2H2 = C5H5P + H2	k = 3.80E-10 EXP(0./T)
549)	C3H5P + C2H4 = C5HNP + H2	k = 1.19E-10 EXP(0./T)
550)	C3H5P + C2H4 + M = C5HNP + M	k0 = 1.00E-27 EXP(0./T)
		koo = 5.10E-11 EXP(0./T)
551)	C3H5P + CH3C2H = C-C6H7P + H2	k = 1.00E-09 EXP(0./T)
552)	C3H5P + A1 = C-C6H7P + CH3C2H	k = 1.15E-10 EXP(0./T)
553)	C4P + H2 = C4HP + H	k = 3.00E-10 EXP(0./T)
554)	C4HP + H2 = C4H2P + H	k = 7.00E-10 EXP(0./T)
555)	C4HP + CH4 = C5H3P + H2	k = 1.10E-09 EXP(0./T)
556)	C4HP + C3H3 = C7HNP	k = 2.50E-09 EXP(0./T)
557)	C4H2P + H = C4H3P	k = 1.24E-11 T** -0.1 EXP(0./T)
558)	C4H2P + C = C5P + H2	k = 5.00E-10 EXP(0./T)
559)	C4H2P + C = C5HP + H	k = 5.00E-10 EXP(0./T)
560)	C4H2P + CH4 = C5H4P + H2	k = 2.00E-10 EXP(0./T)
561)	C4H2P + CH4 = C5H5P + H	k = 5.00E-10 EXP(0./T)
562)	C4H2P + C2H2 = C6H3P + H	k = 1.40E-11 EXP(0./T)
563)	C4H2P + C2H2 = C6H4P	k = 2.66E-10 EXP(0./T)
564)	C4H2P + C2H4 = C6H4P + H2	k = 2.00E-10 EXP(0./T)
565)	C4H2P + C2H4 = C6H5P + H	k = 8.00E-10 EXP(0./T)

566)	C4H2P + C3H2 = C7HNP + H	k = 2.20E-09 EXP(0./T)	
567)	C4H2P + C3H3 = C7HNP	k = 2.50E-09 EXP(0./T)	
568)	C4H3P + H = C4H4P	k = 3.25E-12 T** -0.7 EXP(0./T)	
569)	C4H3P + C = C5HP + H2	k = 5.00E-10 EXP(0./T)	
570)	C4H3P + CH4 = C5H5P + H2	k = 5.00E-10 EXP(0./T)	
571)	C4H3P + C2H2 = C-C6H5P	k = 2.20E-10 EXP(0./T)	
572)	C4H3P + A1 = C-C6H7P + C4H2	k = 1.00E-09 EXP(0./T)	
573)	C4H3P + C = C5H2P + H	k = 5.00E-10 EXP(0./T)	
574)	C4H3P + C3H2 = C7HNP + H	k = 1.50E-09 EXP(0./T)	
575)	C4H3P + C3H3 = C7HNP	k = 2.00E-09 EXP(0./T)	
576)	C4H4P + C2H2 = C6H4P + H2	k = 1.20E-11 EXP(0./T)	
577)	C4H4P + C2H2 = C-C6H5P + H	k = 9.00E-11 EXP(0./T)	
578)	C4H5P + C2H2 + M = C-C6H7P + M	k0 = 1.00E-27 EXP(0./T)	
		koo = 1.00E-09 EXP(0./T)	
579)	C4H5P + CH3C2H = C6H5P + CH4	k = 4.00E-10 EXP(0./T)	
580)	C4H5P + CH3C2H = C7HNP + H2	k = 6.00E-10 EXP(0./T)	
581)	C4H5P + C4H2 = C6H5P + C2H2	k = 1.00E-09 EXP(0./T)	
582)	C4H5P + C4H4 = C6H7P + C2H2	k = 1.00E-09 EXP(0./T)	
583)	C5P + H2 = C5HP + H	k = 7.30E-10 EXP(0./T)	
584)	C5HP + H2 = C5H2P + H	k = 1.00E-17 EXP(0./T)	
585)	C5HP + C = C6P + H	k = 1.00E-09 EXP(0./T)	
586)	C5H2P + C = C6P + H2	k = 5.00E-10 EXP(0./T)	
587)	C5H2P + C = C6HP + H	k = 5.00E-10 EXP(0./T)	
588)	C5H2P + CH4 = C6H4P + H2	k = 2.00E-10 EXP(0./T)	
589)	C5H2P + CH4 = C6H5P + H	k = 8.00E-10 EXP(0./T)	
590)	C5H2P + C2H2 = C7HNP	k = 1.00E-09 EXP(0./T)	
591)	C5H2P + C2H4 = C7HNP	k = 1.00E-09 EXP(0./T)	
592)	C5H2P + C3H2 = C8HNP	k = 1.80E-09 EXP(0./T)	
593)	C5H2P + C3H3 = C8HNP	k = 1.40E-09 EXP(0./T)	
594)	C5H3P + C = C6HP + H2	k = 5.00E-10 EXP(0./T)	
595)	C5H3P + C = C6H2P + H	k = 5.00E-10 EXP(0./T)	
596)	C5H5P + C2H2 = C7HNP	k = 3.10E-11 EXP(0./T)	
597)	C5H5P + CH3C2H = C-C6H7P + C2H2	k = 5.60E-10 EXP(0./T)	
598)	C5H5P + CH3C2H = C8HNP + H2	k = 4.40E-10 EXP(0./T)	
599)	C5H5P + C4H2 = C7HNP + C2H2	k = 1.76E-10 EXP(0./T)	
600)	C5H5P + C4H2 = C7HNP + C2	k = 3.30E-11 EXP(0./T)	
601)	C6P + H2 = C6HP + H	k = 7.00E-11 EXP(0./T)	
602)	C6P + H2 = C6H2P	k = 9.01E-13 T** -0.5 EXP(0./T)	
603)	C6HP + H2 = C6H2P + H	k = 9.50E-13 EXP(0./T)	
604)	C6H2P + CH4 = C7HNP	k = 1.00E-09 EXP(0./T)	
605)	C6H2P + C2H2 = C8HNP	k = 1.00E-09 EXP(0./T)	
606)	C6H2P + C2H4 = C8HNP + H2	k = 1.00E-09 EXP(0./T)	
607)	C6H2P + C3H2 = C9HNP	k = 1.80E-09 EXP(0./T)	
608)	C6H2P + C3H3 = C9HNP	k = 1.42E-09 EXP(0./T)	
609)	C6H3P + C = C7HNP	k = 1.00E-09 EXP(0./T)	
610)	C6H4P + H + M = C6H5P + M	k0 = 1.00E-27 EXP(0./T)	
		koo = 3.30E-11 EXP(0./T)	
611)	C6H5P + H2 = C6H7P	k = 5.00E-11 EXP(0./T)	
612)	C-C6H5P + H2 = C-C6H7P	k = 6.00E-11 EXP(0./T)	
613)	C6H7P + CH3C2H = C7HNP + C2H4	k = 1.00E-09 EXP(0./T)	
614)	HP + EL = H	k = 1.91E-10 T** -0.7 EXP(0./T)	
615)	HEP + EL = HE	k = 1.91E-10 T** -0.7 EXP(0./T)	
616)	H2P + EL = 2H	k = 2.25E-06 T** -0.4 EXP(0./T)	
617)	HEHP + EL = HE + H	k = 3.06E-07 T** -0.6 EXP(0./T)	
618)	H3P + EL = 3H	k = 3.52E-06 T** -0.6 EXP(0./T)	
619)	H3P + EL = H2 + H	k = 1.17E-06 T** -0.6 EXP(0./T)	
620)	CP + EL = C	k = 1.91E-10 T** -0.7 EXP(0./T)	
621)	CHP + EL = C + H	k = 1.65E-06 T** -0.4 EXP(0./T)	
622)	CH2P + EL = C + H2	k = 2.17E-06 T** -0.5 EXP(0./T)	
623)	CH2P + EL = CH + H	k = 2.17E-06 T** -0.5 EXP(0./T)	
624)	CH3P + EL = CH + 2H	k = 1.34E-06 T** -0.5 EXP(0./T)	

625)	CH3P	+	EL	=	CH	+	H2			k	=	3.38E-06	T** -0.5 EXP(0./T)
626)	CH3P	+	EL	=	(3)CH2	+	H			k	=	1.34E-06	T** -0.5 EXP(0./T)
627)	CH3P	+	EL	=	CH3					k	=	1.91E-09	T** -0.5 EXP(0./T)
628)	CH4P	+	EL	=	CH3	+	H			k	=	6.06E-06	T** -0.5 EXP(0./T)
629)	CH5P	+	EL	=	CH	+	2H2			k	=	1.84E-07	T** -0.5 EXP(0./T)
630)	CH5P	+	EL	=	(3)CH2	+	H	+	H2	k	=	1.03E-06	T** -0.5 EXP(0./T)
631)	CH5P	+	EL	=	CH3	+	2H			k	=	3.69E-06	T** -0.5 EXP(0./T)
632)	CH5P	+	EL	=	CH3	+	H2			k	=	3.30E-07	T** -0.5 EXP(0./T)
633)	CH5P	+	EL	=	CH4	+	H			k	=	1.75E-07	T** -0.5 EXP(0./T)
634)	C2P	+	EL	=	2C					k	=	5.20E-06	T** -0.5 EXP(0./T)
635)	C2HP	+	EL	=	CH	+	C			k	=	2.34E-06	T** -0.5 EXP(0./T)
636)	C2HP	+	EL	=	C2	+	PROD			k	=	2.34E-06	T** -0.5 EXP(0./T)
637)	C2H2P	+	EL	=	C2	+	2H			k	=	1.56E-06	T** -0.5 EXP(0./T)
638)	C2H2P	+	EL	=	2CH					k	=	1.56E-06	T** -0.5 EXP(0./T)
639)	C2H2P	+	EL	=	C2H	+	H			k	=	1.56E-06	T** -0.5 EXP(0./T)
640)	C2H3P	+	EL	=	(3)CH2	+	CH			k	=	3.98E-06	T** -0.5 EXP(0./T)
641)	C2H3P	+	EL	=	C2H2	+	H			k	=	3.98E-06	T** -0.5 EXP(0./T)
642)	C2H4P	+	EL	=	C2H2	+	2H			k	=	5.20E-06	T** -0.5 EXP(0./T)
643)	C2H5P	+	EL	=	C2H	+	2H2			k	=	2.60E-06	T** -0.5 EXP(0./T)
644)	C2H5P	+	EL	=	C2H2	+	H2	+	H	k	=	5.20E-06	T** -0.5 EXP(0./T)
645)	C2H5P	+	EL	=	C2H3	+	H2			k	=	2.60E-06	T** -0.5 EXP(0./T)
646)	C2H5P	+	EL	=	C2H4	+	H			k	=	2.60E-05	T** -0.5 EXP(0./T)
647)	C2H6P	+	EL	=	C2H4	+	H2			k	=	2.60E-06	T** -0.5 EXP(0./T)
648)	C2H6P	+	EL	=	C2H5	+	PROD			k	=	2.60E-06	T** -0.5 EXP(0./T)
649)	C2H7P	+	EL	=	C2H5	+	H2			k	=	2.60E-06	T** -0.5 EXP(0./T)
650)	C2H7P	+	EL	=	C2H6	+	H			k	=	2.60E-06	T** -0.5 EXP(0./T)
651)	C3P	+	EL	=	C2	+	C			k	=	5.20E-06	T** -0.5 EXP(0./T)
652)	C3HP	+	EL	=	C3	+	H			k	=	2.60E-06	T** -0.5 EXP(0./T)
653)	C3HP	+	EL	=	C2H	+	C			k	=	2.60E-06	T** -0.5 EXP(0./T)
654)	C-C3H2P	+	EL	=	C2H2	+	C			k	=	5.20E-07	T** -0.5 EXP(0./T)
655)	C-C3H2P	+	EL	=	C3	+	H2			k	=	1.04E-06	T** -0.5 EXP(0./T)
656)	C-C3H2P	+	EL	=	C3	+	2H			k	=	1.04E-06	T** -0.5 EXP(0./T)
657)	C-C3H2P	+	EL	=	C2	+	(3)CH2			k	=	5.20E-07	T** -0.5 EXP(0./T)
658)	C-C3H2P	+	EL	=	C3H	+	H			k	=	5.20E-06	T** -0.5 EXP(0./T)
659)	C3H3P	+	EL	=	C3H2	+	H			k	=	8.66E-07	T** -0.5 EXP(0./T)
660)	C3H3P	+	EL	=	C2H2	+	CH			k	=	8.66E-07	T** -0.5 EXP(0./T)
661)	C-C3H3P	+	EL	=	C3HN					k	=	8.66E-07	T** -0.5 EXP(0./T)
662)	CH3C2HP	+	EL	=	C3H2	+	H2			k	=	3.46E-06	T** -0.5 EXP(0./T)
663)	CH3C2HP	+	EL	=	C3H3	+	H			k	=	3.46E-06	T** -0.5 EXP(0./T)
664)	C3H5P	+	EL	=	C3H3	+	H2			k	=	2.60E-06	T** -0.5 EXP(0./T)
665)	C3H5P	+	EL	=	CH3C2H	+	H			k	=	2.60E-06	T** -0.5 EXP(0./T)
666)	C4P	+	EL	=	2C2					k	=	5.20E-06	T** -0.5 EXP(0./T)
667)	C4HP	+	EL	=	C4HN					k	=	5.20E-06	T** -0.5 EXP(0./T)
668)	C4H2P	+	EL	=	C4H	+	H			k	=	5.20E-06	T** -0.5 EXP(0./T)
669)	C4H3P	+	EL	=	C4H	+	H2			k	=	5.37E-06	T** -0.5 EXP(0./T)
670)	C4H3P	+	EL	=	C4H2	+	H			k	=	5.37E-06	T** -0.5 EXP(0./T)
671)	C4H4P	+	EL	=	C4H3	+	H			k	=	5.72E-06	T** -0.5 EXP(0./T)
672)	C4H5P	+	EL	=	CH3C2H	+	CH			k	=	2.60E-06	T** -0.5 EXP(0./T)
673)	C4H5P	+	EL	=	C4H2	+	H2	+	H	k	=	2.60E-06	T** -0.5 EXP(0./T)
674)	C5P	+	EL	=	C3	+	C2			k	=	5.20E-06	T** -0.5 EXP(0./T)
675)	C5HP	+	EL	=	C4H	+	C			k	=	5.54E-06	T** -0.3 EXP(0./T)
676)	C5HP	+	EL	=	C5HN					k	=	5.20E-06	T** -0.5 EXP(0./T)
677)	C5H2P	+	EL	=	C5HN					k	=	5.20E-06	T** -0.5 EXP(0./T)
678)	C5H3P	+	EL	=	C5HN					k	=	2.60E-06	T** -0.5 EXP(0./T)
679)	C5H3P	+	EL	=	C5H2	+	H			k	=	2.60E-06	T** -0.5 EXP(0./T)
680)	C5H4P	+	EL	=	C5HN					k	=	5.54E-06	T** -0.3 EXP(0./T)
681)	C5H4P	+	EL	=	C5H2	+	H2			k	=	5.54E-06	T** -0.3 EXP(0./T)
682)	C5H5P	+	EL	=	C5H2	+	H2	+	H	k	=	5.54E-06	T** -0.3 EXP(0./T)
683)	C5H5P	+	EL	=	C5HN	+	H			k	=	5.20E-06	T** -0.5 EXP(0./T)
684)	C6P	+	EL	=	C6HN					k	=	1.11E-05	T** -0.3 EXP(0./T)
685)	C6HP	+	EL	=	C6HN					k	=	1.11E-05	T** -0.3 EXP(0./T)

686)	C6H2P	+	EL	=	C6HN					k =	5.54E-06 T** -0.3 EXP(0./T)
687)	C6H2P	+	EL	=	C6H	+	H			k =	5.54E-06 T** -0.3 EXP(0./T)
688)	C6H3P	+	EL	=	C6H	+	H2			k =	5.54E-06 T** -0.3 EXP(0./T)
689)	C6H3P	+	EL	=	C6H2	+	H			k =	5.54E-06 T** -0.3 EXP(0./T)
690)	C6H4P	+	EL	=	C6H	+	H2	+	H	k =	5.54E-06 T** -0.3 EXP(0./T)
691)	C6H4P	+	EL	=	C6H2	+	H2			k =	5.54E-06 T** -0.3 EXP(0./T)
692)	C6H5P	+	EL	=	C6H	+	2H2			k =	5.54E-06 T** -0.3 EXP(0./T)
693)	C6H5P	+	EL	=	C6H2	+	H2	+	H	k =	5.54E-06 T** -0.3 EXP(0./T)
694)	C6H7P	+	EL	=	C6HN					k =	7.50E-07 EXP(0./T)
695)	C-C6H7P	+	EL	=	A1	+	H			k =	8.66E-06 T** -0.5 EXP(0./T)
696)	C-C6H7P	+	EL	=	C6H2	+	2H2	+	H	k =	8.66E-06 T** -0.5 EXP(0./T)
697)	C3HNP	+	EL	=	C3HN					k =	7.50E-07 EXP(0./T)
698)	C4HNP	+	EL	=	C4HN					k =	7.50E-07 EXP(0./T)
699)	C5HNP	+	EL	=	C5HN					k =	7.50E-07 EXP(0./T)
700)	C7HNP	+	EL	=	C7HN					k =	7.50E-07 EXP(0./T)
701)	C8HNP	+	EL	=	C8HN					k =	7.50E-07 EXP(0./T)
702)	C9HNP	+	EL	=	C9HN					k =	7.50E-07 EXP(0./T)

B.1.5 Model Atmosphere

1MODEL ATMOSPHERE LATITUDE 60.0 DEG

	ALTITUDE (KM)	TEMPERATURE (K)	TOTAL DENSITY (CM-3)	PRESSURE (MBAR)	PRESSURE SCALE HEIGHT (KM)	DENSITY SCALE HEIGHT (KM)	EDDY DIFFUSION (CM+2 SEC-1)	TRANSPORT TIMESCALE (SEC)	WIND VELOCITY (CM SEC-1)	TRANSPORT TIMESCALE (SEC)
1)	-57.0	279.4	1.576E+20	6.078E+03	38.5	57.7	1.000E+03	3.33E+10	1.000E-38	1.00E+35
2)	-44.0	249.8	1.258E+20	4.338E+03	38.5	57.7	1.000E+03	3.33E+10	1.000E-38	1.00E+35
3)	-33.0	225.4	1.015E+20	3.158E+03	34.7	51.2	1.000E+03	2.63E+10	1.000E-38	1.00E+35
4)	-23.0	203.7	8.157E+19	2.293E+03	31.3	45.7	1.000E+03	2.09E+10	1.000E-38	1.00E+35
5)	-14.0	185.0	6.537E+19	1.669E+03	28.3	40.7	1.000E+03	1.65E+10	1.000E-38	1.00E+35
6)	-6.0	169.4	5.235E+19	1.224E+03	25.8	36.0	1.000E+03	1.30E+10	1.000E-38	1.00E+35
7)	2.0	155.3	4.069E+19	8.722E+02	23.6	31.7	1.000E+03	1.01E+10	1.000E-38	1.00E+35
8)	9.0	144.4	3.173E+19	6.324E+02	21.8	28.1	1.000E+03	7.92E+09	1.000E-38	1.00E+35
9)	15.0	135.9	2.512E+19	4.712E+02	20.4	25.7	1.000E+03	6.60E+09	1.000E-38	1.00E+35
10)	21.0	127.8	1.954E+19	3.447E+02	19.2	23.9	1.000E+03	5.71E+09	1.000E-38	1.00E+35
11)	27.0	119.5	1.497E+19	2.469E+02	18.0	22.5	1.000E+03	5.07E+09	1.000E-38	1.00E+35
12)	32.0	113.1	1.176E+19	1.836E+02	16.9	20.7	1.000E+03	4.29E+09	1.000E-38	1.00E+35
13)	37.0	108.8	8.956E+18	1.345E+02	16.1	18.4	1.000E+03	3.37E+09	1.000E-38	1.00E+35
14)	42.0	108.6	6.516E+18	9.768E+01	15.6	15.7	3.941E+03	6.27E+08	1.000E-38	1.00E+35
15)	47.0	113.4	4.553E+18	7.127E+01	15.9	13.9	4.631E+03	4.20E+08	1.000E-38	1.00E+35
16)	52.0	121.0	3.165E+18	5.286E+01	16.7	13.8	5.454E+03	3.47E+08	1.000E-38	1.00E+35
17)	57.0	129.1	2.243E+18	3.997E+01	17.9	14.5	6.368E+03	3.31E+08	1.000E-38	1.00E+35
18)	63.0	137.4	1.540E+18	2.921E+01	19.1	16.0	7.542E+03	3.38E+08	1.000E-38	1.00E+35
19)	69.0	143.0	1.098E+18	2.167E+01	20.1	17.7	8.782E+03	3.58E+08	1.000E-38	1.00E+35
20)	75.0	146.8	8.025E+17	1.626E+01	20.9	19.1	1.011E+04	3.62E+08	1.000E-38	1.00E+35
21)	82.0	149.7	5.671E+17	1.172E+01	21.4	20.2	1.182E+04	3.44E+08	1.000E-38	1.00E+35
22)	89.0	151.8	4.052E+17	8.490E+00	21.7	20.8	1.375E+04	3.15E+08	1.000E-38	1.00E+35
23)	96.0	153.8	2.912E+17	6.182E+00	22.1	21.2	1.596E+04	2.81E+08	1.000E-38	1.00E+35
24)	103.0	155.8	2.101E+17	4.518E+00	22.3	21.4	1.848E+04	2.49E+08	1.000E-38	1.00E+35
25)	110.0	158.0	1.521E+17	3.317E+00	22.7	21.7	2.138E+04	2.20E+08	1.000E-38	1.00E+35
26)	117.0	160.4	1.104E+17	2.444E+00	22.9	21.8	2.469E+04	1.93E+08	1.000E-38	1.00E+35
27)	124.0	163.1	8.045E+16	1.811E+00	23.4	22.1	2.847E+04	1.72E+08	1.000E-38	1.00E+35
28)	131.0	165.9	5.891E+16	1.349E+00	23.8	22.5	3.276E+04	1.54E+08	1.000E-38	1.00E+35
29)	138.0	168.5	4.339E+16	1.009E+00	24.1	22.9	3.759E+04	1.39E+08	1.000E-38	1.00E+35
30)	146.0	171.2	3.083E+16	7.285E-01	24.6	23.4	4.384E+04	1.25E+08	1.000E-38	1.00E+35
31)	154.0	173.5	2.206E+16	5.283E-01	24.9	23.9	5.096E+04	1.12E+08	1.000E-38	1.00E+35
32)	162.0	175.6	1.588E+16	3.849E-01	25.3	24.3	5.909E+04	1.00E+08	1.000E-38	1.00E+35

33)	170.0	177.4	1.148E+16	2.811E-01	25.5	24.7	6.838E+04	8.89E+07	1.000E-38	1.00E+35
34)	178.0	179.1	8.342E+15	2.062E-01	25.8	25.1	7.894E+04	7.95E+07	1.000E-38	1.00E+35
35)	186.0	180.2	6.096E+15	1.516E-01	26.0	25.5	9.091E+04	7.16E+07	1.000E-38	1.00E+35
36)	194.0	180.4	4.482E+15	1.116E-01	26.1	26.0	1.044E+05	6.48E+07	1.000E-38	1.00E+35
37)	202.0	179.9	3.308E+15	8.214E-02	26.1	26.3	1.197E+05	5.80E+07	1.000E-38	1.00E+35
38)	210.0	180.9	2.421E+15	6.045E-02	26.1	25.6	1.377E+05	4.77E+07	1.000E-38	1.00E+35
39)	218.0	186.0	1.741E+15	4.470E-02	26.5	24.3	1.598E+05	3.68E+07	1.000E-38	1.00E+35
40)	226.0	197.0	1.228E+15	3.339E-02	27.4	22.9	1.870E+05	2.81E+07	1.000E-38	1.00E+35
41)	235.0	217.2	8.213E+14	2.462E-02	29.5	22.4	2.241E+05	2.23E+07	1.000E-38	1.00E+35
42)	245.0	245.6	5.360E+14	1.817E-02	32.9	23.4	2.715E+05	2.02E+07	1.000E-38	1.00E+35
43)	256.0	279.7	3.506E+14	1.354E-02	37.4	25.9	3.286E+05	2.04E+07	1.000E-38	1.00E+35
44)	269.0	320.2	2.259E+14	9.984E-03	42.7	29.6	4.005E+05	2.18E+07	1.000E-38	1.00E+35
45)	284.0	364.8	1.458E+14	7.342E-03	48.8	34.3	4.877E+05	2.41E+07	1.000E-38	1.00E+35
46)	301.0	411.1	9.524E+13	5.404E-03	55.5	39.9	5.908E+05	2.70E+07	1.000E-38	1.00E+35
47)	320.0	456.8	6.314E+13	3.981E-03	62.2	46.2	7.108E+05	3.01E+07	1.000E-38	1.00E+35
48)	342.0	502.1	4.175E+13	2.893E-03	68.9	53.2	8.562E+05	3.30E+07	1.000E-38	1.00E+35
49)	366.0	544.2	2.801E+13	2.104E-03	75.3	60.1	1.025E+06	3.53E+07	1.000E-38	1.00E+35
50)	392.0	586.7	1.889E+13	1.530E-03	81.6	66.0	1.223E+06	3.56E+07	1.000E-38	1.00E+35
51)	420.0	633.0	1.273E+13	1.112E-03	87.9	70.9	1.461E+06	3.45E+07	1.000E-38	1.00E+35
52)	450.0	685.8	8.571E+12	8.113E-04	95.1	75.8	1.746E+06	3.29E+07	1.000E-38	1.00E+35
53)	483.0	745.0	5.732E+12	5.894E-04	103.3	82.0	2.092E+06	3.22E+07	1.000E-38	1.00E+35
54)	519.0	805.7	3.844E+12	4.275E-04	112.1	90.1	2.505E+06	3.24E+07	1.000E-38	1.00E+35
55)	558.0	863.4	2.599E+12	3.097E-04	121.0	99.6	2.987E+06	3.32E+07	1.000E-38	1.00E+35
56)	600.0	915.5	1.771E+12	2.238E-04	129.2	109.5	3.550E+06	3.38E+07	1.000E-38	1.00E+35
57)	644.0	965.5	1.218E+12	1.623E-04	137.0	117.5	4.201E+06	3.29E+07	1.000E-38	1.00E+35
58)	691.0	1020.0	8.328E+11	1.173E-04	144.5	123.6	4.985E+06	3.07E+07	1.000E-38	1.00E+35
59)	740.0	1083.0	5.697E+11	8.516E-05	153.2	129.1	5.914E+06	2.82E+07	1.000E-38	1.00E+35
60)	793.0	1156.0	3.857E+11	6.154E-05	163.2	135.9	7.048E+06	2.62E+07	1.000E-38	1.00E+35
61)	849.0	1232.0	2.627E+11	4.467E-05	174.8	145.8	8.378E+06	2.54E+07	1.000E-38	1.00E+35
62)	909.0	1305.0	1.795E+11	3.233E-05	185.6	157.5	9.944E+06	2.50E+07	1.000E-38	1.00E+35
63)	973.0	1371.0	1.233E+11	2.333E-05	196.2	170.4	1.177E+07	2.47E+07	1.000E-38	1.00E+35
64)	1040.0	1431.0	8.544E+10	1.688E-05	206.8	182.7	1.389E+07	2.40E+07	1.000E-38	1.00E+35
65)	1110.0	1487.0	5.942E+10	1.220E-05	215.5	192.7	1.635E+07	2.27E+07	1.000E-38	1.00E+35
66)	1183.0	1541.0	4.138E+10	8.802E-06	223.8	201.8	1.925E+07	2.11E+07	1.000E-38	1.00E+35
67)	1259.0	1595.0	2.883E+10	6.347E-06	232.5	210.3	2.264E+07	1.95E+07	1.000E-38	1.00E+35
68)	1338.0	1647.0	2.012E+10	4.574E-06	241.1	219.6	2.662E+07	1.81E+07	1.000E-38	1.00E+35
69)	1420.0	1695.0	1.407E+10	3.292E-06	249.3	229.3	3.127E+07	1.68E+07	1.000E-38	1.00E+35
70)	1504.0	1736.0	9.896E+09	2.371E-06	256.1	238.7	3.664E+07	1.56E+07	1.000E-38	1.00E+35
71)	1590.0	1771.0	6.991E+09	1.709E-06	262.6	247.5	4.284E+07	1.43E+07	1.000E-38	1.00E+35
72)	1678.0	1802.0	4.951E+09	1.231E-06	268.6	255.0	5.003E+07	1.30E+07	1.000E-38	1.00E+35
73)	1768.0	1830.0	3.510E+09	8.866E-07	273.9	261.6	5.841E+07	1.17E+07	1.000E-38	1.00E+35
74)	1860.0	1854.0	2.488E+09	6.367E-07	277.9	267.3	6.820E+07	1.05E+07	1.000E-38	1.00E+35
75)	1953.0	1876.0	1.769E+09	4.581E-07	282.4	272.7	7.951E+07	9.35E+06	1.000E-38	1.00E+35
76)	2047.0	1897.0	1.260E+09	3.299E-07	286.4	277.0	9.262E+07	8.29E+06	1.000E-38	1.00E+35
77)	2143.0	1918.0	8.952E+08	2.370E-07	290.2	280.8	1.080E+08	7.30E+06	1.000E-38	1.00E+35
78)	2240.0	1940.0	6.366E+08	1.705E-07	294.4	284.5	1.259E+08	6.43E+06	1.000E-38	1.00E+35
79)	2338.0	1964.0	4.530E+08	1.228E-07	298.8	288.0	1.468E+08	5.65E+06	1.000E-38	1.00E+35
80)	2400.0	1980.0	3.658E+08	9.997E-08	301.4	290.0	1.616E+08	5.20E+06	1.000E-38	1.00E+35

B.1.6 Concentration for Fixed Species

CONCENTRATIONS LATITUDE 60.0 DEG LONGITUDE 0.0 DEG:

	PRESSURE	H2	H2V2	H2V4
1)	6.078E+03	1.399E+20	1.652E-03	0.000E+00
2)	4.338E+03	1.117E+20	2.530E-06	0.000E+00

3)	3.158E+03	9.011E+19	3.419E-09	0.000E+00
4)	2.293E+03	7.242E+19	2.578E-12	0.000E+00
5)	1.669E+03	5.804E+19	1.368E-15	0.000E+00
6)	1.224E+03	4.648E+19	7.093E-19	0.000E+00
7)	8.722E+02	3.613E+19	0.000E+00	0.000E+00
8)	6.324E+02	2.817E+19	0.000E+00	0.000E+00
9)	4.712E+02	2.230E+19	0.000E+00	0.000E+00
10)	3.447E+02	1.735E+19	0.000E+00	0.000E+00
11)	2.469E+02	1.329E+19	0.000E+00	0.000E+00
12)	1.836E+02	1.044E+19	0.000E+00	0.000E+00
13)	1.345E+02	7.953E+18	0.000E+00	0.000E+00
14)	9.768E+01	5.787E+18	0.000E+00	0.000E+00
15)	7.127E+01	4.043E+18	0.000E+00	0.000E+00
16)	5.286E+01	2.811E+18	0.000E+00	0.000E+00
17)	3.997E+01	1.992E+18	0.000E+00	0.000E+00
18)	2.921E+01	1.368E+18	0.000E+00	0.000E+00
19)	2.167E+01	9.753E+17	0.000E+00	0.000E+00
20)	1.626E+01	7.128E+17	0.000E+00	0.000E+00
21)	1.172E+01	5.038E+17	0.000E+00	0.000E+00
22)	8.490E+00	3.600E+17	0.000E+00	0.000E+00
23)	6.182E+00	2.587E+17	0.000E+00	0.000E+00
24)	4.518E+00	1.867E+17	0.000E+00	0.000E+00
25)	3.317E+00	1.352E+17	0.000E+00	0.000E+00
26)	2.444E+00	9.815E+16	0.000E+00	0.000E+00
27)	1.811E+00	7.154E+16	0.000E+00	0.000E+00
28)	1.349E+00	5.240E+16	0.000E+00	0.000E+00
29)	1.009E+00	3.861E+16	3.702E-22	0.000E+00
30)	7.285E-01	2.745E+16	1.047E-21	0.000E+00
31)	5.283E-01	1.965E+16	2.347E-21	0.000E+00
32)	3.849E-01	1.415E+16	4.673E-21	0.000E+00
33)	2.811E-01	1.024E+16	7.932E-21	0.000E+00
34)	2.062E-01	7.448E+15	1.270E-20	0.000E+00
35)	1.516E-01	5.448E+15	1.536E-20	0.000E+00
36)	1.116E-01	4.011E+15	1.238E-20	0.000E+00
37)	8.214E-02	2.965E+15	7.291E-21	0.000E+00
38)	6.045E-02	2.173E+15	8.413E-21	0.000E+00
39)	4.470E-02	1.566E+15	5.669E-20	0.000E+00
40)	3.339E-02	1.107E+15	3.357E-18	0.000E+00
41)	2.462E-02	7.424E+14	2.381E-15	0.000E+00
42)	1.817E-02	4.863E+14	4.014E-12	0.000E+00
43)	1.354E-02	3.195E+14	3.993E-09	0.000E+00
44)	9.984E-03	2.070E+14	2.040E-06	2.383E-20
45)	7.342E-03	1.344E+14	3.702E-04	2.184E-16
46)	5.404E-03	8.823E+13	2.315E-02	3.256E-13
47)	3.981E-03	5.877E+13	5.607E-01	9.604E-11

48)	2.893E-03	3.900E+13	6.889E+00	8.976E-09
49)	2.104E-03	2.621E+13	4.526E+01	2.871E-07
50)	1.530E-03	1.766E+13	2.191E+02	5.457E-06
51)	1.112E-03	1.186E+13	9.359E+02	8.388E-05
52)	8.113E-04	7.941E+12	3.814E+03	1.193E-03
53)	5.894E-04	5.265E+12	1.417E+04	1.458E-02
54)	4.275E-04	3.491E+12	4.244E+04	1.234E-01
55)	3.097E-04	2.327E+12	9.790E+04	6.682E-01
56)	2.238E-04	1.559E+12	1.769E+05	2.378E+00
57)	1.623E-04	1.050E+12	2.809E+05	6.756E+00
58)	1.173E-04	7.001E+11	4.356E+05	1.852E+01
59)	8.516E-05	4.649E+11	6.928E+05	5.298E+01
60)	6.154E-05	3.036E+11	1.111E+06	1.550E+02
61)	4.467E-05	1.982E+11	1.668E+06	4.032E+02
62)	3.233E-05	1.287E+11	2.233E+06	8.621E+02
63)	2.333E-05	8.325E+10	2.651E+06	1.498E+03
64)	1.688E-05	5.375E+10	2.889E+06	2.239E+03
65)	1.220E-05	3.438E+10	2.967E+06	3.017E+03
66)	8.802E-06	2.169E+10	2.930E+06	3.801E+03
67)	6.347E-06	1.346E+10	2.826E+06	4.601E+03
68)	4.574E-06	8.193E+09	2.642E+06	5.279E+03
69)	3.292E-06	4.885E+09	2.381E+06	5.683E+03
70)	2.371E-06	2.859E+09	2.053E+06	5.662E+03
71)	1.709E-06	1.637E+09	1.711E+06	5.308E+03
72)	1.231E-06	9.140E+08	1.392E+06	4.777E+03
73)	8.866E-07	4.962E+08	1.112E+06	4.166E+03
74)	6.367E-07	2.614E+08	8.683E+05	3.501E+03
75)	4.581E-07	1.350E+08	6.713E+05	2.891E+03
76)	3.299E-07	6.838E+07	5.155E+05	2.359E+03
77)	2.370E-07	3.380E+07	3.930E+05	1.909E+03
78)	1.705E-07	1.649E+07	2.996E+05	1.548E+03
79)	1.228E-07	7.961E+06	2.292E+05	1.264E+03
80)	9.997E-08	5.105E+06	1.938E+05	1.115E+03
	COLUMN	5.712E+26	2.642E+14	5.129E+11

B.2 Mixing Ratios

Calculated mixing ratio of each species as a function of pressure in the output file of auroral model.

MIXING RATIOS :

	PRESSURE	H	HE	C	CH	(1)CH2	(3)CH2	CH3	CH4	C2	C2H
1)	6.078E+03	8.275E-16	1.100E-01	0.000E+00	6.254E-37	3.199E-33	1.628E-22	8.386E-18	2.200E-03	6.302E-31	5.011E-30

2)	4.338E+03	1.331E-15	1.100E-01	0.000E+00	1.854E-35	7.089E-33	3.034E-21	1.025E-17	2.199E-03	2.676E-30	1.786E-29
3)	3.158E+03	2.556E-15	1.100E-01	0.000E+00	2.879E-33	8.031E-32	2.498E-19	1.486E-17	2.199E-03	1.086E-29	6.163E-29
4)	2.293E+03	7.372E-15	1.100E-01	0.000E+00	1.762E-31	1.110E-30	5.414E-18	3.151E-17	2.198E-03	6.690E-29	3.274E-28
5)	1.669E+03	2.067E-14	1.100E-01	0.000E+00	1.554E-30	8.773E-30	1.728E-17	6.633E-17	2.197E-03	9.017E-28	3.961E-27
6)	1.224E+03	4.163E-14	1.100E-01	0.000E+00	7.606E-30	4.321E-29	4.240E-17	1.740E-16	2.196E-03	1.248E-26	5.257E-26
7)	8.722E+02	6.051E-14	1.099E-01	0.000E+00	3.037E-29	1.746E-28	1.173E-16	9.186E-16	2.194E-03	1.404E-25	6.168E-25
8)	6.324E+02	9.747E-14	1.099E-01	0.000E+00	1.124E-28	6.510E-28	2.712E-16	2.190E-15	2.192E-03	7.978E-25	3.935E-24
9)	4.712E+02	1.836E-13	1.099E-01	3.565E-39	2.571E-28	1.491E-27	3.308E-16	3.047E-15	2.191E-03	2.881E-24	1.660E-23
10)	3.447E+02	3.680E-13	1.099E-01	1.769E-38	5.473E-28	3.177E-27	3.529E-16	3.726E-15	2.188E-03	9.550E-24	6.765E-23
11)	2.469E+02	7.617E-13	1.099E-01	8.643E-38	1.094E-27	6.375E-27	3.428E-16	4.256E-15	2.185E-03	3.032E-23	2.825E-22
12)	1.836E+02	1.359E-12	1.098E-01	3.126E-37	1.892E-27	1.106E-26	3.335E-16	4.802E-15	2.182E-03	7.563E-23	9.063E-22
13)	1.345E+02	2.277E-12	1.098E-01	1.099E-36	3.254E-27	1.901E-26	3.425E-16	5.743E-15	2.177E-03	1.732E-22	2.496E-21
14)	9.768E+01	3.308E-12	1.098E-01	3.639E-36	5.661E-27	3.275E-26	4.063E-16	7.048E-15	2.175E-03	2.866E-22	4.127E-21
15)	7.127E+01	4.240E-12	1.098E-01	1.165E-35	1.000E-26	5.596E-26	5.420E-16	9.914E-15	2.173E-03	4.021E-22	4.614E-21
16)	5.286E+01	4.414E-12	1.097E-01	3.129E-35	1.777E-26	9.214E-26	8.580E-16	1.762E-14	2.171E-03	5.247E-22	4.413E-21
17)	3.997E+01	4.088E-12	1.097E-01	7.448E-35	3.187E-26	1.444E-25	1.453E-15	3.505E-14	2.168E-03	6.664E-22	4.278E-21
18)	2.921E+01	3.940E-12	1.097E-01	2.147E-34	6.440E-26	2.327E-25	2.429E-15	7.418E-14	2.164E-03	8.935E-22	4.637E-21
19)	2.167E+01	4.343E-12	1.096E-01	6.564E-34	1.263E-25	3.552E-25	3.361E-15	1.336E-13	2.159E-03	1.255E-21	5.841E-21
20)	1.626E+01	5.188E-12	1.096E-01	2.056E-33	2.413E-25	5.243E-25	4.149E-15	2.180E-13	2.154E-03	1.832E-21	8.022E-21
21)	1.172E+01	6.807E-12	1.095E-01	7.947E-33	5.021E-25	8.083E-25	4.872E-15	3.579E-13	2.146E-03	2.957E-21	1.243E-20
22)	8.490E+00	9.335E-12	1.094E-01	2.488E-32	8.195E-25	9.733E-25	4.278E-15	5.622E-13	2.136E-03	4.874E-21	1.993E-20
23)	6.182E+00	1.287E-11	1.093E-01	1.007E-31	1.729E-24	1.496E-24	4.769E-15	8.679E-13	2.125E-03	8.053E-21	3.213E-20
24)	4.518E+00	1.801E-11	1.092E-01	4.201E-31	3.716E-24	2.319E-24	5.287E-15	1.308E-12	2.111E-03	1.328E-20	5.180E-20
25)	3.317E+00	2.550E-11	1.091E-01	1.805E-30	8.140E-24	3.633E-24	5.857E-15	1.923E-12	2.095E-03	2.169E-20	8.273E-20
26)	2.444E+00	3.676E-11	1.089E-01	7.979E-30	1.807E-23	5.748E-24	6.446E-15	2.752E-12	2.076E-03	3.502E-20	1.308E-19
27)	1.811E+00	5.397E-11	1.087E-01	3.598E-29	4.025E-23	9.143E-24	7.013E-15	3.834E-12	2.054E-03	5.554E-20	2.034E-19
28)	1.349E+00	8.144E-11	1.085E-01	1.640E-28	8.857E-23	1.455E-23	7.442E-15	5.201E-12	2.028E-03	8.688E-20	3.126E-19
29)	1.009E+00	1.271E-10	1.082E-01	7.500E-28	1.903E-22	2.317E-23	7.656E-15	6.889E-12	1.997E-03	1.350E-19	4.786E-19
30)	7.285E-01	2.199E-10	1.078E-01	4.478E-27	4.648E-22	4.160E-23	8.045E-15	9.341E-12	1.956E-03	2.213E-19	7.724E-19
31)	5.283E-01	3.978E-10	1.074E-01	3.386E-26	1.386E-21	9.486E-23	1.028E-14	1.288E-11	1.907E-03	3.597E-19	1.237E-18
32)	3.849E-01	7.565E-10	1.068E-01	3.420E-25	5.281E-21	2.863E-22	1.656E-14	1.885E-11	1.851E-03	5.745E-19	1.947E-18
33)	2.811E-01	1.520E-09	1.062E-01	3.597E-24	1.994E-20	8.827E-22	2.584E-14	2.887E-11	1.784E-03	9.017E-19	3.013E-18
34)	2.062E-01	3.224E-09	1.055E-01	3.365E-23	6.380E-20	2.362E-21	3.322E-14	4.370E-11	1.708E-03	1.369E-18	4.515E-18
35)	1.516E-01	7.929E-09	1.046E-01	3.002E-22	1.691E-19	5.360E-21	3.125E-14	6.260E-11	1.620E-03	2.024E-18	6.574E-18
36)	1.116E-01	2.735E-08	1.036E-01	3.149E-21	3.789E-19	1.049E-20	1.801E-14	7.992E-11	1.521E-03	2.912E-18	9.281E-18
37)	8.214E-02	1.126E-07	1.024E-01	3.414E-20	7.387E-19	1.804E-20	7.610E-15	8.125E-11	1.409E-03	4.098E-18	1.277E-17
38)	6.045E-02	3.961E-07	1.010E-01	2.982E-19	1.344E-18	2.838E-20	3.490E-15	7.051E-11	1.284E-03	5.469E-18	1.687E-17
39)	4.470E-02	1.118E-06	9.943E-02	2.243E-18	2.550E-18	4.451E-20	2.079E-15	6.723E-11	1.145E-03	6.567E-18	2.092E-17
40)	3.339E-02	2.710E-06	9.757E-02	2.289E-17	7.423E-18	1.014E-19	2.357E-15	9.819E-11	9.922E-04	6.735E-18	2.406E-17
41)	2.462E-02	6.446E-06	9.520E-02	4.782E-16	4.215E-17	4.123E-19	6.716E-15	3.684E-10	8.054E-04	5.651E-18	2.633E-17
42)	1.817E-02	1.503E-05	9.220E-02	1.115E-14	2.638E-16	1.588E-18	3.066E-14	2.891E-09	5.846E-04	3.971E-18	2.997E-17
43)	1.354E-02	3.628E-05	8.846E-02	2.556E-12	1.570E-14	1.403E-17	1.517E-12	4.293E-08	3.378E-04	2.131E-18	1.128E-15
44)	9.984E-03	1.333E-04	8.365E-02	1.287E-09	1.379E-12	1.384E-16	7.530E-11	1.774E-07	9.685E-05	1.147E-17	8.305E-15
45)	7.342E-03	6.838E-04	7.775E-02	2.093E-07	3.484E-11	8.410E-17	7.081E-10	1.701E-07	6.058E-06	1.354E-15	1.564E-14
46)	5.404E-03	2.770E-03	7.088E-02	2.145E-07	9.497E-12	6.777E-17	8.164E-11	1.194E-07	8.961E-07	9.557E-16	9.747E-15
47)	3.981E-03	5.920E-03	6.327E-02	1.713E-07	5.194E-12	4.844E-17	3.157E-11	6.016E-08	2.119E-07	7.347E-16	8.082E-15
48)	2.893E-03	1.086E-02	5.492E-02	1.221E-07	2.970E-12	2.329E-17	1.367E-11	1.958E-08	5.387E-08	4.823E-16	5.613E-15
49)	2.104E-03	1.765E-02	4.653E-02	7.053E-08	1.323E-12	8.501E-18	4.840E-12	4.895E-09	1.141E-08	1.868E-16	2.313E-15
50)	1.530E-03	2.661E-02	3.848E-02	3.277E-08	5.116E-13	2.776E-18	1.549E-12	1.104E-09	2.006E-09	4.481E-17	5.915E-16
51)	1.112E-03	3.715E-02	3.105E-02	1.298E-08	1.613E-13	8.026E-19	4.299E-13	2.200E-10	3.051E-10	6.748E-18	9.453E-17
52)	8.113E-04	4.897E-02	2.452E-02	4.559E-09	4.463E-14	2.274E-19	1.100E-13	4.286E-11	4.585E-11	7.542E-19	1.119E-17
53)	5.894E-04	6.252E-02	1.889E-02	1.418E-09	1.079E-14	4.838E-20	2.510E-14	6.229E-12	4.980E-12	4.948E-20	7.757E-19
54)	4.275E-04	7.754E-02	1.425E-02	3.973E-10	2.133E-15	7.705E-21	4.690E-15	6.788E-13	4.102E-13	2.006E-21	3.297E-20
55)	3.097E-04	9.399E-02	1.056E-02	1.017E-10	3.054E-16	7.519E-22	6.292E-16	4.566E-14	2.094E-14	4.403E-23	7.527E-22
56)	2.238E-04	1.122E-01	7.688E-03	2.380E-11	4.172E-17	7.399E-23	7.927E-17	3.122E-15	1.108E-15	9.064E-25	1.598E-23
57)	1.623E-04	1.324E-01	5.539E-03	5.299E-12	5.672E-18	7.462E-24	9.883E-18	2.208E-16	6.131E-17	1.842E-26	3.335E-25
58)	1.173E-04	1.555E-01	3.919E-03	1.088E-12	8.316E-19	8.746E-25	1.327E-18	1.807E-17	3.961E-18	3.996E-28	7.425E-27
59)	8.516E-05	1.812E-01	2.748E-03	2.171E-13	1.227E-19	1.298E-25	1.803E-19	1.875E-18	3.379E-19	1.026E-29	1.957E-28
60)	6.154E-05	2.110E-01	1.888E-03	3.994E-14	1.837E-20	2.204E-26	2.481E-20	2.208E-19	3.295E-20	2.676E-31	5.249E-30
61)	4.467E-05	2.443E-01	1.285E-03	7.123E-15	3.025E-21	4.518E-27	3.724E-21	3.163E-20	3.919E-21	7.952E-33	1.599E-31
62)	3.233E-05	2.820E-01	8.577E-04	1.184E-15	5.354E-22	1.039E-27	5.916E-22	5.113E-21	5.215E-22	2.439E-34	5.008E-33

63)	2.333E-05	3.243E-01	5.609E-04	1.830E-16	8.993E-23	2.301E-28	8.770E-23	8.018E-22	6.667E-23	6.662E-36	1.392E-34
64)	1.688E-05	3.706E-01	3.608E-04	2.701E-17	1.655E-23	5.409E-29	1.409E-23	1.349E-22	9.083E-24	1.874E-37	3.970E-36
65)	1.220E-05	4.211E-01	2.266E-04	3.725E-18	3.400E-24	1.343E-29	2.501E-24	2.409E-23	1.301E-24	5.359E-39	1.149E-37
66)	8.802E-06	4.756E-01	1.385E-04	4.768E-19	8.016E-25	3.517E-30	5.057E-25	4.552E-24	1.951E-25	0.000E+00	3.444E-39
67)	6.347E-06	5.332E-01	8.202E-05	5.675E-20	2.076E-25	9.143E-31	1.116E-25	8.547E-25	2.874E-26	0.000E+00	0.000E+00
68)	4.574E-06	5.927E-01	4.692E-05	6.309E-21	5.514E-26	2.185E-31	2.512E-26	1.477E-25	3.849E-27	0.000E+00	0.000E+00
69)	3.292E-06	6.528E-01	2.580E-05	6.609E-22	1.421E-26	4.549E-32	5.452E-27	2.228E-26	4.431E-28	0.000E+00	0.000E+00
70)	2.371E-06	7.110E-01	1.364E-05	6.803E-23	3.473E-27	8.248E-33	1.119E-27	2.935E-27	4.392E-29	0.000E+00	0.000E+00
71)	1.709E-06	7.658E-01	6.911E-06	7.122E-24	7.899E-28	1.312E-33	2.136E-28	3.398E-28	3.753E-30	0.000E+00	0.000E+00
72)	1.231E-06	8.154E-01	3.348E-06	7.779E-25	1.652E-28	1.848E-34	3.763E-29	3.481E-29	2.770E-31	0.000E+00	0.000E+00
73)	8.866E-07	8.586E-01	1.549E-06	8.869E-26	3.153E-29	2.318E-35	6.091E-30	3.169E-30	1.760E-32	0.000E+00	0.000E+00
74)	6.367E-07	8.949E-01	6.835E-07	1.026E-26	5.441E-30	2.570E-36	8.973E-31	2.541E-31	9.383E-34	0.000E+00	0.000E+00
75)	4.581E-07	9.237E-01	2.918E-07	1.228E-27	8.704E-31	2.662E-37	1.236E-31	1.905E-32	4.424E-35	0.000E+00	0.000E+00
76)	3.299E-07	9.457E-01	1.210E-07	1.489E-28	1.292E-31	2.547E-38	1.582E-32	1.322E-33	1.796E-36	0.000E+00	0.000E+00
77)	2.370E-07	9.622E-01	4.858E-08	1.759E-29	1.747E-32	0.000E+00	1.827E-33	8.130E-35	5.878E-38	0.000E+00	0.000E+00
78)	1.705E-07	9.741E-01	1.919E-08	2.072E-30	2.224E-33	0.000E+00	1.948E-34	4.673E-36	0.000E+00	0.000E+00	0.000E+00
79)	1.228E-07	9.824E-01	7.500E-09	2.213E-31	2.649E-34	0.000E+00	1.927E-35	2.357E-37	0.000E+00	0.000E+00	0.000E+00
80)	9.997E-08	9.860E-01	4.133E-09	5.192E-32	6.602E-35	0.000E+00	4.437E-36	4.610E-38	0.000E+00	0.000E+00	0.000E+00

	PRESSURE	C2H2	C2H3	C2H4	C2H5	C2H6	C3	C3H	C3H2	C3H3	CH3C2H
1)	6.078E+03	1.937E-14	1.026E-22	1.185E-15	2.056E-19	9.863E-09	3.475E-31	3.475E-31	1.062E-17	2.817E-17	7.045E-16
2)	4.338E+03	3.623E-14	1.477E-21	1.722E-15	6.662E-19	1.235E-08	5.469E-31	5.469E-31	1.145E-17	3.540E-17	1.074E-15
3)	3.158E+03	6.575E-14	2.435E-20	2.701E-15	2.524E-18	1.498E-08	6.915E-31	6.915E-31	9.645E-18	3.612E-17	1.516E-15
4)	2.293E+03	1.763E-13	8.889E-19	7.210E-15	1.080E-17	1.794E-08	3.678E-31	3.678E-31	3.297E-18	1.544E-17	1.228E-15
5)	1.669E+03	1.050E-12	3.191E-17	3.357E-14	3.036E-17	2.126E-08	1.674E-31	1.674E-31	9.976E-19	5.633E-18	8.434E-16
6)	1.224E+03	6.860E-12	1.699E-16	1.559E-13	9.306E-17	2.493E-08	4.510E-31	4.510E-31	1.705E-18	1.215E-17	2.569E-15
7)	8.722E+02	3.712E-11	4.689E-16	5.438E-13	2.184E-16	2.957E-08	3.830E-30	3.830E-30	9.660E-18	8.022E-17	1.827E-14
8)	6.324E+02	1.152E-10	7.768E-16	1.215E-12	3.542E-16	3.475E-08	1.168E-29	1.168E-29	2.032E-17	1.907E-16	5.042E-14
9)	4.712E+02	2.530E-10	9.791E-16	2.242E-12	5.063E-16	4.037E-08	1.558E-29	1.558E-29	1.903E-17	2.015E-16	7.097E-14
10)	3.447E+02	5.119E-10	1.088E-15	3.768E-12	6.555E-16	4.748E-08	1.659E-29	1.659E-29	1.392E-17	1.669E-16	8.063E-14
11)	2.469E+02	9.741E-10	1.028E-15	5.572E-12	7.203E-16	5.667E-08	1.619E-29	1.619E-29	9.077E-18	1.248E-16	8.265E-14
12)	1.836E+02	1.569E-09	8.985E-16	6.974E-12	7.082E-16	6.657E-08	1.962E-29	1.962E-29	7.698E-18	1.188E-16	9.684E-14
13)	1.345E+02	2.361E-09	8.625E-16	8.733E-12	7.646E-16	7.951E-08	3.442E-29	3.442E-29	9.453E-18	1.588E-16	1.472E-13
14)	9.768E+01	2.748E-09	9.851E-16	1.046E-11	9.556E-16	8.668E-08	6.369E-29	6.369E-29	1.282E-17	2.137E-16	2.014E-13
15)	7.127E+01	3.002E-09	1.781E-15	1.485E-11	1.802E-15	9.261E-08	1.291E-28	1.291E-28	2.047E-17	3.026E-16	2.722E-13
16)	5.286E+01	3.276E-09	3.980E-15	2.167E-11	3.966E-15	1.000E-07	3.820E-28	3.820E-28	4.984E-17	6.226E-16	4.496E-13
17)	3.997E+01	3.617E-09	8.586E-15	2.963E-11	8.063E-15	1.091E-07	1.444E-27	1.444E-27	1.573E-16	1.668E-15	8.682E-13
18)	2.921E+01	4.151E-09	1.795E-14	4.026E-11	1.585E-14	1.227E-07	6.254E-27	6.254E-27	5.509E-16	4.960E-15	1.852E-12
19)	2.167E+01	4.853E-09	3.006E-14	5.204E-11	2.594E-14	1.393E-07	1.937E-26	1.937E-26	1.381E-15	1.095E-14	3.377E-12
20)	1.626E+01	5.751E-09	4.456E-14	6.583E-11	3.831E-14	1.594E-07	4.756E-26	4.756E-26	2.764E-15	1.966E-14	5.448E-12
21)	1.172E+01	7.090E-09	6.433E-14	8.547E-11	5.565E-14	1.878E-07	1.134E-25	1.134E-25	5.251E-15	3.311E-14	8.647E-12
22)	8.490E+00	8.802E-09	8.869E-14	1.109E-10	7.741E-14	2.221E-07	2.420E-25	2.420E-25	9.083E-15	5.050E-14	1.296E-11
23)	6.182E+00	1.097E-08	1.210E-13	1.439E-10	1.051E-13	2.634E-07	4.954E-25	4.954E-25	1.543E-14	7.431E-14	1.885E-11
24)	4.518E+00	1.370E-08	1.632E-13	1.867E-10	1.396E-13	3.128E-07	9.621E-25	9.621E-25	2.544E-14	1.041E-13	2.642E-11
25)	3.317E+00	1.707E-08	2.185E-13	2.419E-10	1.814E-13	3.715E-07	1.765E-24	1.765E-24	4.062E-14	1.383E-13	3.539E-11
26)	2.444E+00	2.119E-08	2.880E-13	3.111E-10	2.287E-13	4.411E-07	3.012E-24	3.012E-24	6.177E-14	1.713E-13	4.468E-11
27)	1.811E+00	2.615E-08	3.722E-13	3.956E-10	2.782E-13	5.231E-07	4.703E-24	4.703E-24	8.788E-14	1.949E-13	5.239E-11
28)	1.349E+00	3.202E-08	4.647E-13	4.943E-10	3.225E-13	6.194E-07	6.560E-24	6.560E-24	1.139E-13	1.991E-13	5.619E-11
29)	1.009E+00	3.882E-08	5.546E-13	6.042E-10	3.531E-13	7.318E-07	8.050E-24	8.050E-24	1.317E-13	1.799E-13	5.463E-11
30)	7.285E-01	4.766E-08	6.433E-13	7.404E-10	3.671E-13	8.826E-07	8.730E-24	8.730E-24	1.350E-13	1.386E-13	4.693E-11
31)	5.283E-01	5.745E-08	7.051E-13	8.889E-10	3.604E-13	1.060E-06	8.203E-24	8.203E-24	1.202E-13	9.319E-14	3.607E-11
32)	3.849E-01	6.781E-08	7.349E-13	1.062E-09	3.431E-13	1.268E-06	6.826E-24	6.826E-24	9.440E-14	5.580E-14	2.530E-11
33)	2.811E-01	7.801E-08	7.266E-13	1.276E-09	3.207E-13	1.508E-06	5.065E-24	5.065E-24	6.516E-14	2.992E-14	1.631E-11
34)	2.062E-01	8.692E-08	6.820E-13	1.531E-09	2.952E-13	1.784E-06	3.299E-24	3.299E-24	3.856E-14	1.415E-14	9.522E-12
35)	1.516E-01	9.283E-08	5.987E-13	1.785E-09	2.597E-13	2.095E-06	1.692E-24	1.692E-24	1.679E-14	5.304E-15	4.674E-12
36)	1.116E-01	9.420E-08	4.863E-13	1.883E-09	2.037E-13	2.441E-06	7.707E-25	7.707E-25	4.662E-15	1.781E-15	1.929E-12
37)	8.214E-02	9.170E-08	3.710E-13	1.678E-09	1.343E-13	2.823E-06	7.563E-25	7.563E-25	1.706E-15	1.296E-15	1.347E-12
38)	6.045E-02	8.898E-08	2.818E-13	1.357E-09	8.133E-14	3.245E-06	1.389E-24	1.389E-24	1.159E-15	1.748E-15	1.818E-12
39)	4.470E-02	8.923E-08	2.251E-13	1.102E-09	5.135E-14	3.712E-06	3.533E-24	3.533E-24	1.175E-15	3.206E-15	3.172E-12
40)	3.339E-02	9.255E-08	1.906E-13	9.755E-10	3.854E-14	4.226E-06	1.080E-23	1.080E-23	1.563E-15	6.931E-15	5.951E-12
41)	2.462E-02	9.681E-08	1.628E-13	1.107E-09	5.371E-14	4.864E-06	4.135E-23	4.135E-23	2.850E-15	1.780E-14	1.039E-11

42)	1.817E-02	9.292E-08	1.264E-13	2.431E-09	2.677E-13	5.644E-06	1.818E-22	1.819E-22	8.468E-15	5.126E-14	2.196E-11
43)	1.354E-02	5.320E-08	3.292E-13	2.878E-08	4.822E-12	6.590E-06	1.756E-19	2.806E-19	3.526E-12	2.475E-11	4.537E-09
44)	9.984E-03	1.942E-07	6.692E-13	1.571E-07	1.286E-11	3.745E-06	4.453E-16	1.557E-15	4.068E-11	8.307E-11	5.220E-09
45)	7.342E-03	1.668E-07	2.467E-13	2.986E-08	1.480E-12	4.771E-08	1.518E-12	5.314E-12	1.949E-09	6.479E-11	9.707E-10
46)	5.404E-03	3.326E-08	3.127E-14	3.331E-09	1.053E-13	1.732E-09	1.117E-12	3.909E-12	5.696E-10	1.298E-11	6.307E-11
47)	3.981E-03	1.048E-08	7.271E-15	7.110E-10	8.671E-15	4.285E-11	5.521E-13	1.932E-12	2.167E-10	4.400E-12	9.547E-12
48)	2.893E-03	3.097E-09	1.290E-15	1.082E-10	5.640E-16	5.015E-13	1.761E-13	6.159E-13	6.150E-11	1.110E-12	1.171E-12
49)	2.104E-03	6.400E-10	1.470E-16	8.964E-12	2.812E-17	4.651E-15	2.986E-14	1.043E-13	9.654E-12	1.549E-13	8.641E-14
50)	1.530E-03	8.453E-11	1.182E-17	4.605E-13	9.775E-19	4.124E-17	2.669E-15	9.302E-15	7.753E-13	1.098E-14	3.363E-15
51)	1.112E-03	7.453E-12	6.752E-19	1.567E-14	2.310E-20	3.108E-19	1.516E-16	5.266E-16	3.634E-14	4.465E-16	7.594E-17
52)	8.113E-04	5.563E-13	3.379E-20	4.849E-16	4.996E-22	2.307E-21	6.487E-18	2.245E-17	1.261E-15	1.311E-17	1.243E-18
53)	5.894E-04	1.910E-14	7.984E-22	7.009E-18	5.027E-24	9.655E-24	1.408E-19	4.832E-19	1.581E-17	1.332E-19	7.046E-21
54)	4.275E-04	3.658E-16	1.057E-23	5.354E-20	2.671E-26	2.527E-26	1.396E-21	4.702E-21	7.518E-20	4.833E-22	1.463E-23
55)	3.097E-04	3.274E-18	6.518E-26	1.458E-22	5.072E-29	2.931E-29	4.611E-24	1.487E-23	9.937E-23	4.229E-25	7.581E-27
56)	2.238E-04	3.061E-20	4.195E-28	4.175E-25	1.014E-31	4.088E-32	1.056E-26	3.165E-26	9.877E-26	2.379E-28	2.610E-30
57)	1.623E-04	2.986E-22	2.838E-30	1.266E-27	2.162E-34	6.664E-35	2.189E-29	5.879E-29	9.064E-29	1.054E-31	7.227E-34
58)	1.173E-04	3.361E-24	2.212E-32	5.170E-30	6.164E-37	1.441E-37	4.841E-32	1.135E-31	9.268E-32	4.701E-35	2.005E-37
59)	8.516E-05	5.589E-26	2.553E-34	3.866E-32	3.219E-39	0.000E+00	1.585E-34	3.343E-34	1.772E-34	4.288E-38	0.000E+00
60)	6.154E-05	1.034E-27	3.253E-36	3.861E-34	0.000E+00	0.000E+00	5.669E-37	1.090E-36	4.073E-37	0.000E+00	0.000E+00
61)	4.467E-05	2.332E-29	5.087E-38	5.780E-36	0.000E+00	0.000E+00	0.000E+00	4.386E-39	0.000E+00	0.000E+00	0.000E+00
62)	3.233E-05	5.494E-31	0.000E+00	1.071E-37	0.000E+00	0.000E+00	0.000E+00	0.000E+00	0.000E+00	0.000E+00	0.000E+00
63)	2.333E-05	1.137E-32	0.000E+00	0.000E+00	0.000E+00	0.000E+00	0.000E+00	0.000E+00	0.000E+00	0.000E+00	0.000E+00
64)	1.688E-05	2.353E-34	0.000E+00	0.000E+00	0.000E+00	0.000E+00	0.000E+00	0.000E+00	0.000E+00	0.000E+00	0.000E+00
65)	1.220E-05	4.742E-36	0.000E+00	0.000E+00	0.000E+00	0.000E+00	0.000E+00	0.000E+00	0.000E+00	0.000E+00	0.000E+00
66)	8.802E-06	9.515E-38	0.000E+00	0.000E+00	0.000E+00	0.000E+00	0.000E+00	0.000E+00	0.000E+00	0.000E+00	0.000E+00
67)	6.347E-06	0.000E+00	0.000E+00	0.000E+00	0.000E+00	0.000E+00	0.000E+00	0.000E+00	0.000E+00	0.000E+00	0.000E+00
68)	4.574E-06	0.000E+00	0.000E+00	0.000E+00	0.000E+00	0.000E+00	0.000E+00	0.000E+00	0.000E+00	0.000E+00	0.000E+00
69)	3.292E-06	0.000E+00	0.000E+00	0.000E+00	0.000E+00	0.000E+00	0.000E+00	0.000E+00	0.000E+00	0.000E+00	0.000E+00
70)	2.371E-06	0.000E+00	0.000E+00	0.000E+00	0.000E+00	0.000E+00	0.000E+00	0.000E+00	0.000E+00	0.000E+00	0.000E+00
71)	1.709E-06	0.000E+00	0.000E+00	0.000E+00	0.000E+00	0.000E+00	0.000E+00	0.000E+00	0.000E+00	0.000E+00	0.000E+00
72)	1.231E-06	0.000E+00	0.000E+00	0.000E+00	0.000E+00	0.000E+00	0.000E+00	0.000E+00	0.000E+00	0.000E+00	0.000E+00
73)	8.866E-07	0.000E+00	0.000E+00	0.000E+00	0.000E+00	0.000E+00	0.000E+00	0.000E+00	0.000E+00	0.000E+00	0.000E+00
74)	6.367E-07	0.000E+00	0.000E+00	0.000E+00	0.000E+00	0.000E+00	0.000E+00	0.000E+00	0.000E+00	0.000E+00	0.000E+00
75)	4.581E-07	0.000E+00	0.000E+00	0.000E+00	0.000E+00	0.000E+00	0.000E+00	0.000E+00	0.000E+00	0.000E+00	0.000E+00
76)	3.299E-07	0.000E+00	0.000E+00	0.000E+00	0.000E+00	0.000E+00	0.000E+00	0.000E+00	0.000E+00	0.000E+00	0.000E+00
77)	2.370E-07	0.000E+00	0.000E+00	0.000E+00	0.000E+00	0.000E+00	0.000E+00	0.000E+00	0.000E+00	0.000E+00	0.000E+00
78)	1.705E-07	0.000E+00	0.000E+00	0.000E+00	0.000E+00	0.000E+00	0.000E+00	0.000E+00	0.000E+00	0.000E+00	0.000E+00
79)	1.228E-07	0.000E+00	0.000E+00	0.000E+00	0.000E+00	0.000E+00	0.000E+00	0.000E+00	0.000E+00	0.000E+00	0.000E+00
80)	9.997E-08	0.000E+00	0.000E+00	0.000E+00	0.000E+00	0.000E+00	0.000E+00	0.000E+00	0.000E+00	0.000E+00	0.000E+00

	PRESSURE	CH2CCH2	C3H5	C3H6	C3H7	C3H8	C4H	C4H2	C4H3	C4H4	C4H5
1)	6.078E+03	1.254E-16	1.028E-18	1.298E-16	1.054E-22	2.183E-12	1.049E-32	1.461E-18	7.034E-20	3.936E-21	3.631E-30
2)	4.338E+03	1.718E-16	1.239E-18	1.753E-16	1.353E-21	2.838E-12	2.986E-32	2.182E-18	6.317E-20	4.885E-21	1.447E-29
3)	3.158E+03	2.301E-16	1.432E-18	2.496E-16	2.380E-20	3.738E-12	5.956E-32	2.289E-18	3.941E-20	5.742E-21	6.267E-29
4)	2.293E+03	1.970E-16	1.124E-18	3.435E-16	3.172E-19	4.965E-12	5.525E-32	1.071E-18	1.046E-20	5.029E-21	2.961E-28
5)	1.669E+03	1.398E-16	6.936E-19	4.309E-16	4.502E-19	6.542E-12	5.389E-31	5.144E-18	2.763E-20	3.027E-20	1.114E-26
6)	1.224E+03	3.772E-16	1.014E-18	8.348E-16	6.221E-19	8.481E-12	1.922E-29	9.027E-17	2.656E-19	5.240E-19	7.232E-25
7)	8.722E+02	2.318E-15	4.071E-18	3.787E-15	1.979E-18	1.110E-11	3.353E-28	7.254E-16	1.107E-18	3.075E-18	1.569E-23
8)	6.324E+02	5.954E-15	8.083E-18	1.002E-14	3.959E-18	1.380E-11	1.835E-27	1.928E-15	1.624E-18	6.771E-18	1.124E-22
9)	4.712E+02	8.140E-15	7.763E-18	1.403E-14	4.544E-18	1.608E-11	4.724E-27	2.578E-15	1.296E-18	8.266E-18	4.210E-22
10)	3.447E+02	9.038E-15	5.805E-18	1.593E-14	4.374E-18	1.824E-11	1.241E-26	3.351E-15	9.723E-19	7.873E-18	1.320E-21
11)	2.469E+02	9.008E-15	3.803E-18	1.631E-14	3.797E-18	2.074E-11	6.786E-26	8.336E-15	1.281E-18	7.180E-18	3.653E-21
12)	1.836E+02	1.031E-14	3.082E-18	1.822E-14	3.664E-18	2.432E-11	4.633E-25	2.854E-14	2.526E-18	1.007E-17	9.274E-21
13)	1.345E+02	1.551E-14	3.484E-18	2.504E-14	4.526E-18	3.125E-11	2.483E-24	8.358E-14	4.932E-18	1.884E-17	3.099E-20
14)	9.768E+01	2.144E-14	4.803E-18	3.379E-14	6.529E-18	3.702E-11	4.448E-24	1.054E-13	6.121E-18	2.392E-17	5.336E-20
15)	7.127E+01	2.979E-14	8.631E-18	4.741E-14	1.254E-17	4.359E-11	3.612E-24	8.361E-14	7.666E-18	3.068E-17	5.347E-20
16)	5.286E+01	5.119E-14	2.329E-17	7.897E-14	3.162E-17	5.388E-11	2.243E-24	5.919E-14	1.038E-17	4.418E-17	5.580E-20
17)	3.997E+01	1.036E-13	7.905E-17	1.542E-13	9.093E-17	6.886E-11	1.729E-24	5.193E-14	1.672E-17	8.563E-17	7.834E-20
18)	2.921E+01	2.332E-13	3.004E-16	3.410E-13	2.883E-16	9.393E-11	2.168E-24	6.892E-14	3.840E-17	2.196E-16	1.298E-19
19)	2.167E+01	4.417E-13	7.989E-16	6.266E-13	6.721E-16	1.268E-10	3.683E-24	1.087E-13	8.464E-17	4.553E-16	2.076E-19
20)	1.626E+01	7.338E-13	1.667E-15	9.971E-13	1.260E-15	1.673E-10	6.505E-24	1.657E-13	1.599E-16	7.879E-16	3.230E-19

21)	1.172E+01	1.197E-12	3.240E-15	1.519E-12	2.188E-15	2.233E-10	1.232E-23	2.500E-13	2.825E-16	1.287E-15	5.301E-19
22)	8.490E+00	1.844E-12	5.619E-15	2.154E-12	3.411E-15	2.882E-10	2.256E-23	3.552E-13	4.489E-16	1.942E-15	8.622E-19
23)	6.182E+00	2.763E-12	9.338E-15	2.976E-12	5.097E-15	3.610E-10	4.026E-23	4.921E-13	6.900E-16	2.867E-15	1.393E-18
24)	4.518E+00	4.009E-12	1.477E-14	3.990E-12	7.311E-15	4.396E-10	6.886E-23	6.550E-13	1.016E-15	4.096E-15	2.213E-18
25)	3.317E+00	5.601E-12	2.231E-14	5.201E-12	1.014E-14	5.202E-10	1.106E-22	8.270E-13	1.429E-15	5.623E-15	3.407E-18
26)	2.444E+00	7.444E-12	3.178E-14	6.532E-12	1.346E-14	5.984E-10	1.643E-22	9.731E-13	1.883E-15	7.280E-15	5.003E-18
27)	1.811E+00	9.298E-12	4.239E-14	7.870E-12	1.704E-14	6.694E-10	2.216E-22	1.053E-12	2.302E-15	8.793E-15	6.890E-18
28)	1.349E+00	1.074E-11	5.188E-14	8.981E-12	2.014E-14	7.289E-10	2.711E-22	1.040E-12	2.564E-15	9.747E-15	8.815E-18
29)	1.009E+00	1.136E-11	5.724E-14	9.637E-12	2.183E-14	7.751E-10	3.061E-22	9.437E-13	2.585E-15	9.877E-15	1.050E-17
30)	7.285E-01	1.088E-11	5.643E-14	9.794E-12	2.167E-14	8.124E-10	3.285E-22	7.855E-13	2.379E-15	9.214E-15	1.186E-17
31)	5.283E-01	9.458E-12	4.918E-14	9.567E-12	1.984E-14	8.383E-10	3.463E-22	6.366E-13	2.075E-15	8.233E-15	1.259E-17
32)	3.849E-01	7.634E-12	3.873E-14	9.319E-12	1.744E-14	8.582E-10	3.734E-22	5.256E-13	1.808E-15	7.529E-15	1.284E-17
33)	2.811E-01	5.720E-12	2.735E-14	8.897E-12	1.447E-14	8.757E-10	4.325E-22	4.617E-13	1.632E-15	7.572E-15	1.330E-17
34)	2.062E-01	3.868E-12	1.684E-14	7.879E-12	1.082E-14	8.939E-10	5.357E-22	4.315E-13	1.535E-15	8.967E-15	1.590E-17
35)	1.516E-01	2.198E-12	8.058E-15	5.790E-12	6.511E-15	9.163E-10	6.464E-22	3.829E-13	1.319E-15	1.226E-14	2.959E-17
36)	1.116E-01	1.057E-12	2.808E-15	2.860E-12	2.558E-15	9.494E-10	6.166E-22	2.504E-13	7.988E-16	1.657E-14	9.484E-17
37)	8.214E-02	7.912E-13	1.540E-15	1.004E-12	6.967E-16	1.003E-09	5.734E-22	1.352E-13	3.855E-16	2.317E-14	3.120E-16
38)	6.045E-02	1.007E-12	1.731E-15	4.303E-13	2.316E-16	1.086E-09	7.249E-22	8.698E-14	2.236E-16	4.010E-14	7.712E-16
39)	4.470E-02	1.494E-12	2.522E-15	2.890E-13	1.235E-16	1.207E-09	1.108E-21	7.479E-14	1.785E-16	7.776E-14	1.609E-15
40)	3.339E-02	2.126E-12	3.738E-15	2.962E-13	1.041E-16	1.367E-09	1.811E-21	1.093E-13	2.387E-16	1.722E-13	3.351E-15
41)	2.462E-02	2.531E-12	4.618E-15	4.734E-13	1.427E-16	1.596E-09	3.544E-21	3.477E-13	6.368E-16	5.413E-13	8.077E-15
42)	1.817E-02	3.203E-12	6.405E-15	8.138E-13	2.646E-16	1.911E-09	1.533E-20	2.924E-12	4.034E-15	2.798E-12	2.213E-14
43)	1.354E-02	4.908E-10	8.283E-13	1.163E-11	2.847E-15	2.354E-09	3.165E-18	7.752E-10	7.472E-13	5.742E-11	1.749E-13
44)	9.984E-03	6.180E-10	6.413E-13	7.076E-11	1.686E-14	3.483E-09	2.480E-17	3.238E-09	2.062E-12	2.282E-10	2.474E-13
45)	7.342E-03	2.039E-10	8.260E-14	2.304E-12	6.853E-16	4.388E-11	1.335E-14	1.097E-08	4.563E-12	6.052E-10	2.464E-13
46)	5.404E-03	1.951E-11	3.743E-15	3.419E-15	4.580E-18	1.108E-13	9.107E-15	1.302E-09	3.614E-13	7.415E-11	1.222E-14
47)	3.981E-03	3.439E-12	3.902E-16	2.069E-17	6.139E-20	5.170E-16	3.956E-15	3.185E-10	5.992E-14	9.152E-12	6.708E-16
48)	2.893E-03	4.710E-13	3.262E-17	3.197E-19	4.954E-22	1.665E-18	8.824E-16	5.348E-11	6.813E-15	6.759E-13	2.363E-17
49)	2.104E-03	3.781E-14	1.656E-18	7.510E-21	2.900E-24	4.470E-21	7.144E-17	3.988E-12	3.490E-16	2.485E-14	4.514E-19
50)	1.530E-03	1.583E-15	4.448E-20	1.093E-22	2.236E-26	1.761E-23	2.315E-18	1.215E-13	7.335E-18	5.159E-16	5.065E-21
51)	1.112E-03	3.826E-17	6.922E-22	9.897E-25	3.077E-28	1.385E-25	3.495E-20	1.910E-15	7.906E-20	8.104E-18	4.355E-23
52)	8.113E-04	6.694E-19	7.804E-24	7.376E-27	3.767E-30	9.406E-28	3.588E-22	2.168E-17	6.150E-22	9.711E-20	2.867E-25
53)	5.894E-04	4.048E-21	3.028E-26	2.597E-29	2.516E-32	3.478E-30	1.197E-24	8.297E-20	1.547E-24	6.835E-22	1.112E-27
54)	4.275E-04	8.901E-24	4.307E-29	4.783E-32	8.881E-35	7.168E-33	1.668E-27	1.499E-22	1.797E-27	2.744E-24	2.531E-30
55)	3.097E-04	4.848E-27	1.539E-32	3.336E-35	1.692E-37	8.657E-36	1.275E-30	1.924E-25	1.483E-30	6.382E-27	3.476E-33
56)	2.238E-04	1.740E-30	3.678E-36	1.909E-38	0.000E+00	6.180E-39	1.058E-33	2.433E-28	1.254E-33	8.702E-30	2.911E-36
57)	1.623E-04	5.009E-34	0.000E+00	0.000E+00	0.000E+00	0.000E+00	9.020E-37	2.933E-31	1.030E-36	8.349E-33	0.000E+00
58)	1.173E-04	1.446E-37	0.000E+00	0.000E+00	0.000E+00	0.000E+00	0.000E+00	2.552E-34	0.000E+00	5.030E-36	0.000E+00
59)	8.516E-05	0.000E+00	0.000E+00	0.000E+00	0.000E+00	0.000E+00	0.000E+00	1.844E-37	0.000E+00	0.000E+00	0.000E+00
60)	6.154E-05	0.000E+00	0.000E+00	0.000E+00	0.000E+00	0.000E+00	0.000E+00	0.000E+00	0.000E+00	0.000E+00	0.000E+00
61)	4.467E-05	0.000E+00	0.000E+00	0.000E+00	0.000E+00	0.000E+00	0.000E+00	0.000E+00	0.000E+00	0.000E+00	0.000E+00
62)	3.233E-05	0.000E+00	0.000E+00	0.000E+00	0.000E+00	0.000E+00	0.000E+00	0.000E+00	0.000E+00	0.000E+00	0.000E+00
63)	2.333E-05	0.000E+00	0.000E+00	0.000E+00	0.000E+00	0.000E+00	0.000E+00	0.000E+00	0.000E+00	0.000E+00	0.000E+00
64)	1.688E-05	0.000E+00	0.000E+00	0.000E+00	0.000E+00	0.000E+00	0.000E+00	0.000E+00	0.000E+00	0.000E+00	0.000E+00
65)	1.220E-05	0.000E+00	0.000E+00	0.000E+00	0.000E+00	0.000E+00	0.000E+00	0.000E+00	0.000E+00	0.000E+00	0.000E+00
66)	8.802E-06	0.000E+00	0.000E+00	0.000E+00	0.000E+00	0.000E+00	0.000E+00	0.000E+00	0.000E+00	0.000E+00	0.000E+00
67)	6.347E-06	0.000E+00	0.000E+00	0.000E+00	0.000E+00	0.000E+00	0.000E+00	0.000E+00	0.000E+00	0.000E+00	0.000E+00
68)	4.574E-06	0.000E+00	0.000E+00	0.000E+00	0.000E+00	0.000E+00	0.000E+00	0.000E+00	0.000E+00	0.000E+00	0.000E+00
69)	3.292E-06	0.000E+00	0.000E+00	0.000E+00	0.000E+00	0.000E+00	0.000E+00	0.000E+00	0.000E+00	0.000E+00	0.000E+00
70)	2.371E-06	0.000E+00	0.000E+00	0.000E+00	0.000E+00	0.000E+00	0.000E+00	0.000E+00	0.000E+00	0.000E+00	0.000E+00
71)	1.709E-06	0.000E+00	0.000E+00	0.000E+00	0.000E+00	0.000E+00	0.000E+00	0.000E+00	0.000E+00	0.000E+00	0.000E+00
72)	1.231E-06	0.000E+00	0.000E+00	0.000E+00	0.000E+00	0.000E+00	0.000E+00	0.000E+00	0.000E+00	0.000E+00	0.000E+00
73)	8.866E-07	0.000E+00	0.000E+00	0.000E+00	0.000E+00	0.000E+00	0.000E+00	0.000E+00	0.000E+00	0.000E+00	0.000E+00
74)	6.367E-07	0.000E+00	0.000E+00	0.000E+00	0.000E+00	0.000E+00	0.000E+00	0.000E+00	0.000E+00	0.000E+00	0.000E+00
75)	4.581E-07	0.000E+00	0.000E+00	0.000E+00	0.000E+00	0.000E+00	0.000E+00	0.000E+00	0.000E+00	0.000E+00	0.000E+00
76)	3.299E-07	0.000E+00	0.000E+00	0.000E+00	0.000E+00	0.000E+00	0.000E+00	0.000E+00	0.000E+00	0.000E+00	0.000E+00
77)	2.370E-07	0.000E+00	0.000E+00	0.000E+00	0.000E+00	0.000E+00	0.000E+00	0.000E+00	0.000E+00	0.000E+00	0.000E+00
78)	1.705E-07	0.000E+00	0.000E+00	0.000E+00	0.000E+00	0.000E+00	0.000E+00	0.000E+00	0.000E+00	0.000E+00	0.000E+00
79)	1.228E-07	0.000E+00	0.000E+00	0.000E+00	0.000E+00	0.000E+00	0.000E+00	0.000E+00	0.000E+00	0.000E+00	0.000E+00
80)	9.997E-08	0.000E+00	0.000E+00	0.000E+00	0.000E+00	0.000E+00	0.000E+00	0.000E+00	0.000E+00	0.000E+00	0.000E+00

	PRESSURE	1-C4H6	1,2-C4H6	1,3-C4H6	C4H8	C4H9	C4H10	C6H	C6H2	C6H3	C6H6
1)	6.078E+03	9.274E-19	6.333E-20	2.967E-21	8.340E-19	1.562E-25	9.159E-15	1.223E-38	1.703E-24	1.670E-25	6.039E-18
2)	4.338E+03	1.178E-18	7.769E-20	4.131E-21	1.161E-18	3.069E-28	1.292E-14	2.588E-37	1.891E-23	2.340E-24	7.695E-18
3)	3.158E+03	1.518E-18	9.270E-20	6.332E-21	1.780E-18	5.890E-28	1.996E-14	1.057E-36	4.064E-23	6.539E-24	6.516E-18
4)	2.293E+03	1.601E-18	6.758E-20	1.013E-20	2.821E-18	1.644E-27	3.168E-14	4.822E-36	9.350E-23	1.924E-23	9.638E-19
5)	1.669E+03	1.147E-17	4.169E-20	1.199E-19	5.527E-18	1.055E-26	4.954E-14	5.100E-35	4.868E-22	1.199E-22	1.056E-19
6)	1.224E+03	2.035E-16	1.912E-19	2.369E-18	2.205E-17	1.003E-25	7.508E-14	4.713E-34	2.213E-21	6.067E-22	4.094E-19
7)	8.722E+02	1.219E-15	5.110E-18	1.401E-17	9.294E-17	1.163E-24	1.139E-13	6.439E-33	1.393E-20	4.058E-21	1.347E-17
8)	6.324E+02	2.727E-15	2.247E-17	3.019E-17	1.989E-16	6.104E-24	1.585E-13	6.297E-32	6.615E-20	1.981E-20	5.930E-17
9)	4.712E+02	3.423E-15	2.600E-17	3.825E-17	2.703E-16	1.671E-23	2.023E-13	2.943E-31	1.606E-19	4.873E-20	5.233E-17
10)	3.447E+02	3.270E-15	2.032E-17	3.706E-17	2.921E-16	4.092E-23	2.551E-13	1.310E-30	3.537E-19	1.081E-19	2.781E-17
11)	2.469E+02	2.354E-15	1.312E-17	2.571E-17	2.593E-16	1.034E-22	3.374E-13	6.947E-30	8.534E-19	2.615E-19	1.179E-17
12)	1.836E+02	1.847E-15	1.090E-17	1.603E-17	2.868E-16	2.500E-22	4.753E-13	3.836E-29	2.363E-18	7.242E-19	8.265E-18
13)	1.345E+02	2.310E-15	1.302E-17	1.247E-17	4.940E-16	6.409E-22	7.669E-13	2.510E-28	8.450E-18	2.585E-18	1.099E-17
14)	9.768E+01	2.745E-15	1.538E-17	1.323E-17	7.953E-16	9.820E-22	1.034E-12	4.912E-28	1.164E-17	3.546E-18	1.413E-17
15)	7.127E+01	3.982E-15	2.119E-17	2.808E-17	1.294E-15	1.171E-21	1.361E-12	3.137E-28	7.261E-18	2.197E-18	1.951E-17
16)	5.286E+01	8.389E-15	5.358E-17	8.853E-17	2.459E-15	1.591E-21	1.905E-12	1.781E-28	4.702E-18	1.408E-18	5.698E-17
17)	3.997E+01	2.223E-14	2.002E-16	2.782E-16	5.229E-15	2.531E-21	2.751E-12	1.489E-28	4.473E-18	1.322E-18	2.841E-16
18)	2.921E+01	6.162E-14	8.499E-16	8.155E-16	1.241E-14	4.632E-21	4.273E-12	1.783E-28	5.670E-18	1.643E-18	1.665E-15
19)	2.167E+01	1.247E-13	2.384E-15	1.625E-15	2.458E-14	8.210E-21	6.442E-12	2.723E-28	8.035E-18	2.283E-18	5.668E-15
20)	1.626E+01	2.079E-13	5.060E-15	2.619E-15	4.264E-14	1.389E-20	9.306E-12	4.625E-28	1.178E-17	3.282E-18	1.315E-14
21)	1.172E+01	3.259E-13	9.812E-15	3.895E-15	7.214E-14	2.418E-20	1.354E-11	9.180E-28	1.862E-17	5.072E-18	2.605E-14
22)	8.490E+00	4.743E-13	1.670E-14	5.362E-15	1.142E-13	3.944E-20	1.872E-11	1.537E-27	2.419E-17	6.435E-18	4.291E-14
23)	6.182E+00	6.773E-13	2.709E-14	7.278E-15	1.771E-13	6.155E-20	2.476E-11	3.236E-27	3.948E-17	1.021E-17	6.612E-14
24)	4.518E+00	9.400E-13	4.103E-14	9.716E-15	2.665E-13	9.076E-20	3.143E-11	6.897E-27	6.533E-17	1.635E-17	9.284E-14
25)	3.317E+00	1.258E-12	5.769E-14	1.280E-14	3.864E-13	1.257E-19	3.827E-11	1.465E-26	1.086E-16	2.612E-17	1.175E-13
26)	2.444E+00	1.594E-12	7.386E-14	1.633E-14	5.298E-13	1.624E-19	4.464E-11	3.085E-26	1.801E-16	4.123E-17	1.299E-13
27)	1.811E+00	1.887E-12	8.490E-14	2.002E-14	6.785E-13	1.942E-19	4.987E-11	6.355E-26	2.945E-16	6.352E-17	1.216E-13
28)	1.349E+00	2.052E-12	8.581E-14	2.294E-14	7.948E-13	2.137E-19	5.330E-11	1.277E-25	4.697E-16	9.433E-17	9.244E-14
29)	1.009E+00	2.036E-12	7.553E-14	2.408E-14	8.396E-13	2.168E-19	5.461E-11	2.526E-25	7.282E-16	1.347E-16	5.567E-14
30)	7.285E-01	1.833E-12	5.605E-14	2.298E-14	7.964E-13	2.010E-19	5.371E-11	5.673E-25	1.222E-15	2.029E-16	2.370E-14
31)	5.283E-01	1.533E-12	3.721E-14	1.980E-14	6.947E-13	1.704E-19	5.097E-11	1.525E-24	2.467E-15	3.627E-16	7.877E-15
32)	3.849E-01	1.248E-12	2.347E-14	1.570E-14	5.884E-13	1.316E-19	4.715E-11	4.896E-24	6.117E-15	7.859E-16	2.266E-15
33)	2.811E-01	1.083E-12	1.394E-14	1.142E-14	4.810E-13	9.247E-20	4.268E-11	1.513E-23	1.451E-14	1.613E-15	8.747E-16
34)	2.062E-01	1.338E-12	7.287E-15	7.600E-15	3.669E-13	5.863E-20	3.795E-11	3.863E-23	2.800E-14	2.676E-15	9.379E-16
35)	1.516E-01	3.104E-12	2.936E-15	4.524E-15	2.553E-13	3.089E-20	3.350E-11	7.603E-23	3.949E-14	3.244E-15	1.528E-15
36)	1.116E-01	1.033E-11	9.751E-16	2.495E-15	1.832E-13	1.141E-20	3.005E-11	1.077E-22	3.461E-14	2.446E-15	2.184E-15
37)	8.214E-02	3.599E-11	5.814E-16	1.523E-15	1.678E-13	3.601E-21	2.825E-11	1.482E-22	2.246E-14	1.363E-15	2.027E-15
38)	6.045E-02	1.211E-10	1.768E-15	1.228E-15	1.864E-13	1.380E-21	2.840E-11	2.473E-22	1.530E-14	7.793E-16	1.291E-15
39)	4.470E-02	3.842E-10	2.186E-14	1.539E-15	2.765E-13	6.819E-22	3.059E-11	4.309E-22	1.229E-14	5.015E-16	6.917E-16
40)	3.339E-02	1.131E-09	2.947E-13	4.524E-15	8.628E-13	4.102E-22	3.485E-11	7.064E-22	1.602E-14	4.865E-16	4.216E-16
41)	2.462E-02	3.380E-09	4.057E-12	3.074E-14	5.894E-12	3.002E-22	4.220E-11	1.129E-21	4.053E-14	7.956E-16	2.477E-16
42)	1.817E-02	9.919E-09	5.512E-11	2.653E-13	5.074E-11	3.079E-22	5.335E-11	1.938E-21	1.424E-13	1.587E-15	1.460E-16
43)	1.354E-02	2.751E-08	7.012E-10	2.191E-12	4.276E-10	1.504E-20	6.863E-11	2.383E-19	5.842E-11	3.474E-13	9.499E-15
44)	9.984E-03	4.522E-08	3.556E-09	3.960E-12	7.245E-10	2.492E-19	8.195E-11	8.452E-19	1.918E-10	5.851E-13	5.305E-15
45)	7.342E-03	3.308E-08	1.469E-09	6.073E-13	9.836E-11	7.862E-21	1.814E-11	1.027E-15	4.557E-10	7.294E-13	2.759E-16
46)	5.404E-03	5.336E-09	1.385E-10	4.096E-14	6.474E-12	7.208E-23	2.973E-12	1.212E-16	1.310E-11	1.160E-14	9.368E-19
47)	3.981E-03	5.728E-10	9.771E-12	2.137E-15	3.368E-13	3.339E-24	3.692E-13	9.851E-18	9.390E-13	4.866E-16	9.024E-21
48)	2.893E-03	3.948E-11	3.941E-13	8.199E-17	1.292E-14	1.039E-25	3.026E-14	4.372E-19	4.822E-14	1.507E-17	1.086E-22
49)	2.104E-03	1.892E-12	9.799E-15	2.563E-18	4.046E-16	1.449E-27	1.662E-15	6.504E-21	1.256E-15	2.470E-19	5.579E-25
50)	1.530E-03	6.162E-14	1.649E-16	6.257E-20	9.900E-18	8.483E-30	5.730E-17	2.478E-23	1.700E-17	2.146E-21	9.480E-28
51)	1.112E-03	1.297E-15	1.971E-18	1.069E-21	1.693E-19	1.966E-32	1.160E-18	3.589E-26	1.083E-19	8.858E-24	6.130E-31
52)	8.113E-04	1.715E-17	1.682E-20	1.180E-23	1.864E-21	2.056E-35	1.350E-20	3.591E-29	3.393E-22	1.810E-26	2.018E-34
53)	5.894E-04	1.241E-19	8.908E-23	7.098E-26	1.114E-23	6.488E-39	7.843E-23	1.637E-32	4.438E-25	1.549E-29	1.578E-38
54)	4.275E-04	4.943E-22	2.880E-25	2.322E-28	3.598E-26	0.000E+00	2.314E-25	9.077E-36	2.312E-28	5.352E-33	0.000E+00
55)	3.097E-04	1.119E-24	5.692E-28	4.272E-31	6.479E-29	0.000E+00	3.619E-28	0.000E+00	4.540E-32	7.095E-37	0.000E+00
56)	2.238E-04	1.453E-27	6.794E-31	4.496E-34	6.570E-32	0.000E+00	3.052E-31	0.000E+00	4.494E-36	0.000E+00	0.000E+00
57)	1.623E-04	1.302E-30	5.760E-34	3.268E-37	4.534E-35	0.000E+00	1.700E-34	0.000E+00	0.000E+00	0.000E+00	0.000E+00
58)	1.173E-04	7.055E-34	3.018E-37	0.000E+00	1.859E-38	0.000E+00	5.442E-38	0.000E+00	0.000E+00	0.000E+00	0.000E+00
59)	8.516E-05	2.957E-37	0.000E+00	0.000E+00	0.000E+00	0.000E+00	0.000E+00	0.000E+00	0.000E+00	0.000E+00	0.000E+00
60)	6.154E-05	0.000E+00	0.000E+00	0.000E+00	0.000E+00	0.000E+00	0.000E+00	0.000E+00	0.000E+00	0.000E+00	0.000E+00

61)	4.467E-05	0.000E+00	0.000E+00	0.000E+00	0.000E+00	0.000E+00	0.000E+00	0.000E+00	0.000E+00	0.000E+00	0.000E+00
62)	3.233E-05	0.000E+00	0.000E+00	0.000E+00	0.000E+00	0.000E+00	0.000E+00	0.000E+00	0.000E+00	0.000E+00	0.000E+00
63)	2.333E-05	0.000E+00	0.000E+00	0.000E+00	0.000E+00	0.000E+00	0.000E+00	0.000E+00	0.000E+00	0.000E+00	0.000E+00
64)	1.688E-05	0.000E+00	0.000E+00	0.000E+00	0.000E+00	0.000E+00	0.000E+00	0.000E+00	0.000E+00	0.000E+00	0.000E+00
65)	1.220E-05	0.000E+00	0.000E+00	0.000E+00	0.000E+00	0.000E+00	0.000E+00	0.000E+00	0.000E+00	0.000E+00	0.000E+00
66)	8.802E-06	0.000E+00	0.000E+00	0.000E+00	0.000E+00	0.000E+00	0.000E+00	0.000E+00	0.000E+00	0.000E+00	0.000E+00
67)	6.347E-06	0.000E+00	0.000E+00	0.000E+00	0.000E+00	0.000E+00	0.000E+00	0.000E+00	0.000E+00	0.000E+00	0.000E+00
68)	4.574E-06	0.000E+00	0.000E+00	0.000E+00	0.000E+00	0.000E+00	0.000E+00	0.000E+00	0.000E+00	0.000E+00	0.000E+00
69)	3.292E-06	0.000E+00	0.000E+00	0.000E+00	0.000E+00	0.000E+00	0.000E+00	0.000E+00	0.000E+00	0.000E+00	0.000E+00
70)	2.371E-06	0.000E+00	0.000E+00	0.000E+00	0.000E+00	0.000E+00	0.000E+00	0.000E+00	0.000E+00	0.000E+00	0.000E+00
71)	1.709E-06	0.000E+00	0.000E+00	0.000E+00	0.000E+00	0.000E+00	0.000E+00	0.000E+00	0.000E+00	0.000E+00	0.000E+00
72)	1.231E-06	0.000E+00	0.000E+00	0.000E+00	0.000E+00	0.000E+00	0.000E+00	0.000E+00	0.000E+00	0.000E+00	0.000E+00
73)	8.866E-07	0.000E+00	0.000E+00	0.000E+00	0.000E+00	0.000E+00	0.000E+00	0.000E+00	0.000E+00	0.000E+00	0.000E+00
74)	6.367E-07	0.000E+00	0.000E+00	0.000E+00	0.000E+00	0.000E+00	0.000E+00	0.000E+00	0.000E+00	0.000E+00	0.000E+00
75)	4.581E-07	0.000E+00	0.000E+00	0.000E+00	0.000E+00	0.000E+00	0.000E+00	0.000E+00	0.000E+00	0.000E+00	0.000E+00
76)	3.299E-07	0.000E+00	0.000E+00	0.000E+00	0.000E+00	0.000E+00	0.000E+00	0.000E+00	0.000E+00	0.000E+00	0.000E+00
77)	2.370E-07	0.000E+00	0.000E+00	0.000E+00	0.000E+00	0.000E+00	0.000E+00	0.000E+00	0.000E+00	0.000E+00	0.000E+00
78)	1.705E-07	0.000E+00	0.000E+00	0.000E+00	0.000E+00	0.000E+00	0.000E+00	0.000E+00	0.000E+00	0.000E+00	0.000E+00
79)	1.228E-07	0.000E+00	0.000E+00	0.000E+00	0.000E+00	0.000E+00	0.000E+00	0.000E+00	0.000E+00	0.000E+00	0.000E+00
80)	9.997E-08	0.000E+00	0.000E+00	0.000E+00	0.000E+00	0.000E+00	0.000E+00	0.000E+00	0.000E+00	0.000E+00	0.000E+00

	PRESSURE	C8H2	C5H2	C5H3	C6H4	NC6H5	C6H7	A1-	A1	HP	HEP
1)	6.078E+03	7.979E-33	5.080E-08	1.443E-25	1.020E-19	1.022E-22	3.866E-25	1.989E-18	1.864E-16	0.000E+00	0.000E+00
2)	4.338E+03	8.597E-32	6.363E-08	1.728E-25	1.192E-19	1.179E-22	4.516E-24	1.617E-18	1.946E-16	0.000E+00	0.000E+00
3)	3.158E+03	1.387E-30	7.715E-08	1.686E-25	1.172E-19	9.457E-23	4.466E-23	8.588E-19	1.600E-16	0.000E+00	0.000E+00
4)	2.293E+03	3.734E-29	9.239E-08	2.614E-26	2.451E-19	1.317E-22	1.286E-22	1.051E-19	4.579E-17	0.000E+00	0.000E+00
5)	1.669E+03	8.934E-28	1.095E-07	2.068E-26	1.877E-18	1.182E-21	8.839E-23	6.210E-21	6.247E-18	0.000E+00	0.000E+00
6)	1.224E+03	1.720E-26	1.284E-07	6.638E-26	2.009E-17	1.600E-20	3.277E-22	1.545E-21	2.517E-18	0.000E+00	0.000E+00
7)	8.722E+02	3.033E-25	1.524E-07	8.978E-26	1.844E-16	1.747E-19	7.667E-21	7.089E-21	1.277E-17	0.000E+00	0.000E+00
8)	6.324E+02	3.320E-24	1.792E-07	4.901E-26	5.541E-16	5.470E-19	2.400E-20	1.170E-20	2.623E-17	0.000E+00	0.000E+00
9)	4.712E+02	2.142E-23	2.085E-07	1.963E-26	7.248E-16	7.077E-19	1.540E-20	5.880E-21	1.960E-17	0.000E+00	0.000E+00
10)	3.447E+02	1.411E-22	2.458E-07	1.638E-26	8.767E-16	8.462E-19	5.757E-21	2.014E-21	1.034E-17	0.000E+00	0.000E+00
11)	2.469E+02	1.030E-21	2.939E-07	6.574E-26	1.634E-15	1.578E-18	1.624E-21	6.532E-22	5.208E-18	0.000E+00	0.000E+00
12)	1.836E+02	6.188E-21	3.454E-07	3.912E-25	3.521E-15	3.421E-18	7.897E-22	4.333E-22	4.697E-18	0.000E+00	0.000E+00
13)	1.345E+02	3.091E-20	4.118E-07	1.878E-24	6.567E-15	6.403E-18	7.627E-22	5.381E-22	7.268E-18	0.000E+00	0.000E+00
14)	9.768E+01	4.016E-20	4.478E-07	3.328E-24	7.132E-15	6.937E-18	8.283E-22	8.013E-22	1.138E-17	0.000E+00	0.000E+00
15)	7.127E+01	2.502E-20	4.769E-07	3.387E-24	7.288E-15	7.041E-18	1.163E-21	1.649E-21	2.172E-17	0.000E+00	0.000E+00
16)	5.286E+01	1.310E-20	5.123E-07	2.612E-24	8.413E-15	8.042E-18	3.659E-21	6.398E-21	6.369E-17	0.000E+00	0.000E+00
17)	3.997E+01	7.966E-21	5.552E-07	2.263E-24	1.177E-14	1.113E-17	1.890E-20	3.580E-20	2.317E-16	0.000E+00	0.000E+00
18)	2.921E+01	7.497E-21	6.178E-07	3.551E-24	2.019E-14	1.909E-17	1.058E-19	2.389E-19	9.581E-16	0.000E+00	0.000E+00
19)	2.167E+01	1.331E-20	6.939E-07	1.143E-23	3.383E-14	3.233E-17	3.162E-19	9.556E-19	2.892E-15	0.000E+00	0.000E+00
20)	1.626E+01	3.408E-20	7.845E-07	8.497E-23	5.189E-14	5.010E-17	6.150E-19	2.577E-18	6.667E-15	0.000E+00	0.000E+00
21)	1.172E+01	1.164E-19	9.105E-07	1.147E-21	7.671E-14	7.442E-17	9.587E-19	5.995E-18	1.422E-14	0.000E+00	0.000E+00
22)	8.490E+00	4.173E-19	1.062E-06	1.398E-20	1.040E-13	1.008E-16	1.219E-18	1.163E-17	2.714E-14	0.000E+00	0.000E+00
23)	6.182E+00	1.469E-18	1.241E-06	1.067E-19	1.332E-13	1.298E-16	1.443E-18	2.202E-17	5.267E-14	0.000E+00	0.000E+00
24)	4.518E+00	4.917E-18	1.455E-06	6.256E-19	1.613E-13	1.582E-16	1.551E-18	4.526E-17	1.207E-13	0.000E+00	0.000E+00
25)	3.317E+00	1.553E-17	1.707E-06	2.892E-18	1.842E-13	1.818E-16	1.504E-18	1.214E-16	3.755E-13	0.000E+00	0.000E+00
26)	2.444E+00	4.619E-17	2.004E-06	1.084E-17	1.968E-13	1.945E-16	1.275E-18	4.253E-16	1.438E-12	0.000E+00	0.000E+00
27)	1.811E+00	1.295E-16	2.352E-06	3.384E-17	1.956E-13	1.920E-16	9.202E-19	1.587E-15	5.588E-12	0.000E+00	0.000E+00
28)	1.349E+00	3.427E-16	2.757E-06	8.986E-17	1.806E-13	1.732E-16	5.407E-19	5.393E-15	1.983E-11	0.000E+00	0.000E+00
29)	1.009E+00	8.582E-16	3.226E-06	2.069E-16	1.564E-13	1.434E-16	2.515E-19	1.564E-14	6.193E-11	0.000E+00	0.000E+00
30)	7.285E-01	2.267E-15	3.849E-06	4.597E-16	1.286E-13	1.092E-16	7.976E-20	4.180E-14	1.893E-10	0.000E+00	0.000E+00
31)	5.283E-01	5.655E-15	4.570E-06	8.999E-16	1.150E-13	8.797E-17	1.972E-20	8.881E-14	4.887E-10	0.000E+00	0.000E+00
32)	3.849E-01	1.330E-14	5.399E-06	1.630E-15	1.288E-13	8.812E-17	4.226E-21	1.493E-13	1.069E-09	0.000E+00	0.000E+00
33)	2.811E-01	2.955E-14	6.337E-06	2.862E-15	1.754E-13	1.110E-16	1.213E-21	2.010E-13	2.015E-09	0.000E+00	0.000E+00
34)	2.062E-01	6.222E-14	7.388E-06	4.928E-15	2.382E-13	1.440E-16	9.697E-22	2.221E-13	3.345E-09	0.000E+00	0.000E+00
35)	1.516E-01	1.244E-13	8.547E-06	8.153E-15	2.647E-13	1.559E-16	1.175E-21	1.882E-13	5.011E-09	0.000E+00	0.000E+00
36)	1.116E-01	2.365E-13	9.800E-06	1.257E-14	2.000E-13	1.162E-16	1.241E-21	1.034E-13	6.916E-09	0.000E+00	0.000E+00
37)	8.214E-02	4.288E-13	1.113E-05	1.777E-14	1.044E-13	6.033E-17	8.472E-22	4.419E-14	8.954E-09	0.000E+00	0.000E+00
38)	6.045E-02	7.427E-13	1.251E-05	2.338E-14	5.333E-14	3.019E-17	4.009E-22	2.123E-14	1.105E-08	0.000E+00	0.000E+00
39)	4.470E-02	1.232E-12	1.393E-05	2.921E-14	3.228E-14	1.718E-17	1.648E-22	1.246E-14	1.317E-08	0.000E+00	0.000E+00

40)	3.339E-02	1.954E-12	1.536E-05	3.508E-14	3.024E-14	1.426E-17	8.017E-23	8.448E-15	1.524E-08	0.000E+00	3.868E-39
41)	2.462E-02	3.105E-12	1.697E-05	4.166E-14	4.179E-14	1.596E-17	3.807E-23	6.108E-15	1.751E-08	2.638E-29	4.142E-29
42)	1.817E-02	4.822E-12	1.871E-05	4.863E-14	8.139E-14	2.367E-17	1.801E-23	4.582E-15	1.983E-08	1.897E-19	2.538E-19
43)	1.354E-02	7.150E-12	2.044E-05	5.557E-14	8.325E-12	1.816E-15	9.217E-22	3.519E-15	2.203E-08	7.502E-16	8.237E-16
44)	9.984E-03	1.015E-11	2.055E-05	6.989E-14	9.362E-12	1.525E-15	3.889E-22	1.491E-15	9.805E-09	1.789E-14	9.738E-15
45)	7.342E-03	1.331E-11	1.100E-05	2.815E-13	4.133E-12	5.104E-16	1.481E-23	3.571E-16	1.337E-10	1.965E-12	1.039E-13
46)	5.404E-03	2.614E-12	3.217E-06	9.032E-14	4.585E-14	4.375E-18	3.611E-26	9.006E-18	3.856E-12	3.101E-11	3.954E-13
47)	3.981E-03	2.909E-13	6.310E-07	2.594E-14	6.084E-16	4.554E-20	2.471E-28	8.654E-19	1.783E-13	1.923E-10	1.122E-12
48)	2.893E-03	1.521E-14	7.212E-08	3.792E-15	1.415E-17	8.328E-22	2.070E-30	5.197E-20	5.394E-15	7.544E-10	2.303E-12
49)	2.104E-03	3.735E-16	4.827E-09	2.672E-16	1.482E-19	6.944E-24	7.399E-33	1.055E-21	5.984E-17	2.370E-09	3.689E-12
50)	1.530E-03	3.927E-18	1.788E-10	9.671E-18	6.378E-22	2.392E-26	8.727E-36	5.161E-24	1.697E-19	5.654E-09	6.245E-12
51)	1.112E-03	1.588E-20	3.473E-12	1.795E-19	1.063E-24	3.182E-29	3.896E-39	9.079E-27	1.780E-22	1.330E-08	6.898E-12
52)	8.113E-04	2.376E-23	3.534E-14	1.724E-21	7.536E-28	1.785E-32	0.000E+00	1.019E-29	1.195E-25	2.368E-08	5.815E-12
53)	5.894E-04	1.043E-26	1.645E-16	7.473E-24	2.120E-31	3.900E-36	0.000E+00	2.303E-33	1.606E-29	5.577E-08	6.902E-12
54)	4.275E-04	1.350E-30	3.603E-19	1.505E-26	2.552E-35	0.000E+00	0.000E+00	3.088E-37	1.288E-33	1.316E-07	7.760E-12
55)	3.097E-04	5.452E-35	3.923E-22	1.486E-29	0.000E+00	0.000E+00	0.000E+00	0.000E+00	1.086E-37	3.336E-07	1.033E-11
56)	2.238E-04	0.000E+00	2.173E-25	7.371E-33	0.000E+00	0.000E+00	0.000E+00	0.000E+00	0.000E+00	7.126E-07	1.207E-11
57)	1.623E-04	0.000E+00	7.622E-29	2.293E-36	0.000E+00	0.000E+00	0.000E+00	0.000E+00	0.000E+00	1.417E-06	1.302E-11
58)	1.173E-04	0.000E+00	1.465E-32	0.000E+00	0.000E+00	0.000E+00	0.000E+00	0.000E+00	0.000E+00	2.600E-06	1.427E-11
59)	8.516E-05	0.000E+00	2.052E-36	0.000E+00	0.000E+00	0.000E+00	0.000E+00	0.000E+00	0.000E+00	3.865E-06	1.411E-11
60)	6.154E-05	0.000E+00	0.000E+00	0.000E+00	0.000E+00	0.000E+00	0.000E+00	0.000E+00	0.000E+00	5.275E-06	1.236E-11
61)	4.467E-05	0.000E+00	0.000E+00	0.000E+00	0.000E+00	0.000E+00	0.000E+00	0.000E+00	0.000E+00	6.699E-06	1.219E-11
62)	3.233E-05	0.000E+00	0.000E+00	0.000E+00	0.000E+00	0.000E+00	0.000E+00	0.000E+00	0.000E+00	8.298E-06	1.568E-11
63)	2.333E-05	0.000E+00	0.000E+00	0.000E+00	0.000E+00	0.000E+00	0.000E+00	0.000E+00	0.000E+00	1.025E-05	1.909E-11
64)	1.688E-05	0.000E+00	0.000E+00	0.000E+00	0.000E+00	0.000E+00	0.000E+00	0.000E+00	0.000E+00	1.285E-05	1.233E-11
65)	1.220E-05	0.000E+00	0.000E+00	0.000E+00	0.000E+00	0.000E+00	0.000E+00	0.000E+00	0.000E+00	1.654E-05	8.782E-12
66)	8.802E-06	0.000E+00	0.000E+00	0.000E+00	0.000E+00	0.000E+00	0.000E+00	0.000E+00	0.000E+00	2.175E-05	5.670E-12
67)	6.347E-06	0.000E+00	0.000E+00	0.000E+00	0.000E+00	0.000E+00	0.000E+00	0.000E+00	0.000E+00	2.891E-05	4.105E-12
68)	4.574E-06	0.000E+00	0.000E+00	0.000E+00	0.000E+00	0.000E+00	0.000E+00	0.000E+00	0.000E+00	3.843E-05	2.761E-12
69)	3.292E-06	0.000E+00	0.000E+00	0.000E+00	0.000E+00	0.000E+00	0.000E+00	0.000E+00	0.000E+00	5.061E-05	2.045E-12
70)	2.371E-06	0.000E+00	0.000E+00	0.000E+00	0.000E+00	0.000E+00	0.000E+00	0.000E+00	0.000E+00	6.550E-05	1.403E-12
71)	1.709E-06	0.000E+00	0.000E+00	0.000E+00	0.000E+00	0.000E+00	0.000E+00	0.000E+00	0.000E+00	8.319E-05	9.958E-13
72)	1.231E-06	0.000E+00	0.000E+00	0.000E+00	0.000E+00	0.000E+00	0.000E+00	0.000E+00	0.000E+00	1.039E-04	6.551E-13
73)	8.866E-07	0.000E+00	0.000E+00	0.000E+00	0.000E+00	0.000E+00	0.000E+00	0.000E+00	0.000E+00	1.278E-04	4.317E-13
74)	6.367E-07	0.000E+00	0.000E+00	0.000E+00	0.000E+00	0.000E+00	0.000E+00	0.000E+00	0.000E+00	1.557E-04	2.742E-13
75)	4.581E-07	0.000E+00	0.000E+00	0.000E+00	0.000E+00	0.000E+00	0.000E+00	0.000E+00	0.000E+00	1.877E-04	1.767E-13
76)	3.299E-07	0.000E+00	0.000E+00	0.000E+00	0.000E+00	0.000E+00	0.000E+00	0.000E+00	0.000E+00	2.246E-04	1.150E-13
77)	2.370E-07	0.000E+00	0.000E+00	0.000E+00	0.000E+00	0.000E+00	0.000E+00	0.000E+00	0.000E+00	2.679E-04	7.702E-14
78)	1.705E-07	0.000E+00	0.000E+00	0.000E+00	0.000E+00	0.000E+00	0.000E+00	0.000E+00	0.000E+00	3.180E-04	5.314E-14
79)	1.228E-07	0.000E+00	0.000E+00	0.000E+00	0.000E+00	0.000E+00	0.000E+00	0.000E+00	0.000E+00	3.764E-04	3.786E-14
80)	9.997E-08	0.000E+00	0.000E+00	0.000E+00	0.000E+00	0.000E+00	0.000E+00	0.000E+00	0.000E+00	4.179E-04	3.097E-14

	PRESSURE	H2P	H3P	HEHP	CP	CHP	CH2P	CH3P	CH4P	CH5P	C2P
1)	6.078E+03	0.000E+00	0.000E+00	0.000E+00	0.000E+00	0.000E+00	0.000E+00	0.000E+00	0.000E+00	0.000E+00	0.000E+00
2)	4.338E+03	0.000E+00	0.000E+00	0.000E+00	0.000E+00	0.000E+00	0.000E+00	0.000E+00	0.000E+00	0.000E+00	0.000E+00
3)	3.158E+03	0.000E+00	0.000E+00	0.000E+00	0.000E+00	0.000E+00	0.000E+00	0.000E+00	0.000E+00	0.000E+00	0.000E+00
4)	2.293E+03	0.000E+00	0.000E+00	0.000E+00	0.000E+00	0.000E+00	0.000E+00	0.000E+00	0.000E+00	0.000E+00	0.000E+00
5)	1.669E+03	0.000E+00	0.000E+00	0.000E+00	0.000E+00	0.000E+00	0.000E+00	0.000E+00	0.000E+00	0.000E+00	0.000E+00
6)	1.224E+03	0.000E+00	0.000E+00	0.000E+00	0.000E+00	0.000E+00	0.000E+00	0.000E+00	0.000E+00	0.000E+00	0.000E+00
7)	8.722E+02	0.000E+00	0.000E+00	0.000E+00	0.000E+00	0.000E+00	0.000E+00	0.000E+00	0.000E+00	0.000E+00	0.000E+00
8)	6.324E+02	0.000E+00	0.000E+00	0.000E+00	0.000E+00	0.000E+00	0.000E+00	0.000E+00	0.000E+00	0.000E+00	0.000E+00
9)	4.712E+02	0.000E+00	0.000E+00	0.000E+00	0.000E+00	0.000E+00	0.000E+00	0.000E+00	0.000E+00	0.000E+00	0.000E+00
10)	3.447E+02	0.000E+00	0.000E+00	0.000E+00	0.000E+00	0.000E+00	0.000E+00	0.000E+00	0.000E+00	0.000E+00	0.000E+00
11)	2.469E+02	0.000E+00	0.000E+00	0.000E+00	0.000E+00	0.000E+00	0.000E+00	0.000E+00	0.000E+00	0.000E+00	0.000E+00
12)	1.836E+02	0.000E+00	0.000E+00	0.000E+00	0.000E+00	0.000E+00	0.000E+00	0.000E+00	0.000E+00	0.000E+00	0.000E+00
13)	1.345E+02	0.000E+00	0.000E+00	0.000E+00	0.000E+00	0.000E+00	0.000E+00	0.000E+00	0.000E+00	0.000E+00	0.000E+00
14)	9.768E+01	0.000E+00	0.000E+00	0.000E+00	0.000E+00	0.000E+00	0.000E+00	0.000E+00	0.000E+00	0.000E+00	0.000E+00
15)	7.127E+01	0.000E+00	0.000E+00	0.000E+00	0.000E+00	0.000E+00	0.000E+00	0.000E+00	0.000E+00	0.000E+00	0.000E+00
16)	5.286E+01	0.000E+00	0.000E+00	0.000E+00	0.000E+00	0.000E+00	0.000E+00	0.000E+00	0.000E+00	0.000E+00	0.000E+00
17)	3.997E+01	0.000E+00	0.000E+00	0.000E+00	0.000E+00	0.000E+00	0.000E+00	0.000E+00	0.000E+00	0.000E+00	0.000E+00
18)	2.921E+01	0.000E+00	0.000E+00	0.000E+00	0.000E+00	0.000E+00	0.000E+00	0.000E+00	0.000E+00	0.000E+00	0.000E+00

19)	2.167E+01	0.000E+00	0.000E+00	0.000E+00	0.000E+00	0.000E+00	0.000E+00	0.000E+00	0.000E+00	0.000E+00	0.000E+00
20)	1.626E+01	0.000E+00	0.000E+00	0.000E+00	0.000E+00	0.000E+00	0.000E+00	0.000E+00	0.000E+00	0.000E+00	0.000E+00
21)	1.172E+01	0.000E+00	0.000E+00	0.000E+00	0.000E+00	0.000E+00	0.000E+00	0.000E+00	0.000E+00	0.000E+00	0.000E+00
22)	8.490E+00	0.000E+00	0.000E+00	0.000E+00	0.000E+00	0.000E+00	0.000E+00	0.000E+00	0.000E+00	0.000E+00	0.000E+00
23)	6.182E+00	0.000E+00	0.000E+00	0.000E+00	0.000E+00	0.000E+00	0.000E+00	0.000E+00	0.000E+00	0.000E+00	0.000E+00
24)	4.518E+00	0.000E+00	0.000E+00	0.000E+00	0.000E+00	0.000E+00	0.000E+00	0.000E+00	0.000E+00	0.000E+00	0.000E+00
25)	3.317E+00	0.000E+00	0.000E+00	0.000E+00	0.000E+00	0.000E+00	0.000E+00	0.000E+00	0.000E+00	0.000E+00	0.000E+00
26)	2.444E+00	0.000E+00	0.000E+00	0.000E+00	0.000E+00	0.000E+00	0.000E+00	0.000E+00	0.000E+00	0.000E+00	0.000E+00
27)	1.811E+00	0.000E+00	0.000E+00	0.000E+00	0.000E+00	0.000E+00	0.000E+00	0.000E+00	0.000E+00	0.000E+00	0.000E+00
28)	1.349E+00	0.000E+00	0.000E+00	0.000E+00	0.000E+00	0.000E+00	0.000E+00	0.000E+00	0.000E+00	0.000E+00	0.000E+00
29)	1.009E+00	0.000E+00	0.000E+00	0.000E+00	0.000E+00	0.000E+00	0.000E+00	0.000E+00	0.000E+00	0.000E+00	0.000E+00
30)	7.285E-01	0.000E+00	0.000E+00	0.000E+00	0.000E+00	0.000E+00	0.000E+00	0.000E+00	0.000E+00	0.000E+00	0.000E+00
31)	5.283E-01	0.000E+00	0.000E+00	0.000E+00	0.000E+00	0.000E+00	0.000E+00	0.000E+00	0.000E+00	0.000E+00	0.000E+00
32)	3.849E-01	0.000E+00	0.000E+00	0.000E+00	0.000E+00	0.000E+00	0.000E+00	0.000E+00	0.000E+00	0.000E+00	0.000E+00
33)	2.811E-01	0.000E+00	0.000E+00	0.000E+00	0.000E+00	0.000E+00	0.000E+00	0.000E+00	0.000E+00	0.000E+00	0.000E+00
34)	2.062E-01	0.000E+00	0.000E+00	0.000E+00	0.000E+00	0.000E+00	0.000E+00	0.000E+00	0.000E+00	0.000E+00	0.000E+00
35)	1.516E-01	0.000E+00	0.000E+00	0.000E+00	0.000E+00	0.000E+00	0.000E+00	0.000E+00	0.000E+00	0.000E+00	0.000E+00
36)	1.116E-01	0.000E+00	0.000E+00	0.000E+00	0.000E+00	0.000E+00	0.000E+00	0.000E+00	0.000E+00	0.000E+00	0.000E+00
37)	8.214E-02	0.000E+00	0.000E+00	0.000E+00	0.000E+00	0.000E+00	0.000E+00	0.000E+00	0.000E+00	0.000E+00	0.000E+00
38)	6.045E-02	0.000E+00	0.000E+00	0.000E+00	0.000E+00	0.000E+00	0.000E+00	0.000E+00	0.000E+00	0.000E+00	0.000E+00
39)	4.470E-02	0.000E+00	0.000E+00	0.000E+00	0.000E+00	0.000E+00	0.000E+00	0.000E+00	0.000E+00	3.239E-39	0.000E+00
40)	3.339E-02	0.000E+00	6.600E-39	0.000E+00	0.000E+00	0.000E+00	0.000E+00	7.508E-38	1.458E-36	1.171E-31	0.000E+00
41)	2.462E-02	2.283E-34	6.597E-29	1.164E-32	1.698E-34	7.323E-33	3.462E-32	3.757E-28	1.021E-28	3.419E-24	5.954E-36
42)	1.817E-02	2.081E-22	3.396E-19	7.122E-23	4.747E-25	3.243E-23	1.533E-22	8.023E-19	8.091E-21	7.619E-17	3.484E-26
43)	1.354E-02	1.446E-17	3.279E-14	2.312E-19	3.659E-21	6.058E-20	2.863E-19	2.934E-15	5.011E-16	2.934E-12	6.451E-23
44)	9.984E-03	1.155E-16	9.163E-13	2.733E-18	2.088E-19	2.598E-19	1.024E-18	5.401E-14	2.312E-14	3.713E-11	2.770E-21
45)	7.342E-03	8.272E-16	9.696E-11	2.916E-17	2.169E-14	3.673E-16	3.805E-16	2.084E-11	4.629E-12	1.456E-09	2.524E-20
46)	5.404E-03	2.570E-15	1.461E-09	1.108E-16	1.626E-12	1.256E-15	1.301E-15	1.710E-10	3.843E-11	3.001E-09	1.905E-20
47)	3.981E-03	5.525E-15	6.088E-09	3.137E-16	1.555E-11	2.261E-15	2.344E-15	4.691E-10	5.959E-11	2.189E-09	1.696E-20
48)	2.893E-03	9.926E-15	1.240E-08	6.417E-16	5.472E-11	2.789E-15	2.902E-15	6.020E-10	4.124E-11	8.306E-10	1.024E-20
49)	2.104E-03	1.465E-14	1.730E-08	1.024E-15	8.219E-11	2.163E-15	2.262E-15	4.183E-10	1.649E-11	2.051E-10	3.385E-21
50)	1.530E-03	2.411E-14	2.280E-08	1.723E-15	7.934E-11	1.310E-15	1.379E-15	1.995E-10	4.790E-12	3.959E-11	7.576E-22
51)	1.112E-03	3.539E-14	2.599E-08	1.890E-15	5.110E-11	5.888E-16	6.243E-16	6.980E-11	1.089E-12	6.446E-12	7.402E-23
52)	8.113E-04	4.690E-14	2.744E-08	1.581E-15	2.550E-11	2.178E-16	2.328E-16	2.094E-11	2.249E-13	1.008E-12	4.684E-24
53)	5.894E-04	7.372E-14	2.759E-08	1.860E-15	1.044E-11	6.810E-17	7.345E-17	4.208E-12	3.147E-14	1.100E-13	1.925E-25
54)	4.275E-04	1.179E-13	2.438E-08	2.071E-15	3.295E-12	1.687E-17	1.838E-17	5.800E-13	3.077E-15	8.618E-15	4.194E-27
55)	3.097E-04	1.739E-13	1.663E-08	2.725E-15	7.212E-13	2.956E-18	3.259E-18	4.679E-14	1.755E-16	4.022E-16	5.067E-29
56)	2.238E-04	2.472E-13	1.166E-08	3.144E-15	1.464E-13	4.868E-19	5.438E-19	3.824E-15	1.026E-17	1.951E-17	5.630E-31
57)	1.623E-04	3.490E-13	8.435E-09	3.343E-15	2.903E-14	7.885E-20	8.946E-20	3.217E-16	6.166E-19	9.830E-19	6.049E-33
58)	1.173E-04	5.405E-13	7.105E-09	3.601E-15	6.193E-15	1.374E-20	1.588E-20	3.129E-17	4.258E-20	5.712E-20	7.651E-35
59)	8.516E-05	6.964E-13	6.141E-09	3.490E-15	1.341E-15	2.390E-21	2.829E-21	3.755E-18	3.834E-21	4.348E-21	1.296E-36
60)	6.154E-05	9.048E-13	5.806E-09	2.983E-15	3.017E-16	4.205E-22	5.140E-22	4.985E-19	3.897E-22	3.725E-22	2.176E-38
61)	4.467E-05	1.231E-12	6.143E-09	2.860E-15	7.571E-17	8.037E-23	1.027E-22	7.763E-20	4.761E-23	3.843E-23	0.000E+00
62)	3.233E-05	1.868E-12	7.365E-09	3.554E-15	2.091E-17	1.626E-23	2.216E-23	1.323E-20	6.413E-24	4.366E-24	0.000E+00
63)	2.333E-05	2.720E-12	8.401E-09	4.149E-15	6.098E-18	2.918E-24	4.561E-24	2.127E-21	8.147E-25	4.674E-25	0.000E+00
64)	1.688E-05	4.218E-12	9.925E-09	2.549E-15	1.974E-18	5.188E-25	1.032E-24	3.654E-22	1.097E-25	5.321E-26	0.000E+00
65)	1.220E-05	6.818E-12	1.174E-08	1.710E-15	6.941E-19	8.657E-26	2.624E-25	6.771E-23	1.565E-26	6.441E-27	0.000E+00
66)	8.802E-06	1.170E-11	1.420E-08	1.026E-15	2.551E-19	1.373E-26	7.722E-26	1.398E-23	2.423E-27	8.523E-28	0.000E+00
67)	6.347E-06	2.093E-11	1.739E-08	6.803E-16	9.421E-20	2.054E-27	2.521E-26	3.108E-24	3.908E-28	1.191E-28	0.000E+00
68)	4.574E-06	3.813E-11	2.124E-08	4.114E-16	3.392E-20	2.869E-28	8.532E-27	7.019E-25	6.176E-29	1.669E-29	0.000E+00
69)	3.292E-06	7.057E-11	2.591E-08	2.681E-16	1.165E-20	3.777E-29	2.838E-27	1.534E-25	9.131E-30	2.253E-30	0.000E+00
70)	2.371E-06	1.246E-10	2.989E-08	1.579E-16	3.793E-21	4.620E-30	9.058E-28	3.186E-26	1.255E-30	2.928E-31	0.000E+00
71)	1.709E-06	2.090E-10	3.238E-08	9.365E-17	1.162E-21	5.396E-31	2.725E-28	6.179E-27	1.586E-31	3.617E-32	0.000E+00
72)	1.231E-06	3.312E-10	3.276E-08	4.996E-17	3.331E-22	6.138E-32	7.642E-29	1.104E-27	1.820E-32	4.180E-33	0.000E+00
73)	8.866E-07	5.030E-10	3.123E-08	2.585E-17	8.911E-23	6.867E-33	1.981E-29	1.795E-28	1.874E-33	4.441E-34	0.000E+00
74)	6.367E-07	7.312E-10	2.794E-08	1.248E-17	2.215E-23	7.317E-34	4.693E-30	2.614E-29	1.697E-34	4.242E-35	0.000E+00
75)	4.581E-07	1.026E-09	2.381E-08	5.941E-18	5.246E-24	7.719E-35	1.031E-30	3.488E-30	1.392E-35	3.727E-36	0.000E+00
76)	3.299E-07	1.409E-09	1.960E-08	2.789E-18	1.190E-24	8.042E-36	2.085E-31	4.239E-31	1.031E-36	2.981E-37	0.000E+00
77)	2.370E-07	1.905E-09	1.568E-08	1.313E-18	2.569E-25	8.073E-37	3.777E-32	4.568E-32	6.755E-38	2.101E-38	0.000E+00
78)	1.705E-07	2.557E-09	1.244E-08	6.264E-19	5.413E-26	8.252E-38	6.230E-33	4.510E-33	4.134E-39	0.000E+00	0.000E+00
79)	1.228E-07	3.429E-09	1.002E-08	3.047E-19	1.124E-26	8.103E-39	9.446E-34	4.234E-34	0.000E+00	0.000E+00	0.000E+00

80)	9.997E-08	3.987E-09	8.945E-09	2.007E-19	4.153E-27	0.000E+00	2.833E-34	9.579E-35	0.000E+00	0.000E+00	0.000E+00

	PRESSURE	C2HP	C2H2P	C2H3P	C2H4P	C2H5P	C2H6P	C2H7P	C3P	C3HP	C3H2P
1)	6.078E+03	0.000E+00	0.000E+00	0.000E+00	0.000E+00	0.000E+00	0.000E+00	0.000E+00	0.000E+00	0.000E+00	0.000E+00
2)	4.338E+03	0.000E+00	0.000E+00	0.000E+00	0.000E+00	0.000E+00	0.000E+00	0.000E+00	0.000E+00	0.000E+00	0.000E+00
3)	3.158E+03	0.000E+00	0.000E+00	0.000E+00	0.000E+00	0.000E+00	0.000E+00	0.000E+00	0.000E+00	0.000E+00	0.000E+00
4)	2.293E+03	0.000E+00	0.000E+00	0.000E+00	0.000E+00	0.000E+00	0.000E+00	0.000E+00	0.000E+00	0.000E+00	0.000E+00
5)	1.669E+03	0.000E+00	0.000E+00	0.000E+00	0.000E+00	0.000E+00	0.000E+00	0.000E+00	0.000E+00	0.000E+00	0.000E+00
6)	1.224E+03	0.000E+00	0.000E+00	0.000E+00	0.000E+00	0.000E+00	0.000E+00	0.000E+00	0.000E+00	0.000E+00	0.000E+00
7)	8.722E+02	0.000E+00	0.000E+00	0.000E+00	0.000E+00	0.000E+00	0.000E+00	0.000E+00	0.000E+00	0.000E+00	0.000E+00
8)	6.324E+02	0.000E+00	0.000E+00	0.000E+00	0.000E+00	0.000E+00	0.000E+00	0.000E+00	0.000E+00	0.000E+00	0.000E+00
9)	4.712E+02	0.000E+00	0.000E+00	0.000E+00	0.000E+00	0.000E+00	0.000E+00	0.000E+00	0.000E+00	0.000E+00	0.000E+00
10)	3.447E+02	0.000E+00	0.000E+00	0.000E+00	0.000E+00	0.000E+00	0.000E+00	0.000E+00	0.000E+00	0.000E+00	0.000E+00
11)	2.469E+02	0.000E+00	0.000E+00	0.000E+00	0.000E+00	0.000E+00	0.000E+00	0.000E+00	0.000E+00	0.000E+00	0.000E+00
12)	1.836E+02	0.000E+00	0.000E+00	0.000E+00	0.000E+00	0.000E+00	0.000E+00	0.000E+00	0.000E+00	0.000E+00	0.000E+00
13)	1.345E+02	0.000E+00	0.000E+00	0.000E+00	0.000E+00	0.000E+00	0.000E+00	0.000E+00	0.000E+00	0.000E+00	0.000E+00
14)	9.768E+01	0.000E+00	0.000E+00	0.000E+00	0.000E+00	0.000E+00	0.000E+00	0.000E+00	0.000E+00	0.000E+00	0.000E+00
15)	7.127E+01	0.000E+00	0.000E+00	0.000E+00	0.000E+00	0.000E+00	0.000E+00	0.000E+00	0.000E+00	0.000E+00	0.000E+00
16)	5.286E+01	0.000E+00	0.000E+00	0.000E+00	0.000E+00	0.000E+00	0.000E+00	0.000E+00	0.000E+00	0.000E+00	0.000E+00
17)	3.997E+01	0.000E+00	0.000E+00	0.000E+00	0.000E+00	0.000E+00	0.000E+00	0.000E+00	0.000E+00	0.000E+00	0.000E+00
18)	2.921E+01	0.000E+00	0.000E+00	0.000E+00	0.000E+00	0.000E+00	0.000E+00	0.000E+00	0.000E+00	0.000E+00	0.000E+00
19)	2.167E+01	0.000E+00	0.000E+00	0.000E+00	0.000E+00	0.000E+00	0.000E+00	0.000E+00	0.000E+00	0.000E+00	0.000E+00
20)	1.626E+01	0.000E+00	0.000E+00	0.000E+00	0.000E+00	0.000E+00	0.000E+00	0.000E+00	0.000E+00	0.000E+00	0.000E+00
21)	1.172E+01	0.000E+00	0.000E+00	0.000E+00	0.000E+00	0.000E+00	0.000E+00	0.000E+00	0.000E+00	0.000E+00	0.000E+00
22)	8.490E+00	0.000E+00	0.000E+00	0.000E+00	0.000E+00	0.000E+00	0.000E+00	0.000E+00	0.000E+00	0.000E+00	0.000E+00
23)	6.182E+00	0.000E+00	0.000E+00	0.000E+00	0.000E+00	0.000E+00	0.000E+00	0.000E+00	0.000E+00	0.000E+00	0.000E+00
24)	4.518E+00	0.000E+00	0.000E+00	0.000E+00	0.000E+00	0.000E+00	0.000E+00	0.000E+00	0.000E+00	0.000E+00	0.000E+00
25)	3.317E+00	0.000E+00	0.000E+00	0.000E+00	0.000E+00	0.000E+00	0.000E+00	0.000E+00	0.000E+00	0.000E+00	0.000E+00
26)	2.444E+00	0.000E+00	0.000E+00	0.000E+00	0.000E+00	0.000E+00	0.000E+00	0.000E+00	0.000E+00	0.000E+00	0.000E+00
27)	1.811E+00	0.000E+00	0.000E+00	0.000E+00	0.000E+00	0.000E+00	0.000E+00	0.000E+00	0.000E+00	0.000E+00	0.000E+00
28)	1.349E+00	0.000E+00	0.000E+00	0.000E+00	0.000E+00	0.000E+00	0.000E+00	0.000E+00	0.000E+00	0.000E+00	0.000E+00
29)	1.009E+00	0.000E+00	0.000E+00	0.000E+00	0.000E+00	0.000E+00	0.000E+00	0.000E+00	0.000E+00	0.000E+00	0.000E+00
30)	7.285E-01	0.000E+00	0.000E+00	0.000E+00	0.000E+00	0.000E+00	0.000E+00	0.000E+00	0.000E+00	0.000E+00	0.000E+00
31)	5.283E-01	0.000E+00	0.000E+00	0.000E+00	0.000E+00	0.000E+00	0.000E+00	0.000E+00	0.000E+00	0.000E+00	0.000E+00
32)	3.849E-01	0.000E+00	0.000E+00	0.000E+00	0.000E+00	0.000E+00	0.000E+00	0.000E+00	0.000E+00	0.000E+00	0.000E+00
33)	2.811E-01	0.000E+00	0.000E+00	0.000E+00	0.000E+00	0.000E+00	0.000E+00	0.000E+00	0.000E+00	0.000E+00	0.000E+00
34)	2.062E-01	0.000E+00	0.000E+00	0.000E+00	0.000E+00	0.000E+00	0.000E+00	0.000E+00	0.000E+00	0.000E+00	0.000E+00
35)	1.516E-01	0.000E+00	0.000E+00	0.000E+00	0.000E+00	0.000E+00	0.000E+00	0.000E+00	0.000E+00	0.000E+00	0.000E+00
36)	1.116E-01	0.000E+00	0.000E+00	0.000E+00	0.000E+00	0.000E+00	0.000E+00	0.000E+00	0.000E+00	0.000E+00	0.000E+00
37)	8.214E-02	0.000E+00	0.000E+00	0.000E+00	0.000E+00	0.000E+00	0.000E+00	0.000E+00	0.000E+00	0.000E+00	0.000E+00
38)	6.045E-02	0.000E+00	0.000E+00	0.000E+00	0.000E+00	0.000E+00	0.000E+00	6.055E-38	0.000E+00	0.000E+00	0.000E+00
39)	4.470E-02	0.000E+00	2.691E-37	2.756E-34	2.457E-34	2.502E-33	0.000E+00	6.233E-32	0.000E+00	0.000E+00	0.000E+00
40)	3.339E-02	0.000E+00	1.618E-31	1.872E-28	1.102E-28	2.180E-27	3.133E-35	3.933E-26	0.000E+00	0.000E+00	8.722E-35
41)	2.462E-02	1.872E-35	6.899E-26	9.472E-23	6.993E-23	1.845E-21	7.160E-29	1.824E-20	0.000E+00	4.782E-33	7.145E-29
42)	1.817E-02	1.196E-25	1.908E-20	3.316E-17	5.159E-17	1.560E-15	2.025E-22	5.865E-15	0.000E+00	1.016E-26	5.711E-23
43)	1.354E-02	2.575E-22	3.121E-16	5.929E-13	2.792E-13	8.423E-12	7.130E-18	1.373E-10	0.000E+00	4.591E-23	1.059E-19
44)	9.984E-03	1.796E-20	2.294E-14	2.164E-11	1.288E-12	3.822E-11	9.076E-18	2.862E-10	0.000E+00	2.759E-20	1.339E-17
45)	7.342E-03	5.853E-18	2.124E-12	4.219E-10	1.014E-12	2.156E-11	1.676E-19	9.715E-11	0.000E+00	4.247E-16	3.971E-14
46)	5.404E-03	4.221E-17	4.689E-12	2.309E-10	2.924E-13	5.206E-12	4.702E-21	4.595E-12	0.000E+00	1.178E-15	2.753E-14
47)	3.981E-03	9.109E-17	5.334E-12	1.233E-10	9.985E-14	1.546E-12	1.171E-22	5.155E-14	0.000E+00	1.493E-15	1.652E-14
48)	2.893E-03	8.481E-17	3.765E-12	4.758E-11	2.399E-14	2.791E-13	1.344E-24	1.926E-16	0.000E+00	1.090E-15	6.655E-15
49)	2.104E-03	3.613E-17	1.473E-12	1.147E-11	3.772E-15	2.586E-14	1.132E-26	7.543E-19	0.000E+00	3.363E-16	1.280E-15
50)	1.530E-03	8.541E-18	3.237E-13	1.669E-12	4.070E-16	1.453E-15	1.096E-28	4.718E-21	0.000E+00	4.644E-17	1.187E-16
51)	1.112E-03	1.310E-18	4.456E-14	1.639E-13	3.215E-17	5.549E-17	8.684E-31	2.904E-23	0.000E+00	3.584E-18	6.673E-18
52)	8.113E-04	1.490E-19	4.758E-15	1.320E-14	2.177E-18	1.904E-18	6.481E-33	1.810E-25	0.000E+00	1.833E-19	2.610E-19
53)	5.894E-04	1.031E-20	2.349E-16	5.054E-16	7.153E-20	3.153E-20	3.339E-35	4.870E-28	0.000E+00	4.516E-21	5.074E-21
54)	4.275E-04	4.294E-22	6.071E-18	1.038E-17	1.288E-21	2.694E-22	1.126E-37	6.268E-31	0.000E+00	4.647E-23	4.203E-23
55)	3.097E-04	9.374E-24	6.844E-20	9.456E-20	1.053E-23	7.861E-25	0.000E+00	2.299E-34	0.000E+00	1.471E-25	1.090E-25
56)	2.238E-04	1.860E-25	7.597E-22	8.551E-22	8.753E-26	2.340E-27	0.000E+00	1.116E-37	0.000E+00	3.007E-28	1.844E-28
57)	1.623E-04	3.615E-27	8.573E-24	7.893E-24	7.539E-28	7.254E-30	0.000E+00	0.000E+00	0.000E+00	5.161E-31	2.653E-31
58)	1.173E-04	7.523E-29	1.105E-25	8.281E-26	7.400E-30	3.014E-32	0.000E+00	0.000E+00	0.000E+00	8.859E-34	3.838E-34

59)	8.516E-05	1.884E-30	2.077E-27	1.278E-27	1.056E-31	2.291E-34	0.000E+00	0.000E+00	0.000E+00	2.351E-36	8.600E-37
60)	6.154E-05	4.848E-32	4.311E-29	2.178E-29	1.643E-33	2.329E-36	0.000E+00	0.000E+00	0.000E+00	6.957E-39	0.000E+00
61)	4.467E-05	1.426E-33	1.079E-30	4.492E-31	3.093E-35	3.564E-38	0.000E+00	0.000E+00	0.000E+00	0.000E+00	0.000E+00
62)	3.233E-05	4.313E-35	2.794E-32	9.542E-33	6.044E-37	0.000E+00	0.000E+00	0.000E+00	0.000E+00	0.000E+00	0.000E+00
63)	2.333E-05	1.155E-36	6.290E-34	1.752E-34	1.034E-38	0.000E+00	0.000E+00	0.000E+00	0.000E+00	0.000E+00	0.000E+00
64)	1.688E-05	3.179E-38	1.404E-35	3.167E-36	0.000E+00	0.000E+00	0.000E+00	0.000E+00	0.000E+00	0.000E+00	0.000E+00
65)	1.220E-05	0.000E+00	3.039E-37	5.491E-38	0.000E+00	0.000E+00	0.000E+00	0.000E+00	0.000E+00	0.000E+00	0.000E+00
66)	8.802E-06	0.000E+00	6.543E-39	0.000E+00	0.000E+00	0.000E+00	0.000E+00	0.000E+00	0.000E+00	0.000E+00	0.000E+00
67)	6.347E-06	0.000E+00	0.000E+00	0.000E+00	0.000E+00	0.000E+00	0.000E+00	0.000E+00	0.000E+00	0.000E+00	0.000E+00
68)	4.574E-06	0.000E+00	0.000E+00	0.000E+00	0.000E+00	0.000E+00	0.000E+00	0.000E+00	0.000E+00	0.000E+00	0.000E+00
69)	3.292E-06	0.000E+00	0.000E+00	0.000E+00	0.000E+00	0.000E+00	0.000E+00	0.000E+00	0.000E+00	0.000E+00	0.000E+00
70)	2.371E-06	0.000E+00	0.000E+00	0.000E+00	0.000E+00	0.000E+00	0.000E+00	0.000E+00	0.000E+00	0.000E+00	0.000E+00
71)	1.709E-06	0.000E+00	0.000E+00	0.000E+00	0.000E+00	0.000E+00	0.000E+00	0.000E+00	0.000E+00	0.000E+00	0.000E+00
72)	1.231E-06	0.000E+00	0.000E+00	0.000E+00	0.000E+00	0.000E+00	0.000E+00	0.000E+00	0.000E+00	0.000E+00	0.000E+00
73)	8.866E-07	0.000E+00	0.000E+00	0.000E+00	0.000E+00	0.000E+00	0.000E+00	0.000E+00	0.000E+00	0.000E+00	0.000E+00
74)	6.367E-07	0.000E+00	0.000E+00	0.000E+00	0.000E+00	0.000E+00	0.000E+00	0.000E+00	0.000E+00	0.000E+00	0.000E+00
75)	4.581E-07	0.000E+00	0.000E+00	0.000E+00	0.000E+00	0.000E+00	0.000E+00	0.000E+00	0.000E+00	0.000E+00	0.000E+00
76)	3.299E-07	0.000E+00	0.000E+00	0.000E+00	0.000E+00	0.000E+00	0.000E+00	0.000E+00	0.000E+00	0.000E+00	0.000E+00
77)	2.370E-07	0.000E+00	0.000E+00	0.000E+00	0.000E+00	0.000E+00	0.000E+00	0.000E+00	0.000E+00	0.000E+00	0.000E+00
78)	1.705E-07	0.000E+00	0.000E+00	0.000E+00	0.000E+00	0.000E+00	0.000E+00	0.000E+00	0.000E+00	0.000E+00	0.000E+00
79)	1.228E-07	0.000E+00	0.000E+00	0.000E+00	0.000E+00	0.000E+00	0.000E+00	0.000E+00	0.000E+00	0.000E+00	0.000E+00
80)	9.997E-08	0.000E+00	0.000E+00	0.000E+00	0.000E+00	0.000E+00	0.000E+00	0.000E+00	0.000E+00	0.000E+00	0.000E+00

	PRESSURE	C-C3H2P	C3H3P	C-C3H3P	CH3C2HP	C3H5P	C4P	C4HP	C4H2P	C4H3P	C4H4P
1)	6.078E+03	0.000E+00	0.000E+00	0.000E+00	0.000E+00	0.000E+00	0.000E+00	0.000E+00	0.000E+00	0.000E+00	0.000E+00
2)	4.338E+03	0.000E+00	0.000E+00	0.000E+00	0.000E+00	0.000E+00	0.000E+00	0.000E+00	0.000E+00	0.000E+00	0.000E+00
3)	3.158E+03	0.000E+00	0.000E+00	0.000E+00	0.000E+00	0.000E+00	0.000E+00	0.000E+00	0.000E+00	0.000E+00	0.000E+00
4)	2.293E+03	0.000E+00	0.000E+00	0.000E+00	0.000E+00	0.000E+00	0.000E+00	0.000E+00	0.000E+00	0.000E+00	0.000E+00
5)	1.669E+03	0.000E+00	0.000E+00	0.000E+00	0.000E+00	0.000E+00	0.000E+00	0.000E+00	0.000E+00	0.000E+00	0.000E+00
6)	1.224E+03	0.000E+00	0.000E+00	0.000E+00	0.000E+00	0.000E+00	0.000E+00	0.000E+00	0.000E+00	0.000E+00	0.000E+00
7)	8.722E+02	0.000E+00	0.000E+00	0.000E+00	0.000E+00	0.000E+00	0.000E+00	0.000E+00	0.000E+00	0.000E+00	0.000E+00
8)	6.324E+02	0.000E+00	0.000E+00	0.000E+00	0.000E+00	0.000E+00	0.000E+00	0.000E+00	0.000E+00	0.000E+00	0.000E+00
9)	4.712E+02	0.000E+00	0.000E+00	0.000E+00	0.000E+00	0.000E+00	0.000E+00	0.000E+00	0.000E+00	0.000E+00	0.000E+00
10)	3.447E+02	0.000E+00	0.000E+00	0.000E+00	0.000E+00	0.000E+00	0.000E+00	0.000E+00	0.000E+00	0.000E+00	0.000E+00
11)	2.469E+02	0.000E+00	0.000E+00	0.000E+00	0.000E+00	0.000E+00	0.000E+00	0.000E+00	0.000E+00	0.000E+00	0.000E+00
12)	1.836E+02	0.000E+00	0.000E+00	0.000E+00	0.000E+00	0.000E+00	0.000E+00	0.000E+00	0.000E+00	0.000E+00	0.000E+00
13)	1.345E+02	0.000E+00	0.000E+00	0.000E+00	0.000E+00	0.000E+00	0.000E+00	0.000E+00	0.000E+00	0.000E+00	0.000E+00
14)	9.768E+01	0.000E+00	0.000E+00	0.000E+00	0.000E+00	0.000E+00	0.000E+00	0.000E+00	0.000E+00	0.000E+00	0.000E+00
15)	7.127E+01	0.000E+00	0.000E+00	0.000E+00	0.000E+00	0.000E+00	0.000E+00	0.000E+00	0.000E+00	0.000E+00	0.000E+00
16)	5.286E+01	0.000E+00	0.000E+00	0.000E+00	0.000E+00	0.000E+00	0.000E+00	0.000E+00	0.000E+00	0.000E+00	0.000E+00
17)	3.997E+01	0.000E+00	0.000E+00	0.000E+00	0.000E+00	0.000E+00	0.000E+00	0.000E+00	0.000E+00	0.000E+00	0.000E+00
18)	2.921E+01	0.000E+00	0.000E+00	0.000E+00	0.000E+00	0.000E+00	0.000E+00	0.000E+00	0.000E+00	0.000E+00	0.000E+00
19)	2.167E+01	0.000E+00	0.000E+00	0.000E+00	0.000E+00	0.000E+00	0.000E+00	0.000E+00	0.000E+00	0.000E+00	0.000E+00
20)	1.626E+01	0.000E+00	0.000E+00	0.000E+00	0.000E+00	0.000E+00	0.000E+00	0.000E+00	0.000E+00	0.000E+00	0.000E+00
21)	1.172E+01	0.000E+00	0.000E+00	0.000E+00	0.000E+00	0.000E+00	0.000E+00	0.000E+00	0.000E+00	0.000E+00	0.000E+00
22)	8.490E+00	0.000E+00	0.000E+00	0.000E+00	0.000E+00	0.000E+00	0.000E+00	0.000E+00	0.000E+00	0.000E+00	0.000E+00
23)	6.182E+00	0.000E+00	0.000E+00	0.000E+00	0.000E+00	0.000E+00	0.000E+00	0.000E+00	0.000E+00	0.000E+00	0.000E+00
24)	4.518E+00	0.000E+00	0.000E+00	0.000E+00	0.000E+00	0.000E+00	0.000E+00	0.000E+00	0.000E+00	0.000E+00	0.000E+00
25)	3.317E+00	0.000E+00	0.000E+00	0.000E+00	0.000E+00	0.000E+00	0.000E+00	0.000E+00	0.000E+00	0.000E+00	0.000E+00
26)	2.444E+00	0.000E+00	0.000E+00	0.000E+00	0.000E+00	0.000E+00	0.000E+00	0.000E+00	0.000E+00	0.000E+00	0.000E+00
27)	1.811E+00	0.000E+00	0.000E+00	0.000E+00	0.000E+00	0.000E+00	0.000E+00	0.000E+00	0.000E+00	0.000E+00	0.000E+00
28)	1.349E+00	0.000E+00	0.000E+00	0.000E+00	0.000E+00	0.000E+00	0.000E+00	0.000E+00	0.000E+00	0.000E+00	0.000E+00
29)	1.009E+00	0.000E+00	0.000E+00	0.000E+00	0.000E+00	0.000E+00	0.000E+00	0.000E+00	0.000E+00	0.000E+00	0.000E+00
30)	7.285E-01	0.000E+00	0.000E+00	0.000E+00	0.000E+00	0.000E+00	0.000E+00	0.000E+00	0.000E+00	0.000E+00	0.000E+00
31)	5.283E-01	0.000E+00	0.000E+00	6.059E-39	0.000E+00	0.000E+00	0.000E+00	0.000E+00	0.000E+00	0.000E+00	0.000E+00
32)	3.849E-01	0.000E+00	0.000E+00	6.462E-35	0.000E+00	0.000E+00	0.000E+00	0.000E+00	0.000E+00	0.000E+00	0.000E+00
33)	2.811E-01	0.000E+00	0.000E+00	2.985E-31	0.000E+00	0.000E+00	0.000E+00	0.000E+00	0.000E+00	0.000E+00	0.000E+00
34)	2.062E-01	0.000E+00	0.000E+00	5.523E-28	0.000E+00	0.000E+00	0.000E+00	0.000E+00	0.000E+00	0.000E+00	0.000E+00
35)	1.516E-01	0.000E+00	0.000E+00	3.733E-25	0.000E+00	0.000E+00	0.000E+00	0.000E+00	0.000E+00	0.000E+00	0.000E+00
36)	1.116E-01	0.000E+00	0.000E+00	7.844E-23	0.000E+00	0.000E+00	0.000E+00	0.000E+00	0.000E+00	0.000E+00	0.000E+00
37)	8.214E-02	0.000E+00	0.000E+00	4.438E-21	0.000E+00	0.000E+00	0.000E+00	0.000E+00	3.068E-37	0.000E+00	0.000E+00

38)	6.045E-02	0.000E+00	1.865E-36	1.170E-19	3.124E-39	1.235E-35	0.000E+00	5.542E-38	7.760E-35	0.000E+00	0.000E+00
39)	4.470E-02	3.085E-39	3.959E-31	2.662E-18	1.329E-33	4.892E-30	0.000E+00	9.460E-36	1.488E-32	2.230E-37	3.146E-36
40)	3.339E-02	1.736E-33	5.133E-26	6.432E-17	3.144E-28	1.176E-24	0.000E+00	2.330E-33	4.237E-30	7.741E-33	1.987E-31
41)	2.462E-02	7.098E-28	4.776E-21	2.035E-15	4.846E-23	1.986E-19	0.000E+00	1.536E-30	3.456E-27	4.936E-27	9.218E-27
42)	1.817E-02	1.911E-22	2.758E-16	7.800E-14	4.216E-18	1.988E-14	7.826E-36	1.372E-27	6.200E-24	2.283E-21	2.910E-22
43)	1.354E-02	1.195E-17	6.599E-13	5.937E-13	1.619E-14	8.216E-11	1.117E-28	5.021E-24	5.863E-20	4.207E-17	1.035E-18
44)	9.984E-03	4.898E-14	4.933E-12	6.005E-12	9.575E-14	2.553E-10	2.294E-22	2.215E-20	4.398E-16	2.558E-14	7.887E-16
45)	7.342E-03	5.578E-11	1.223E-11	9.645E-13	1.116E-13	6.410E-11	4.222E-17	4.047E-17	2.947E-12	1.002E-11	5.071E-13
46)	5.404E-03	2.020E-11	1.125E-11	2.712E-13	9.299E-15	1.451E-12	1.559E-17	1.718E-17	6.531E-13	5.696E-12	5.377E-13
47)	3.981E-03	5.762E-12	8.173E-12	1.384E-13	1.191E-15	9.618E-14	3.535E-18	5.215E-18	1.145E-13	1.985E-12	2.140E-13
48)	2.893E-03	1.201E-12	2.757E-12	5.081E-14	1.203E-16	5.958E-15	5.231E-19	9.725E-19	1.297E-14	3.658E-13	4.412E-14
49)	2.104E-03	1.531E-13	3.989E-13	9.262E-15	6.635E-18	2.169E-16	3.847E-20	7.692E-20	6.567E-16	2.648E-14	3.693E-15
50)	1.530E-03	1.004E-14	2.642E-14	7.084E-16	1.978E-19	4.337E-18	1.173E-21	2.364E-21	1.356E-17	7.278E-16	1.068E-16
51)	1.112E-03	4.288E-16	9.316E-16	2.922E-17	4.054E-21	5.462E-20	1.991E-23	3.619E-23	1.450E-19	9.444E-18	1.392E-18
52)	8.113E-04	1.456E-17	2.501E-17	8.175E-19	6.722E-23	5.868E-22	2.387E-25	3.862E-25	1.132E-21	8.747E-20	1.288E-20
53)	5.894E-04	1.980E-19	1.900E-19	8.626E-21	5.296E-25	2.231E-24	1.019E-27	1.311E-27	2.709E-24	2.076E-22	2.359E-23
54)	4.275E-04	1.050E-21	4.427E-22	3.295E-23	1.826E-27	3.462E-27	1.531E-30	1.610E-30	2.329E-27	1.756E-25	1.304E-26
55)	3.097E-04	1.480E-24	2.016E-25	3.244E-26	1.836E-30	1.452E-30	5.602E-34	5.182E-34	5.329E-31	6.628E-29	2.629E-30
56)	2.238E-04	1.486E-27	7.921E-29	2.225E-29	1.097E-33	6.287E-34	1.339E-37	1.187E-37	9.132E-35	2.864E-32	6.474E-34
57)	1.623E-04	1.324E-30	3.151E-32	1.348E-32	5.004E-37	2.948E-37	0.000E+00	0.000E+00	1.364E-38	1.300E-35	1.742E-37
58)	1.173E-04	1.275E-33	1.639E-35	8.677E-36	0.000E+00	0.000E+00	0.000E+00	0.000E+00	0.000E+00	5.361E-39	0.000E+00
59)	8.516E-05	2.324E-36	1.894E-38	1.058E-38	0.000E+00	0.000E+00	0.000E+00	0.000E+00	0.000E+00	0.000E+00	0.000E+00
60)	6.154E-05	5.085E-39	0.000E+00	0.000E+00	0.000E+00	0.000E+00	0.000E+00	0.000E+00	0.000E+00	0.000E+00	0.000E+00
61)	4.467E-05	0.000E+00	0.000E+00	0.000E+00	0.000E+00	0.000E+00	0.000E+00	0.000E+00	0.000E+00	0.000E+00	0.000E+00
62)	3.233E-05	0.000E+00	0.000E+00	0.000E+00	0.000E+00	0.000E+00	0.000E+00	0.000E+00	0.000E+00	0.000E+00	0.000E+00
63)	2.333E-05	0.000E+00	0.000E+00	0.000E+00	0.000E+00	0.000E+00	0.000E+00	0.000E+00	0.000E+00	0.000E+00	0.000E+00
64)	1.688E-05	0.000E+00	0.000E+00	0.000E+00	0.000E+00	0.000E+00	0.000E+00	0.000E+00	0.000E+00	0.000E+00	0.000E+00
65)	1.220E-05	0.000E+00	0.000E+00	0.000E+00	0.000E+00	0.000E+00	0.000E+00	0.000E+00	0.000E+00	0.000E+00	0.000E+00
66)	8.802E-06	0.000E+00	0.000E+00	0.000E+00	0.000E+00	0.000E+00	0.000E+00	0.000E+00	0.000E+00	0.000E+00	0.000E+00
67)	6.347E-06	0.000E+00	0.000E+00	0.000E+00	0.000E+00	0.000E+00	0.000E+00	0.000E+00	0.000E+00	0.000E+00	0.000E+00
68)	4.574E-06	0.000E+00	0.000E+00	0.000E+00	0.000E+00	0.000E+00	0.000E+00	0.000E+00	0.000E+00	0.000E+00	0.000E+00
69)	3.292E-06	0.000E+00	0.000E+00	0.000E+00	0.000E+00	0.000E+00	0.000E+00	0.000E+00	0.000E+00	0.000E+00	0.000E+00
70)	2.371E-06	0.000E+00	0.000E+00	0.000E+00	0.000E+00	0.000E+00	0.000E+00	0.000E+00	0.000E+00	0.000E+00	0.000E+00
71)	1.709E-06	0.000E+00	0.000E+00	0.000E+00	0.000E+00	0.000E+00	0.000E+00	0.000E+00	0.000E+00	0.000E+00	0.000E+00
72)	1.231E-06	0.000E+00	0.000E+00	0.000E+00	0.000E+00	0.000E+00	0.000E+00	0.000E+00	0.000E+00	0.000E+00	0.000E+00
73)	8.866E-07	0.000E+00	0.000E+00	0.000E+00	0.000E+00	0.000E+00	0.000E+00	0.000E+00	0.000E+00	0.000E+00	0.000E+00
74)	6.367E-07	0.000E+00	0.000E+00	0.000E+00	0.000E+00	0.000E+00	0.000E+00	0.000E+00	0.000E+00	0.000E+00	0.000E+00
75)	4.581E-07	0.000E+00	0.000E+00	0.000E+00	0.000E+00	0.000E+00	0.000E+00	0.000E+00	0.000E+00	0.000E+00	0.000E+00
76)	3.299E-07	0.000E+00	0.000E+00	0.000E+00	0.000E+00	0.000E+00	0.000E+00	0.000E+00	0.000E+00	0.000E+00	0.000E+00
77)	2.370E-07	0.000E+00	0.000E+00	0.000E+00	0.000E+00	0.000E+00	0.000E+00	0.000E+00	0.000E+00	0.000E+00	0.000E+00
78)	1.705E-07	0.000E+00	0.000E+00	0.000E+00	0.000E+00	0.000E+00	0.000E+00	0.000E+00	0.000E+00	0.000E+00	0.000E+00
79)	1.228E-07	0.000E+00	0.000E+00	0.000E+00	0.000E+00	0.000E+00	0.000E+00	0.000E+00	0.000E+00	0.000E+00	0.000E+00
80)	9.997E-08	0.000E+00	0.000E+00	0.000E+00	0.000E+00	0.000E+00	0.000E+00	0.000E+00	0.000E+00	0.000E+00	0.000E+00

	PRESSURE	C4H5P	C5P	C5HP	C5H2P	C5H3P	C5H4P	C5H5P	C6P	C6HP	C6H2P
1)	6.078E+03	0.000E+00	0.000E+00	0.000E+00	0.000E+00	1.201E-23	9.124E-24	0.000E+00	0.000E+00	0.000E+00	0.000E+00
2)	4.338E+03	0.000E+00	0.000E+00	0.000E+00	0.000E+00	1.506E-23	1.153E-23	0.000E+00	0.000E+00	0.000E+00	0.000E+00
3)	3.158E+03	0.000E+00	0.000E+00	0.000E+00	0.000E+00	1.841E-23	1.469E-23	0.000E+00	0.000E+00	0.000E+00	0.000E+00
4)	2.293E+03	0.000E+00	0.000E+00	0.000E+00	0.000E+00	2.242E-23	1.944E-23	0.000E+00	0.000E+00	0.000E+00	0.000E+00
5)	1.669E+03	0.000E+00	0.000E+00	0.000E+00	0.000E+00	2.707E-23	2.563E-23	0.000E+00	0.000E+00	0.000E+00	0.000E+00
6)	1.224E+03	0.000E+00	0.000E+00	0.000E+00	0.000E+00	3.259E-23	3.454E-23	0.000E+00	0.000E+00	0.000E+00	0.000E+00
7)	8.722E+02	0.000E+00	0.000E+00	0.000E+00	0.000E+00	3.957E-23	4.581E-23	0.000E+00	0.000E+00	0.000E+00	0.000E+00
8)	6.324E+02	0.000E+00	0.000E+00	0.000E+00	0.000E+00	4.815E-23	6.345E-23	0.000E+00	0.000E+00	0.000E+00	0.000E+00
9)	4.712E+02	0.000E+00	0.000E+00	0.000E+00	0.000E+00	5.705E-23	7.926E-23	0.000E+00	0.000E+00	0.000E+00	0.000E+00
10)	3.447E+02	0.000E+00	0.000E+00	0.000E+00	0.000E+00	6.967E-23	1.097E-22	0.000E+00	0.000E+00	0.000E+00	0.000E+00
11)	2.469E+02	0.000E+00	0.000E+00	0.000E+00	0.000E+00	8.414E-23	1.326E-22	0.000E+00	0.000E+00	0.000E+00	0.000E+00
12)	1.836E+02	0.000E+00	0.000E+00	0.000E+00	0.000E+00	1.004E-22	1.636E-22	0.000E+00	0.000E+00	0.000E+00	0.000E+00
13)	1.345E+02	0.000E+00	0.000E+00	0.000E+00	0.000E+00	1.208E-22	1.984E-22	0.000E+00	0.000E+00	0.000E+00	0.000E+00
14)	9.768E+01	0.000E+00	0.000E+00	0.000E+00	0.000E+00	1.327E-22	2.248E-22	0.000E+00	0.000E+00	0.000E+00	0.000E+00
15)	7.127E+01	0.000E+00	0.000E+00	0.000E+00	0.000E+00	1.422E-22	2.454E-22	0.000E+00	0.000E+00	0.000E+00	0.000E+00
16)	5.286E+01	0.000E+00	0.000E+00	0.000E+00	0.000E+00	1.535E-22	2.680E-22	0.000E+00	0.000E+00	0.000E+00	0.000E+00

17)	3.997E+01	0.000E+00	0.000E+00	0.000E+00	0.000E+00	1.675E-22	2.973E-22	0.000E+00	0.000E+00	0.000E+00	0.000E+00
18)	2.921E+01	0.000E+00	0.000E+00	0.000E+00	0.000E+00	1.881E-22	3.419E-22	0.000E+00	0.000E+00	0.000E+00	0.000E+00
19)	2.167E+01	0.000E+00	0.000E+00	0.000E+00	0.000E+00	2.132E-22	3.977E-22	0.000E+00	0.000E+00	0.000E+00	0.000E+00
20)	1.626E+01	0.000E+00	0.000E+00	0.000E+00	0.000E+00	2.433E-22	4.654E-22	0.000E+00	0.000E+00	0.000E+00	0.000E+00
21)	1.172E+01	0.000E+00	0.000E+00	0.000E+00	0.000E+00	2.852E-22	5.590E-22	0.000E+00	0.000E+00	0.000E+00	0.000E+00
22)	8.490E+00	0.000E+00	0.000E+00	0.000E+00	0.000E+00	3.353E-22	6.699E-22	0.000E+00	0.000E+00	0.000E+00	0.000E+00
23)	6.182E+00	0.000E+00	0.000E+00	0.000E+00	0.000E+00	3.954E-22	8.043E-22	0.000E+00	0.000E+00	0.000E+00	0.000E+00
24)	4.518E+00	0.000E+00	0.000E+00	0.000E+00	0.000E+00	4.668E-22	9.640E-22	0.000E+00	0.000E+00	0.000E+00	0.000E+00
25)	3.317E+00	0.000E+00	0.000E+00	0.000E+00	0.000E+00	5.514E-22	1.153E-21	0.000E+00	0.000E+00	0.000E+00	0.000E+00
26)	2.444E+00	0.000E+00	0.000E+00	0.000E+00	0.000E+00	6.514E-22	1.375E-21	0.000E+00	0.000E+00	0.000E+00	0.000E+00
27)	1.811E+00	0.000E+00	0.000E+00	0.000E+00	0.000E+00	7.692E-22	1.637E-21	0.000E+00	0.000E+00	0.000E+00	0.000E+00
28)	1.349E+00	0.000E+00	0.000E+00	0.000E+00	0.000E+00	9.072E-22	1.945E-21	0.000E+00	0.000E+00	0.000E+00	0.000E+00
29)	1.009E+00	0.000E+00	0.000E+00	0.000E+00	0.000E+00	1.068E-21	2.303E-21	0.000E+00	0.000E+00	0.000E+00	0.000E+00
30)	7.285E-01	0.000E+00	0.000E+00	0.000E+00	0.000E+00	1.283E-21	2.782E-21	0.000E+00	0.000E+00	0.000E+00	0.000E+00
31)	5.283E-01	0.000E+00	0.000E+00	0.000E+00	0.000E+00	1.536E-21	3.344E-21	0.000E+00	0.000E+00	0.000E+00	0.000E+00
32)	3.849E-01	0.000E+00	0.000E+00	0.000E+00	0.000E+00	1.829E-21	3.997E-21	0.000E+00	0.000E+00	0.000E+00	0.000E+00
33)	2.811E-01	0.000E+00	0.000E+00	0.000E+00	0.000E+00	2.167E-21	4.748E-21	0.000E+00	0.000E+00	0.000E+00	0.000E+00
34)	2.062E-01	0.000E+00	0.000E+00	0.000E+00	0.000E+00	2.553E-21	5.606E-21	0.000E+00	0.000E+00	0.000E+00	0.000E+00
35)	1.516E-01	7.679E-38	0.000E+00	0.000E+00	0.000E+00	2.989E-21	6.572E-21	5.641E-38	0.000E+00	0.000E+00	0.000E+00
36)	1.116E-01	1.776E-33	0.000E+00	0.000E+00	0.000E+00	3.473E-21	7.647E-21	1.215E-34	0.000E+00	6.431E-39	7.190E-39
37)	8.214E-02	1.954E-29	0.000E+00	0.000E+00	0.000E+00	4.004E-21	8.825E-21	7.638E-32	0.000E+00	8.025E-38	9.699E-38
38)	6.045E-02	9.945E-26	0.000E+00	0.000E+00	0.000E+00	4.578E-21	1.010E-20	2.035E-29	0.000E+00	8.003E-37	1.063E-36
39)	4.470E-02	2.294E-22	0.000E+00	0.000E+00	0.000E+00	5.195E-21	1.147E-20	7.207E-26	0.000E+00	6.816E-36	1.017E-35
40)	3.339E-02	2.386E-19	0.000E+00	7.879E-36	0.000E+00	5.873E-21	1.321E-20	1.321E-21	0.000E+00	7.851E-35	1.355E-34
41)	2.462E-02	1.340E-16	0.000E+00	3.474E-31	3.900E-36	7.927E-21	2.847E-20	1.835E-17	0.000E+00	2.207E-33	4.706E-33
42)	1.817E-02	4.001E-14	5.218E-38	1.025E-26	1.810E-31	9.806E-20	3.075E-19	1.569E-13	0.000E+00	6.342E-31	1.872E-30
43)	1.354E-02	6.498E-13	1.127E-31	1.940E-22	1.647E-25	2.870E-17	3.866E-17	4.782E-12	7.775E-33	4.238E-26	3.426E-25
44)	9.984E-03	4.272E-12	4.232E-25	1.922E-17	1.727E-19	4.441E-14	7.852E-15	2.189E-11	3.874E-25	3.282E-20	6.028E-19
45)	7.342E-03	7.757E-13	4.583E-19	5.516E-13	1.486E-13	1.081E-11	9.786E-13	1.569E-11	2.029E-18	1.452E-15	2.368E-13
46)	5.404E-03	2.908E-14	1.036E-19	1.242E-13	2.520E-13	4.781E-13	2.479E-14	4.967E-13	8.269E-19	1.484E-16	1.929E-14
47)	3.981E-03	5.227E-15	1.443E-20	1.807E-14	6.487E-14	3.227E-14	1.657E-15	2.184E-14	1.327E-19	1.884E-17	1.262E-15
48)	2.893E-03	8.545E-16	1.161E-21	1.476E-15	6.205E-15	1.698E-15	1.004E-16	6.431E-16	8.539E-21	1.140E-18	4.695E-17
49)	2.104E-03	5.848E-17	3.390E-23	4.515E-17	2.017E-16	4.252E-17	2.695E-18	7.285E-18	1.570E-22	2.047E-20	6.198E-19
50)	1.530E-03	1.430E-18	3.255E-25	4.154E-19	1.920E-18	3.445E-19	2.256E-20	2.578E-20	6.879E-25	8.781E-23	1.941E-21
51)	1.112E-03	1.534E-20	1.383E-27	1.591E-21	7.514E-21	1.204E-21	7.716E-23	3.893E-23	1.063E-27	1.327E-25	2.234E-24
52)	8.113E-04	1.082E-22	3.816E-30	4.080E-24	1.963E-23	2.817E-24	1.697E-25	4.422E-26	9.749E-31	1.191E-28	1.622E-27
53)	5.894E-04	1.414E-25	2.865E-33	1.904E-27	9.299E-27	9.330E-28	5.113E-29	7.491E-30	1.442E-34	1.653E-32	1.437E-31
54)	4.275E-04	3.946E-29	6.979E-37	2.479E-31	1.232E-30	5.651E-32	2.731E-33	2.895E-34	5.376E-39	5.460E-37	2.433E-36
55)	3.097E-04	1.326E-33	0.000E+00	1.084E-35	5.550E-35	3.902E-37	1.514E-38	0.000E+00	0.000E+00	0.000E+00	0.000E+00
56)	2.238E-04	3.060E-38	0.000E+00	0.000E+00	0.000E+00	0.000E+00	0.000E+00	0.000E+00	0.000E+00	0.000E+00	0.000E+00
57)	1.623E-04	0.000E+00	0.000E+00	0.000E+00	0.000E+00	0.000E+00	0.000E+00	0.000E+00	0.000E+00	0.000E+00	0.000E+00
58)	1.173E-04	0.000E+00	0.000E+00	0.000E+00	0.000E+00	0.000E+00	0.000E+00	0.000E+00	0.000E+00	0.000E+00	0.000E+00
59)	8.516E-05	0.000E+00	0.000E+00	0.000E+00	0.000E+00	0.000E+00	0.000E+00	0.000E+00	0.000E+00	0.000E+00	0.000E+00
60)	6.154E-05	0.000E+00	0.000E+00	0.000E+00	0.000E+00	0.000E+00	0.000E+00	0.000E+00	0.000E+00	0.000E+00	0.000E+00
61)	4.467E-05	0.000E+00	0.000E+00	0.000E+00	0.000E+00	0.000E+00	0.000E+00	0.000E+00	0.000E+00	0.000E+00	0.000E+00
62)	3.233E-05	0.000E+00	0.000E+00	0.000E+00	0.000E+00	0.000E+00	0.000E+00	0.000E+00	0.000E+00	0.000E+00	0.000E+00
63)	2.333E-05	0.000E+00	0.000E+00	0.000E+00	0.000E+00	0.000E+00	0.000E+00	0.000E+00	0.000E+00	0.000E+00	0.000E+00
64)	1.688E-05	0.000E+00	0.000E+00	0.000E+00	0.000E+00	0.000E+00	0.000E+00	0.000E+00	0.000E+00	0.000E+00	0.000E+00
65)	1.220E-05	0.000E+00	0.000E+00	0.000E+00	0.000E+00	0.000E+00	0.000E+00	0.000E+00	0.000E+00	0.000E+00	0.000E+00
66)	8.802E-06	0.000E+00	0.000E+00	0.000E+00	0.000E+00	0.000E+00	0.000E+00	0.000E+00	0.000E+00	0.000E+00	0.000E+00
67)	6.347E-06	0.000E+00	0.000E+00	0.000E+00	0.000E+00	0.000E+00	0.000E+00	0.000E+00	0.000E+00	0.000E+00	0.000E+00
68)	4.574E-06	0.000E+00	0.000E+00	0.000E+00	0.000E+00	0.000E+00	0.000E+00	0.000E+00	0.000E+00	0.000E+00	0.000E+00
69)	3.292E-06	0.000E+00	0.000E+00	0.000E+00	0.000E+00	0.000E+00	0.000E+00	0.000E+00	0.000E+00	0.000E+00	0.000E+00
70)	2.371E-06	0.000E+00	0.000E+00	0.000E+00	0.000E+00	0.000E+00	0.000E+00	0.000E+00	0.000E+00	0.000E+00	0.000E+00
71)	1.709E-06	0.000E+00	0.000E+00	0.000E+00	0.000E+00	0.000E+00	0.000E+00	0.000E+00	0.000E+00	0.000E+00	0.000E+00
72)	1.231E-06	0.000E+00	0.000E+00	0.000E+00	0.000E+00	0.000E+00	0.000E+00	0.000E+00	0.000E+00	0.000E+00	0.000E+00
73)	8.866E-07	0.000E+00	0.000E+00	0.000E+00	0.000E+00	0.000E+00	0.000E+00	0.000E+00	0.000E+00	0.000E+00	0.000E+00
74)	6.367E-07	0.000E+00	0.000E+00	0.000E+00	0.000E+00	0.000E+00	0.000E+00	0.000E+00	0.000E+00	0.000E+00	0.000E+00
75)	4.581E-07	0.000E+00	0.000E+00	0.000E+00	0.000E+00	0.000E+00	0.000E+00	0.000E+00	0.000E+00	0.000E+00	0.000E+00
76)	3.299E-07	0.000E+00	0.000E+00	0.000E+00	0.000E+00	0.000E+00	0.000E+00	0.000E+00	0.000E+00	0.000E+00	0.000E+00
77)	2.370E-07	0.000E+00	0.000E+00	0.000E+00	0.000E+00	0.000E+00	0.000E+00	0.000E+00	0.000E+00	0.000E+00	0.000E+00

78)	1.705E-07	0.000E+00	0.000E+00	0.000E+00	0.000E+00	0.000E+00	0.000E+00	0.000E+00	0.000E+00	0.000E+00	0.000E+00
79)	1.228E-07	0.000E+00	0.000E+00	0.000E+00	0.000E+00	0.000E+00	0.000E+00	0.000E+00	0.000E+00	0.000E+00	0.000E+00
80)	9.997E-08	0.000E+00	0.000E+00	0.000E+00	0.000E+00	0.000E+00	0.000E+00	0.000E+00	0.000E+00	0.000E+00	0.000E+00

	PRESSURE	C6H3P	C6H4P	C6H5P	C-C6H5P	C6H7P	C-C6H7P	PAH	CC	C3HN	C4HN
1)	6.078E+03	8.044E-29	0.000E+00	0.000E+00	0.000E+00	0.000E+00	1.346E-18	6.246E-11	5.686E-11	7.403E-09	4.377E-08
2)	4.338E+03	1.017E-28	0.000E+00	0.000E+00	0.000E+00	0.000E+00	1.694E-18	7.823E-11	7.123E-11	9.274E-09	5.482E-08
3)	3.158E+03	1.296E-28	0.000E+00	0.000E+00	0.000E+00	0.000E+00	2.108E-18	9.485E-11	8.637E-11	1.124E-08	6.647E-08
4)	2.293E+03	1.714E-28	0.000E+00	0.000E+00	0.000E+00	0.000E+00	2.665E-18	1.136E-10	1.034E-10	1.347E-08	7.960E-08
5)	1.669E+03	2.259E-28	0.000E+00	0.000E+00	0.000E+00	0.000E+00	3.353E-18	1.346E-10	1.226E-10	1.596E-08	9.432E-08
6)	1.224E+03	3.046E-28	0.000E+00	0.000E+00	0.000E+00	0.000E+00	4.264E-18	1.578E-10	1.438E-10	1.872E-08	1.106E-07
7)	8.722E+02	4.038E-28	0.000E+00	0.000E+00	0.000E+00	0.000E+00	5.415E-18	1.872E-10	1.707E-10	2.221E-08	1.313E-07
8)	6.324E+02	5.593E-28	0.000E+00	0.000E+00	0.000E+00	0.000E+00	7.044E-18	2.202E-10	2.009E-10	2.614E-08	1.545E-07
9)	4.712E+02	6.987E-28	0.000E+00	0.000E+00	0.000E+00	0.000E+00	8.600E-18	2.561E-10	2.338E-10	3.041E-08	1.797E-07
10)	3.447E+02	9.666E-28	0.000E+00	0.000E+00	0.000E+00	0.000E+00	1.123E-17	3.018E-10	2.757E-10	3.585E-08	2.118E-07
11)	2.469E+02	1.169E-27	0.000E+00	0.000E+00	0.000E+00	0.000E+00	1.364E-17	3.607E-10	3.299E-10	4.288E-08	2.534E-07
12)	1.836E+02	1.442E-27	0.000E+00	0.000E+00	0.000E+00	0.000E+00	1.662E-17	4.238E-10	3.881E-10	5.042E-08	2.978E-07
13)	1.345E+02	1.748E-27	0.000E+00	0.000E+00	0.000E+00	0.000E+00	2.014E-17	5.050E-10	4.632E-10	6.014E-08	3.552E-07
14)	9.768E+01	1.981E-27	0.000E+00	0.000E+00	0.000E+00	0.000E+00	2.252E-17	5.490E-10	5.040E-10	6.541E-08	3.863E-07
15)	7.127E+01	2.162E-27	0.000E+00	0.000E+00	0.000E+00	0.000E+00	2.439E-17	5.845E-10	5.370E-10	6.967E-08	4.114E-07
16)	5.286E+01	2.361E-27	0.000E+00	0.000E+00	0.000E+00	0.000E+00	2.652E-17	6.277E-10	5.771E-10	7.486E-08	4.419E-07
17)	3.997E+01	2.619E-27	0.000E+00	0.000E+00	0.000E+00	0.000E+00	2.922E-17	6.800E-10	6.259E-10	8.115E-08	4.790E-07
18)	2.921E+01	3.012E-27	0.000E+00	0.000E+00	0.000E+00	0.000E+00	3.327E-17	7.564E-10	6.972E-10	9.034E-08	5.332E-07
19)	2.167E+01	3.503E-27	0.000E+00	0.000E+00	0.000E+00	0.000E+00	3.828E-17	8.490E-10	7.838E-10	1.015E-07	5.989E-07
20)	1.626E+01	4.099E-27	0.000E+00	0.000E+00	0.000E+00	0.000E+00	4.431E-17	9.592E-10	8.873E-10	1.148E-07	6.773E-07
21)	1.172E+01	4.922E-27	0.000E+00	0.000E+00	0.000E+00	0.000E+00	5.267E-17	1.112E-09	1.032E-09	1.334E-07	7.864E-07
22)	8.490E+00	5.898E-27	0.000E+00	0.000E+00	0.000E+00	0.000E+00	6.263E-17	1.295E-09	1.205E-09	1.556E-07	9.173E-07
23)	6.182E+00	7.079E-27	0.000E+00	0.000E+00	0.000E+00	0.000E+00	7.462E-17	1.512E-09	1.413E-09	1.822E-07	1.073E-06
24)	4.518E+00	8.482E-27	0.000E+00	0.000E+00	0.000E+00	0.000E+00	8.885E-17	1.768E-09	1.661E-09	2.138E-07	1.259E-06
25)	3.317E+00	1.014E-26	0.000E+00	0.000E+00	0.000E+00	0.000E+00	1.057E-16	2.069E-09	1.957E-09	2.512E-07	1.478E-06
26)	2.444E+00	1.209E-26	0.000E+00	0.000E+00	0.000E+00	0.000E+00	1.255E-16	2.421E-09	2.307E-09	2.955E-07	1.737E-06
27)	1.811E+00	1.439E-26	0.000E+00	0.000E+00	0.000E+00	0.000E+00	1.489E-16	2.828E-09	2.721E-09	3.475E-07	2.040E-06
28)	1.349E+00	1.708E-26	0.000E+00	0.000E+00	0.000E+00	0.000E+00	1.762E-16	3.290E-09	3.209E-09	4.084E-07	2.395E-06
29)	1.009E+00	2.021E-26	0.000E+00	0.000E+00	0.000E+00	0.000E+00	2.079E-16	3.795E-09	3.783E-09	4.794E-07	2.807E-06
30)	7.285E-01	2.439E-26	0.000E+00	0.000E+00	0.000E+00	0.000E+00	2.503E-16	4.387E-09	4.555E-09	5.741E-07	3.355E-06
31)	5.283E-01	2.927E-26	0.000E+00	0.000E+00	0.000E+00	6.374E-38	2.999E-16	4.914E-09	5.472E-09	6.850E-07	3.993E-06
32)	3.849E-01	3.494E-26	0.000E+00	0.000E+00	0.000E+00	6.131E-34	3.573E-16	5.274E-09	6.552E-09	8.137E-07	4.730E-06
33)	2.811E-01	4.144E-26	0.000E+00	0.000E+00	0.000E+00	2.524E-30	4.230E-16	5.384E-09	7.815E-09	9.614E-07	5.571E-06
34)	2.062E-01	4.883E-26	0.000E+00	1.178E-37	0.000E+00	4.098E-27	4.977E-16	5.227E-09	9.284E-09	1.130E-06	6.520E-06
35)	1.516E-01	5.712E-26	0.000E+00	3.905E-35	0.000E+00	2.384E-24	5.813E-16	4.845E-09	1.098E-08	1.319E-06	7.576E-06
36)	1.116E-01	6.628E-26	1.591E-37	3.383E-33	0.000E+00	4.204E-22	6.735E-16	4.320E-09	1.292E-08	1.528E-06	8.733E-06
37)	8.214E-02	7.625E-26	2.948E-35	1.334E-31	0.000E+00	1.935E-20	7.736E-16	3.735E-09	1.511E-08	1.756E-06	9.976E-06
38)	6.045E-02	8.694E-26	2.629E-33	4.740E-30	0.000E+00	3.984E-19	8.806E-16	3.136E-09	1.757E-08	2.001E-06	1.129E-05
39)	4.470E-02	9.837E-26	2.378E-31	1.877E-28	0.000E+00	6.554E-18	9.944E-16	2.545E-09	2.034E-08	2.262E-06	1.266E-05
40)	3.339E-02	1.129E-25	4.077E-29	8.506E-27	3.352E-38	9.802E-17	1.128E-15	1.982E-09	2.343E-08	2.536E-06	1.408E-05
41)	2.462E-02	2.502E-25	2.584E-26	4.812E-25	3.428E-33	1.216E-15	1.956E-15	1.413E-09	2.734E-08	2.861E-06	1.571E-05
42)	1.817E-02	3.358E-24	5.111E-23	4.822E-23	6.561E-26	2.638E-15	4.368E-14	8.960E-10	3.217E-08	3.232E-06	1.753E-05
43)	1.354E-02	1.665E-22	4.576E-21	1.618E-19	2.415E-22	3.752E-14	2.801E-12	4.888E-10	3.788E-08	3.627E-06	1.939E-05
44)	9.984E-03	2.291E-18	3.490E-17	1.745E-18	2.135E-20	1.494E-13	4.029E-12	2.066E-10	4.203E-08	3.259E-06	1.847E-05
45)	7.342E-03	2.536E-14	7.580E-14	1.777E-17	6.790E-18	4.740E-13	4.685E-13	6.060E-11	3.674E-08	1.793E-06	9.021E-06
46)	5.404E-03	1.269E-15	5.583E-15	3.984E-18	7.790E-19	4.929E-14	2.110E-14	1.149E-11	2.505E-08	7.737E-07	3.147E-06
47)	3.981E-03	7.746E-17	1.914E-16	2.407E-19	8.561E-20	1.630E-15	1.324E-15	1.272E-12	1.539E-08	2.580E-07	7.959E-07
48)	2.893E-03	2.930E-18	3.194E-18	5.846E-21	4.665E-21	2.470E-17	4.667E-17	6.498E-14	8.283E-09	6.033E-08	1.284E-07
49)	2.104E-03	4.336E-20	1.874E-20	4.037E-23	7.020E-23	1.234E-19	5.283E-19	1.508E-15	3.976E-09	9.909E-09	1.340E-08
50)	1.530E-03	1.654E-22	2.953E-23	6.822E-26	2.558E-25	1.478E-22	1.431E-21	1.433E-17	1.702E-09	1.113E-09	8.696E-10
51)	1.112E-03	2.472E-25	1.974E-26	4.110E-29	2.937E-28	6.480E-26	1.270E-24	5.012E-20	6.504E-10	8.436E-11	3.395E-11
52)	8.113E-04	2.297E-28	1.015E-29	1.630E-32	2.042E-31	1.969E-29	7.135E-28	6.204E-23	2.249E-10	4.410E-12	8.042E-13
53)	5.894E-04	2.467E-32	6.384E-34	8.400E-37	1.657E-35	6.217E-34	5.013E-32	2.139E-26	6.901E-11	1.483E-13	1.046E-14
54)	4.275E-04	3.426E-37	6.087E-39	0.000E+00	0.000E+00	3.626E-39	1.450E-36	2.061E-30	1.909E-11	3.312E-15	7.707E-17
55)	3.097E-04	0.000E+00	0.000E+00	0.000E+00	0.000E+00	0.000E+00	0.000E+00	5.875E-35	4.823E-12	5.115E-17	3.379E-19
56)	2.238E-04	0.000E+00	0.000E+00	0.000E+00	0.000E+00	0.000E+00	0.000E+00	0.000E+00	1.117E-12	5.549E-19	8.989E-22

57)	1.623E-04	0.000E+00	0.000E+00	0.000E+00	0.000E+00	0.000E+00	0.000E+00	0.000E+00	2.466E-13	4.816E-21	1.724E-24
58)	1.173E-04	0.000E+00	0.000E+00	0.000E+00	0.000E+00	0.000E+00	0.000E+00	0.000E+00	5.029E-14	3.058E-23	2.124E-27
59)	8.516E-05	0.000E+00	0.000E+00	0.000E+00	0.000E+00	0.000E+00	0.000E+00	0.000E+00	9.958E-15	1.677E-25	2.098E-30
60)	6.154E-05	0.000E+00	0.000E+00	0.000E+00	0.000E+00	0.000E+00	0.000E+00	0.000E+00	1.818E-15	6.784E-28	1.350E-33
61)	4.467E-05	0.000E+00	0.000E+00	0.000E+00	0.000E+00	0.000E+00	0.000E+00	0.000E+00	3.215E-16	2.392E-30	7.098E-37
62)	3.233E-05	0.000E+00	0.000E+00	0.000E+00	0.000E+00	0.000E+00	0.000E+00	0.000E+00	5.288E-17	6.513E-33	0.000E+00
63)	2.333E-05	0.000E+00	0.000E+00	0.000E+00	0.000E+00	0.000E+00	0.000E+00	0.000E+00	8.051E-18	1.359E-35	0.000E+00
64)	1.688E-05	0.000E+00	0.000E+00	0.000E+00	0.000E+00	0.000E+00	0.000E+00	0.000E+00	1.162E-18	2.370E-38	0.000E+00
65)	1.220E-05	0.000E+00	0.000E+00	0.000E+00	0.000E+00	0.000E+00	0.000E+00	0.000E+00	1.553E-19	0.000E+00	0.000E+00
66)	8.802E-06	0.000E+00	0.000E+00	0.000E+00	0.000E+00	0.000E+00	0.000E+00	0.000E+00	1.895E-20	0.000E+00	0.000E+00
67)	6.347E-06	0.000E+00	0.000E+00	0.000E+00	0.000E+00	0.000E+00	0.000E+00	0.000E+00	2.097E-21	0.000E+00	0.000E+00
68)	4.574E-06	0.000E+00	0.000E+00	0.000E+00	0.000E+00	0.000E+00	0.000E+00	0.000E+00	2.082E-22	0.000E+00	0.000E+00
69)	3.292E-06	0.000E+00	0.000E+00	0.000E+00	0.000E+00	0.000E+00	0.000E+00	0.000E+00	1.824E-23	0.000E+00	0.000E+00
70)	2.371E-06	0.000E+00	0.000E+00	0.000E+00	0.000E+00	0.000E+00	0.000E+00	0.000E+00	1.419E-24	0.000E+00	0.000E+00
71)	1.709E-06	0.000E+00	0.000E+00	0.000E+00	0.000E+00	0.000E+00	0.000E+00	0.000E+00	9.701E-26	0.000E+00	0.000E+00
72)	1.231E-06	0.000E+00	0.000E+00	0.000E+00	0.000E+00	0.000E+00	0.000E+00	0.000E+00	5.784E-27	0.000E+00	0.000E+00
73)	8.866E-07	0.000E+00	0.000E+00	0.000E+00	0.000E+00	0.000E+00	0.000E+00	0.000E+00	2.994E-28	0.000E+00	0.000E+00
74)	6.367E-07	0.000E+00	0.000E+00	0.000E+00	0.000E+00	0.000E+00	0.000E+00	0.000E+00	1.334E-29	0.000E+00	0.000E+00
75)	4.581E-07	0.000E+00	0.000E+00	0.000E+00	0.000E+00	0.000E+00	0.000E+00	0.000E+00	5.395E-31	0.000E+00	0.000E+00
76)	3.299E-07	0.000E+00	0.000E+00	0.000E+00	0.000E+00	0.000E+00	0.000E+00	0.000E+00	2.005E-32	0.000E+00	0.000E+00
77)	2.370E-07	0.000E+00	0.000E+00	0.000E+00	0.000E+00	0.000E+00	0.000E+00	0.000E+00	6.718E-34	0.000E+00	0.000E+00
78)	1.705E-07	0.000E+00	0.000E+00	0.000E+00	0.000E+00	0.000E+00	0.000E+00	0.000E+00	2.149E-35	0.000E+00	0.000E+00
79)	1.228E-07	0.000E+00	0.000E+00	0.000E+00	0.000E+00	0.000E+00	0.000E+00	0.000E+00	6.684E-37	0.000E+00	0.000E+00
80)	9.997E-08	0.000E+00	0.000E+00	0.000E+00	0.000E+00	0.000E+00	0.000E+00	0.000E+00	7.431E-38	0.000E+00	0.000E+00

	PRESSURE	C5HN	C6HN	C7HN	C8HN	C9HN	CCP	C3HNP	C4HNP	C5HNP	C7HNP
1)	6.078E+03	4.923E-08	2.098E-09	2.546E-09	2.517E-10	1.078E-12	0.000E+00	5.306E-18	1.312E-17	2.882E-19	3.455E-17
2)	4.338E+03	6.167E-08	2.628E-09	3.189E-09	3.153E-10	1.351E-12	0.000E+00	6.669E-18	1.648E-17	3.622E-19	4.341E-17
3)	3.158E+03	7.477E-08	3.186E-09	3.867E-09	3.823E-10	1.638E-12	0.000E+00	8.231E-18	2.035E-17	4.471E-19	5.358E-17
4)	2.293E+03	8.954E-08	3.816E-09	4.630E-09	4.578E-10	1.961E-12	0.000E+00	1.022E-17	2.526E-17	5.552E-19	6.654E-17
5)	1.669E+03	1.061E-07	4.521E-09	5.486E-09	5.424E-10	2.323E-12	0.000E+00	1.261E-17	3.116E-17	6.846E-19	8.205E-17
6)	1.224E+03	1.244E-07	5.303E-09	6.434E-09	6.362E-10	2.725E-12	0.000E+00	1.558E-17	3.850E-17	8.459E-19	1.014E-16
7)	8.722E+02	1.477E-07	6.292E-09	7.634E-09	7.548E-10	3.233E-12	0.000E+00	1.933E-17	4.778E-17	1.050E-18	1.258E-16
8)	6.324E+02	1.737E-07	7.402E-09	8.980E-09	8.878E-10	3.802E-12	0.000E+00	2.420E-17	5.981E-17	1.314E-18	1.575E-16
9)	4.712E+02	2.021E-07	8.611E-09	1.045E-08	1.033E-09	4.423E-12	0.000E+00	2.912E-17	7.196E-17	1.581E-18	1.894E-16
10)	3.447E+02	2.382E-07	1.015E-08	1.231E-08	1.217E-09	5.211E-12	0.000E+00	3.649E-17	9.017E-17	1.981E-18	2.373E-16
11)	2.469E+02	2.848E-07	1.213E-08	1.472E-08	1.455E-09	6.229E-12	0.000E+00	4.445E-17	1.098E-16	2.412E-18	2.889E-16
12)	1.836E+02	3.348E-07	1.426E-08	1.729E-08	1.709E-09	7.318E-12	0.000E+00	5.359E-17	1.324E-16	2.908E-18	3.482E-16
13)	1.345E+02	3.992E-07	1.700E-08	2.061E-08	2.037E-09	8.719E-12	0.000E+00	6.492E-17	1.603E-16	3.521E-18	4.216E-16
14)	9.768E+01	4.341E-07	1.848E-08	2.241E-08	2.214E-09	9.479E-12	0.000E+00	7.175E-17	1.772E-16	3.892E-18	4.659E-16
15)	7.127E+01	4.623E-07	1.968E-08	2.386E-08	2.358E-09	1.009E-11	0.000E+00	7.720E-17	1.907E-16	4.187E-18	5.011E-16
16)	5.286E+01	4.966E-07	2.114E-08	2.563E-08	2.532E-09	1.084E-11	0.000E+00	8.363E-17	2.065E-16	4.534E-18	5.427E-16
17)	3.997E+01	5.382E-07	2.291E-08	2.777E-08	2.743E-09	1.174E-11	0.000E+00	9.160E-17	2.262E-16	4.966E-18	5.942E-16
18)	2.921E+01	5.989E-07	2.549E-08	3.090E-08	3.052E-09	1.306E-11	0.000E+00	1.034E-16	2.553E-16	5.604E-18	6.704E-16
19)	2.167E+01	6.726E-07	2.862E-08	3.469E-08	3.425E-09	1.466E-11	0.000E+00	1.179E-16	2.910E-16	6.387E-18	7.640E-16
20)	1.626E+01	7.605E-07	3.235E-08	3.920E-08	3.871E-09	1.656E-11	0.000E+00	1.353E-16	3.339E-16	7.328E-18	8.762E-16
21)	1.172E+01	8.827E-07	3.754E-08	4.547E-08	4.489E-09	1.920E-11	0.000E+00	1.595E-16	3.935E-16	8.634E-18	1.032E-15
22)	8.490E+00	1.029E-06	4.376E-08	5.299E-08	5.229E-09	2.236E-11	0.000E+00	1.885E-16	4.649E-16	1.020E-17	1.218E-15
23)	6.182E+00	1.204E-06	5.116E-08	6.192E-08	6.109E-09	2.611E-11	0.000E+00	2.233E-16	5.505E-16	1.207E-17	1.441E-15
24)	4.518E+00	1.411E-06	5.993E-08	7.251E-08	7.149E-09	3.055E-11	0.000E+00	2.648E-16	6.525E-16	1.430E-17	1.706E-15
25)	3.317E+00	1.655E-06	7.028E-08	8.498E-08	8.376E-09	3.577E-11	0.000E+00	3.140E-16	7.734E-16	1.694E-17	2.020E-15
26)	2.444E+00	1.944E-06	8.245E-08	9.963E-08	9.814E-09	4.189E-11	0.000E+00	3.723E-16	9.164E-16	2.006E-17	2.389E-15
27)	1.811E+00	2.281E-06	9.669E-08	1.168E-07	1.149E-08	4.902E-11	0.000E+00	4.412E-16	1.085E-15	2.374E-17	2.824E-15
28)	1.349E+00	2.675E-06	1.133E-07	1.366E-07	1.344E-08	5.728E-11	0.000E+00	5.222E-16	1.283E-15	2.805E-17	3.332E-15
29)	1.009E+00	3.131E-06	1.324E-07	1.596E-07	1.568E-08	6.676E-11	0.000E+00	6.170E-16	1.515E-15	3.308E-17	3.923E-15
30)	7.285E-01	3.736E-06	1.578E-07	1.899E-07	1.863E-08	7.923E-11	0.000E+00	7.446E-16	1.825E-15	3.981E-17	4.711E-15
31)	5.283E-01	4.438E-06	1.871E-07	2.247E-07	2.202E-08	9.351E-11	0.000E+00	8.951E-16	2.190E-15	4.770E-17	5.631E-15
32)	3.849E-01	5.244E-06	2.206E-07	2.645E-07	2.586E-08	1.097E-10	0.000E+00	1.072E-15	2.617E-15	5.690E-17	6.696E-15
33)	2.811E-01	6.158E-06	2.584E-07	3.091E-07	3.016E-08	1.276E-10	0.000E+00	1.277E-15	3.111E-15	6.749E-17	7.913E-15
34)	2.062E-01	7.184E-06	3.005E-07	3.585E-07	3.490E-08	1.473E-10	0.000E+00	1.514E-15	3.678E-15	7.960E-17	9.294E-15
35)	1.516E-01	8.315E-06	3.467E-07	4.123E-07	4.002E-08	1.685E-10	0.000E+00	1.786E-15	4.322E-15	9.327E-17	1.084E-14

36)	1.116E-01	9.541E-06	3.962E-07	4.696E-07	4.544E-08	1.907E-10	0.000E+00	2.093E-15	5.046E-15	1.085E-16	1.254E-14
37)	8.214E-02	1.084E-05	4.483E-07	5.292E-07	5.102E-08	2.135E-10	0.000E+00	2.436E-15	5.847E-15	1.252E-16	1.437E-14
38)	6.045E-02	1.220E-05	5.019E-07	5.898E-07	5.663E-08	2.361E-10	0.000E+00	2.817E-15	6.725E-15	1.434E-16	1.633E-14
39)	4.470E-02	1.360E-05	5.562E-07	6.504E-07	6.217E-08	2.581E-10	0.000E+00	3.238E-15	7.683E-15	1.630E-16	1.839E-14
40)	3.339E-02	1.501E-05	6.101E-07	7.095E-07	6.750E-08	2.790E-10	0.000E+00	3.729E-15	8.785E-15	1.853E-16	2.056E-14
41)	2.462E-02	1.661E-05	6.701E-07	7.744E-07	7.325E-08	3.013E-10	0.000E+00	5.969E-15	1.395E-14	2.922E-16	2.904E-14
42)	1.817E-02	1.834E-05	7.336E-07	8.418E-07	7.913E-08	3.237E-10	0.000E+00	1.585E-13	3.682E-13	7.587E-15	5.280E-13
43)	1.354E-02	2.006E-05	7.954E-07	9.049E-07	8.459E-08	3.441E-10	0.000E+00	3.035E-12	1.128E-11	1.463E-12	5.496E-14
44)	9.984E-03	2.088E-05	8.430E-07	9.477E-07	7.825E-08	3.604E-10	0.000E+00	2.330E-12	2.116E-11	8.912E-12	2.999E-13
45)	7.342E-03	1.450E-05	8.163E-07	8.604E-07	4.119E-08	3.664E-10	0.000E+00	6.814E-14	9.680E-13	1.320E-13	9.439E-13
46)	5.404E-03	4.657E-06	2.654E-07	2.013E-07	8.450E-09	6.904E-11	0.000E+00	8.039E-15	8.994E-15	1.539E-16	8.893E-15
47)	3.981E-03	9.862E-07	4.709E-08	2.863E-08	1.017E-09	7.129E-12	0.000E+00	2.969E-16	6.746E-17	1.185E-18	2.523E-16
48)	2.893E-03	1.205E-07	4.382E-09	2.062E-09	5.808E-11	3.277E-13	0.000E+00	2.853E-18	2.157E-19	6.940E-21	5.354E-18
49)	2.104E-03	8.621E-09	2.205E-10	7.500E-11	1.560E-12	6.612E-15	0.000E+00	1.445E-20	5.411E-22	1.512E-23	3.575E-20
50)	1.530E-03	3.453E-10	5.657E-12	1.271E-12	1.791E-14	5.248E-17	0.000E+00	5.027E-23	1.299E-24	1.102E-26	4.904E-23
51)	1.112E-03	7.387E-12	6.933E-14	9.245E-15	7.954E-17	1.459E-19	0.000E+00	1.249E-25	2.661E-27	3.449E-30	2.013E-26
52)	8.113E-04	8.453E-14	4.022E-16	2.826E-17	1.324E-19	1.359E-22	0.000E+00	3.306E-28	5.377E-30	8.837E-34	4.772E-30
53)	5.894E-04	4.540E-16	9.395E-19	2.996E-20	6.599E-23	3.285E-26	0.000E+00	2.913E-31	2.589E-33	3.011E-38	8.555E-35
54)	4.275E-04	1.179E-18	9.059E-22	1.121E-23	9.939E-27	2.058E-30	0.000E+00	9.773E-35	3.815E-37	0.000E+00	0.000E+00
55)	3.097E-04	1.562E-21	3.816E-25	1.567E-27	4.788E-31	3.530E-35	0.000E+00	6.215E-39	0.000E+00	0.000E+00	0.000E+00
56)	2.238E-04	1.080E-24	7.193E-29	8.392E-32	7.555E-36	0.000E+00	0.000E+00	0.000E+00	0.000E+00	0.000E+00	0.000E+00
57)	1.623E-04	4.818E-28	7.802E-33	2.297E-36	0.000E+00	0.000E+00	0.000E+00	0.000E+00	0.000E+00	0.000E+00	0.000E+00
58)	1.173E-04	1.206E-31	4.125E-37	0.000E+00	0.000E+00	0.000E+00	0.000E+00	0.000E+00	0.000E+00	0.000E+00	0.000E+00
59)	8.516E-05	2.231E-35	0.000E+00	0.000E+00	0.000E+00	0.000E+00	0.000E+00	0.000E+00	0.000E+00	0.000E+00	0.000E+00
60)	6.154E-05	0.000E+00	0.000E+00	0.000E+00	0.000E+00	0.000E+00	0.000E+00	0.000E+00	0.000E+00	0.000E+00	0.000E+00
61)	4.467E-05	0.000E+00	0.000E+00	0.000E+00	0.000E+00	0.000E+00	0.000E+00	0.000E+00	0.000E+00	0.000E+00	0.000E+00
62)	3.233E-05	0.000E+00	0.000E+00	0.000E+00	0.000E+00	0.000E+00	0.000E+00	0.000E+00	0.000E+00	0.000E+00	0.000E+00
63)	2.333E-05	0.000E+00	0.000E+00	0.000E+00	0.000E+00	0.000E+00	0.000E+00	0.000E+00	0.000E+00	0.000E+00	0.000E+00
64)	1.688E-05	0.000E+00	0.000E+00	0.000E+00	0.000E+00	0.000E+00	0.000E+00	0.000E+00	0.000E+00	0.000E+00	0.000E+00
65)	1.220E-05	0.000E+00	0.000E+00	0.000E+00	0.000E+00	0.000E+00	0.000E+00	0.000E+00	0.000E+00	0.000E+00	0.000E+00
66)	8.802E-06	0.000E+00	0.000E+00	0.000E+00	0.000E+00	0.000E+00	0.000E+00	0.000E+00	0.000E+00	0.000E+00	0.000E+00
67)	6.347E-06	0.000E+00	0.000E+00	0.000E+00	0.000E+00	0.000E+00	0.000E+00	0.000E+00	0.000E+00	0.000E+00	0.000E+00
68)	4.574E-06	0.000E+00	0.000E+00	0.000E+00	0.000E+00	0.000E+00	0.000E+00	0.000E+00	0.000E+00	0.000E+00	0.000E+00
69)	3.292E-06	0.000E+00	0.000E+00	0.000E+00	0.000E+00	0.000E+00	0.000E+00	0.000E+00	0.000E+00	0.000E+00	0.000E+00
70)	2.371E-06	0.000E+00	0.000E+00	0.000E+00	0.000E+00	0.000E+00	0.000E+00	0.000E+00	0.000E+00	0.000E+00	0.000E+00
71)	1.709E-06	0.000E+00	0.000E+00	0.000E+00	0.000E+00	0.000E+00	0.000E+00	0.000E+00	0.000E+00	0.000E+00	0.000E+00
72)	1.231E-06	0.000E+00	0.000E+00	0.000E+00	0.000E+00	0.000E+00	0.000E+00	0.000E+00	0.000E+00	0.000E+00	0.000E+00
73)	8.866E-07	0.000E+00	0.000E+00	0.000E+00	0.000E+00	0.000E+00	0.000E+00	0.000E+00	0.000E+00	0.000E+00	0.000E+00
74)	6.367E-07	0.000E+00	0.000E+00	0.000E+00	0.000E+00	0.000E+00	0.000E+00	0.000E+00	0.000E+00	0.000E+00	0.000E+00
75)	4.581E-07	0.000E+00	0.000E+00	0.000E+00	0.000E+00	0.000E+00	0.000E+00	0.000E+00	0.000E+00	0.000E+00	0.000E+00
76)	3.299E-07	0.000E+00	0.000E+00	0.000E+00	0.000E+00	0.000E+00	0.000E+00	0.000E+00	0.000E+00	0.000E+00	0.000E+00
77)	2.370E-07	0.000E+00	0.000E+00	0.000E+00	0.000E+00	0.000E+00	0.000E+00	0.000E+00	0.000E+00	0.000E+00	0.000E+00
78)	1.705E-07	0.000E+00	0.000E+00	0.000E+00	0.000E+00	0.000E+00	0.000E+00	0.000E+00	0.000E+00	0.000E+00	0.000E+00
79)	1.228E-07	0.000E+00	0.000E+00	0.000E+00	0.000E+00	0.000E+00	0.000E+00	0.000E+00	0.000E+00	0.000E+00	0.000E+00
80)	9.997E-08	0.000E+00	0.000E+00	0.000E+00	0.000E+00	0.000E+00	0.000E+00	0.000E+00	0.000E+00	0.000E+00	0.000E+00

	PRESSURE	C8HNP	C9HNP
1)	6.078E+03	8.935E-20	1.606E-34
2)	4.338E+03	1.123E-19	2.019E-34
3)	3.158E+03	1.386E-19	2.492E-34
4)	2.293E+03	1.721E-19	3.094E-34
5)	1.669E+03	2.122E-19	3.815E-34
6)	1.224E+03	2.622E-19	4.713E-34
7)	8.722E+02	3.254E-19	5.850E-34
8)	6.324E+02	4.072E-19	7.321E-34
9)	4.712E+02	4.898E-19	8.805E-34
10)	3.447E+02	6.136E-19	1.103E-33
11)	2.469E+02	7.471E-19	1.343E-33
12)	1.836E+02	9.004E-19	1.618E-33
13)	1.345E+02	1.090E-18	1.959E-33
14)	9.768E+01	1.204E-18	2.164E-33

15)	7.127E+01	1.295E-18	2.328E-33
16)	5.286E+01	1.403E-18	2.520E-33
17)	3.997E+01	1.536E-18	2.759E-33
18)	2.921E+01	1.733E-18	3.113E-33
19)	2.167E+01	1.974E-18	3.546E-33
20)	1.626E+01	2.264E-18	4.066E-33
21)	1.172E+01	2.666E-18	4.788E-33
22)	8.490E+00	3.146E-18	5.649E-33
23)	6.182E+00	3.721E-18	6.680E-33
24)	4.518E+00	4.404E-18	7.904E-33
25)	3.317E+00	5.212E-18	9.350E-33
26)	2.444E+00	6.163E-18	1.105E-32
27)	1.811E+00	7.280E-18	1.305E-32
28)	1.349E+00	8.585E-18	1.538E-32
29)	1.009E+00	1.010E-17	1.808E-32
30)	7.285E-01	1.212E-17	2.167E-32
31)	5.283E-01	1.447E-17	2.585E-32
32)	3.849E-01	1.718E-17	3.065E-32
33)	2.811E-01	2.027E-17	3.612E-32
34)	2.062E-01	2.376E-17	4.227E-32
35)	1.516E-01	2.765E-17	4.908E-32
36)	1.116E-01	3.190E-17	5.650E-32
37)	8.214E-02	3.648E-17	6.443E-32
38)	6.045E-02	4.131E-17	7.275E-32
39)	4.470E-02	4.638E-17	8.140E-32
40)	3.339E-02	5.199E-17	9.091E-32
41)	2.462E-02	8.059E-17	1.403E-31
42)	1.817E-02	1.799E-15	3.567E-30
43)	1.354E-02	4.949E-14	5.890E-27
44)	9.984E-03	9.373E-14	1.411E-21
45)	7.342E-03	3.114E-14	4.933E-16
46)	5.404E-03	2.625E-16	5.379E-18
47)	3.981E-03	5.809E-18	7.277E-20
48)	2.893E-03	7.664E-20	4.768E-22
49)	2.104E-03	2.582E-22	7.127E-25
50)	1.530E-03	1.332E-25	1.270E-28
51)	1.112E-03	1.737E-29	5.011E-33
52)	8.113E-04	1.197E-33	9.754E-38
53)	5.894E-04	4.497E-39	0.000E+00
54)	4.275E-04	0.000E+00	0.000E+00
55)	3.097E-04	0.000E+00	0.000E+00
56)	2.238E-04	0.000E+00	0.000E+00
57)	1.623E-04	0.000E+00	0.000E+00
58)	1.173E-04	0.000E+00	0.000E+00
59)	8.516E-05	0.000E+00	0.000E+00
60)	6.154E-05	0.000E+00	0.000E+00
61)	4.467E-05	0.000E+00	0.000E+00
62)	3.233E-05	0.000E+00	0.000E+00
63)	2.333E-05	0.000E+00	0.000E+00
64)	1.688E-05	0.000E+00	0.000E+00
65)	1.220E-05	0.000E+00	0.000E+00
66)	8.802E-06	0.000E+00	0.000E+00
67)	6.347E-06	0.000E+00	0.000E+00
68)	4.574E-06	0.000E+00	0.000E+00
69)	3.292E-06	0.000E+00	0.000E+00
70)	2.371E-06	0.000E+00	0.000E+00
71)	1.709E-06	0.000E+00	0.000E+00
72)	1.231E-06	0.000E+00	0.000E+00
73)	8.866E-07	0.000E+00	0.000E+00
74)	6.367E-07	0.000E+00	0.000E+00
75)	4.581E-07	0.000E+00	0.000E+00

```
76)  3.299E-07   0.000E+00  0.000E+00
77)  2.370E-07   0.000E+00  0.000E+00
78)  1.705E-07   0.000E+00  0.000E+00
79)  1.228E-07   0.000E+00  0.000E+00
80)  9.997E-08   0.000E+00  0.000E+00
```

Bibliography

Ajello, J. M., D. Shemansky, W. Pryor, K. Tobiska, C. Hord, S. Stephens, I. Stewart, J. Clarke, K. Simmons, W. McClintock, C. Barth, J. Gebben, D. Miller, and B. Sandel 1998. Galileo orbiter ultraviolet observations of Jupiter aurora. *J. Geophys. Res.* **103**, 20125–20148.

Ajello, J. M., D. E. Shemansky, W. R. Pryor, A. I. Stewart, K. E. Simmons, T. Majeed, J. H. Waite, and G. R. Glandstone 2000. Spectroscopic evidence for high altitude aurora at Jupiter from Galileo extreme ultraviolet spectrometer and Hopkins ultraviolet telescope observations. *Icarus* **152**, 151–171.

Allen, M., J. P. Pinto, and Y. L. Yung 1980. Titan: Aerosol photochemistry and variations related to the sunspot cycle. *Astrophys. J.* **242**, L125–L128.

Allen, M., and Y. L. Yung 1985. A simple photochemical model for forming benzene in the Jovian atmosphere. *Bull. Am. Astron. Soc.* **17**, 710.

Anicich, V. G., and M. J. McEwan 1997. Ion-molecule chemistry in Titan's ionosphere. *Planet. Space Sci.* **45**, 897–921.

Anicich, V. G., D. B. Milligan, D. A. Fairley, and M. J. McEwan 2000. Termolecular ion-molecule reactions in Titan's atmosphere. I. Principal ions with principal neutrals. *Icarus* **146**, 118–124.

Ashfold, M. N. R., M. A. Fullstone, G. Hancock, and G. W. Ketley 1981. Singlet methylene kinetics: Direct measurements of removal rates of $\tilde{a}^1A_1$ and $\tilde{b}^1B_1$ CH_2 and CD_2. *Chem. Phys.* **55**, 245–257.

Atreya, S. K., T. M. Donahue, and W. R. Kuhn 1978. Evolution of a nitrogen atmosphere on Titan. *Science* **201**, 611.

Atreya, S. K. 1986. *Atmospheres and Ionospheres of the Outer Planets and Their Satellites.* Springer-Verlag, Berlin.

Bézard, B., P. Drossart, Th. Encrenaz, and H. Feuchtgruber 2001. Benzene on the giant planets. *Icarus*, in press.

Chamberlain, J. W., and D. M. Hunten 1987. *Theory of Planetary Atmospheres*, Academic Press, pp. 34–36.

Chen, I. C., W. H. Green, and C. B. Moore 1988. Bond breaking without barriers — photofragmentation of ketene at the singlet threshold. *J. Chem. Phys.* **89**, 314.

Clarke, J. T., L. B. Jaffel, A. Vidal-Madjar, G. R. Gladstone, J. H. Waite Jr., R. Prangé, J.-C. Gérard, J. Ajello, and G. James 1994. Hubble Space Telescope Goddard high-resolution spectrograph H_2 rotational spectra of Jupiter's aurora. *Astrophys. J.* **430**, L73–L76.

Colket, M. B. 1986. in *Twenty-first Symposium (International) on Combustion*, The Combustion Institute, Pittsburgh, p. 851.

Coustenis, A., B. Bézard, and D. Gautier 1989. Titan's atmosphere from Voyager infrared observations. II. The CH^3D abundance and D/H ratio from the 900–1200 cm^{-1} spectral region. *Icarus* **82**, 67.

Coustenis, A., A. Salama, E. Lellouch, Th. Encrenaz, G. L. Bjoraker, R. E. Samuelson, Th. de Graauw, H. Feuchtgruber, and M. F. Kessler 1998. Evidence for water vapor in Titan's atmosphere from ISO/SWS data. *Astron. Astrophys.* **336**, L85–L89.

Coustenis, A., and F. Taylor 1999. *Titan: the Earth-like Moon*, World Scientific, pp. 96–97.

Cui, Q., and K. Morokuma 1997. Ab initio study of nonadiabatic interactions in the photodissociation of ketene. *J. Chem. Phys.* **107**, 4951.

D'Anna, A., A. D'Alessio, and J. Kent 2001. A computational study of hydrocarbon growth and the formation of aromatics in coflowing laminar diffusion flames of ethylene. *Combust. Flame* **125**, 1196–1206.

Darwin, D. C., and C. B. Moore 1995. Reaction-rate constants (295 K) for $^3CH_2$ with H_2S, SO_2, and NO_2: Upper-bounds for rate constants with less reactive partners. *J. Phys. Chem.* **99**, 13467–13470.

De Bergh, C., B. L. Lutz, T. Owen, and J. Chauville 1988. Monodeuterated methane in the outer solar system. III. Its abundance on Titan. *Astrophys. J.* **329**, 951.

Deters, R., M. Otting, H. Gg. Wagner, F. Temps, B. László, S. Dóbé, and T. Bérces 1998. A direct investigation of the reaction CH_3 + OH: Overall rate constant and CH_2 formation at T=298 K. *Ber. Bunsenges. Phys. Chem.* **102**, 58–72.

Dubouloz, N., F. Raulin, E. Lellouch, and D. Gautier 1989. Titan's hypothesized ocean properties: the influence of surface temperature and atmospheric composition uncertainties. *Icarus* **82**, 81.

Encrenaz, Th., E. Lellouch, H. Feuchtgruber, B. Altieri, B. Beézard, M. G. Davis, Th. de Graauw, P. Drossart, M. J. Griffin, M. F. Kessler, and P. G. Oldham 1997. The giant planets as seen by ISO. in *Proc. First* ISO *Workshop on Analytical Spectroscopy*, ed. M. Kessler (ESA-SP 419; Noordwijk: ESA), 125–130.

Fenimore, C. P. 1968. Destruction of methane in water gas by reaction of CH_3 with OH radicals. in *The Twelfth Symposium (International) on Combustion*, The Combustion Institute, Pittsburgh, p. 463.

Geiss, J., and J. Gloeckler 1998. Abundances of deuterium and helium 3 in the protosolar cloud from solar wind measurements. *Space Sci. Rev.* **84**, 239.

Gladstone, G. R., M. Allen, and Y. L. Yung 1996. Hydrocarbon photochemistry in the upper atmosphere of Jupiter. *Icarus* **119**, 1–52.

Grodent, D., J. H. Waite Jr., and J.-C. Gérard 2000. A self-consistent model of the Jovian auroral thermal structure. *J. Geophys. Res.* **106**, 12933–12952.

Gurwell, M. A., and D. O. Muhleman 1995. CO on Titan: Evidence for a well-mixed vertical profile. *Icarus* **117**, 375–382.

Gurwell, M. A., and D. O. Muhleman 2000. CO on Titan: More evidence for a well-mixed vertical profile. *Icarus* **145**, 653–656.

Harris, W., J. T. Clarkes, M. A. McGrath, and G. E. Ballester 1996. Analysis of Jovian auroral H Ly-α emission (1981–1991). *Icarus* **124**, 350–365.

Hidayat, T., A. Marten, B. Bézard, D. Gautier, T. Owen, H. E. Matthews, and G. Paubert 1997. Millimeter and submillimeter heterodyne observations of Titan: Retrieval of the vertical profile of HCN and the $^{12}C/^{13}C$ ratio. *Icarus* **126**, 170–182.

Hidayat, T., and A. Marten 1998. Evidence for a strong $^{15}N/^{14}N$ enrichment in Titan's atmosphere from millimeter observations. *Annales Geophysicae* **16**, (Suppl. III) C998 (Abstract).

Humpfer, R., H. Oser, and H. H. Grotheer 1995. Formation of HCOH + H_2 through the reaction CH_3 + OH; experimental evidence for a hitherto undetected product channel. *Int. J. Chem. Kinet.* **27**, 577–595.

Kass, D. M., and Y. L. Yung 1995. Loss of atmosphere from Mars due to solar wind-induced sputtering. *Science* **268**, 697.

Keifer, J. H., L. J. Mizerka, M. R. Patel, and H.-C. Wei 1985. A shock tube investigation of major pathways in the high-temperature pyrolysis on benzene. *J. Phys. Chem.* **10**, 2013–2019.

Keller, C. N., V. G. Anicich, and T. E. Cravens 1998. Model of Titan's ionosphere with detailed hydrocarbon ion chemistry. *Planet. Space Sci.* **46**, 1157–1174.

Kim, S. J. et al. 1985. Infrared polar brightening on Jupiter. *Icarus* **64**, 233.

Kim, Y. H., and J. L. Fox 1994. The chemistry of hydrocarbon ions in the Jovian ionosphere. *Icarus* **112**, 310–325.

Kim, Y. H., J. J. Caldwell, and J. L. Fox 1995. High-resolution ultraviolet spectroscopy of Jupiter's aurora with the Hubble Space Telescope. *Astrophys. J.* **477**, 906–914.

Kim, Y. H., J. L. Fox, and J. J. Caldwell 1997. Temperature and altitudes of Jupiter's ultraviolet aurora inferred from GHRS observations with the Hubble Space Telescope. *Icarus* **128**, 189–201.

Lammer, H., W. Stumptner, G. J. Molina-Cuberos, S. J. Bauer, and T. Owen 2000. Nitrogen isotope fractionation and its consequence for Titan's atmospheric evolution. *Planet. Space Sci.* **48**, 529–543.

Langford, A. O., H. Petek, and C. B. Moore 1983. Collisional removal of $CH_2(^1A_1)$: Absolute rate constants for atomic and molecular collisional partners at 295 K. *J. Chem. Phys.* **78**, 6650–6659.

Lara, L. M., E. Lellouch, J. J. López-Moreno, and R. Rodrigo 1996. Vertical distribution of Titan's atmospheric neutral constituents. *J. Geophys. Res.* **101**, 23261–23283.

Lara, L. M. et al. 1998. Correction to "Vertical distribution of Titan's atmospheric neutral constituents." *J. Geophys. Res.* **103**, 25775.

Laufer, A. H., and A. M. Bass 1977. Reaction between triplet methylene and CO_2: rate constant determination. *Chem. Phys. Lett.* **46**, 151–155.

Lee, A. Y. T., Y. L. Yung, and J. Moses 2000. Photochemical modeling of CH_3 abundances in the outer solar system. *J. Geophys. Res.* **105**, 22207–20225.

Lee, A. Y. T. 2001. Atmospheric chemistry and transport modeling in the outer solar system. Ph.D. dissertation, Caltech.

Le Teuff, Y. H., and A. J. Markwick 2000. The UMIST databse for astrochemistry 1999. *Astron. Astrophys. Supp.* **146**, 157–168.

Lewis, J. 1971. Satellites of the outer planets: their physical and chemical nature. *Icarus* **15**, 174.

Lindstedt, P. 1989. Modeling of the chemical complexities of flames. in *Twenty-Seventh Symposium (International) on Combustion*, The Combustion Institute, Pittsburgh, p. 269–285.

Liu, W., and A. Dalgarno 1996. The ultraviolet spectra of the Jovian aurora. *Astrophys. J.* **467**, 446.

Livengood, T. A., D. F. Strobel, and H. W. Woos 1990. Long-term study of longitudinal dependence in primary particle precipitation in the north Jovian aurora. *J. Geophys. Res.* **95**, 10375–10388.

Lorenz, R. D., C. P. McKay, and J. I. Lunine 1997. Photochemically driven collapse of Titan's atmosphere. *Science* **275**, 642–644.

Lovejoy, E. R., S. K. Kim, R. A. Alvarez, and C. B. Moore 1991. Kinetics of intramolecular carbon-atom exchange in ketene. *J. Chem. Phys.* **95**, 4081.

Lovejoy, E. R., and C. B. Moore 1993. Structures in the energy-dependence of the rate-constant for ketene isomerization. *J. Chem. Phys.* **98**, 7846.

Lunine, J. I., Y. L. Yung, and R. D. Lorenz 1999. On the volatile inventory of Titan from isotopic abundances in nitrogen and methane. *Planet. Space Sci.* **47**, 1291–1303.

Lutz, B. L., C. de Bergh, and T. Owen 1983. Titan: Discovery of carbon monoxide in its atmosphere. *Science* **220**, 1374–1375.

Millar, T. J., P. R. A. Farquhar, and K. Willacy 1997. The UMIST database for astrochemistry 1995. *Astron. Astrophys. Supp.* **121**, 139–185.

Mahaffy, P. R., T. M. Donahue, S. K. Atreya, T. C. Owen, and H. B. Niemann 1998. Galileo probe measurements of D/H and 3He/4He in Jupiter's atmosphere. *Space Sci. Rev.* **84**, 251.

Marten, A., D. Gautier, L. Tanguy, A. Lecacheux, C. Rosolen, and G. Paubert 1988. Abundance of carbon monoxide in the stratosphere of Titan from millimeter heterodyne observations. *Icarus* **76**, 558–562.

McElroy, M. B., and Y. L. Yung 1976. Oxygen isotopes in the Martian atmosphere: Implications for the evolution of volatiles. *Planet. Space Sci.* **24**, 1107.

McEwan, M. J., G. B. I. Scott, N. G. Adams, L. M. Babcock, R. Terzieva, and E. Herbst 1999. New H and H_2 reactions with small hydrocarbon ions and their roles in benzene synthesis in dense interstellar clouds. *Astrophys. J.* **513**, 287–293.

Montague, D. C., and F. S. Rowland 1971. Oxirene intermediate in the reaction of singlet methylene with carbon monoxide. *J. Am. Chem. Soc.* **93**, 5381–5387.

Muhleman, D. O., G. L. Berge, and R. T. Clancy 1984. Microwave measurements of carbon monoxide on Titan. *Science* **223**, 393.

Moses, J. I., B. Bézard, E. Lellouch, G. R. Gladstone, H. Feuchtgruber, and M. Allen 2000a. Photochemistry of Saturn's atmosphere. I. Hydrocarbon chemistry and comparisons with ISO observations. *Icarus* **143**, 244–298.

Moses, J. I., E. Lellouch, B. Bézard, G. R. Gladstone, H. Feuchtgruber, and M. Allen 2000b. Photochemistry of Saturn's atmosphere. II. Effects of an influx of external oxygen. *Icarus* **145**, 166–202.

Niemann, H. B., S. K. Atreya, G. R. Carignan, T. M. Donahue, J. A. Haberman, D. N. Harpold, R. E. Hartle, D. M. Hunten, W. T. Kasprzak, P. R. Mahaffy, T. C. Owen, and S. H. Way 1998. The composition of the Jovian atmosphere as determined by the Galileo probe mass spectrometer. *J. Geophys. Res.* **103**, E22831–22845.

Noll, K. S., T. R. Geballe, R. F. Knacke, and Y. J. Pendleton 1996. Titan's 5 μm spectral window: Carbon monoxide and the albedo of the surface. *Icarus* **124**, 625–631.

Orton, G. S. 1992. in *Symposium on Titan.* ESA SP-338, Noordwijk, Netherlands, 81.

Oser, H., N. D. Stothard, R. Humpfer, and H. H. Grotheer 1992. Direct measurement of the reaction CH_3 + OH at ambient temperature in the pressure range 0.3–6.2 mbar. *J. Phys. Chem.* **96**, 5359–5363.

Owen, T., N. Biver, A. Marten, H. Matthews, and R. Meier 1999. IAU Circular 7307.

Pepin, R. O. 1991. On the origin and early evolution of terrestrial planet atmospheres and meteoritic volatiles. *Icarus* **92**, 2.

Pereira, R. A., D. L. Baulch, M. J. Pilling, S. H. Robertson, and G. Zeng 1997. Temperature and pressure dependence of the multichannel rate coefficients for the CH_3 + OH system. *J. Phys. Chem.* **A 101**, 9681–9693.

Perry, J. J., Y. H. Kim, J. L. Fox, and H. S. Porter 1999. Chemistry of Jovian auroral ionosphere. *J. Geophys. Res.* **104**, 16541–16565.

Pinto, J. P., J. I. Lunine, S. J. Kim, and Y. L. Yung 1986. D to H ratio and the origin and evolution of Titan's atmosphere. *Nature* **319**, 388–390.

Pryor, W. R., and C. W. Hord 1991. A study of photopolarimeter system UV absorption data on Jupiter, Saturn, Uranus, and Neptune: Implications for auroral haze formation. *Icarus* **91**, 161–172.

Pryor, W. R., J. M. Ajello, W. K. Tobiska, D. E. Shemansky, G. K. James, C. W. Hord, S. K. Stephens, R. A. West, A. I. F. Stewart, W. E. McClintock, K. E. Simmons, A. R. Hendrix, and D. A. Miller 1998. Galileo ultraviolet spectrometer observations of Jupiter's auroral spectrum from 1600–3200 Å. *J. Geophys. Res.* **103**, 20149–20158.

Pryor, J. R., A. I. F. Stewart, K. E. Simmons, W. E. McClintock, W. D. Sweet, J. M. Ajello, G. K. James, W. K. Tobiska, G. R. Gladstone, J. H. Waite, T. Majeed, D. E. Shemansky, A. R. Vasavada, and J. T. Clarke 2000. Jupiter's ultraviolet aurora on Galileo orbit G7. *Icarus*, submitted.

Rebrion-Rowe, C., L. Lehfaoui, B. R. Rowe, and J. B. A. Mitchell 1998. The dissociative recombination of hydrocarbon ions. II. Alkene and alkyne derived species. *J. Chem. Phys.* **108**, 7185–7189.

Röckmann, T., C. A. M. Brenninkmeijer, G. Saueressig, P. Bergamaschi, J. N. Crowley, H. Fischer, and P. J. Crutzen 1998. Mass-independent oxygen isotope fractionation in atmospheric CO as a result of the reaction CO + OH. *Science* **281**, 544–546.

Sagan, C. B., B. N. Khare, W. R. Thompson, G. D. McDonald, M. R. Wing, J. L. Bada, V. D. Tuan, and E. T. Arakawa 1993. Polycyclic aromatic-hydrocarbons in the atmospheres of Titan and Jupiter. *Astrophys. J.* **414**, 399–405.

Scott, G. B. I., A. D. Fairley, C. G. Freeman, M. J. McEwan, N. G. Adams, and L. M. Babcock 1997. $C_mH_n^+$ reactions with H and H_2: An experimental study. *J. Phys. Chem.* **101**, 4973–4978.

Shemansky, D. E., J. M. Ajello, and D. T. Hall 1985. Electron impact excitation of H_2: Rydberg band systems and the benchmark cross section for H Lyman-α. *Astrophys. J.* **296**, 765–773.

Steinfeld, J. I., J. S. Francisco, and W. L. Hase 1989. *Chemical Kinetics and Dynamics*, Prentice-Hill: Englewood Cliffs, New Jersey, pp. 248–250.

Strobel, D. F. 1974. The photochemistry of hydrocarbons in the atmosphere of Titan. *Icarus* **21**, 466–470.

Summers, M. E., and D. F. Strobel 1989. Photochemistry of the atmosphere of Uranus. *Astrophys. J.* **346**, 495–508.

Trafton, L. M., J. C. Gérard, G. Munhoven, and J. H. Waite, Jr. 1994. High resolution spectra of Jupiter's northern auroral ultraviolet emission with the Hubble Space Telescope. *Astrophys. J.* **421**, 816–827.

Van Dishoeck, E. F., G. A. Blake, B. T. Draine, and J. I. Lunine 1993. in Levy, E. H., Lunine, J. I. (Eds.), *Protostars and Planets III*, University of Arizona Press, Tucson, pp. 163–241.

Vinckier, C., M. P. Gardner, and K. Bayes 1962. A study of some primary and secondary chemi-ionization reactions in hydrocarbon oxidations. in *Sixteenth Symposium (International) on Combustion*, The Combustion Institute, Pittsburgh.

Waganer, R. J., J. Caldwell, T. Owen, S.-J. Kim, Th. Encrenaz, and M. Combes 1985. The Jovian stratosphere in the ultraviolet. *Icarus* **60**, 222–236.

Wang, H., and M. Frenklach 1994. Calculations of rate coefficients for the chemically activated reactions of acetylene with vinylic and aromatic radicals. *J. Phys. Chem.* **98**, 11465–11489.

Wang, H., and M. Frenklach 1997. A detailed kinetic modeling study of aromatics formation in laminar premixed acetylene and ethylene flames. *Combust. Flame* **110**, 173–221.

West, R. A. 1988. Voyager-2 imaging eclipse observations of the Jovian high-altitude haze. *Icarus* **75**, 381.

Westmoreland, P. R., A. M. Dean, J. B. Howard, and J. P. Longwell 1989. Forming benzene in flames by chemically activated isomerization. *J. Phys. Chem.* **93**, 8171–8180.

Wolven, B. C., and P. D. Feldman 1998. Self-absorption by vibrationally excited H_2 in the Astro-2 Hopkins Ultraviolet Telescope spectrum of the Jovian aurora. *Geophys. Res. Lett.* **25**, 1537.

Wong, A. S., A. Y. T. Lee, Y. L. Yung, and J. M. Ajello 2000. Jupiter: Aerosol chemistry in the polar atmosphere. *Astrophys. J.* **543**, L215–217.

Yaws, C. L. 1994. *Handbook of Vapor Pressure*, Texas: Gulf Publishing Company.

Yung, Y. L., G. R. Gladstone, K. M. Change, J. M. Ajello, and S. K. Srivastava 1982. H_2 fluorescence spectrum from 1200 to 1700 Å by electron impact: Laboratory study and application to Jovian aurora. *Astrophys. J.* **254**, L65–L69.

Yung, Y. L., M. Allen, and J. P. Pinto 1984. Photochemistry of the atmosphere of Titan: Comparison between model and observations. *Astrophys. J. Supp.* **55**, 465–506.

Yung, Y. L., and W. B. DeMore 1999. *Photochemistry of Planetary Atmospheres*, New York: Oxford University Press.